CRANFIELD UNIVERSITY

SOPHIE BECKETT

INTER-SPECIES VARIATION IN BONE MINERAL

CRANFIELD DEFENCE AND SECURITY

PhD THESIS

2009

SUPERVISOR: PROFESSOR KEITH D. ROGERS

June 2009

CRANFIELD UNIVERSITY

CRANFIELD DEFENCE AND SECURITY

PhD THESIS

2009

SOPHIE BECKETT

INTER-SPECIES VARIATION IN BONE MINERAL

SUPERVISOR: PROFESSOR KEITH D. ROGERS

June 2009

ABSTRACT

Bone is a complex heterogeneous composite material with organic and inorganic components. The inorganic component; bone mineral, is a poorly crystalline, non-stoichiometric form of calcium hydroxylapatite. A model for the general structure and composition of bone mineral has been established within the literature. However, the nature and extent of variation in bone mineral composition and structure has, to date, been poorly understood. This situation also applies to the general response of bone mineral to heat treatment and variation in this response.

This thesis presents the results of an investigation of inter-species variation in bone mineral characteristics of unheated bone and bone heated to temperatures of 600 °C and 1400 °C. Twelve different animal species were investigated, including human bone. X-ray diffraction analysis was the primary analytical technique employed. The Rietveld method of full profile fitting of diffraction data was used to quantitatively investigate characteristics of unheated and heated bone such as the weight percentages of the thermal decomposition products of bone mineral. Infrared spectroscopy, inductively coupled plasma – atomic emission spectrometry, pyrohydrolysis – ion chromatography and combustion – gas chromatography were also employed to obtain further data regarding the chemical composition of bone. Biological

control of bone mineral composition and structure and the chemical basis for the variation observed within the results were explored.

Significant inter-species variation in bone mineral composition and structure and also, the response of bone to heat treatment have been demonstrated by the results of this thesis. In particular, human bone is significantly different from bone of all other species investigated.

ACKNOWLEDGEMENTS

Grateful acknowledgements are given to all those who have provided me with help and support in the creation of this thesis.

Many, many thanks are extended to Professor Keith Rogers for his previous work and initial proposal of the research, his supervision, his confidence in my capabilities and my future potential, and particularly for, being a pleasure to work for and his extreme patience.

The continual belief, encouragement and support from my family and friends helped me to reach the point of undertaking PhD research and have greatly helped me through my PhD studies and I wholeheartedly thank them all for this.

On moving onto post-doctoral research, I take with me friends and colleagues from DMMS/DMAS/DASSR, Shrivenham and Eastbury Way with whom it has been lovely working and socialising during the last few years. I cannot imagine how the three plus years as a PhD student would have been without Melanie Sapsford being a fellow conspirator and constant source of support, encouragement and entertaining gossip. I would like to thank Adrian Mustey, for all his help with everything practical. Also, this thesis has benefited from the considerable number of inter-library loans obtained by Iain Mckay and I have

benefited from many cheery chats, library snacks and the library survey i-pod prize.

This thesis would not exist without the help of those who responded to requests for bone samples and their faith in the potential of my research. I especially thank Professor John Clement for access to samples from the Melbourne Femur Collection, his collaboration, advice, continual support and for his inspiring interest in my research. Along with John, I would also like to thank, David Thomas and Sherie Blackwell from the University of Melbourne for their assistance and for their hospitality. I would like to thank the North London Tissue Bank for providing (via Dr Peter Zioupos from Cranfield University) human bone samples from individuals from the United Kingdom. I also especially thank Mick Kirby from the Veterinary Laboratories Agency for all his generous help and support and for providing me with cow, goat, pig and sheep bone samples. I would like to thank Dr Martin Owen from the University of Bristol for dog bone samples, Dr Niall Martin for the monkey bone sample and Whipsnade Zoo (via Dr Peter Zioupos from Cranfield University and Dr Richard Cook, now at the University of Southampton) for the elephant bone sample. In addition, I would like to thank various local butchers and abattoirs for providing chicken, cow, deer, goat, pig, rabbit and sheep bone samples and local pet food shops for providing rat bone samples.

Acknowledgements are given to Catherine Unsworth and Dr Sarah James from the Natural History Museum, London for carrying out the analysis of my

specimens using inductively coupled plasma – atomic emission spectrometry, pyrohydrolysis – ion chromatography and combustion – gas chromatography; their help was greatly appreciated.

Acknowledgement is given to the Engineering and Physical Sciences Research Council for Doctoral Training Account funding and for Roberts' Money funding. I would also like to thank the International Centre for Diffraction Data for the award of a Ludo Frevel scholarship in 2008. Thanks are also given to the British Association for Human Identification for the award of the prize for best student presentation at the association's annual conference meeting in 2006. I would like to thank the Royal Society of Chemistry for the following bursaries: Analytical Chemistry Division travel bursary, Corday Morgan Memorial Fund – stop-over in Commonwealth Countries bursary, Public Activities Small Grant and a Faraday Discussion 136 – Crystal Growth and Nucleation conference bursary. I would also like to thank the Society for Chemical Industry, UK Resource Centre for Women in Science Engineering and Technology, Australian and New Zealand Bone and Mineral Society and, Cranfield Student Association for each awarding me travel bursaries.

Finally, thanks to everyone who has proof read this thesis and provided me with many helpful comments.

CONTENTS

ABSTRACT I

ACKNOWLEDGEMENTS III

CONTENTS VI

LIST OF TABLES X

LIST OF FIGURES XIX

GLOSSARY XXIX

CHAPTER 1 – INTRODUCTION 1

1.1 – THESIS OUTLINE 1

1.2 – BIOLOGICAL CLASSIFICATION 2

1.3 – SPECIES IDENTIFICATION OF SKELETAL MATERIAL 5

1.4 – PRACTICAL APPLICATION OF SPECIES IDENTIFICATION 9

CHAPTER 2 – BONE MINERAL AND ITS VARIATION 16

2.1 – BONE 16

2.2 – CALCIUM HYDROXYLAPATITE 17

2.3 – BONE MINERAL (BIO-APATITE) 21

2.4 – BONE MINERAL VARIATION 24

2.5 – HEAT TREAMENT OF BONE 27

CHAPTER 3 – ANALYTICAL TECHNIQUES 33

3.1 – X-RAY DIFFRACTION ANALYSIS 34

3.2 – INFRARED SPECTROSCOPY 42

3.3 – INDUCTIVELY COUPLED PLASMA – ATOMIC EMISSION SPECTROMETRY 44

3.4 – PYROHYDROLYSIS – ION CHROMATOGRAPHY AND COMBUSTION – GAS CHROMATOGRAPHY 45

CHAPTER 4 – AIMS, HYPOTHESES, MATERIALS AND METHODS 48

4.1 – AIMS AND HYPOTHESES 48

4.2 – BONE MATERIAL 54

4.3 – SPECIMEN PREPARATION 57

4.4 – X-RAY DIFFRACTION (XRD) ANALYSIS 64

4.5 – INFRARED (IR) SPECTROSCOPY 69

4.6 – INDUCTIVELY COUPLED PLASMA – ATOMIC EMISSION SPECTROMETRY (ICP-AES) 73

4.7 – PYROHYDROLYSIS – ION CHROMATOGRAPHY (P-IC) 74

4.8 – COMBUSTION – GAS CHROMATOGRAPHY (C-GC) 76

4.9 – MEASUREMENT OF MASS CHANGE DUE TO HEAT TREATMENT 77

4.10 – STATISTICAL ANALYSIS OF DATA 78

CHAPTER 5 – RESULTS 81

5.1 – X-RAY DIFFRACTION ANALYSIS OF UNHEATED BONE 82

5.2 – INDUCTIVELY COUPLED PLASMA – ATOMIC EMISSION SPECTROMETRY OF BONE HEATED TO 600 °C 83

5.3 – PYROHYDROLYSIS – ION CHROMATOGRAPHY OF BONE HEATED TO 600 °C 86

5.4 – COMBUSTION – GAS CHROMATOGRAPHY OF BONE HEATED TO 600 °C.....87

5.5 – INFRARED SPECTROSCOPY OF BONE HEATED TO 600 °C 88

5.6 – MASS CHANGE ON HEATING.....89

5.7 – X-RAY DIFFRACTION ANALYSIS OF BONE HEATED TO 600 °C 90

5.8 – X-RAY DIFFRACTION ANALYSIS OF BONE HEATED TO 1400 °C 94

5.9 – INTER-SPECIES VARIATION.....99

5.10 – KENDALL'S TAU CORRELATIONS OF BONE MINERAL CHARACTERISTICS 135

CHAPTER 6 – DISCUSSION.....143

6.1 – GENERAL COMPOSITION AND STUCTURE OF BONE MINERAL 143

6.2 – BIOLOGICAL CONTROL OF COMPOSITION AND STRUCTURE 145

6.3 – GENERAL RESPONSE OF BONE TO HEAT TREATMENT 147

6.4 – CHEMICAL BASIS FOR VARIATION IN RESPONSE OF BONE TO HEAT TREATMENT 151

6.5 – INTER-SPECIES VARIATION IN COMPOSTITION AND STRUCTURE.....155

6.6 – INTER-SPECIES VARIATION IN RESPONSE TO HEAT TREATMENT 157

6.7 – SPECIES IDENTIFICATION.....158

CHAPTER 7 – CONCLUSIONS 161

7.1 – RESEARCH CONCLUSIONS 161

7.2 – CONTRIBUTION TO KNOWLEDGE 162

7.3 – FUTURE WORK 164

REFERENCES 166

A – APPENDIX 181

LIST OF TABLES

Table 4.1 – Total number of individuals investigated for each species and the numbers of individuals of each species used for each analytical technique 56

Table 5.1 – XRD analysis results for HAP %, HAP <00ℓ>, HAP 'a' and HAP 'c' obtained from unheated bone specimens, including all species investigated (unheated rat bone was not investigated using this technique). Data presented as two groups: one that excludes human AUS and one that includes human AUS 82

Table 5.2 – ICP-AES results for Ca % and P %, calculated $Ca/P_{(atomic)}$ and calculated $Ca/P_{(weight)}$ obtained from bone specimens heated to 600 °C, including all species investigated (elephant and rat not investigated using this technique). Data presented as two groups: one that excludes human AUS and one that includes human AUS 84

Table 5.3 – ICP-AES results for Na ppm, Mg ppm, K ppm, Sr ppm and Fe ppm obtained from bone specimens heated to 600 °C, including all species investigated (elephant and rat not investigated using this technique). Data presented as two groups: one that excludes human AUS and one that includes human AUS 85

Table 5.4 – P-IC results for F ppm and Cl ppm obtained from bone specimens heated to 600 °C, including all species investigated (elephant and rat not investigated using this technique). Data presented as two groups: one that excludes human AUS and one that includes human AUS..86

Table 5.5 – C-GC results for C %, N % and H % obtained from bone specimens heated to 600 °C, including all species investigated (elephant and rat not investigated using this technique). Data presented as two groups: one that excludes human AUS and one that includes human AUS 87

Table 5.6 – IR spectroscopy results for CO_3 % and *SF* obtained from bone specimens heated to 600 °C, including all species investigated (elephant, rat and human AUS not investigated using this technique) 88

Table 5.7 – Mass change results for mass change on heating bone specimens to 600 °C and on heating bone specimens to 1400 °C, including all species investigated. Data presented as two groups: one that excludes human AUS and one that includes human AUS.....89
Table 5.8 – XRD analysis results for HAP %, HAP <00ℓ>, HAP 'a', and HAP 'c' obtained from bone specimens heated to 600 °C, including all species investigated. Data presented as two groups: one that excludes human AUS and one that includes human AUS.....91
Table 5.9 – XRD analysis results for β-TCP and MgO obtained from bone specimens heated to 600 °C, including all species investigated. Data presented as two groups: one that excludes human AUS and one that includes human AUS.....93
Table 5.10 – XRD analysis results for HAP %, HAP 'a' and HAP 'c' obtained from bone specimens heated to 1400 °C, including all species investigated. Data presented as two groups: one that excludes human AUS and one that includes human AUS.....95
Table 5.11 – XRD analysis results for β-TCP and MgO obtained from bone specimens heated to 1400 °C, including all species investigated. Data presented as two groups: one that excludes human AUS and one that includes human AUS.....96
Table 5.12 – XRD analysis results for TTCP, CaO and α-TCP obtained from bone specimens heated to 600 °C, including all species investigated. Data presented as two groups: one that excludes human AUS and one that includes human AUS.....98
Table 5.13 – Kendall's Tau correlation results for HAP <00ℓ>, HAP 'a' and HAP 'c' obtained from XRD analysis of unheated bone specimens, HAP <00ℓ>, HAP 'a', HAP 'c', β-TCP %, β-TCP 'a' and β-TCP 'c' obtained from XRD analysis of bone specimens heated to 600 °C and mass change results for bone specimens heated to 600 °C, tested against each other. Data presented includes all species investigated with the exception of tests involving data from unheated bone specimens for which rat was not included and tests for β-TCP %, β-TCP 'a' and β-TCP 'c' obtained from bone specimens heated to 600 °C for which only rat, chicken and sheep were included. In each test result 'box' the correlation coefficient is presented above the number of individuals used for the test 137
Table 5.14 – Kendall's Tau correlation results for bone mineral characteristics obtained from ICP-AES, P-IC, C-GC and IR spectroscopy of bone specimens heated to 600 °C tested against

characteristics obtained from XRD analysis of unheated bone specimens, bone specimens heated to 600 °C and to 1400 °C and for mass change results for 600 °C and 1400 °C. Data includes all species investigated with the exception of tests involving data from unheated bone for which rat was not included and tests for β-TCP %, β-TCP 'a' and β-TCP 'c' obtained from bone specimens heated to 600 °C for which only rat, chicken and sheep were included. In each test result 'box' the correlation coefficient is presented above the number of individuals used for the test.....138

Table 5.15 – Kendall's Tau correlation results for bone mineral characteristics obtained from XRD analysis of bone specimens heated to 600 °C and mass change results for bone specimens heated to 600 °C tested against bone mineral characteristics obtained from XRD analysis of bone specimens heated to 1400 °C and mass change results for bone specimens heated to 1400 °C. Data presented includes all species investigated with the exception of tests involving data from unheated bone specimens for which rat was not included, tests for β-TCP %, β-TCP 'a' and β-TCP 'c' obtained from bone specimens heated to 600 °C for which only rat, chicken and sheep were included and tests for α-TCP % for which only chicken, human AUS and rat were included. In each test result 'box' the correlation coefficient is presented above the number of individuals used for the test 141

Table A.1 – XRD analysis results for HAP %, HAP <00ℓ>, HAP 'a' and HAP 'c' obtained from unheated bone specimens, grouped by species. For elephant and monkey the 'mean' values represent data from one individual from each species and so no standard error of the mean, minimum or maximum values are presented. Unheated rat bone was not investigated using this technique.....234

Table A.2 – ICP-AES results for Ca % and P %, calculated $Ca/P_{(atomic)}$ and calculated $Ca/P_{(weight)}$ obtained from bone specimens heated to 600 °C, grouped by species. For all species except cow, human AUS and rat the 'mean' values represent data from one individual from each species and so no standard error of the mean, minimum or maximum values are presented. Rat bone was not investigated using this technique.....235

Table A.3 – ICP-AES results for Na ppm, Mg ppm, K ppm, Sr ppm and Fe ppm obtained from bone specimens heated to 600 °C, grouped by species. For all species except cow, human AUS and rat the 'mean' values represent data from one individual from each species and so no standard error of the mean, minimum or maximum values are presented. Rat bone was not investigated using this technique 236

Table A.4 – P-IC results for F ppm and Cl ppm obtained from bone specimens heated to 600 °C, grouped by species. For all species except cow, human AUS and rat the 'mean' values represent data from one individual from each species and so no standard error of the mean, minimum or maximum values are presented. Rat bone was not investigated using this technique. Data obtained for rabbit was semi-quantitative and so is not presented 237

Table A.5 – C-GC results for N %, C % and H % obtained from bone specimens heated to 600 °C, grouped by species. For all species except cow, human AUS and rat the 'mean' values represent data from one individual from each species and so no standard error of the mean, minimum or maximum values are presented. Rat bone was not investigated using this technique 238

Table A.6 – IR spectroscopy results for CO_3 % and SF obtained from bone specimens heated to 600 °C, grouped by species. For all species except cow, human AUS, elephant and rat the 'mean' values represent data from one individual from each species and so no standard error of the mean, minimum or maximum values are presented. Rat, human AUS and elephant bone were not investigated using this technique 239

Table A.7 – Mass change results obtained from bone specimens heated to 600 °C and 1400 °C, grouped by species. For elephant and monkey the 'mean' values represent data from one individual from each species and so no standard error of the mean, minimum or maximum values are presented 240

Table A.8 – XRD analysis results for HAP %, HAP <00ℓ>, HAP 'a' and HAP 'c' obtained from bone specimens heated to 600 °C, grouped by species. For elephant and monkey the 'mean' values represent data from one individual from each species and so no standard error of the mean, minimum or maximum values are presented 241

Table A.9 – XRD analysis results for XRD analysis results for β-TCP and MgO obtained from bone specimens heated to 600 °C, grouped by species. For elephant and monkey the 'mean' values represent data from one individual from each species and so no standard error of the mean, minimum or maximum values are presented. The phase β-TCP was only detected in chicken, rat and sheep and MgO was only detected in human UK and monkey bone specimens 242
Table A.10 – XRD analysis results for HAP %, HAP 'a' and HAP 'c' obtained from bone specimens heated to 1400 °C, grouped by species. For elephant and monkey the 'mean' values represent data from one individual from each species and so no standard error of the mean, minimum or maximum values are presented.....243
Table A.11 – XRD analysis results for β-TCP and MgO obtained from bone specimens heated to 1400 °C, grouped by species. For elephant and monkey the 'mean' values represent data from one individual from each species and so no standard error of the mean, minimum or maximum values are presented.....244
Table A.12 – XRD analysis results for α-TCP, TTCP and CaO obtained from bone specimens heated to 1400 °C, grouped by species. For elephant and monkey the 'mean' values represent data from one individual from each species and so no standard error of the mean, minimum or maximum values are presented. The phase α-TCP was only detected in chicken, human AUS and rat bone specimens and CaO was not detected in rat or monkey bone specimens.....245
Table A.13 – Chicken and rat: Kendall's Tau correlation results for bone mineral characteristics obtained from XRD analysis of unheated bone and bone heated to 600 °C and mass change results for bone heated to 600 °C, tested against each other. Unheated rat bone was not investigated using XRD analysis. In each test result 'box' the correlation coefficient is presented above the number of individuals used for the test. A grey shaded box indicates $p < 0.05$ and a black box indicates $p < 0.01$ 246
Table A.14 – Chicken: Kendall's Tau correlation results for bone mineral characteristics obtained from XRD analysis of bone heated to 1400 °C and mass change results for bone heated to 1400 °C, each tested against bone mineral characteristics obtained from XRD analysis of unheated bone and bone heated to 600 °C and mass change results for bone

heated to 600 °C. In each test result ‘box’ the correlation coefficient is presented above the number of individuals used for the test. A grey shaded box indicates $p < 0.05$ and a black box indicates $p < 0.01$ 247
Table A.15 – Rat: Kendall’s Tau correlation results for bone mineral characteristics obtained from XRD analysis of bone heated to 1400 °C and mass change results for bone heated to 1400 °C, each tested against bone mineral characteristics obtained from XRD analysis of bone heated to 600 °C and mass change results for bone heated to 600 °C. Unheated rat bone was not investigated using XRD analysis. In each test result ‘box’ the correlation coefficient is presented above the number of individuals used for the test. A grey shaded box indicates $p < 0.05$ and a black box indicates $p < 0.01$ 248
Table A.16 – Deer and rabbit: Kendall’s Tau correlation results for bone mineral characteristics obtained from XRD analysis of unheated bone and bone heated to 600 °C and mass change results for bone heated to 600 °C, tested against each other. In each test result ‘box’ the correlation coefficient is presented above the number of individuals used for the test. In each test result ‘box’ the correlation coefficient is presented above the number of individuals used for the test. A grey shaded box indicates $p < 0.05$ and a black box indicates $p < 0.01$ 249
Table A.17 – Deer: Kendall’s Tau correlation results for bone mineral characteristics obtained from XRD analysis of bone heated to 1400 °C and mass change results for bone heated to 1400 °C, each tested against bone mineral characteristics obtained from XRD analysis of unheated bone and bone heated to 600 °C and mass change results for bone heated to 600 °C. In each test result ‘box’ the correlation coefficient is presented above the number of individuals used for the test. A grey shaded box indicates $p < 0.05$ and a black box indicates $p < 0.01$ ... 250
Table A.18 – Rabbit: Kendall’s Tau correlation results for bone mineral characteristics obtained from XRD analysis of bone heated to 1400 °C and mass change results for bone heated to 1400 °C, each tested against bone mineral characteristics obtained from XRD analysis of unheated bone and bone heated to 600 °C and mass change results for bone heated to 600 °C. In each test result ‘box’ the correlation coefficient is presented above the number of individuals used for the test. A grey shaded box indicates $p < 0.05$ and a black box indicates $p < 0.01$ ... 251

Table A.19 – Goat and Sheep: Kendall's Tau correlation results for bone mineral characteristics obtained from XRD analysis of unheated bone and bone heated to 600 °C and mass change results for bone heated to 600 °C, tested against each other. In each test result 'box' the correlation coefficient is presented above the number of individuals used for the test. In each test result 'box' the correlation coefficient is presented above the number of individuals used for the test. A grey shaded box indicates $p < 0.05$ and a black box indicates $p < 0.01$ 252
Table A.20 – Goat: Kendall's Tau correlation results for bone mineral characteristics obtained from XRD analysis of bone heated to 1400 °C and mass change results for bone heated to 1400 °C, each tested against bone mineral characteristics obtained from XRD analysis of unheated bone and bone heated to 600 °C and mass change results for bone heated to 600 °C. In each test result 'box' the correlation coefficient is presented above the number of individuals used for the test. A grey shaded box indicates $p < 0.05$ and a black box indicates $p < 0.01$ ... 253
Table A.21 – Sheep: Kendall's Tau correlation results for bone mineral characteristics obtained from XRD analysis of bone heated to 1400 °C and mass change results for bone heated to 1400 °C, each tested against bone mineral characteristics obtained from XRD analysis of unheated bone and bone heated to 600 °C and mass change results for bone heated to 600 °C. In each test result 'box' the correlation coefficient is presented above the number of individuals used for the test. A grey shaded box indicates $p < 0.05$ and a black box indicates $p < 0.01$ ... 254
Table A.22 – Dog and pig: Kendall's Tau correlation results for bone mineral characteristics obtained from XRD analysis of unheated bone and bone heated to 600 °C and mass change results for bone heated to 600 °C, tested against each other. In each test result 'box' the correlation coefficient is presented above the number of individuals used for the test. In each test result 'box' the correlation coefficient is presented above the number of individuals used for the test. A grey shaded box indicates $p < 0.05$ and a black box indicates $p < 0.01$ 255
Table A.23 – Dog: Kendall's Tau correlation results for bone mineral characteristics obtained from XRD analysis of bone heated to 1400 °C and mass change results for bone heated to 1400 °C, each tested against bone mineral characteristics obtained from XRD analysis of unheated bone and bone heated to 600 °C and mass change results for bone heated to 600 °C.

In each test result ‘box’ the correlation coefficient is presented above the number of individuals used for the test. A grey shaded box indicates $p < 0.05$ and a black box indicates $p < 0.01$ ...256
Table A.24 – Pig: Kendall’s Tau correlation results for bone mineral characteristics obtained from XRD analysis of bone heated to 1400 °C and mass change results for bone heated to 1400 °C, each tested against bone mineral characteristics obtained from XRD analysis of unheated bone and bone heated to 600 °C and mass change results for bone heated to 600 °C. In each test result ‘box’ the correlation coefficient is presented above the number of individuals used for the test. A grey shaded box indicates $p < 0.05$ and a black box indicates $p < 0.01$ ...257
Table A.25 – Human UK and human AUS: Kendall’s Tau correlation results for bone mineral characteristics obtained from XRD analysis of unheated bone and bone heated to 600 °C and mass change results for bone heated to 600 °C, tested against each other. In each test result ‘box’ the correlation coefficient is presented above the number of individuals used for the test. In each test result ‘box’ the correlation coefficient is presented above the number of individuals used for the test. A grey shaded box indicates $p < 0.05$ and a black box indicates $p < 0.01$ ...258
Table A.26 – Human AUS: Kendall’s Tau correlation results for bone mineral characteristics obtained from XRD analysis of bone heated to 1400 °C, mass change results for bone heated to 1400 °C, sex and age data, each tested against bone mineral characteristics obtained from XRD analysis of unheated bone and bone heated to 600 °C and mass change results for bone heated to 600 °C. In each test result ‘box’ the correlation coefficient is presented above the number of individuals used for the test. A grey shaded box indicates $p < 0.05$ and a black box indicates $p < 0.01$.....259
Table A.27 – Human UK: Kendall’s Tau correlation results for bone mineral characteristics obtained from XRD analysis of bone heated to 1400 °C, mass change results for bone heated to 1400 °C, sex and age data, each tested against bone mineral characteristics obtained from XRD analysis of unheated bone and bone heated to 600 °C and mass change results for bone heated to 600 °C. In each test result ‘box’ the correlation coefficient is presented above the number of individuals used for the test. A grey shaded box indicates $p < 0.05$ and a black box indicates $p < 0.01$.....260

Table A.28 – Cow: Kendall's Tau correlation results for bone mineral characteristics obtained from XRD analysis of unheated bone and bone heated to 600 °C and mass change results for bone heated to 600 °C, tested against each other. In each test result 'box' the correlation coefficient is presented above the number of individuals used for the test. In each test result 'box' the correlation coefficient is presented above the number of individuals used for the test. A grey shaded box indicates $p < 0.05$ and a black box indicates $p < 0.01$.....261
Table A.29 – Cow: Kendall's Tau correlation results for bone mineral characteristics obtained from XRD analysis of bone heated to 1400 °C, mass change results for bone heated to 1400 °C, sex and age data, each tested against bone mineral characteristics obtained from XRD analysis of unheated bone and bone heated to 600 °C and mass change results for bone heated to 600 °C. In each test result 'box' the correlation coefficient is presented above the number of individuals used for the test. A grey shaded box indicates $p < 0.05$ and a black box indicates $p < 0.01$.....262
Table A.30 – Human AUS: Kendall's Tau correlation results for bone mineral characteristics obtained from ICP-AES, P-IC and C-GC of bone specimens heated to 600 °C tested against characteristics obtained from XRD analysis of unheated bone specimens, bone specimens heated to 600 °C and to 1400 °C and for mass change results for 600 °C and 1400 °C. In each test result 'box' the correlation coefficient is presented above the number of individuals used for the test.....263
Table A.31 – Cow: Kendall's Tau correlation results for bone mineral characteristics obtained from ICP-AES, P-IC, C-GC and IR spectroscopy of bone specimens heated to 600 °C tested against characteristics obtained from XRD analysis of unheated bone specimens, bone specimens heated to 600 °C and to 1400 °C and for mass change results for 600 °C and 1400 °C. In each test result 'box' the correlation coefficient is presented above the number of individuals used for the test.....264

LIST OF FIGURES

Figure 1.1 – Overview of taxonomic classification categories, from phylum to species levels, using the species investigated within this thesis as examples 3

Figure 1.2 – Diagram showing anterior (left of diagram) and posterior (right of diagram) aspects of the human skeleton[2] 4

Figure 2.1 – Structural features of bone [61] 17

Figure 2.2 – Crystal lattice structure of stoichiometric calcium hydroxylapatite (HAP) with hydrogen atoms omitted and atomic radii reduced for clarity. The diagram shows the crystal lattice viewed down the 'c' axis and shows two unit cells along each axis: a, b and, c (diagram created using Crystallographica software, version 1.53) 19

Figure 3.1 – Photograph of X-ray diffractometer employed for this research 37

Figure 4.1 – Diagram showing example of cut bone specimen segment 58

Figure 4.2 – Diagram showing preliminary data and observations used to help determine the choice of 600 °C and 1400 °C as the heat temperatures investigated. Values of the HAP lattice parameter 'a' and the weight percentage of HAP are presented for cow, human and sheep bone specimens heated to a range of temperatures, each heated for two hours (one individual per species). Values obtained for the HAP lattice parameter 'c' and weight percentage values for thermal decomposition products of HAP are referred to but not presented. Rietveld fitting errors are shown for HAP 'a' values, those for HAP % are all within the limits of the data markers and are therefore omitted for clarity 61

Figure 4.3 – Photograph of the Carbolite tube furnace (CTF 16/75) used for the heating of bone specimens 63

Figure 4.4 – Diagram of set-up of furnace apparatus for the heating of bone specimens showing one specimen placed within the furnace and ceramic fibre bungs used at each end of the furnace tube 63

Figure 4.5 - Calibration graph for calculation of carbonate weight percentage values (CO_3 %) from the total carbonate peak area (A), measured using IR spectroscopy 71

Figure 4.6 – Section of IR spectrum obtained from a bone specimen heated to 600 °C showing phosphate ion splitting factor measurement points. Peaks correspond to the ν_4 P-O stretching and bending vibration bands 72
Figure 4.7 – Diagram of pyrohydrolysis apparatus set up for pyrohydrolysis – ion chromatography of bone specimens previously heated to 600 °C (courtesy of Natural History Museum).....75
Figure 5.1 – X-ray diffractograms from bone specimens heated to 1400 °C showing evidence for detection of MgO presented using Topas software. XRD data is represented by the blue line, the Rietveld refinement data is represented by the red line. Rietveld refinement has been carried out for all mineral phases except MgO in order to highlight MgO peaks (indicated by arrows). A weight percentage of 0.36 % MgO was obtained from the lower diffractogram (peak at approximately 1.38 d-spacing is not observed due to low weight percentage of MgO) and 1.4 % MgO was obtained from the upper diffractogram 93
Figure 5.2 – Results of Bonferroni ANOVA post-hoc tests for statistical significance of inter-species variation for a selection of bone mineral characteristics measured using X-ray diffraction analysis and for mass change on heating. Results presented for elephant and monkey represent one individual from each species and one sample t-tests were carried out for these species. An 'X' within a box indicates that no test was carried out for the corresponding species pair for a particular bone mineral characteristic due to absence of data or insufficient data 100
Figure 5.3 – XRD analysis results for HAP <00ℓ> obtained from unheated bone specimens, grouped by species, showing mean (line within a box), minimum (lower limit of a box) and maximum (upper limit of a box) values. Unheated rat bone was not investigated and data presented for elephant and monkey represents one individual from each species.....103
Figure 5.4 – XRD analysis results for HAP 'a' obtained from unheated bone specimens, grouped by species, showing mean (line within a box), minimum (lower limit of a box) and maximum (upper limit of a box) values. Unheated rat bone rat was not investigated and data presented for elephant and monkey represents one individual from each species 104
Figure 5.5 – XRD analysis results for HAP 'c' obtained from unheated bone specimens, grouped by species, showing mean (line within a box), minimum (lower limit of a box) and maximum

(upper limit of a box) values. Unheated rat bone rat was not investigated and data presented for elephant and monkey represents one individual from each species 105
Figure 5.6 – ICP-AES results for Ca %, P % and calculated Ca/P $_{(atomic)}$ obtained from bone specimens heated to 600 °C, grouped by species. Data for one individual from each species presented with the exception of cow and human AUS (mean (line within a box), minimum (lower limit of a box) and maximum (upper limit of a box) values shown for these species) and elephant and rat which were not investigated using this technique 107
Figure 5.7 – ICP-AES results for K ppm, Mg ppm and Na ppm obtained from bone specimens heated to 600 °C, grouped by species. Data for one individual from each species presented with the exception of cow and human AUS (mean (line within a box), minimum (lower limit of a box) and maximum (upper limit of a box) values shown for these species) and elephant and rat which were not investigated using this technique..... 109
Figure 5.8 – ICP-AES results for Fe ppm and Sr ppm obtained from bone specimens heated to 600 °C, grouped by species. Data for one individual from each species presented with the exception of cow and human AUS (mean (line within a box), minimum (lower limit of a box) and maximum (upper limit of a box) values shown for these species) and elephant and rat which were not investigated using this technique..... 111
Figure 5.9 – P-IC results for Cl ppm and F ppm obtained from bone specimens heated to 600 °C, grouped by species. Data for one individual from each species presented with the exception of cow and human AUS (mean (line within a box), minimum (lower limit of a box) and maximum (upper limit of a box) values shown for these species), elephant and rat which were not investigated using this technique and rabbit, for which semi-quantitative results were obtained 113
Figure 5.10 – C-GC results for N %, C % and H % obtained from bone specimens heated to 600 °C, grouped by species. Data for one individual from each species presented with the exception of cow and human AUS (mean (line within a box), minimum (lower limit of a box) and maximum (upper limit of a box) values shown for these species) and elephant and rat which were not investigated using this technique 115

Figure 5.11 – IR spectroscopy results for CO_3 % obtained from bone specimens heated to 600 °C, grouped by species. Data for one individual from each species presented with the exception of cow (mean (line within a box), minimum (lower limit of a box) and maximum (upper limit of a box) values shown for this species) and elephant, human AUS and rat which were not investigated using this technique 116
Figure 5.12 – IR spectroscopy results for phosphate splitting factor (*SF*) obtained from bone specimens heated to 600 °C, grouped by species. Data for one individual from each species presented with the exception of cow (mean (line within a box), minimum (lower limit of a box) and maximum (upper limit of a box) values shown for this species) and elephant, human AUS and rat which were not investigated using this technique 117
Figure 5.13 – Mass change results for mass change on heating bone specimens to 600 °C, grouped by species, showing mean (line within a box), minimum (lower limit of a box) and maximum (upper limit of a box) values. Data presented for elephant and monkey represents one individual from each species 119
Figure 5.14 – Mass change results for mass change on heating bone specimens to 1400 °C, grouped by species, showing mean (line within a box), minimum (lower limit of a box) and maximum (upper limit of a box) values. Data presented for elephant and monkey represents one individual from each species 120
Figure 5.15 – XRD analysis results for HAP <00ℓ> obtained from bone specimens heated to 600 °C, grouped by species, showing mean (line within a box), minimum (lower limit of a box) and maximum (upper limit of a box) values. Data presented for elephant and monkey represents one individual from each species 122
Figure 5.16 – XRD analysis results for HAP ‘a’ obtained from bone specimens heated to 600 °C, grouped by species, showing mean (line within a box), minimum (lower limit of a box) and maximum (upper limit of a box) values. Data presented for elephant and monkey represents one individual from each species 123
Figure 5.17 – XRD analysis results for HAP ‘c’ obtained from bone specimens heated to 600 °C, grouped by species, showing mean (line within a box), minimum (lower limit of a box) and

maximum (upper limit of a box) values. Data presented for elephant and monkey represents one individual from each species 124
Figure 5.18 – XRD analysis results for HAP % obtained from bone specimens heated to 1400 °C, grouped by species, showing mean (line within a box), minimum (lower limit of a box) and maximum (upper limit of a box) values. Data presented for elephant and monkey represents one individual from each species 126
Figure 5.19 – XRD analysis results for HAP ‘a’ obtained from bone specimens heated to 1400 °C, grouped by species, showing mean (line within a box), minimum (lower limit of a box) and maximum (upper limit of a box) values. Data presented for elephant and monkey represents one individual from each species 127
Figure 5.20 – XRD analysis results for HAP ‘c’ obtained from bone specimens heated to 1400 °C, grouped by species, showing mean (line within a box), minimum (lower limit of a box) and maximum (upper limit of a box) values. Data presented for elephant and monkey represents one individual from each species 127
Figure 5.21 – XRD analysis results for β-TCP % obtained from bone specimens heated to 1400 °C, grouped by species, showing mean (line within a box), minimum (lower limit of a box) and maximum (upper limit of a box) values. Data presented for elephant and monkey represents one individual from each species 129
Figure 5.22 – XRD analysis results for β-TCP ‘a’ obtained from bone specimens heated to 1400 °C, grouped by species, showing mean (line within a box), minimum (lower limit of a box) and maximum (upper limit of a box) values. Data presented for elephant and monkey represents one individual from each species 130
Figure 5.23 – XRD analysis results for β-TCP ‘c’ obtained from bone specimens heated to 1400 °C, grouped by species, showing mean (line within a box), minimum (lower limit of a box) and maximum (upper limit of a box) values. Data presented for elephant and monkey represents one individual from each species 131
Figure 5.24 – XRD analysis results for α-TCP % and TTCP % obtained from bone specimens heated to 1400 °C, grouped by species, showing mean (line within a box), minimum (lower limit of a box) and maximum (upper limit of a box) values. Data presented for elephant and monkey

represents one individual from each species. The phase α-TCP was only detected in chicken, human AUS and rat bone specimens. Data for individuals for which mineral phase weight percentage was equal to zero are not presented and not included in calculation of mean values 133

Figure 5.25 – XRD analysis results for CaO % and MgO % obtained from bone specimens heated to 1400 °C, grouped by species, showing mean (line within a box), minimum (lower limit of a box) and maximum (upper limit of a box) values. Data presented for elephant and monkey represents one individual from each species. The phase CaO was not detected in monkey and rat bone specimens. Data for individuals for which mineral phase weight percentage was equal to zero are not presented and not included in calculation of mean values 134

Figure A.1 – Diffractograms obtained from chicken bone specimens from five individuals. Lower five: unheated bone specimens, middle five; bone specimens heated to 600 °C, upper five; bone specimens heated to 1400 °C..... 183

Figure A.2 – Diffractograms obtained from unheated cow bone specimens from ten individuals 184

Figure A.3 – Diffractograms obtained from cow bone specimens from ten individuals. All bone specimens heated to 600 °C. 185

Figure A.4 – Diffractograms obtained from cow bone specimens from ten individuals. All bone specimens heated to 1400 °C. 186

Figure A.5 – Diffractograms obtained from deer bone specimens from five individuals. Lower five; unheated bone specimens, middle five; bone specimens heated to 600 °C, upper five; bone specimens heated to 1400 °C..... 187

Figure A.6 – Diffractograms obtained from unheated dog bone specimens from twelve individuals..... 188

Figure A.7 – Diffractograms obtained from dog bone specimens from twelve individuals. All bone specimens heated to 600 °C..... 189

Figure A.8 – Diffractograms obtained from dog bone specimens from twelve individuals. All bone specimens heated to 1400 °C..... 190

Figure A.9 – Diffractograms obtained from unheated goat bone specimens from eight individuals. 191
Figure A.10 – Diffractograms obtained from goat bone specimens from eight individuals. All bone specimens heated to 600 °C. 192
Figure A.11 – Diffractograms obtained from goat bone specimens from eight individuals. All bone specimens heated to 1400 °C. 193
Figure A.12 – Diffractograms obtained from unheated human AUS bone specimens from ten individuals. Group A, of groups A – E (a total of 50 individuals) 194
Figure A.13 – Diffractograms obtained from unheated human AUS bone specimens from ten individuals. Group B, of groups A – E (a total of 50 individuals) 195
Figure A.14 – Diffractograms obtained from unheated human AUS bone specimens from seven individuals. Group C, of groups A – E (a total of 50 individuals). Unheated bone specimen data was not collected for three of the ten individuals within group C. 196
Figure A.15 – Diffractograms obtained from unheated human AUS bone specimens from ten individuals. Group D, of groups A – E (a total of 50 individuals). 197
Figure A.16 – Diffractograms obtained from unheated human AUS bone specimens from ten individuals. Group E, of groups A – E (a total of 50 individuals) 198
Figure A.17 – Diffractograms obtained from human AUS bone specimens from ten individuals. Group A, of groups A – E (a total of 50 individuals). All bone specimens heated to 600 °C. 199
Figure A.18 – Diffractograms obtained from human AUS bone specimens from ten individuals. Group B, of groups A – E (a total of 50 individuals). All bone specimens heated to 600 °C. 200
Figure A.19 – Diffractograms obtained from human AUS bone specimens from ten individuals. Group C, of groups A – E (a total of 50 individuals). All bone specimens heated to 600 °C. ... 201
Figure A.20 – Diffractograms obtained from human AUS bone specimens from ten individuals. Group D, of groups A – E (a total of 50 individuals). All bone specimens heated to 600 °C. ... 202
Figure A.21 – Diffractograms obtained from human AUS bone specimens from ten individuals. Group E, of groups A – E (a total of 50 individuals). All bone specimens heated to 600 °C. 203
Figure A.22 – Diffractograms obtained from human AUS bone specimens from ten individuals. Group A, of groups A – E (a total of 50 individuals). All bone specimens heated to 1400 °C... 204

Figure A.23 – Diffractograms obtained from human AUS bone specimens from ten individuals. Group B, of groups A – E (a total of 50 individuals). All bone specimens heated to 1400 °C...205
Figure A.24 – Diffractograms obtained from human AUS bone specimens from ten individuals. Group C, of groups A – E (a total of 50 individuals). All bone specimens heated to 1400 °C ..206
Figure A.25 – Diffractograms obtained from human AUS bone specimens from ten individuals. Group D, of groups A – E (a total of 50 individuals). All bone specimens heated to 1400 °C ..207
Figure A.26 – Diffractograms obtained from human AUS bone specimens from ten individuals. Group E, of groups A – E (a total of 50 individuals). All bone specimens heated to 1400 °C...208
Figure A.27 – Diffractograms obtained from unheated human UK bone specimens from eight individuals.....209
Figure A.28 – Diffractograms obtained from human UK bone specimens from eight individuals. All bone specimens heated to 600 °C.....210
Figure A.29 – Diffractograms obtained from human UK bone specimens from eight individuals. All bone specimens heated to 1400 °C.....211
Figure A.30 – Diffractograms obtained from elephant and monkey bone specimens, from one individual from each species. Within each set of three diffractograms: lower profile; unheated bone specimen, middle profile; bone specimen heated to 600 °C, upper profile; bone specimen heated to 1400 °C.....212
Figure A.31 – Diffractograms obtained from unheated pig bone specimens from seven individuals and from unheated sheep bone specimens from six individuals.....213
Figure A.32 – Diffractograms obtained from pig bone specimens from seven individuals and from sheep bone specimens from six individuals. All bone specimens heated to 600 °C.....214
Figure A.33 – Diffractograms obtained from pig bone specimens from seven individuals and from sheep bone specimens from six individuals. All bone specimens heated to 1400 °C.....215
Figure A.34 – Diffractograms obtained from rabbit bone specimens from five individuals. Lower five; unheated bone specimens, middle five; bone specimens heated to 600 °C, upper five; bone specimens heated to 1400 °C.....216
Figure A.35 – Diffractograms obtained from rat bone specimens from five individuals. Lower five; bone specimens heated to 600 °C, upper five; bone specimens heated to 1400 °C.....217

Figure A.36 – Stick representations of diffractograms for several mineral phases. The five highest intensity peaks are presented for each phase. Data obtained from International Centre for Diffraction Data, Powder Diffraction Files: HAP (9-432), β-TCP (9-169), α-TCP (29-359), TTCP (25-1137), CaO (37-1497), MgO (45-946) 218
Figure A.37 – Infrared spectrum obtained from a chicken bone specimen (J01) heated to 600 °C 219
Figure A.38 – Infrared spectrum obtained from a cow bone specimen (C02) heated to 600 °C 220
Figure A.39 – Infrared spectrum obtained from a cow bone specimen (C11) heated to 600 °C 221
Figure A.40 – Infrared spectrum obtained from a cow bone specimen (C12) heated to 600 °C 222
Figure A.41 – Infrared spectrum obtained from a cow bone specimen (C13) heated to 600 °C 223
Figure A.42 – Infrared spectrum obtained from a cow bone specimen (C14) heated to 600 °C 224
Figure A.43 – Infrared spectrum obtained from a cow bone specimen (C15) heated to 600 °C 225
Figure A.44 – Infrared spectrum obtained from a deer bone specimen (K01) heated to 600 °C 226
Figure A.45 – Infrared spectrum obtained from a dog bone specimen (D01) heated to 600 °C 227
Figure A.46 – Infrared spectrum obtained from a goat bone specimen (G01) heated to 600 °C 228
Figure A.47 – Infrared spectrum obtained from a human UK bone specimen (H02) heated to 600 °C 229
Figure A.48 – Infrared spectrum obtained from a monkey bone specimen (M01) heated to 600 °C 230
Figure A.49 – Infrared spectrum obtained from a pig bone specimen (P02) heated to 600 °C 231

Figure A.50 – Infrared spectrum obtained from a rabbit bone specimen (L03) heated to 600 °C 232
Figure A.51 – Infrared spectrum obtained from a sheep bone specimen (S02) heated to 600 °C 233

GLOSSARY

SYMBOLS

α	alpha
β	beta
θ	(theta) diffraction angle
λ	(lambda) wavelength of X-radiation
τ	(tau) Kendall's tau correlation co-efficient
>	greater than (relationship between two values)
<	less than (relationship between two values)
±	plus or minus (prefix to an error value)
A	total area of carbonate peak in the region of 858 – 892 cm^{-1}
d	d – spacing
F_s	the full width half maximum contribution of each specimen (F_s) to the measured HAP 002 full width at half maximum
F_o	measured HAP 002 full width half maximum
F_i	the full width half maximum contribution of X-ray diffractometer instrument to measured HAP 002 full width half maximum
(g)	gas
p	p-value
S	scale factor
S_e	scale factor fitting error

W	weight percentage value
W_e	fitting error for weight percentage value (W)
y_a	y-axis value for point ‘a’ (defined in Figure 4.6)
y_b	y-axis value for point ‘b’ (defined in Figure 4.6)
y_c	y-axis value for point ‘c’ (defined in Figure 4.6)

UNITS

Å	Ångström (1 Å = 0.1 nm)
cm	centimetre (1 cm = 1 x 10^{-2} m)
°C	degree Celsius (or degree Centigrade)
g	gram
l	litre
m	metre
mg	milligram (1mg = 1 x 10^{-3} g)
ml	millilitre (1 ml = 1 x 10^{-3} L)
mm	millimetre (1 mm = 1 x 10^{-3} m)
μm	micrometre (1 μm = 1 x 10^{-6} m)
nm	nanometre (1 nm = 1 x 10^{-9} m, 1 nm = 10 Å)
ppm	parts per million
%	percent
cm^{-1}	wavenumber

ABBREVIATIONS

See also specific lists of chemical element, ion and compound abbreviations and mineral phase abbreviations

ANOVA	one-way analysis of variance
AUS	Australian (within this thesis, AUS is used to refer to bone samples and specimens from Australian individuals, obtained from the Melbourne Femur Collection)
Ca/P	calcium phosphorous ratio
CCP Inc.	Clarkson Chromatography Products Incorporated, 213 South Main Street, South Williamsport, Pennsylvania, USA 17702
C-GC	combustion – gas chromatography
CTF	Carbolite tube furnace
DNA	deoxyribonucleic acid
excl.	excluding
FWHM	full width at half maximum of a diffraction peak
GADDS	General Area Detector Diffraction System
ICDD	International Centre for Diffraction Data
ICP-AES	inductively coupled plasma – atomic emission spectrometry
incl.	including
IR	infrared
HAP <00ℓ>	relative coherence length of calcium hydroxylapatite crystallites in the <00 ℓ > direction

HAP ‘a’	lattice parameter ‘a’ for calcium hydroxylapatite
HAP ‘c’	lattice parameter ‘c’ for calcium hydroxylapatite
P-IC	pyrohydrolysis – ion chromatography
PDF	powder diffraction file
MFC	Melbourne Femur Collection (curated by Professor John Clement and held at the Victorian Institute of Forensic Medicine)
Max	maximum value
Min	minimum value
NBS	National Bureau of Standards (now National Institute of Standards and Technology)
No. Det	number of individuals for which a mineral phase was detected within XRD data
Rwp	weighted residual value
SF	phosphate ion splitting factor
Std. Error	standard error of the mean
Stoich.	Stoichiometric value
UK	United Kingdom (within this thesis, UK is used to refer to bone samples and specimens from individuals from the United Kingdom, obtained from the North London Tissue Bank)
XRD	X-ray diffraction

CHEMICAL ELEMENT, ION AND COMPOUND ABBREVIATIONS

Al	aluminium
Al_2O_3	aluminium oxide (or corundum)
Br	bromine
C	carbon
Ca	calcium
Ca^{2+}	calcium ion
Cl	chlorine
CO_3^{2-}	carbonate ion (also referred to as CO_3 within this thesis)
F	fluorine
Fe	iron
H	hydrogen
HNO_3	nitric acid
HPO_4^{2-}	hydrogen phosphate ion (or acid phosphate ion)
K	potassium
KBr	potassium bromide
Mg	magnesium
N	nitrogen
Na	sodium
O^{2-}	oxygen ion
O	oxygen
OH^-	hydroxyl ion
P	phosphorous

PO_4^{3-}	phosphate ion
Si	silicon
Sr	strontium

MINERAL PHASE ABBREVIATIONS

α-TCP	alpha-tri-calcium phosphate (see also TCP) $\alpha Ca_3(PO_4)_2$
β-TCP	beta-tri-calcium phosphate (see also TCP) $\beta Ca_3(PO_4)_2$
b-HAP	bio-apatite (bone mineral: a poorly crystalline non-stoichiometric form of calcium hydroxylapatite – see Equation 2.2)
brushite	hydrated calcium hydrogen phosphate $CaH(PO_4)\cdot 2H_2O$
CaO	calcium oxide CaO
Cl-AP	calcium chloroapatite (section 2.2: when single crystals of chloroapatite are heated in steam at 1200 °C, chloride ions (Cl^-) are replaced by hydroxyl ions (OH^-) to form monoclinic HAP) $Ca_5(PO_4)_3(Cl)$

HAP	calcium hydroxylapatite (or calcium hydroxyapatite) $Ca_5(PO_4)_3(OH)$
monetite	calcium hydrogen phosphate $CaHPO_4$
MgO	magnesium oxide MgO
OAP	calcium oxyapatite (metastable phase believed to form during the thermal decomposition of HAP to β-TCP) $Ca_{10}(PO_4)_6O$
TCP	tri-calcium phosphate (Both α and β polymorphs: α-TCP and β-TCP are referred to within this thesis) $Ca_3(PO_4)_2$
TTCP	tetra-calcium phosphate $Ca_4(PO_4)_2(O)$

CHAPTER 1 – INTRODUCTION

1.1 – THESIS OUTLINE

This thesis presents the results of an investigation into inter-species variation in bone mineral characteristics of unheated bone and bone heated to 600 °C and 1400 °C. The research employed the analytical techniques of X-ray diffraction (XRD) analysis, infrared (IR) spectroscopy, inductively coupled plasma – atomic emission spectrometry (ICP-AES), pyrohydrolysis – ion chromatography (P-IC) and combustion – gas chromatography (C-GC). Each technique is introduced in chapter 3. Bone mineral is introduced in chapter 2 within the context of current knowledge of bone mineral composition and structure characteristics.

The rationale for the investigation into inter-species variation in bone mineral characteristics is discussed in chapter 1 within the context of species identification of skeletal material. The potential for the development of a new method of species identification using X-ray diffraction analysis is proposed.

The research aims and hypotheses are presented in chapter 4 together with details of the materials used and methods employed. Results are presented in chapter 5. These are discussed in chapter 6 within the contexts of: defining general characteristics of unheated and heated bone, the extent of inter-species variation, the explanation of the observed variation from both a biological and

chemical basis and, the implications for the proposed method of species identification using XRD analysis.

The conclusions of the research, a summary of the contribution to knowledge resulting from the work and a number of suggestions for further research are presented in chapter 7.

1.2 – BIOLOGICAL CLASSIFICATION

The diversity of life on Earth is tremendous as many millions of different organisms exist. The study of biological variation between different organisms, over many years, has enabled their classification into groups (taxonomy). An organism can therefore be identified as a member of a particular group based on its biological traits (characteristics).

One level of classification is the assignment of organisms as either vertebrate or invertebrate (at the sub-phylum level). The vertebrate category contains many classes, including the Mammalian, Avian (bird), Reptilian and Amphibian animal classes. Each of these classes is further divided into genus categories and each genus category can contain many different species. Figure 1.1 shows an overview of taxonomic classification categories from the phylum level to species level, using species investigated in this thesis as examples. Names that are commonly used to refer to each species or genus are shown in brackets and for ease of reference, these terms are used throughout this thesis. The rationale for the choice of these species is discussed within chapter 4.

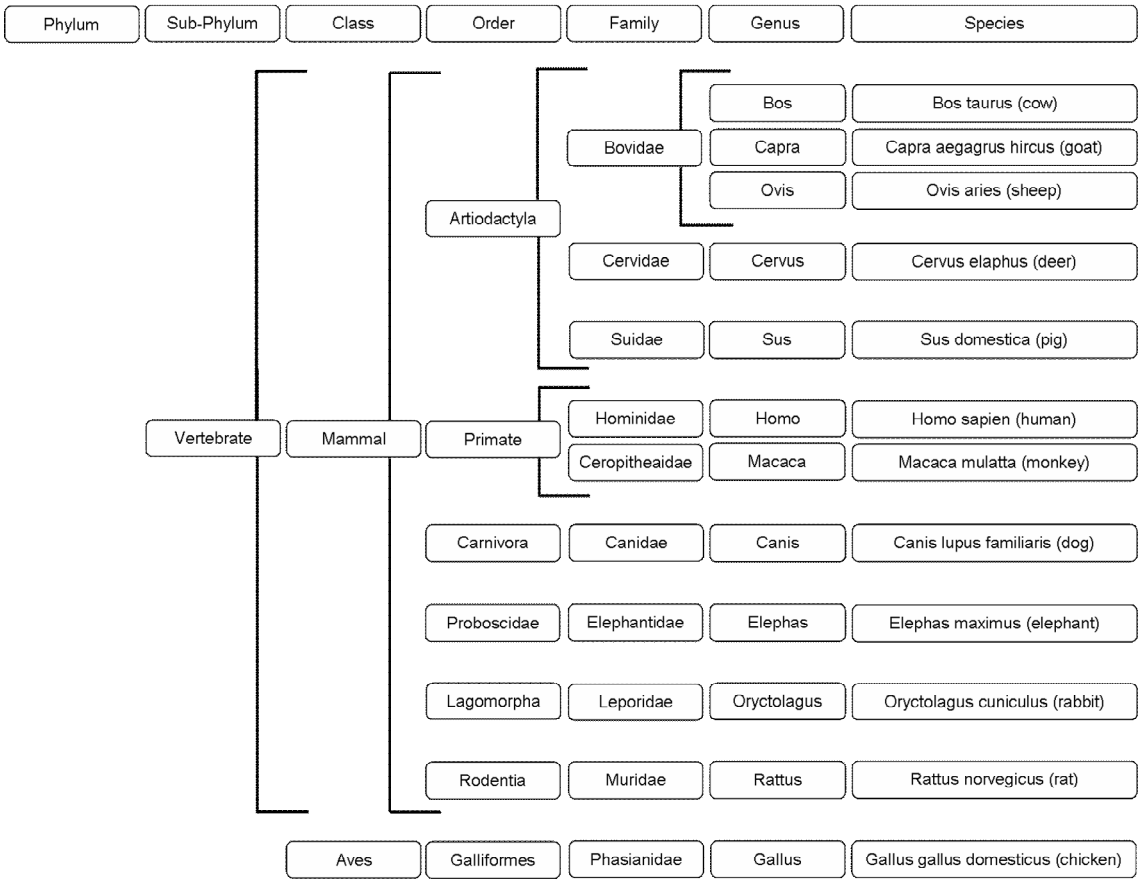

Figure 1.1 – Overview of taxonomic classification categories, from phylum to species levels, using the species investigated within this thesis as examples

Membership of the vertebrate category is generally defined by the possession of a vertebral column (spine), a brain case and an endo-skeleton (internal skeleton). Generally, the internal skeleton is comprised of a hard mineralised tissue (bone) and is a jointed system of a number of skeletal elements (bones) [1]. A diagram of the anterior and posterior aspects of the human internal skeleton is shown in Figure 1.2.

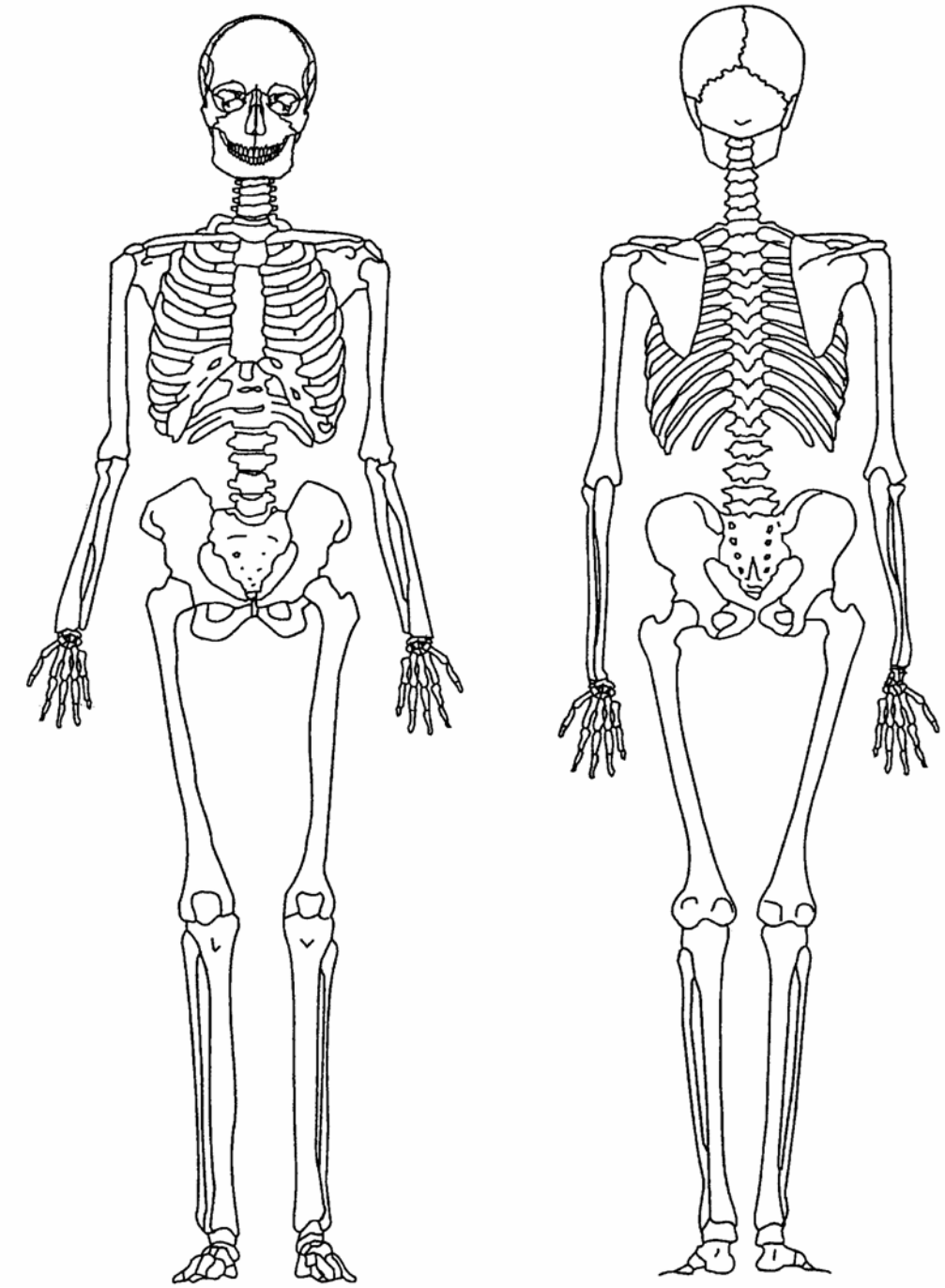

Figure 1.2 – Diagram showing anterior (left of diagram) and posterior (right of diagram) aspects of the human skeleton[2]

Many biological characteristics are used in the taxonomic system of classification of organisms. These include anatomical characteristics of the soft tissues as well as characteristics of the internal skeleton. However, it is not always possible to consider all biological characteristics when classifying an organism. For example, when the remains of an organism are discovered in an archaeological context, often only the internal skeleton is present and so soft tissues cannot be considered. In such cases, it is often still possible to distinguish between different species due to known inter-species variation of skeletal characteristics [3, 4].

1.3 – SPECIES IDENTIFICATION OF SKELETAL MATERIAL

Skeletal characteristics can be grouped into sets of similar characteristics such as; macro-scale morphology (size and shape), micro-scale histology (microscopic structural architecture), immunohistochemistry (specific antibody to antigen binding in bone tissue proteins), and DNA (deoxyribonucleic acid) characteristic groupings. These sets are used in established methods of species identification of skeletal material [5].

Groups of skeletal characteristics are used to unequivocally determine species because, in most cases, it is not possible to distinguish all species from each other based on a single skeletal characteristic. The range of variation in a skeletal characteristic between organisms of the same species (intra-species variation) can be considerable and ranges of intra-species variation can overlap for some species resulting in no significant inter-species difference. For the

same reasons, it may not be possible to distinguish between the internal skeletons of some species based on a single group of skeletal characteristics and it may be necessary to consider several groups of characteristics together [6].

There are numerous practical applications that rely on being able to identify species from skeletal material (see section 1.4). Several general approaches for the identification of species have been developed, each based on a group of characteristics. These are briefly discussed in sections 1.3.2 – 1.3.5. In most cases, these are successful methods. However, each method has limitations that prevent success in some situations.

1.3.1 – BONE ALTERATION

The alteration of bone is a major limiting factor for all methods of species identification. Alteration generally occurs through natural or anthropogenic (human activity) processes once bone is removed from an organism [7-9]. Alteration can also be induced *in vivo*, through anthropogenic processes such as enforced diets or surgical procedures [10, 11]. Examples of some of the many processes that can result in the alteration of bone include; diagenetic processes (change due to burial), specimen preparation and storage processes prior to analysis of bone in research studies and, the heat treatment of bone [8, 12-19]. Alteration results in changes to skeletal characteristics from their biologically controlled state *in vivo* (within a living organism). Severe alteration of bone can even obliterate some skeletal characteristics. Inevitably, the

measurement or observation of skeletal characteristics is mostly carried out on bone that has been altered to some extent.

1.3.2 – DNA ANALYSIS

Species identification using DNA (deoxyribonucleic acid) obtained from bone has a greater ability to successfully identify the species of an organism, compared to other methods. However, DNA characteristics of bone are very susceptible to bone alteration and it is not always possible to obtain DNA [20, 21]. Even if DNA can be obtained, DNA characteristics of bone may not be considered when identifying species from skeletal material, due to the high cost of DNA analysis [22].

1.3.3 – MACRO-SCALE MORPHOLOGY

The consideration of macro-scale morphological characteristics of the internal skeleton is the most common approach used for species identification of skeletal material. Biological variation in morphological characteristics of the internal skeleton and individual bones is related to the considerable variation between species; in the average size of an organism and its locomotion (movement and stance). This method results in a good ability to discriminate between species and has an advantage over other methods, in terms of cost. However, the method is particularly limited for skeletal material that has been altered by fragmentation, weathering, burning or pulverization.

1.3.4 – HISTOLOGY

A method of species identification based on micro-scale histology was initially developed prior to the development of DNA analysis [23-27]. It is now generally only employed when methods based on macro-scale morphology and DNA characteristics have not been successful or when a budget for DNA analysis is not available. It has a poor ability to distinguish species, primarily because variation in histology characteristics of bone is difficult to quantify. In general, it is only possible to classify an organism to a group of many possible species based on histology characteristics [28]. Even so, there is continued research into the development of this method due to the cost implications of DNA analysis [29, 30].

1.3.5 – IMMUNOHISTOCHEMISTRY

Species identification based on immunohistochemistry characteristics of bone is occasionally used when it is not possible to apply any of the techniques previously discussed in this chapter. It is particularly limited when alteration of bone results in poor preservation of species-specific proteins within bone tissue [31]. It is also restricted by the need for a candidate list of possible species and the considerable length of time taken for the analysis [5, 32, 33].

1.4 – PRACTICAL APPLICATION OF SPECIES IDENTIFICATION

The methods of species identification that have been discussed within this chapter are used in a variety of practical applications that require the species identification of skeletal material. Despite their limitations, they are used in the absence of any suitable alternative methods. Examples of such practical applications include the analysis of bone in; forensic investigations, archaeology, custom authority investigations and, in the screening of animal feed. Each of the examples is briefly discussed in sections 1.4.1 through to 1.4.4.

1.4.1 – FORENSIC INVESTIGATIONS

Bone is often recovered during forensic investigations. These may include single murder cases, multiple murder cases and disaster victim identification operations. Bone recovered in these cases is often fragmented and has undergone extensive weathering; in some cases it may have been burnt or pulverised [34-36]. Examples of investigations where bone has been recovered in such conditions include; the collapse of the World Trade Centre towers in 2001, the London Underground bombings in 2005 and the investigation into mass murder, believed to have been carried out by Canadian pig farmer, Robert Picton over a number of years, since approximately 1980.

Identification of species is the primary line of enquiry in the analysis of bone recovered in these cases and further investigation is restricted when species identification cannot be determined [37]. Unfortunately, poor bone condition can prevent conventional methods of species identification from being successfully applied [38].

An example of a homicide forensic investigation within which, bone shards were recovered and species identification was attempted, has been published in the forensic academic literature [39]. A microscopic examination of the shards was conducted in an attempt to determine whether the fragments were human or deer bone. The study concluded that the bone fragments were human and, faced with this information, the suspect in the case confessed to the murder. However, the results of the study were never tested in court [39] and the limitations of bone microscopy as a method of species identification could have made a strong argument for the defence, against the admissibility of the study as evidence. The case occurred prior to recent significant advances in the capability of DNA analysis. However, it is doubtful, if it had been available, whether DNA analysis would have been successful in identifying the bone as deer or human, due to the small amount of bone available for analysis. It could also be debated whether DNA analysis would even have been used due to the high cost of the analysis.

DNA analysis is generally used in forensic cases for the purpose of identification of human individuals. DNA analysis to determine human identity is different to that used to determine species [40]. An ideal approach would be to firstly determine species and whether the bone is human. Further analysis can then be conducted on human bone to establish human personal identity. However, DNA analysis is often carried out to establish human identity without the species first being identified. This is due to the time taken for DNA analysis and the limitations imposed by small bone samples, in addition to high costs. However, a limitation of this approach is that uncertainties arise when the DNA analysis is not successful in producing results. These could be due to the fact that the bone is human but DNA analysis is not possible, or that the bone is non-human. An example of an investigation where this approach was adopted was in the disaster victim identification operation following the collapse of the World Trade Centre towers.

1.4.2 – ARCHAEOLOGY

Bone assemblages are often recovered during archaeological excavations and are an important component of archaeological evidence. The interpretations made from the study of archaeological bone can be of considerable value to the understanding of past human activity and culture [41, 42]. An integral part of these studies is the determination of species from bone fragments. Identification of species is the initial step in any archaeological analysis of bone and all subsequent interpretations rest upon that determination [43]. For example, the identification of bone as sheep or goat bone is important to studies that

investigate the development and expansion of prehistoric pastoral economies, herding strategies and animal production. Sheep and goat species differ in terms of their diet and environmental requirements and are often kept by humans for different economic purposes [44]. However, there are few macro-scale morphology characteristics that exhibit sufficient inter-species variation for sheep and goat bone to be distinguished.

Furthermore, mixtures of human and non-human bone are often recovered from within the same archaeological context (deposit) [45, 46]. Both human and non-human archaeological bone is often fragmented and weathered [47]. Whilst it is possible to identify the majority of bone fragments based on morphological characteristics, this is not always possible [3]. In some cases, it is possible to identify a group of possible species. In the case of sheep and goat, bone is categorised as sheep-goat [48, 49]. In some cases, it is simply only possible to categorise the bone as a fragment from a large or small animal and when this is not possible, bone can only be labelled as ‘unidentified’. Further analysis to identify species is rarely carried out. This decision is generally based on considerations of cost, time and the potential gain in information. However, unidentified fragments can introduce a bias into studies of archaeological bone [50].

1.4.3 – CUSTOM AUTHORITY INVESTIGATIONS

Legislation exists in most countries regarding the export and import of bone material and customs authorities are tasked with ensuring that this legislation is adhered to [51]. In particular, there is concern over the illegal export and import of bone from endangered species [52]. However, bone material encountered by customs authorities is often in the form of carved bone objects or powdered bone, especially in the form of a medicine and therefore mixed with other materials [53]. It is often difficult, or even impossible, to determine the species of origin of such material using methods of species identification that are currently available [54].

1.4.4 – SCREENING OF ANIMAL FEED

The use of animal feed that contains bone material is heavily legislated. Many countries ban the practice of using animal feed that contains bone material from the same species as the animals being fed. Such legislation exists due to concerns about veterinary and human health risks associated with the transmission of diseases such as bovine spongiform encephalopathy (BSE) [55]. Bone material may be present in animal feed due to a variety of reasons. These include; the accidental capture of small animals such as field mice, within the feed at the time of harvest and, the incorporation of bone material from fertilisers that contain bone meal and that are used in growing animal feed crop.

Many countries have well-established animal feed screening protocols in place. In general, current protocols use microscopy to initially determine whether bone fragments are present and, when possible, DNA analysis or immunohistochemistry techniques are used to analyse recovered bone fragments [56]. However, the usefulness of current protocols is often severely limited due to the bone material within animal feed being present in low contamination levels, being of small fragment size and having previously undergone heat treatment as part of feed processing. There have also been published calls for the development of reliable methods of identifying material of ruminant species such as cow, deer, goat and sheep from other species that are also both cost and time-effective [57].

1.4.5 – DEVELOPMENT OF A NEW METHOD OF SPECIES IDENTIFICATION

The above examples of practical applications that rely on species identification of skeletal material demonstrate the need for new methods that overcome the limitations of those currently available. A method of species identification based on the measurement of variation in bone mineral characteristics, using X-ray diffraction (XRD) analysis has the potential of successfully addressing this need. X-ray diffraction analysis is increasingly being used in the analysis of skeletal material within the contexts of these practical applications [35]. The bone mineral component of bone has a general structure and composition that is able to accommodate considerable variation. Also, it is possible to carry out a cost-effective and high-throughput, reliable and highly sensitive analysis of small quantities of bone material, using X-ray diffraction analysis.

In order to determine whether the X-ray diffraction analysis of bone mineral can be developed as a new method of species identification, the nature and extent of inter-species variation in bone mineral characteristics must first be investigated. Such investigations must also utilise other analytical techniques to obtain additional information about the structure and composition of bone mineral which is of valuable assistance in obtaining a more comprehensive understanding of inter-species variation in bone mineral. The analytical techniques employed for this research are introduced and discussed within chapter 3. Prior to this, the structure and composition of bone mineral is introduced in chapter 2, along with a discussion of bone mineral variation.

CHAPTER 2 – BONE MINERAL AND ITS VARIATION

2.1 – BONE

The internal skeleton of an organism fulfils a number of different functional roles. These include mechanical functions of support and protection of the soft tissues of an organism and facilitation of movement [58]. In addition, the internal skeleton fulfils a synthesis role in the production of blood cells. It acts as a reservoir for ions that are essential to metabolic processes and a storage reservoir for fatty acids [59]. It also provides protection against excessive changes to blood pH levels and a mechanism for the removal of toxins, such as heavy metals, from blood [60].

The complexity of both the structure and composition of the internal skeleton is a reflection of the many different functions it fulfils. The internal skeleton is a dynamic collective tissue system that includes marrow, cartilage and blood vessels and, a hard mineralised tissue (bone). Bone itself is also a dynamic and complex composite material with a highly organised hierarchical structure [59] (see Figure 2.1). On the nano-scale bone consists of bone mineral crystals that are located within an organic component matrix of collagen fibrils, non-collagenous proteins and water [59]. The bone mineral component of bone is the focus of subsequent sections of this chapter.

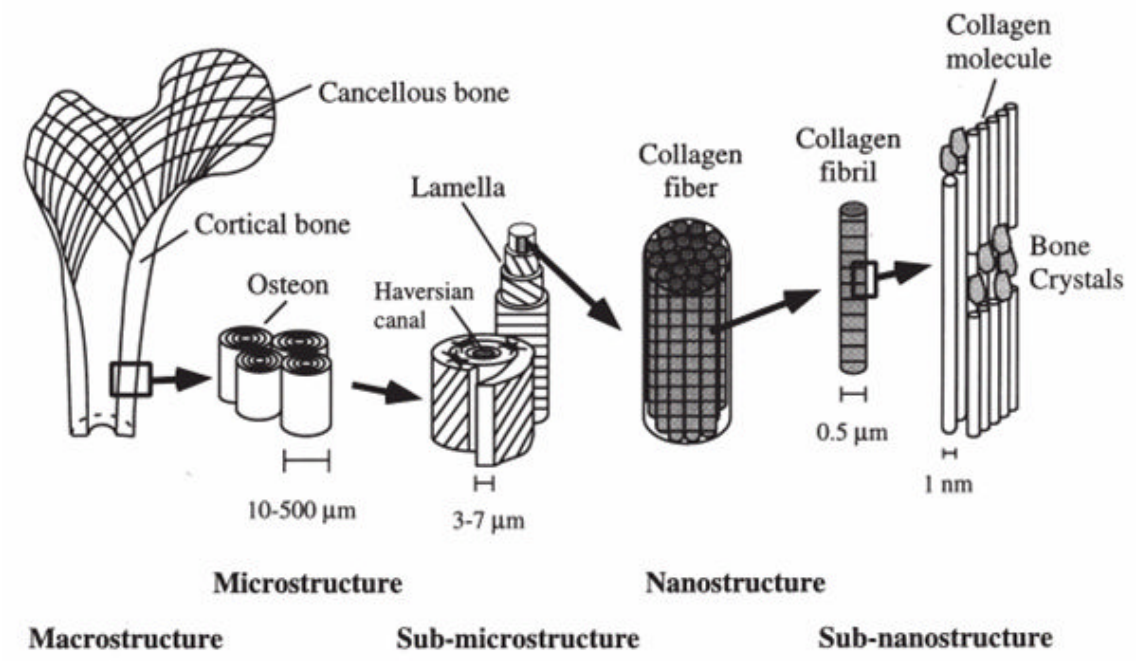

Figure 2.1 – Structural features of bone [61]

2.2 – CALCIUM HYDROXYLAPATITE

Calcium hydroxylapatite (HAP) is a structural prototype for bone mineral [62-65]. It has also been identified as the prototype for the mineral component of teeth [59, 62, 66, 67] and as one of the components of most pathological calcifications (biological stones) such as urinary calculi (kidney, bladder or urether stones) [68]. It also exists as a natural geological mineral and can be produced synthetically [62, 69-71].

Calcium hydroxylapatite (or calcium hydroxyapatite) consists of calcium ions (Ca^{2+}), phosphate ions (PO_4^{3-}) and hydroxyl ions (^{-}OH) [62]. It has the general empirical formula shown in Equation 2.1. It is a crystalline material and its structure consists of unit cells, each containing two general formula units of ions that are in specific positions, relative to one-another [62] (see Figure 2.2). A repetitive array (crystal lattice) of the unit cells form crystals of calcium hydroxylapatite [64].

$$Ca_5(PO_4)_3(OH)$$

Equation 2.1 – General chemical formula of calcium hydroxylapatite

The crystal lattice of calcium hydroxylapatite is dominated by the phosphate ions which are stacked in a closely packed arrangement [62]. There are interstices (holes) between the phosphate ions and the positions of some of these interstices create channels through the structure [62, 72] (see Figure 2.2). The hydroxyl ions and some of the calcium ions are located within the channel interstices [62, 72]. Four calcium ions in each unit cell which are referred to as Ca^{2+} (I) ions are positioned within channel interstices. The remaining six calcium ions in each unit cell are referred to as Ca^{2+} (II) ions [73]. These include two complete ions plus eight ions on the faces of a unit cell that each count as half an ion to the unit cell. They are spatially arranged in sets of triangles, with respect to each other in the crystal lattice [73]. They are located within interstices that are not within the channels but form part of the hydroxyl ion channel walls [72, 73].

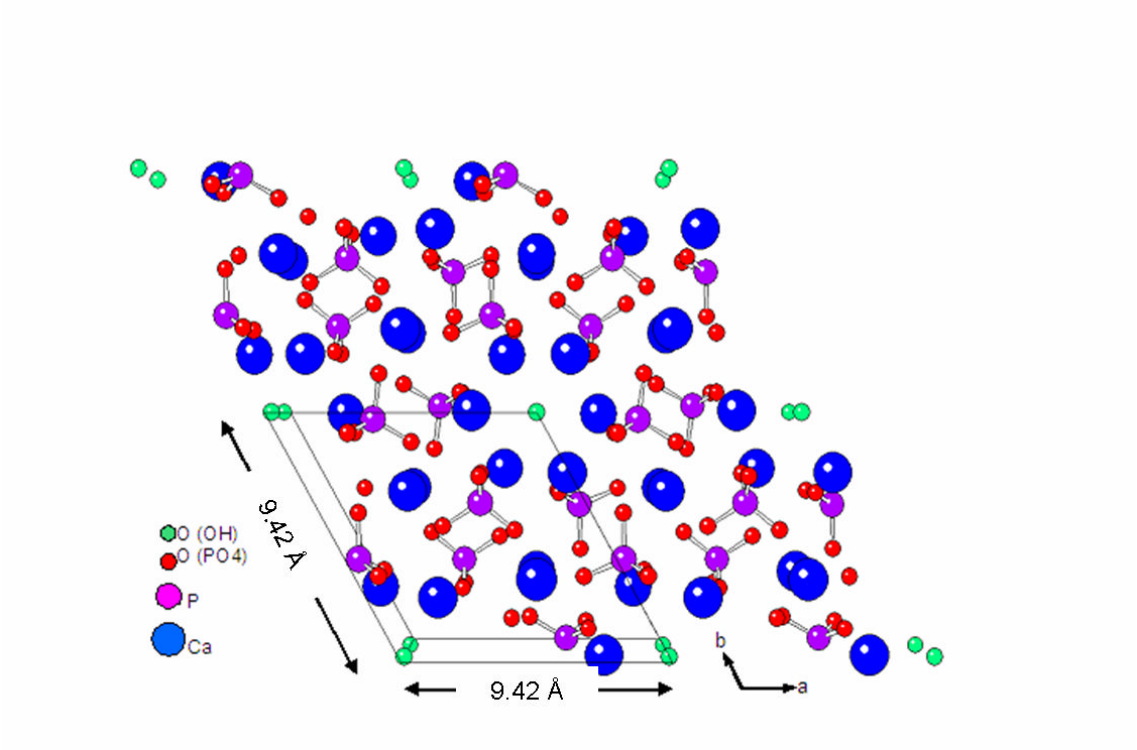

Figure 2.2 – Crystal lattice structure of stoichiometric calcium hydroxylapatite (HAP) with hydrogen atoms omitted and atomic radii reduced for clarity. The diagram shows the crystal lattice viewed down the 'c' axis and shows two unit cells along each axis: a, b and, c (diagram created using Crystallographica software, version 1.53)

The structure of calcium hydroxylapatite can be described in terms of its symmetry and in general, this is hexagonal, with the space group; $P6_3/m$ [62]. It has characteristic unit cell dimensions (lattice parameters) and these are: a = b = 9.42 Å and c = 6.88 Å [62] (see glossary). It also has characteristic atomic and weight ratios of calcium to phosphorous, which are 1.67 (10 atoms per unit cell/6 atoms per unit cell) and 2.16 (39.9 $gmol^{-1}$/18.5 $gmol^{-1}$) respectively [74].

Calcium hydroxylapatite can also adopt a monoclinic structure with a space group of $P2_1/b$ [75]. It has this symmetry due to the ordering of hydroxyl ions within and between channels [75]. HAP with a monoclinic structure has hydroxyl ions that are orientated in the same direction within an ion channel [75]. Rows of channels adopt the same orientation and the orientation alternates between adjacent rows [75]. The unit cell of monoclinic hydroxylapatite is larger than that of hexagonal hydroxylapatite. It contains four of the general formula units and the lattice parameter value for 'b' is double that of 'a' [75]. However, the monoclinic structure is only observed under exceptional conditions such as the heating of calcium chloroapatite (Cl-AP) single crystals in steam at 1200 °C [75] (see glossary).

The above descriptions of the hexagonal and monoclinic structures of calcium hydroxylapatite have assumed stoichiometric compositions and structures. They each relate to a crystal lattice that is free of defects and they can be considered as ideal prototypes. However, crystalline materials can possess defects [76]. These generally exist in the form of ion site vacancies, ion substitutions and interstitial ions. Defects cause structural disorder and lattice strain within crystals [71]. In calcium hydroxylapatite, this includes disorder in the hydroxyl ion channels [76]. Therefore, calcium hydroxylapatite generally adopts the hexagonal structure due to the presence of crystal defects [73, 75]. Furthermore, the prototype hexagonal structure is not strictly stoichiometric because its symmetry allows hydroxyl ion disorder.

Calcium hydroxylapatite has a very stable structure due to the close packed arrangement of the phosphate ions [77]. The HAP crystal lattice is able to tolerate many defects. These can include the substitution of many different ions within the lattice and the adsorption of a range of different ions onto crystal surfaces. Therefore, calcium hydroxylapatite materials, including bone mineral, have complex heterogeneous compositions and structures, with many deviations from stoichiometry [74].

Current knowledge and understanding of the composition and structure of bone mineral has been achieved through the study of other biological, geological and synthetic hydroxylapatites, in addition to direct studies of bone mineral [65, 74, 78-88]. However, the focus of the subsequent discussion is the structure and composition of natural bone mineral in particular.

2.3 – BONE MINERAL (BIO-APATITE)

The calcium hydroxylapatite of bone mineral is widely referred to as bio-apatite (b-HAP) [59, 89]. The use of this term acknowledges that calcium hydroxylapatite is a prototype for bone mineral and also that bone mineral is distinct from stoichiometric calcium hydroxylapatite and from other natural and synthetic calcium hydroxylapatites [59, 79, 88].

A general and simple description of bio-apatite is: a poorly crystalline, nano-crystalline calcium hydroxylapatite that is deficient in calcium and hydroxyl ions, contains carbonate, sodium, magnesium, potassium, fluoride and chloride ions and a variety of other ions in various quantities both within the crystal lattice and on crystal surfaces and which, has a complex and intimate relationship with the organic component of bone [79, 90-92].

$$\left[\left(Ca^{2+}\right)_{10-a-b}\left(Sub^{Ca^{2+}}\right)_a\left(V^{Ca^{2+}}\right)_b\right]\left[\left(PO_4{}^{3-}\right)_{6-c-d}\left(Sub^{PO_4{}^{3-}}\right)_c\left(V^{PO_4{}^{3-}}\right)_d\right]\left[\left(OH^-\right)_{2-e-f}\left(Sub^{OH^-}\right)_e\left(V^{OH^-}\right)_f\right]$$

$Sub^{Ca^{2+}}$ = calcium ion substitution (for example Mg^{2+}, Na^+, K^+, Sr^{2+})

$V^{Ca^{2+}}$ = calcium ion vacancy

$Sub^{PO_4{}^{3-}}$ = phosphate ion substitution (for example $CO_3{}^{2-}$, $HPO_4{}^{2-}$)

$V^{PO_4{}^{3-}}$ = phosphate ion vacancy

Sub^{OH^-} = hydroxyl ion substitution (for example $CO_3{}^{2-}$, F^-, Cl^-)

V^{OH^-} = hydroxyl ion vacancy

$$10 > a > 0 \quad 10 > b > 0 \quad 10 > (a + b)$$

$$6 > c > 0 \quad 6 > d > 0 \quad 6 > (c + d)$$

$$2 > e > 0 \quad 2 > f > 0 \quad 2 > (e + f)$$

Equation 2.2 – Proposed general chemical formula for bone mineral (bio-apatite)

A general chemical formula for bio-apatite is proposed in Equation 2.2. The formula is based on that of stoichiometric calcium hydroxylapatite but considers both lattice substitutions and vacancy defects for calcium, phosphate and hydroxyl ions. Examples of some of the substituting ions are presented below the formula. Individual ions are deliberately not specified within the formula due to uncertainties regarding the quantity of each type of substituting ion. Many different formulae for bio-apatite have been proposed within the literature as a result of previous research into bone mineral chemistry [93]. Generally, these are variations of Equation 2.2 that specify quantities for selections of substituting ions. However, they are inevitably not comprehensive in terms of all ion substitutions present within bio-apatite and represent best approximations. Furthermore, the general formula presented in Equation 2.2 and those presented within the literature do not include adsorbed surface ions.

Despite the complex nature of bone mineral and the challenges of its characterization [62], it is perhaps the most studied natural mineral and as a result of this numerous characteristics of bone mineral have been investigated over many years [62, 94, 95]. These include; the amount of bone mineral in bone and groups of characteristics such as, chemical composition and crystal structure characteristics.

2.4 – BONE MINERAL VARIATION

It is clearly evident from the published results of previous studies that variation exists in bone mineral characteristics between different studies and also within individual studies [96-101]. For example, there is considerable variation in the values reported for the amount of bone mineral, as a percentage of the total mass of organic and inorganic components and in the amount of carbonate in bone mineral, as a percentage of the total mass of the inorganic component [102]. Due to the variation encountered, ranges of values are often quoted when summaries of bone mineral characteristics are presented and referred to within the published literature [69, 94, 103, 104].

2.4.1 – BIOLOGICAL VARIATION

The variation observed in the results of investigations into bone mineral characteristics has often stimulated the proposal and discussion of causal explanations [63, 93, 96]. It is generally accepted that a significant proportion of the variation has arisen as a result of dynamic adaptation in response to changes in biological and environmental functional requirements of bone [58, 105-108]. This adaptation occurs throughout the lifetime of an organism [59, 109-111] and it is likely that sustained adaptation has occurred, through evolution, over many generations. This explanation is supported by evidence of trends within observed variation, due to factors such as age, diet, disease, habitat and habitual activity, for organisms within the same species group [59, 109, 112-128]. Furthermore, studies have shown that there is inter-species

variation for a number of bone mineral characteristics [89, 102, 107, 126, 129-131].

2.4.2 – EXTENT OF BIOLOGICAL VARIATION

Although there is a general acknowledgement of biological variation in bone mineral characteristics within the field of bone mineral research, the nature and extent of this variation is poorly understood for the vast majority of bone mineral characteristics [102]. This situation is due to the fact that bone is a biological composite material that has a complex, and ironically, a highly variable composition and structure. The challenges of the characterisation of bone mineral have resulted in the primary focus of much previous research being the development of a general model for the structure and composition of bio-apatite [62, 81]. This has been achieved through the determination of the general characteristics of bone mineral. Knowledge of the general characteristics is essential to the determination of the boundaries of biological variation of bone mineral characteristics. However, numerous analytical techniques and an even greater number of experimental methods have been employed for investigations of general characteristics, over many years. Inevitably, this has lead to the introduction of variation in presented results for bone mineral characteristics that is not due to biological variation, but is due to experimental factors. In addition, there is variation in the physical meaning of values of characteristics that are reported within the literature as representing the same characteristic. For example the weight percentage of bone mineral in bone is reported in many studies but there is considerable variation in the measurement of this

characteristic. Furthermore, over time there have been changes to general consensus regarding proposed models for bone mineral, such as the dismissal of the proposal that a separate calcium carbonate phase is an additional mineral component of bone [82, 132, 133]. These factors hinder attempts to establish the extent of biological variation from a review of the published literature.

With a general model for bone mineral composition and structure now well established and advances in analytical techniques providing improved capabilities for the measurement of bone mineral characteristics, the lack of understanding of the nature and extent of biological variation in bone mineral characteristics should be addressed. This thesis has done so for a number of characteristics of bone mineral, each of which are introduced in chapter 4. The techniques employed in the measurement of these characteristics are introduced in chapter 3. Characteristics of unheated bone and bone heated to 600 °C and 1400 °C were measured. Therefore, the general response of bone to heat treatment and the rationale for investigating heated bone mineral characteristics are discussed in section 2.5 and also, in section 3.1 with respect to X-ray diffraction analysis. The rationale for using the temperatures of 600 °C and 1400 °C is presented in chapter 4.

2.5 – HEAT TREAMENT OF BONE

2.5.1 – GENERAL RESPONSE OF BONE TO HEAT TREATMENT

Bone is physically and chemically altered when it is subjected to heat treatment [38, 134-137]. On heating, the organic component undergoes combustion and is released from bone as gaseous products such as water vapour ($H_2O_{(g)}$) and carbon dioxide ($CO_{2(g)}$) [103]. The combustion of the organic component results in the shrinkage of bone and a loss of mass [103]. Bone tissue often cracks and fractures during heating or upon cooling [138, 139]. The loss of the organic component also causes heated bone to be more brittle compared to unheated bone [140].

Heat treatment of bone above approximately 500 °C results in the recrystallisation of the bio-apatite mineral phase with increases in crystal size and perfection (crystallinity) [134, 141-148]. An increase in material hardness of heated bone when compared to unheated bone has been attributed to an increase in crystal size on heating bone above approximately 500 °C [149]. Also, the bio-apatite crystal tends towards an equidimensional hexagonal crystal habit [103, 141, 145]. Gases such as water vapour and carbon dioxide are released from the bone mineral lattice and crystal surfaces [104, 150, 151]. However, ions may also be incorporated into the lattice from crystal surfaces. Furthermore, the process of combustion of the organic component alters the local atmospheric environment of the bone mineral and provides another potential source of ions that are available for incorporation into the lattice and

for adsorption on to crystal surfaces. The extent to which any incorporation and adsorption occurs has not as yet been clearly established [152].

When bone is heated to high temperatures (above approximately 800 °C), decomposition of the bio-apatite phase occurs and additional mineral phases are formed as decomposition products [100, 153]. The number of decomposition products detected increases with increasing temperature [143, 154]. Both the combustion of the organic component and changes that occur in the bone mineral cause heated bone to differ in colour compared to unheated bone [155] and for bone to lose macro and micro-architectural structure on heating. Bone melts when heated to temperatures around the melting point of calcium hydroxylapatite (approximately 1600 °C) and calcium hydroxylapatite is no longer detected as the main mineral phase [138].

2.5.2 – VARIATION IN THE RESPONSE OF BONE TO HEAT TREATMENT

The specific response of bone to heat treatment is dependent on the composition, structure and condition of the unheated bone and on heat treatment conditions such as heat time and heating environment [156]. Variation in any of the above factors results in variations in the characteristics of heated bone. The separation of biological variation from experimental factor variation for previously published studies is challenging due to the wide range of heat treatment conditions adopted by different studies. Despite this, the general response of bone to heat treatment described above has been established within the literature and provides a basis from which to measure biological

variation in heated bone characteristics using controlled heat treatment conditions. Furthermore, the study of bone mineral characteristics of heated bone can assist in the explanation of variation observed in unheated bone [103]. Also, the number of characteristics from which to develop a method of species identification is increased by the inclusion of heated bone characteristics and this has the potential to increase the power of any resultant method that is developed. The thermal decomposition of calcium hydroxylapatite is discussed in greater detail in section 2.5.3 in terms of the specific decomposition products formed on heating.

2.5.3 – THERMAL DECOMPOSITION OF CALCIUM HYDROXYLAPATITE

The thermal decomposition of calcium hydroxylapatite (HAP) is widely reported to occur at approximately 800 - 1000 °C [157] and it is generally believed that decomposition occurs through an initial step of dehydroxylation of the HAP lattice [64, 158]. The loss of hydroxyl ions from the lattice through the release of water vapour ($H_2O_{(g)}$) results in the formation of calcium oxyapatite (OAP) which is a transitory, metastable phase in the decomposition process [64, 159] (see Equation 2.3). This proposal for the decomposition pathway is supported by experimental evidence within the literature for; the evolution of H_2O gas from synthetic calcium hydroxylapatites, the suppression of the thermal decomposition of HAP in an atmosphere of high water vapour pressure and the lack of detection of mineral phases that contain hydrogen, such as brushite and monetite (see glossary), in bone heated to high temperatures .

$$Ca_{10}(PO_4)_6(OH)_2 \xrightarrow{dehydroxylation} Ca_{10}(PO_4)_6O + H_2O_{(g)}$$

Equation 2.3 – Proposed formation of calcium oxyapatite and water vapour from calcium hydroxylapatite on heating to approximately 800 - 1000 °C

The mineral phase, beta-tri-calcium phosphate (β-TCP) is widely accepted as a thermal decomposition product of HAP [69] and its detection in heated bone is frequently reported [79, 150]. Tetra-calcium phosphate (TTCP) and calcium oxide (CaO) are also acknowledged as decomposition products of HAP, although their detection is less frequently reported [150, 160, 161]. The mineral products that are believed to result from the decomposition of HAP, through an OAP pathway, are therefore; β-TCP, TTCP and CaO [64, 143, 151, 161] (see Equation 2.4 and Equation 2.5 and glossary).

$$Ca_{10}(PO_4)_6(O) \rightarrow 2\beta Ca_3(PO_4)_2 + Ca_4(PO_4)_2O$$

Equation 2.4 – Proposed formation of β-TCP and TTCP from calcium oxyapatite on heating calcium hydroxylapatite to temperatures above approximately 800 °C

$$Ca_{10}(PO_4)_6(O) \rightarrow 3\beta Ca_3(PO_4)_2 + CaO$$

Equation 2.5 – Formation of β-TCP and CaO from calcium oxyapatite on heating calcium hydroxylapatite to temperatures above approximately 800 °C

In addition to the decomposition of HAP, it is generally accepted that changes and interactions of the HAP decomposition products occur on heating. The mineral phase; β-TCP has been shown to undergo a polymorph transformation into alpha-tri-calcium phosphate (α-TCP) (see glossary) on heating to a temperature of approximately 1300 °C [162]. This transformation has been

shown to be reversible on further heating to higher temperatures and under conditions of slow cooling [162]. The formation of TCP and CaO from TTCP is also a plausible decomposition reaction (see Equation 2.6).

$$Ca_4(PO_4)_2O \rightarrow Ca_3(PO_4)_2 + CaO$$

Equation 2.6 – Proposed formation of TCP and CaO from TTCP on heating calcium hydroxylapatite to temperatures above approximately 800 °C

Equation 2.3 through to Equation 2.6 each assume a stoichiometric HAP starting material. Under this assumption, the weight percentage values obtained for each decomposition product are dependent on the thermal stability of each mineral phase and the heating conditions employed [160, 163]. Variation in heating conditions is likely to account for the majority of variation between different reports of the thermal decomposition products of bone within the literature [160, 161].

However, previous work has shown that variation in the thermal decomposition of non-stoichiometric calcium hydroxylapatites can also occur when temperature and heating atmosphere conditions are controlled [160]. It has been demonstrated that the temperature at which HAP decomposition commences and the amount of each decomposition product formed are dependent on the structure and composition of the HAP phase [154, 160]. For example, magnesium associated with calcium hydroxylapatite results in the favouring of the formation of β-TCP, stabilising the phase and delaying its transformation into α-TCP [154]. Evidence presented within the literature

suggests that the magnesium ions responsible for this effect are originally located as calcium substituting ions within the HAP lattice or on the HAP crystal surfaces and that they stabilise the β-TCP phase by becoming calcium substituting ions within the β-TCP lattice on its formation [154].

In this study, variation due to heating conditions was mitigated against by the employment of a standardised heat treatment regime (see chapter 4). Therefore, it was possible to attribute any variation in terms of the decomposition products obtained on heating to differences in the starting material.

CHAPTER 3 – ANALYTICAL TECHNIQUES

A large number of analytical techniques and research approaches have been employed, over many years, in attempts to measure just some of the many characteristics of bone and bone mineral [13, 62, 81, 108, 134, 161, 164-195]. This is due to; the challenges of the analytical characterization of bone composition, structure and material properties, the debates that have ensued as a result and, the extensive study of bone across a wide range of research fields, each of which were discussed in chapter 2. The use of a wide range of techniques complicates the cross-study comparison of results published within the literature. However, the development of analytical techniques, over time, has helped to clarify and resolve many of the debates surrounding the composition and structure of bone [66, 196].

The techniques used in this research are introduced and discussed within this chapter through brief explanations of general principles. Detailed explanations of the theory underpinning each technique can be found elsewhere [159, 197-200]. The experimental methods and protocols adopted for each technique are detailed in chapter 4.

3.1 – X-RAY DIFFRACTION ANALYSIS

X-ray diffraction (XRD) analysis was the principal analytical technique employed in this research. The development of XRD analysis has played a key, revolutionary role in the study of bone mineral and the understanding of its structure [81, 101, 201-207]. XRD analysis is responsible for resolving much of the debate surrounding the general identity of bone mineral and the development of the calcium hydroxylapatite (bio-apatite) model [81, 142, 184, 208-214].

X-ray diffraction analysis is a technique that can be used to interrogate the structure and composition of a material, on the atomic-scale. It is, in general, used to investigate the structure of crystalline materials. Such structures were described in chapter 2 as regular arrays (crystal lattice) of unit cells, each containing the ions of the general compositional formula of the material, each in specific positions, relative to one-another. Crystalline materials are, in general, inorganic mineral materials, such as the bone mineral prototype calcium hydroxylapatite. X-ray diffraction is therefore well-suited to the analysis of bone mineral.

Diffraction is a phenomenon that occurs when X-ray waves are coherently scattered (elastic scattering) by interaction with a periodic array of electron density (surrounding the nuclei of atoms or ions) and, conditions that result in constructive and destructive interference of scattered waves at specific scattering angles are met by both the waves and the array of electron density.

X-ray waves are sinusoidal waves that can be described by their direction of propagation, their maximum displacement from the line of propagation (amplitude) and the distance between two wave crests (wavelength). Two waves that have the same direction of propagation, the same wavelength and same amplitude but are displaced with respect to each other have a path difference or phase difference. The combination of waves with phase differences results in a combined wave of the same direction of propagation and the same wavelength but with differing amplitude to each of the component waves. When the phase difference between two waves is equal to an integer multiple of whole wavelengths, constructive interference occurs and the amplitude of the resultant wave is an addition of the amplitudes of the component waves. When the phase difference is equal to an odd integer multiple of half wavelengths, destructive interference occurs and the amplitude of the resultant wave is zero.

If the scattering of X-rays by ions within a crystal is considered as a reflection of the incident X-rays the Bragg analogy can be used as an explanation of X-ray diffraction. X-rays that have the same direction of propagation which is at an angle of incidence of theta (θ) to a parallel set of lattice planes of a crystal are scattered or ‘reflected’ and emerge from the lattice planes at an angle of θ from the lattice planes. Diffraction of the X-rays occurs at specific angles of θ when the spacing between the lattice planes (d – spacing) satisfies the Bragg equation (see Equation 3.1).

$$\lambda = 2d \sin\theta$$

Equation 3.1 – Bragg equation

Crystals of different compositions and lattice structures differ in terms of their inter-planar spacing (d – spacing) and so differ in specific diffraction angles on interaction with X-rays. Therefore, the measurement of X-ray diffraction enables the study of the composition and structure of crystalline materials.

The practicalities of measuring diffraction from crystals can be cumbersome as, a crystal must first be rotated to bring a lattice plane into a reflecting position and then a detector must be moved to an appropriate position. These difficulties are overcome by the use of powdered specimens in XRD analysis.

The powdering of crystalline materials generally produces specimens that consist of many crystallites that are randomly orientated. Therefore, whatever the orientation of the specimen, there are always a proportion of the crystallites within the specimen which have lattice plane orientations that will result in diffraction and it is therefore not necessary to rotate the specimen.

Powder XRD analysis is carried out using an X-ray powder diffractometer; the main components of which are an X-ray tube, a specimen stage and an X-ray detector. A beam of X-rays is generated by the X-ray tube and targeted at a flat powder specimen. In general, the specimen is rotated so that the angle of θ is incremented in set steps, with regular step sizes (typically 0.02 °/2θ) and count

times at each step (typically 5 seconds), as the detector scans an angular range of 2θ. The detector counts and records the intensity of X-rays at each step and a diffractogram is produced from the collected data as an output from the analysis. The 2θ increments of the detector enable the collection of diffraction data and the specimen is rotated in order to maintain Bragg-Brentano geometry. Generally, powder diffraction data is presented as a diffractogram (see appendix) with intensity plotted as a function of detector angle, 2θ (or d – spacing).

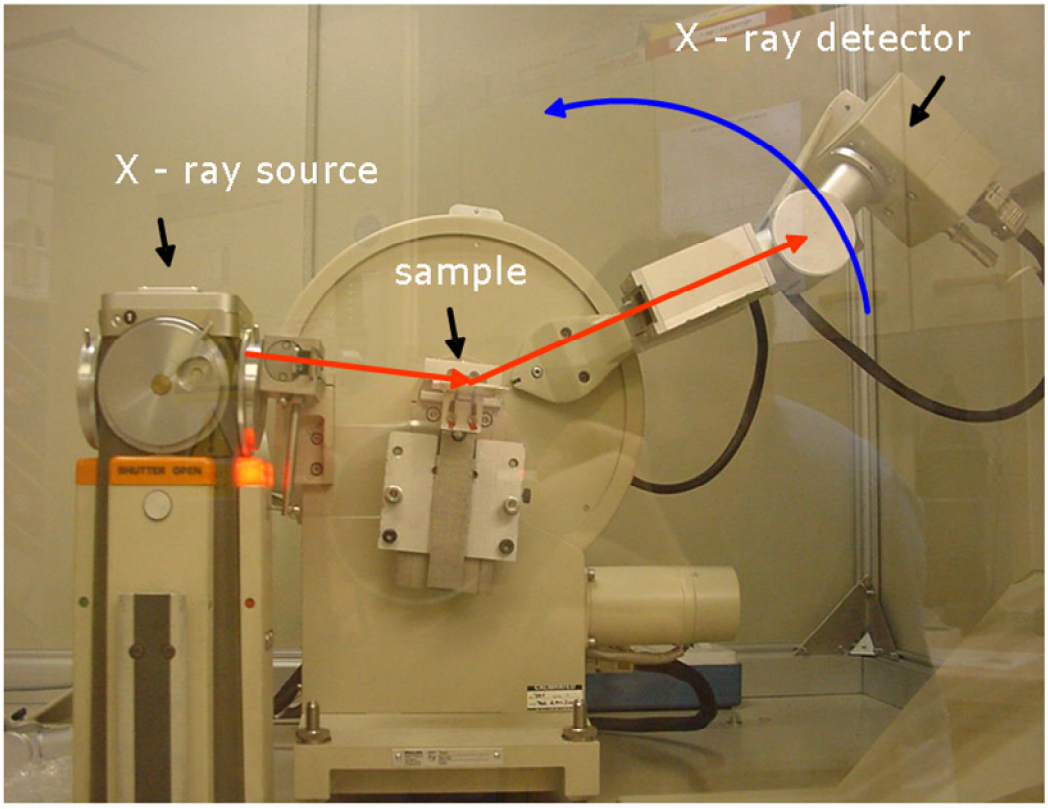

Figure 3.1 – Photograph of X-ray diffractometer employed for this research

The characteristic information that can be obtained from X-ray diffraction analysis includes the identity of the mineral phase(s) present within a specimen, the relative ‘coherence length’ (a combined measure of crystallite size and strain) along a specific crystallographic direction for crystallites of each mineral phase and the lattice parameters (unit cell dimensions) of each mineral phase.

In the analysis of bone, X-ray diffraction suffers, as do many other techniques, from difficulties due to the composite organic and inorganic composition of bone [64, 141]. In the first instance, it is difficult to powder bone. Secondly, the scattering of X-rays from the poorly ordered atoms of the organic portion of bone results in high background intensities within collected XRD data. Also, the amount of mineral being interrogated in a given specimen volume is less for bone than for specimens which are only comprised of a mineral component, resulting in lower intensity diffraction peaks.

In addition, bone mineral is a highly strained nano-material, with small crystals that contain many defects (see chapter 2). Therefore, the diffraction peaks that are obtained from bone specimens are broad, causing peaks to overlap with each other (see appendix). This leads to difficulties in the measurement of coherence lengths and increases the errors associated with the obtained values for coherence length and lattice parameters (see section 4.4.3).

Many previous researchers have heated bone specimens, prior to XRD analysis, in attempts to combat the above limitations. The response of bone to heat treatment was discussed in chapter 2 and changes to the characteristics of bone on heating make it, in some respects, a more suitable candidate for XRD analysis compared to unheated bone. Heated bone is much more easily powdered. The removal of the organic component through combustion results in a specimen that has a higher mineral concentration and that produces a lower background intensity of scattered X-rays (see appendix). This can also be achieved through the chemical removal of the organic component. However, methods of chemical removal are cumbersome and time consuming and can result in the alteration of the chemical composition and structure of bone mineral whilst in solution.

The heating of bone also alters the mineral component from its state in unheated bone (see section 2.5.1). However, changes to bone mineral on heating, far from being a limitation of this study, were exploited as an advantage. The response of bone mineral to heat treatment is dependent on both the composition and structure of the starting material (bone) and the heat treatment conditions (see section 2.5). A standardized, controlled heating regime was used for all heated bone specimens (see chapter 4). Therefore the XRD results obtained from this study have enabled the investigation of variation in the response of bone to heat treatment due to differences in the starting material. The rationale for the use of temperatures of 600 °C and 1400 °C in this research is presented in chapter 4.

There are several approaches that can be adopted within X-ray diffraction analysis, once XRD data has been collected. This is dependent on the level and amount of information required from the analysis. In general, the first approach is to identify the mineral phase(s) represented within the data based on the position and relative intensity of the diffraction peaks. A reference database of d – spacing values with corresponding relative intensities for known mineral phases is generally employed to assist in phase identification. Typically, this is the International Centre for Diffraction Data, Powder Diffraction File. This is a qualitative approach but one which should be done as a preliminary step of any more detailed analyses. It was used within this study prior to undertaking further quantitative analysis of the XRD data.

The quantitative analysis of XRD data to accurately determine the composition of a specimen in terms of the weight percentages of its component mineral phases is a further step in XRD analysis, once the mineral phases represented by the XRD data have been identified. This analysis has greatly benefited from the development of the Rietveld full profile fitting method [215]. This is increasingly being used in the XRD analysis of bone and also geological and synthetic calcium hydroxylapatites [89, 216-223] and it is the quantitative approach that has been employed within this study.

The Rietveld method involves the analysis of the entire diffraction pattern, including the background, rather than analysis based on individual peaks or small subsets of peaks. The parameters used to calculate a simulated

diffraction pattern are refined to fit the experimentally observed diffraction pattern. The calculated pattern is initially generated from data such as the space group symmetry, atomic positions, site occupancies and lattice parameters for each phase that is incorporated into the refinement. Additional information such as parameters that define the profile shape, the background function and, the scale factor for each phase are also used in the refinement. The refinement process involves the minimizing of the sum of the weighted, squared differences between the observed and the simulated intensities at every collected data step. In addition to the quantitative determination of weight percentages for the refined mineral phases, the lattice parameters for each phase can also be obtained [218, 219, 224-226].

For this research, X-ray diffraction analysis was used to identify and quantify each mineral phase(s) present in all unheated bone specimens and all bone specimens heated to 600 °C and 1400 °C (HAP %, β-TCP %, α-TCP %, TTCP % CaO % and MgO %). The coherence length, along the <00ℓ> direction of the calcium hydroxylapatite (HAP) mineral phase (HAP <00ℓ>) was measured for all unheated bone specimens and all bone specimens heated to 600 °C. HAP <00ℓ> was used as an indicator of recrystallisation (an increase in crystal size and perfection) along the <00ℓ> direction on heating bone specimens to 600 °C. Evidence for recrystallisation of bone mineral on heating was also obtained from a visual inspection of the XRD data from unheated bone and bone heated to 600 °C and 1400 °C and was based on the consideration of the width of the XRD peaks. The lattice parameters ‘a’ and ‘c’ were obtained for the

HAP and β-TCP mineral phases, whenever they were detected in a bone specimen (HAP ‘a’, HAP ‘c’, β-TCP ‘a’ and β-TCP ‘c’). The materials and methods employed in the measurement of each of these bone mineral characteristics are detailed in chapter 4.

3.2 – INFRARED SPECTROSCOPY

Infrared (IR) spectroscopy is an analytical tool that provides information about the molecular structure of compounds. Molecules that have covalent bonds with permanent electrical dipoles, such as C–O or O–H vibrate with respect to the bond. They have vibration frequencies that are within the infrared region of the electromagnetic energy spectrum. The frequency of the vibration is specific to the atomic structural environment surrounding the bond. Infrared radiation that interacts with the molecule at the same frequency as that of a particular vibration is absorbed by the molecule. Thus, different molecules will have different, characteristic absorptions and the observation of the frequencies that are absorbed enables the molecular structure of a compound to be determined. The majority of IR analyses that are carried out employ a Fourier Transform infrared spectrometer. This is comprised of an infrared radiation beam source, an interferometer, a specimen stage and an infrared radiation detector.

Solid specimens, in powdered form are generally combined with dry potassium bromide (KBr) powder and compressed into a disc using a press. The detector measures the infrared radiation transmitted through the specimen disc and an infrared transmittance spectrum is obtained as a data output from the analysis .

The x-axis of this spectrum represents infrared radiation frequencies, plotted in wavenumbers (cm^{-1}) and the y-axis represents the transmittance of the incident infrared radiation at each frequency. An infrared transmittance spectrum therefore displays a series of 'peaks' (troughs) that extend below a slowly varying background level of transmittance (see appendix).

An infrared spectrum of bone consists of peaks corresponding to bond vibrations within the organic component such as those of C–H and N–H bonds [227]. Covalent bond vibrations within the inorganic component are also represented. These include those of P–O bonds in the phosphate ions (PO_4^{3-}) and O–H bonds in the hydroxyl ions (OH^-) of the calcium hydroxylapatite lattice [227]. They also include vibrations of bonds within ions substitutions such as C–O bonds in carbonate ions (CO_3^{2-}) and O–H bonds in acid phosphate groups (HPO_4^{2-}) [227].

IR spectroscopy has been used, in combination with the study of synthetic and natural calcium hydroxylapatites, to firstly establish the general chemical composition of bio-apatite and then, confirm the presence of carbonate substitutions within the bio-apatite crystal lattice [80, 82, 104, 147, 228-231]. It has also been used to measure the amount of carbonate substitution and to demonstrate that bio-apatite is hydroxyl ion deficient [90, 154, 232, 233]. The measurement of the splitting resolution between HAP phosphate bond vibration peaks (see Figure 4.6) has also been used as an indication of the degree of short range order within the HAP lattice with respect to the typical atomic

environment surrounding the phosphate groups [122, 230, 234-236]. This measurement is generally referred to as the HAP phosphate ion splitting factor (*SF*) or crystallinity index [234, 237, 238]. The measurement of the HAP phosphate splitting factor calculates the extent of the separation between the ν_4 P-O stretching and bending vibration bands (see section 4.5.3). Values in the range of 2.50 – 3.25 are typically obtained for fresh, unheated bone [238].

For this research, infrared spectroscopy was used to measure the weight percentage of carbonate ions within the bone mineral component of bone heated to 600 °C (CO_3 %). The weight percentage value includes carbonate ions within the HAP crystal lattice in both the phosphate and hydroxyl ion sites and also 'labile' carbonate ions adsorbed onto the HAP crystal surfaces. IR spectroscopy was also used to measure the HAP phosphate ion splitting factor (*SF*) for bone heated to 600 °C. It is not possible to measure either of these bone mineral characteristics using X-ray diffraction analysis. The materials and methods employed in the measurement of each of these bone mineral characteristics are detailed in chapter 4.

3.3 – INDUCTIVELY COUPLED PLASMA – ATOMIC EMISSION SPECTROMETRY

Inductively coupled plasma - atomic emission spectrometry (ICP-AES) is a technique that enables the measurement of the concentration of the compositional elements of a material [196, 239]. This is achieved by the excitation of the atoms within a specimen by the introduction of the specimen as an aerosol to a plasma flow. Plasma is a neutral environment formed under high

temperature conditions by neutral atoms (typically atoms of argon gas) in equilibrium with their ionised state and electrons. In the case of ICP-AES, the energy that is used to form and maintain the plasma is inductively derived from an electric or magnetic field. The optical emission spectrum produced from the excited atoms is detected using a spectrophotometer and used to measure the concentration of specific elements within a specimen.

For this research, ICP-AES was used to measure the weight percentage of calcium (Ca) and phosphorous (P) and the parts per million (ppm) of sodium (Na), magnesium (Mg), potassium (K), strontium (Sr) and iron (Fe) in bone heated to 600 °C (Ca %, P %, Na ppm, Mg ppm, K ppm, Sr ppm and Fe ppm). The materials and methods employed in the measurement of each of these bone mineral characteristics are detailed in chapter 4.

3.4 – PYROHYDROLYSIS – ION CHROMATOGRAPHY AND COMBUSTION – GAS CHROMATOGRAPHY

Analytical chromatography is a technique that involves the separation, isolation and quantitative measurement of specific ionic or organic components of a material. This is achieved by the passing of a specimen (analyte) within a ‘mobile phase’ through a column containing a ‘stationary phase’.

In ion chromatography, the mobile phase consists of a buffered solution in which the analyte is dissolved and the stationary phase consists of spherical polymer particles with micrometre diameters. The stationary phase particle

surfaces are chemically modified to generate surface ion sites and enable ion exchange to occur at these sites with the ions to be separated from the mobile phase. In pyrohydrolysis – ion chromatography, the mobile phase is prepared by incorporating into a solution, the gaseous products collected from the heating of a powdered specimen mixed with a flux.

In gas chromatography, the mobile phase is a gaseous mixture of the analyte in vapour form and a carrier gas (typically helium, nitrogen or hydrogen). The stationary phase is either a liquid that is immobilised by impregnation or bonding to a support column or a porous solid column such as graphite or silica gel and which also allows ion exchange to occur between the mobile phase and stationary phase. In combustion – gas chromatography, the mobile phase is prepared by mixing the gaseous products collected from the combustion of a powdered specimen with the carrier gas.

In both ion chromatography and gas chromatography the mobile phase passes through a detector located at the end of the stationary phase column, the retention time for each constituent ion or element of interest is measured and data output is in the form of a chromatogram. The characterisation and the quantification of constituent ions or elements are determined from the retention time data.

For this research, chromatography was employed as an elemental analysis technique to investigate elemental components of bone that could not be measured using ICP-AES. Pyrohydrolysis – ion chromatography (P-IC) was used to measure the parts per million by weight (ppm) of fluorine (F) and chlorine (Cl) (F ppm and Cl ppm) and combustion – gas chromatography (C-GC) was used to measure the weight percentage of carbon (C), nitrogen (N) and hydrogen (H) (C %, N % and H %). The materials and methods employed in the measurement of each of these bone mineral characteristics are detailed in chapter 4.

CHAPTER 4 – AIMS, HYPOTHESES, MATERIALS AND METHODS

4.1 – AIMS AND HYPOTHESES

This thesis aimed to investigate inter-species variation in bone mineral characteristics of unheated bone and bone heated to 600 °C and 1400 °C. This investigation was conducted by the achievement of a sub-set series of aims and the testing of a number of hypothesis for a range of bone mineral characteristics measured using X-ray diffraction (XRD) analysis, infrared (IR) spectroscopy, inductively coupled plasma – atomic emission spectrometry (ICP-AES), pyrohydrolysis – ion chromatography (P-IC) and combustion – gas chromatography (C-GC). The series of aims are detailed below, together with the hypotheses tested and through which, each aim was achieved.

4.1.1 – GENERAL COMPOSITION AND STRUCTURE OF BONE MINERAL

Aim 1 - Demonstrate that bone mineral has a general composition and structure, common to all individuals of all species investigated.

This aim was set, to establish a consistency with current, commonly held views and to confirm the validity of employing the analytical techniques used for the research (see chapters 2, 3 and 4).

Hypothesis 1 (a) – The phase identity of the mineral component of unheated bone is exclusively that of calcium hydroxylapatite (HAP).

Hypothesis 1 (b) – The HAP phase of unheated bone is poorly crystalline and non-stoichiometric.

Hypothesis 1 (c) – Calcium and phosphorous are major bone mineral compositional components of bone.

Hypothesis 1 (d) – Sodium, magnesium, potassium, strontium, iron, fluorine and chlorine are bone mineral compositional components of bone.

Hypothesis 1 (e) – Nitrogen, hydrogen, carbon, are compositional components of bone and carbonate ions are compositional components of bone mineral.

The hypotheses 1 (c) to 1 (e) were tested using a sub-set of the sample of individuals used to test hypotheses 1 (a) and 1 (b). They were tested using bone heated to 600 °C. The tests relied on the assumptions that; the majority of the organic component is removed on heating and calcium, phosphorous, sodium, magnesium, potassium, iron, fluorine, chlorine, nitrogen, carbon and hydrogen are not incorporated into bone from the atmosphere on heating to 600 °C. Also, the hypotheses do not specify the location of each of the elements within bone. Using the analytical techniques of ICP-AES, P-IC and C-GC, it was not possible to determine whether the elements investigated were specifically

located within the organic component, within the HAP crystal lattice, adsorbed onto crystal surfaces or within a combination of these locations (see sections 3.3 and 3.4).

4.1.2 – BIOLOGICAL CONTROL OF COMPOSITION AND STRUCTURE

Aim 2 – Demonstrate that the biological control of the general composition and structure of bone mineral is similar for all species.

Hypothesis 2 (a) – Values of relative coherence length of calcium hydroxylapatite crystals along the <00ℓ> direction (HAP <00ℓ>) are significantly correlated to values obtained for HAP lattice parameters (HAP ‘a’ and HAP ‘c’), for all unheated bone specimens (see section 4.4.3). This hypothesis is underpinned by the proposal that ion substitutions provide a mechanism for biological control of HAP crystallinity.

Hypothesis 2 (b) – The percentage of magnesium in bone (Mg %) is negatively correlated to HAP <00ℓ> values obtained for unheated bone. This proposal is supported by the currently accepted view that magnesium plays an *in vivo* role in restricting crystallite morphology [79, 240].

Hypothesis 2 (c) – The HAP <00ℓ> values obtained for unheated bone are positively correlated to values obtained for the percentage of fluorine in bone (F ppm). This hypothesis is underpinned by the proposal that fluorine plays an *in vivo* role in enhancing crystallite size and/ or perfection through substitution with

hydroxyl ions (OH^-) within the HAP lattice, thus stabilising bone mineral crystals [79, 166].

Hypotheses 2 (b) and 2 (c) relied on the assumption that magnesium and fluorine are associated with the HAP mineral phase in bone heated to 600 °C.

4.1.3 - GENERAL RESPONSE OF BONE MINERAL TO HEAT TREATMENT

Aim 3 – Demonstrate that there is a measurable, general response of bone to heat treatment, when heat treatment conditions are standardised.

Hypothesis 3 (a) – Mass is lost from all bone specimens on heating.

Hypothesis 3 (b) – The HAP mineral phase undergoes recrystallisation on heating bone to 600 °C (see sections 2.5.1, 3.1 and 4.4.3).

A significant increase in HAP <00ℓ> values obtained for bone heated to 600 °C compared to corresponding values obtained for unheated bone from the same individual was used as a quantitative indicator of recrystallisation. A subjective indication of recrystallisation was also obtained from a visual inspection of the XRD data from unheated bone and bone heated to 600 °C and was based on the consideration of the width of the XRD peaks.

Hypothesis 3 (c) – The HAP lattice parameters (HAP ‘a’ and HAP ‘c’) tend towards stoichiometric HAP values of ‘a’ = 9.420 Å and ‘c’ = 6.880 Å, on heating bone to 600 °C and 1400 °C.

Hypothesis 3 (d) – Thermal decomposition of the HAP mineral phase does not occur on heating bone to 600 °C.

Hypothesis 3 (e) – Thermal decomposition of the HAP mineral phase occurs on heating bone to 1400 °C.

Hypothesis 3 (f) – The mineral phases; β-tri-calcium phosphate (β-TCP) and tetra-calcium phosphate (TTCP) are formed on heating bone to 1400 °C.

4.1.4 – CHEMICAL BASIS FOR VARIATION IN RESPONSE OF BONE TO HEAT TREATMENT

Aim 4 – Demonstrate that the response of bone mineral to heat treatment is related to compositional and structural characteristics of unheated bone and propose developments to current models for the thermal decomposition of bone mineral.

Hypothesis 4 (a) – The characteristics of unheated bone, measured using X-ray diffraction, are correlated to the weight percentage values obtained for the thermal decomposition products of the bone mineral HAP phase.

Hypothesis 4 (b) – The compositional characteristics of bone, measured using ICP-AES, P-IC, C-GC and IR spectroscopy, are correlated to the weight percentage values obtained for the thermal decomposition products of the bone mineral HAP phase.

4.1.5 – INTER-SPECIES VARIATION IN COMPOSITION AND STRUCTURE

Aim 5 – Demonstrate that inter-species variation exists in terms of the general composition and structure of bone mineral.

Hypothesis 5 (a) Significant inter-species differences exist, in terms of the structure and composition of bone mineral.

4.1.6 – INTER-SPECIES VARIATION IN RESPONSE TO HEAT TREATMENT

Aim 6 – Demonstrate that inter-species variation exists in terms of the general response of bone, in particular bone mineral, to heat treatment.

Hypothesis 6 – (a) Significant inter-species differences exist, in terms of the response of bone to the same heat treatment conditions.

4.1.7 – SPECIES IDENTIFICATION

Aim 7 – Evaluate the potential for the development of a new method of species identification based on bone mineral characteristics, measured using X-ray diffraction.

Hypothesis 7 – (a) Human bone can be distinguished from bone of all other species, based on the extent of inter-species variation in bone mineral characteristics of unheated and heated bone.

Hypothesis 7 – (b) Sheep bone can be distinguished from goat bone, based on the extent of inter-species variation in bone mineral characteristics of unheated and heated bone.

Hypothesis 7 – (c) Bone of ruminant species can be distinguished from bone of non-ruminant species, based on the extent of inter-species variation in bone mineral characteristics of unheated and heated bone.

4.2 – BONE MATERIAL

A total of 361 bone specimens from a total of 123 individuals were investigated. This included a range of 12 different animal species and a total of 430 analyses. The numbers of individuals of each species used for each analytical technique are presented in Table 4.1.

Non-human bone material was obtained from several sources: local butchers and a local abattoir, local pet food stores, Bristol Veterinary College, the Department for the Environment and Rural Affairs Veterinary Laboratories Agency (DEFRA VLA) and Whipsnade Zoo. Human bone was obtained from UK individuals from the North London Tissue Bank, UK and from Australian

individuals from the Melbourne Femur Collection, Australia. The range of species investigated was as wide as practically possible and included species that are of relevance to the practical applications of species identification, discussed in chapter 1. Results presented for human bone, in chapter 5, are presented as two separate groups, bone from UK individuals (human UK) and bone from Australian individuals (human AUS). The rationale for this separation is discussed in section 4.3.

Species		Gallus gallus domesticus	Bos taurus	Cervus elaphus	Canis lupus familiaris	Elephas maximus	Capra aegagrus hircus	Homo sapien	Macaca mulatta	Sus domestica	Oryctolagus cuniculus	Rattus norvegicus	Ovis aries
Commonly used name for species		Chicken	Cow	Deer	Dog	Elephant	Goat	Human	Monkey	Pig	Rabbit	Rat	Sheep
Total number of individuals		5	10	5	12	1	8	50 AUS 8 UK	1	7	5	5	6
Number of individuals used in sample set	XRD analysis of unheated bone	5	10	5	12	1	8	47 AUS 8 UK	1	7	5	0	6
	XRD analysis of bone heated to 600 °C	5	10	5	12	1	8	50 AUS 8 UK	1	7	5	5	6
	XRD analysis of bone heated to 1400 °C	5	10	5	12	1	8	50 AUS 8 UK	1	7	5	5	6
	IR spectroscopy of bone heated to 600 °C	1	6	1	1	0	1	0 AUS 1 UK	1	1	1	0	1
	ICP-AES of bone heated to 600 °C	1	6	1	1	0	1	3 AUS 1 UK	1	1	1	0	1
	C-IC of bone heated to 600 °C	1	6	1	1	0	1	3 AUS 1 UK	1	1	1	0	1
	P-IC of bone heated to 600 °C	1	6	1	1	0	1	3 AUS 1 UK	1	1	1	0	1
Same individuals used for ICP-AES, C-IC and P-IC (elemental analyses)		Yes	Yes	Yes	Yes	---	Yes	Yes AUS Yes UK	Yes	Yes	Yes	---	Yes
Same individuals used for elemental analyses and IR spectrocopy		No	5 Yes 1 No	No	No	---	No	--- Yes UK	Yes	No	No	---	No

Table 4.1 – Total number of individuals investigated for each species and the numbers of individuals of each species used for each analytical technique

4.3 – SPECIMEN PREPARATION

4.3.1 – CUTTING OF BONE SPECIMENS

All bone specimens were cut from cortical bone samples, taken from the mid-shafts of femur (thigh) bones. Left femur samples were used if a choice between left or right was available. All bone samples were from modern bone, collected shortly after death and stored frozen with the exception of human bone samples from Australian individuals (human AUS). Prior to their use in the study, they had been stored, long term, at room temperature, in 70 % ethanol solution. Once received for use in this research, the samples were stored frozen, out of ethanol, after rinsing with water. Due to the differences in storage conditions, human bone samples from Australian individuals were grouped as a separate species category to human bone from UK individuals (human UK).

Bone samples were stored frozen as a preservation measure in order to prevent bone alteration by dehydration at room temperature and to prevent decomposition of any adhering soft tissue. This was also the aim in the storage of the human AUS bone samples in ethanol. There is evidence within the literature to suggest that the frozen storage of bone has no detrimental effect on bone mineral characteristics. However, the effect of the storage of bone in ethanol on bone mineral characteristics is not well established.

Any adhering soft tissue was manually removed from bone samples using a scalpel. All samples were rinsed with water and dilute disinfectant. Specimens were cut from bone samples using a band saw and a circular saw or, in the case of small samples, using a scalpel. The saw blades were cooled with water when necessary. Any bone powder adhering to specimen surfaces after cutting was removed by rinsing with water. Specimens were cut as cross-sectional segments that included bone from the periostial to the endostial surfaces (see Figure 4.1).

Figure 4.1 – Diagram showing example of cut bone specimen segment

For each individual, a set of three bone specimens were cut, when possible. Of each set, one specimen was left unheated, one was heated to 600 °C, and one was heated to 1400 °C. For all rat bone samples and three human AUS bone samples, there was only sufficient material from which to cut the two heated bone specimens. The bone specimens that were left unheated were all cut to a segment height of approximately 1 mm due to the requirements of X-ray diffraction analysis for non-powdered bone specimens.

4.3.2 – HEAT TREATMENT

The knowledge gained from a review of the literature regarding the heat treatment of bone and calcium hydroxylapatite materials (see section 2.5) and the results obtained from preliminary experiments were used to determine the choice of heat temperatures investigated. X-ray diffraction analysis data values from these preliminary experiments for calcium hydroxylapatite (HAP) lattice parameter ‘a’ (HAP ‘a’) and the weight percentage of HAP (HAP %) are presented in Figure 4.2 for cow, human and sheep bone specimens (one individual from each species) heated to a range of temperatures, each heated for two hours following the same experimental protocols as those used for this research.

Two temperatures were chosen for which both the number of bone mineral characteristics measurable by X-ray diffraction analysis, the inter-species variation for each characteristic and the potential of each characteristic for use in a method of species identification were optimised.

A temperature of 600 °C was chosen because it lies within the temperature range in which recrystallisation (see section 2.5.1 and section 4.4.3) of the bio-apatite mineral phase occurs [134] and below the expected temperature range for the thermal decomposition of HAP. The variation in HAP lattice parameter values between species was greater for 600 °C than for 500 °C and the Rietveld analysis fitting errors (see section 4.4.3) are lower in value for bone heated to 600 °C than for bone heated to lower temperatures.

A temperature of 1400 °C was chosen because it lies below the expected temperature range for the melting of HAP [141, 143] and difficulties in specimen recovery and specimen powdering are encountered. The number of thermal decomposition products detected and also the inter-species variation in weight percentage values obtained for each decomposition product detected were both greater for bone heated to 1400 °C than for bone heated to 1200 °C. Furthermore, the variation in HAP lattice parameter values between species was also greater for 1400 °C than for 1200 °C.

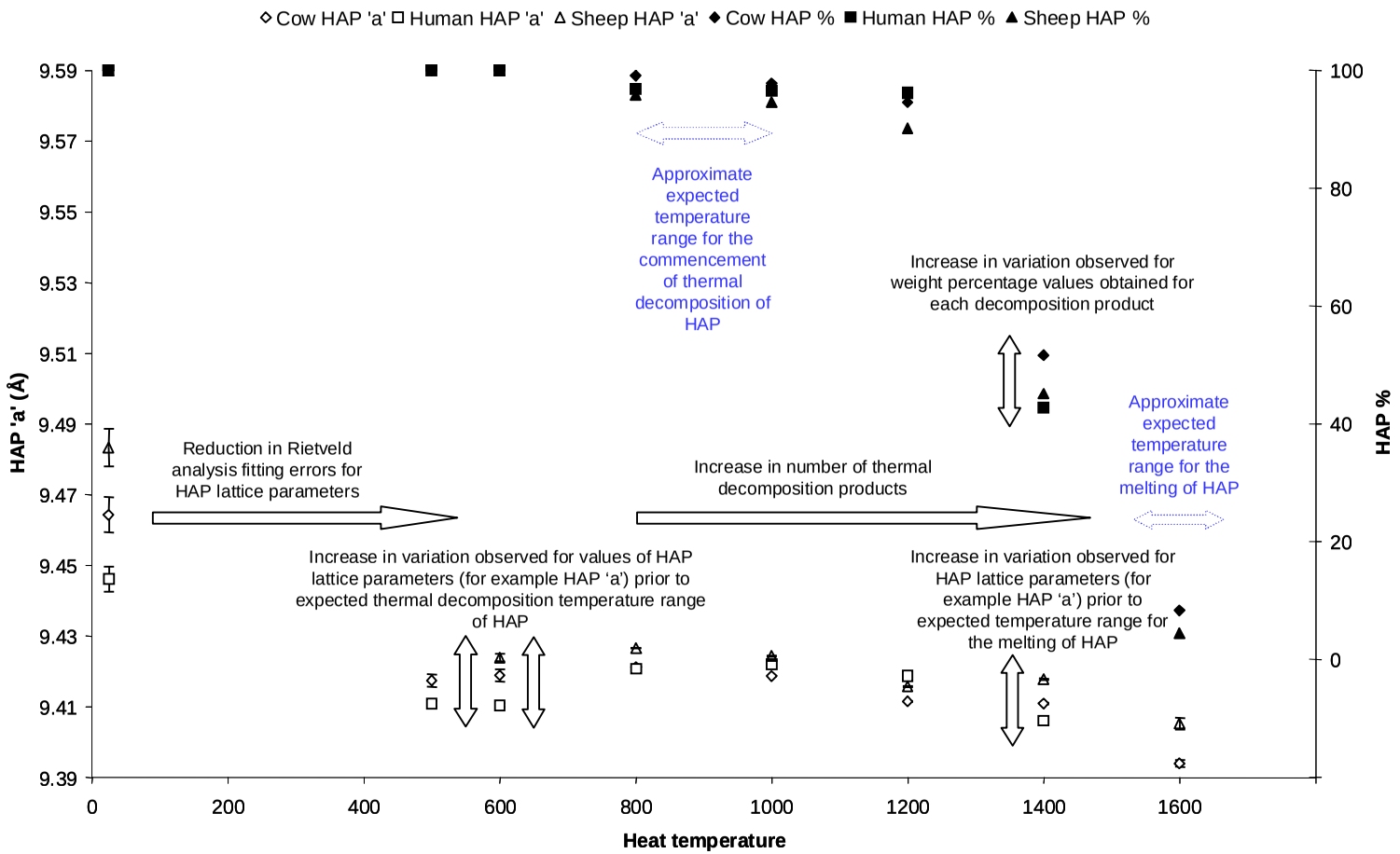

Figure 4.2 – Diagram showing preliminary data and observations used to help determine the choice of 600 °C and 1400 °C as the heat temperatures investigated. Values of the HAP lattice parameter 'a' and the weight percentage of HAP are presented for cow, human and sheep bone specimens heated to a range of temperatures, each heated for two hours (one individual per species). Values obtained for the HAP lattice parameter 'c' and weight percentage values for thermal decomposition products of HAP are referred to but not presented. Rietveld fitting errors are shown for HAP 'a' values, those for HAP % are all within the limits of the data markers and are therefore omitted for clarity

Bone specimens that were subjected to heat treatment were defrosted at room temperature prior to heating. The appearance and the mass of each specimen were recorded before and after heating (see section 4.9). The mass of each specimen prior to heat treatment was in the range of 0.028 – 2.142 g (inclusive) and the experimental error associated with each mass measurement was ± 0.001 g.

The heating of specimens was carried out in a Carbolite tube furnace (CTF 16/75) (see Figure 4.3). Each bone specimen was placed into a separate alumina crucible for heat treatment. Crucibles rested on alumina slabs within the tube of the furnace and specimens were heated in batches of 1, 3 or 4 specimens (see Figure 4.4). For all batches, specimens were placed into the furnace at room temperature. After specimen placement in the furnace, each end of the furnace tube was sealed with a ceramic fibre bung. The temperature of the furnace was increased to the required heat temperature (600 °C or 1400 °C) at a programmed rate of 10 °C per minute. The furnace then followed a set programme of maintaining the required heat temperature for two hours. The furnace was set to automatically switch off at the end of this dwell time and bone specimens were allowed to slowly cool to room temperature before removal from the furnace. A dwell time of 2 hours was adopted to enable comparisons with the results of previous studies and to enable the evaluation of the results with respect to the development of a high-throughput method of species identification.

Figure 4.3 – Photograph of the Carbolite tube furnace (CTF 16/75) used for the heating of bone specimens

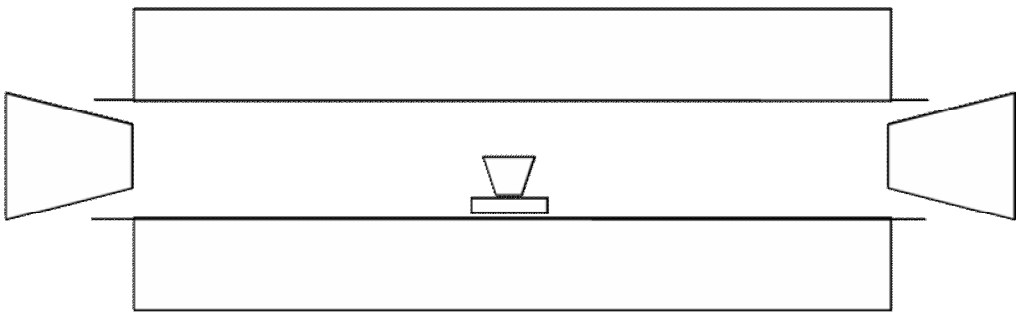

Figure 4.4 – Diagram of set-up of furnace apparatus for the heating of bone specimens showing one specimen placed within the furnace and ceramic fibre bungs used at each end of the furnace tube

4.3.3 – POWDER PREPARATION OF HEATED BONE SPECIMENS

All heated bone specimens were powdered for analysis, using an agate pestle and mortar. The powder from each specimen was individually sieved through a stainless steel mesh of 106 µm. Pestles, mortars and sieves were washed and dried, between use, for each bone specimen.

The powder obtained from each bone specimen was stored in a separate sealed glass vial. Vials were stored in a desiccator, at room temperature, until required for analysis. For some specimens, the bone powder was divided to create separate powder specimens for the different analytical techniques. There was no evidence for alteration of specimens due to deterioration over time with the period of time taken to analyse all specimens.

4.4 – X-RAY DIFFRACTION (XRD) ANALYSIS

4.4.1– XRD ANALYSIS SPECIMEN PREPARATION

Powdered bone specimens were prepared for X-ray diffraction analysis by mounting specimens onto silicon slides. These slides were used because of the low background scattering of X-rays from the slides, during data collection. For each specimen, a thin film of petroleum jelly was applied to the silicon slide. A small mound of specimen powder was placed onto the slide and gently flattened using a microscope slide to produce an even layer of powder with a thickness of approximately 0.5 mm and of an area slightly larger than the incident area of the X-ray beam of the diffractometer. Silicon and microscope slides were re-used

and were cleaned before use for each specimen. After X-ray diffraction analysis, mounted specimens were removed from slides using a spatula and stored in a separate sealed glass vial.

All unheated bone specimens were prepared for XRD analysis by mounting specimen segments onto microscope cover slips. A strip of adhesive tape was used between specimen and slide to secure each specimen in place. Mounted unheated specimens were stored frozen until required for analysis, at which point they were defrosted at room temperature.

4.4.2 – XRD DATA COLLECTION

Powder X-ray diffraction analysis of all heated bone specimens was carried out using Phillips 1820 diffractometers with Cu Kα radiation (approximately 15 Å). The detectors collected data as stepped scans across an angular range of 10 – 80 °/2θ (4.43 – 0.78 Å d-spacing). The count time at each step was 5 seconds, with a 0.02 °/2θ step size.

X-ray diffraction analysis of non-powdered specimens was carried out using a Bruker D8 X-ray diffractometer with Cu Kα radiation. A General Area Detector Diffraction System (GADDS) was used to collect data over an angular range of approximately 21 - 55 °/2θ (2.15 – 0.94 Å d-spacing).

Occasional noise peaks were present in the XRD data. These were characterised by a peak width at the base of the peak that was one step size in

magnitude (°/2θ). They were easily detectable above the background signal on a visual inspection of the XRD data. Noise peaks were removed prior to data analysis by replacing the noise peak value with the mean value obtained from the values of the data points immediately either side of the noise peak.

4.4.3 – XRD DATA ANALYSIS

The main mineral phases present within each specimen were initially identified by comparison of specimen diffractograms with the International Centre for Diffraction Data (ICDD) Powder Diffraction File (version PDF-2, 2004). This comparison was carried out using Crystallographica Search-Match software (version 2,1,1,1 1996 - 2004).

Bruker Topas software (version 2, 2000) was used to carry out Rietveld refinement of all diffraction profiles. All profiles were refined using the same protocol. This included specifying the emission profile for the Cu Kα radiation and instrument details of the diffractometer. Each identified mineral phase was refined, starting with the most prominent until all mineral phases had been included into the refinement and the best possible fit was deemed to have been achieved. The goodness of a refinement fit was judged on the basis of the weighted residual (Rwp) value that was obtained after each refinement run and the visual observation of the residual and fitted peaks on-screen.

The fitting errors (W_e) for the weight percentage values (W) obtained from the Rietveld Refinement were calculated using the scale factor (S) and scale factor fitting errors (S_e) output from Topas (see Equation 4.1).

$$W_e = \left(\frac{S_e}{S} \right) xW$$

Equation 4.1 – Equation for the calculation fitting errors for the weight percentage values obtained from Rietveld Refinement

Topas software (version 2, 2000) was also used to carry out the profile fitting of the calcium hydroxylapatite 002 peak in each diffraction profile obtained from unheated bone specimens and bone specimens heated to 600 °C. This was achieved by using the same protocol for all profiles. The emission profile for the Cu Kα radiation and instrument details of the diffractometer were specified. The refinement range was confined to a 24 – 27 °/2θ angular range and a split pseudo-Voigt peak was refined. This is an approximation to a Voigt function which is a combination of Gaussian and Lorentzian peaks [241].

The HAP 002 full width half maximum contribution of each specimen (F_s) to the measured HAP 002 full width at half maximum (F_o) was calculated using values obtained for peak broadening due to the X-ray diffractometer instrument (F_i) (see Equation 4.2).

$$(F_s)^2 = (F_o)^2 - (F_i)^2$$

Equation 4.2 – Equation for the calculation of the HAP 002 FWHM contribution of a specimen to the measured HAP 002 FWHM

Data collected from a silicon (Si) powder standard (NBS 640c), run routinely on the Phillips 1820 diffractometers and from a corundum (Al_2O_3) standard (NBS 1976), run on the Bruker D8 X-ray diffractometer were used to calculate values of F_i for each instrument.

Values of relative coherence length of calcium hydroxylapatite crystals in the <002> direction (HAP <00ℓ>) were calculated using the Scherrer equation from the values calculated for F_s (converted into radians), theta (θ) from the 2θ position of the peak (in radians), the wavelength of Cu Kα radiation (λ = 15 Å) and a shape factor of 0.9 (see Equation 4.3).

$$HAP < 00\ell >= \frac{0.9\lambda}{(F_s)\cos\theta}$$

Equation 4.3 – Scherrer equation

The unit of Ångström was consistently used for the reporting of HAP <00ℓ> and lattice parameter values. Although the Ångström is not a Standard International unit, it is the unit conventionally used within X-ray crystallography.

The fitting errors associated with the weight percentage values obtained for each identified mineral phase were in the range of 0.69 – 2.01 % for unheated bone specimens. Those for heated bone specimens were all less than 0.62 %. The fitting errors associated with HAP <00ℓ> values were less than 1.3 Å for all bone specimens and those associated with HAP lattice parameter values were in the range of 0.001 – 0.008 Å for unheated bone specimens and less than 0.002 Å for heated bone specimens. The fitting errors associated with β-TCP lattice parameter values were in the range of 0.001 – 0.018 Å for bone specimens heated to 600 °C and less than 0.006 Å for bone specimens heated to 1400 °C.

4.5 – INFRARED (IR) SPECTROSCOPY

4.5.1 – IR SPECTROSCOPY SPECIMEN PREPARATION

A sub-set of the sample of bone specimens heated to 600 °C was analysed using infrared (IR) spectroscopy (see Table 4.1). Bone powder from each specimen (0.005 g) was mixed with 0.3 g of potassium bromide powder, using an agate pestle and mortar. A mass of 0.055 g of the mixture was transferred to a pellet die. The die was pressed under approximately 5 – 10 tonnes for approximately 10 seconds. The pestle and mortar and die plates were cleaned with water and dried in an oven prior to each use. This pellet preparation protocol is slightly amended from standard recommendations for the production of KBr pellets which involve the use of 0.01 g of a specimen and a pressing time

of approximately 30 seconds. Amendments were made after encountering production difficulties due to pellets adhering to die plates after pressing.

4.5.2 – IR SPECTROSCOPY DATA COLLECTION

A Bruker Vector 22 Fourier transform infrared spectrometer was used for the IR analysis. This employed Bruker Opus software (version 3.1) for data collection. A background profile was obtained by scanning a pellet made from 0.055 g of KBr powder at the start of each analysis session. The Opus software automatically accounted for this background for subsequently run bone specimens. A scan resolution of 4 cm^{-1} and 64 scans were used for each data collection run.

4.5.3 – IR SPECTROSCOPY DATA ANALYSIS

Peak Fit software (version 4) was used to obtain values for the total area of the carbonate peak in the region of 858 – 892 cm^{-1} (*A*). This was achieved using the same protocol for all infrared spectra. Peaks were fit after conversion to a y-scale measure of absorbance and an automatic baseline subtraction across the selected region. A second derivative was used to carry out peak detection and fitting and the data was fit to either two or three peaks, depending on the best fit obtained.

The weight percentage of carbonate ions within the bone mineral (CO_3 %) was calculated using a calibration equation (see Equation 4.4). This was created using specimens of carbonated calcium hydroxylapatite standards with known

carbonate weight percentage values (0.5, 1.4, 2.3 and 3.5 %) which were obtained from CCP Inc. (see glossary). Equation 4.4 was obtained from a plot of the values obtained for the total area of the carbonate peak from these standards against the certified weight percentage values (see Figure 4.5).

$$CO_3\% = (4.6155A) - 0.7095$$

Equation 4.4 - Calibration equation for calculation of carbonate weight percentage values (CO_3 %) from the total carbonate peak area (A), measured using IR spectroscopy

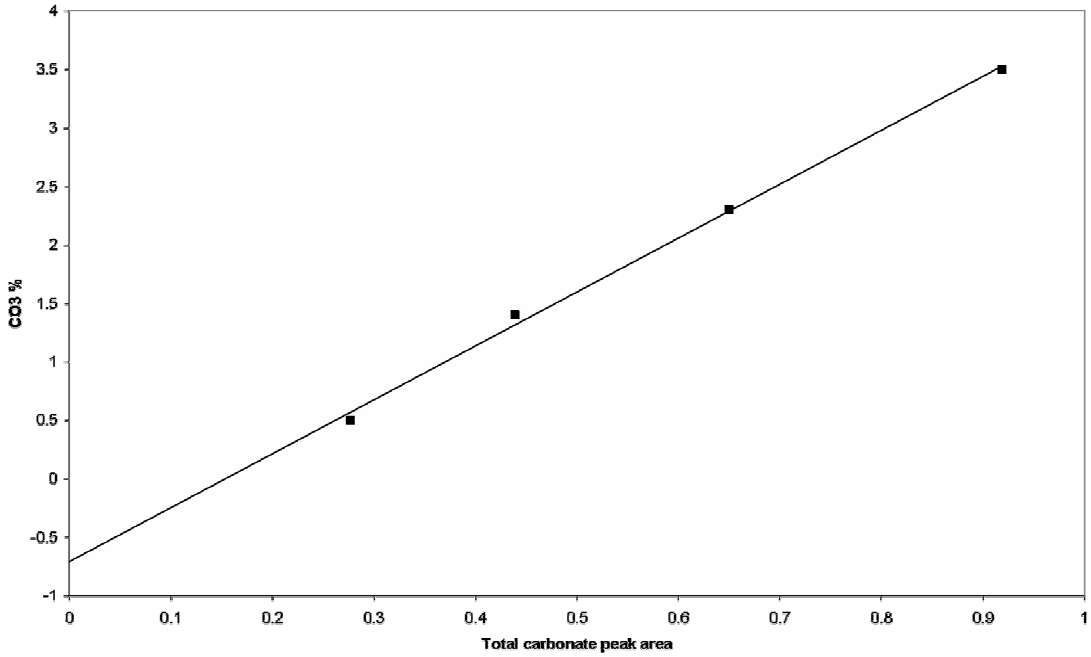

Figure 4.5 - Calibration graph for calculation of carbonate weight percentage values (CO_3 %) from the total carbonate peak area (A), measured using IR spectroscopy

The Peak Fit software was also used to obtain values for the phosphate ion splitting factor (*SF*), again using the same protocol for all infrared spectra. After a conversion to a y-scale measure of absorbance, a region of approximately 450 – 750 cm^{-1} was selected for automatic baseline subtraction. This area encompassed the ν_4 P-O stretching and bending vibration bands from which the splitting factor was determined. The value of 750 cm^{-1} was fixed as the upper limit of this range in all cases. The lower limit was taken from a minimum point in the data in the region of 525 cm^{-1}. Values were recorded for the coordinates of points 'a', 'b' and 'c' (see Figure 4.6).

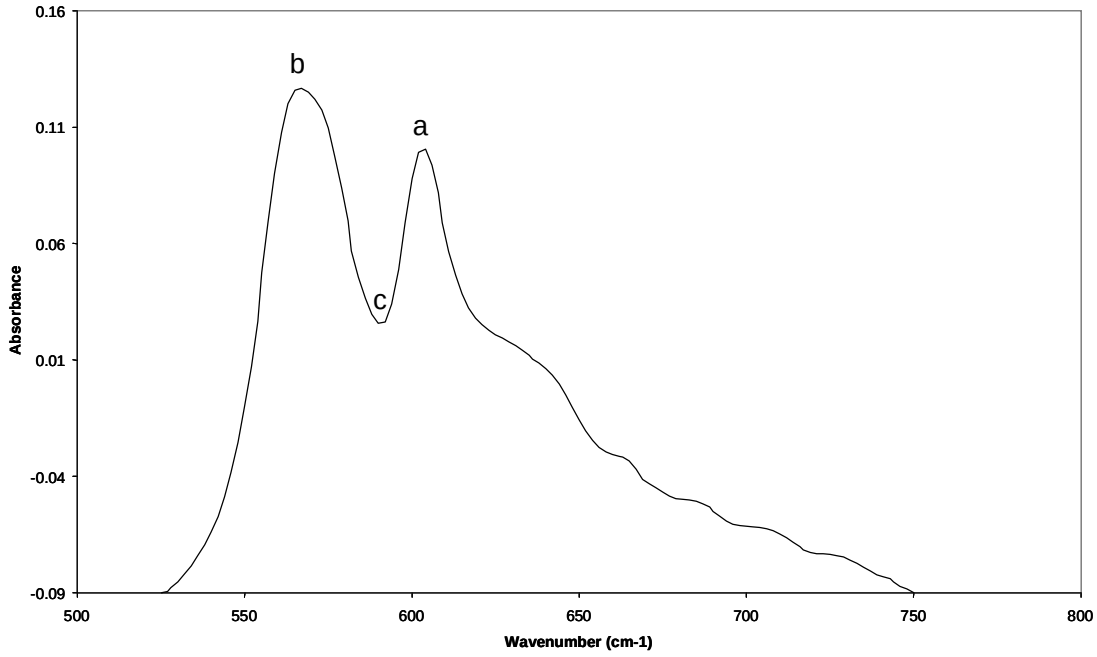

Figure 4.6 – Section of IR spectrum obtained from a bone specimen heated to 600 °C showing phosphate ion splitting factor measurement points. Peaks correspond to the ν_4 P-O stretching and bending vibration bands

$$SF = \frac{(y_a + y_b)}{y_c}$$

Equation 4.5 – Calculation of phosphate ion splitting factor

The phosphate ion splitting factor (*SF*) was calculated using the y-axis values obtained for points ‘a’, ‘b’ and ‘c’ (see Equation 4.5).

4.6 – INDUCTIVELY COUPLED PLASMA – ATOMIC EMISSION SPECTROMETRY (ICP-AES)

4.6.1 – ICP-AES SPECIMEN PREPARATION

A sub-set of the sample of bone specimens heated to 600 °C was analysed using inductively coupled plasma – atomic emission spectrometry (ICP-AES), carried out by staff at the Natural History Museum, London (see Table 4.1).

The majority of specimen solutions were made up from 50 mg (± 5 mg) of bone powder, 2 ml of deionised water and 1 ml of concentrated nitric acid (HNO_3). For one human bone specimen and the deer bone specimen, 3 ml of concentrated nitric acid and 1 ml of hydrogen peroxide (H_2O_2) was used instead of the 1 ml of concentrated HNO_3. Each solution was heated for 1 hour at 40 °C and then made up to a solution of 50 ml by volume using deionised water.

4.6.2 – ICP-AES DATA COLLECTION AND DATA ANALYSIS

A Varian Vista-Pro axial inductively coupled plasma spectrometer, an SPS-5 auto-sampler and ICP Expert software (version 4.1.0) were used for the ICP-AES analysis of the bone specimens. The analysis conditions included a power of 1.1 kW, a plasma flow of 15 l/min, an auxiliary flow of 1.5 l/min and a nebuliser flow of 0.75 l/min, the monitoring of the internal drift throughout each run and 3 replicate analysis runs were obtained from each 50 ml solution. Weight percentage values were reported for calcium (Ca %) and phosphorous (P %) and parts per million values (ppm) were reported for sodium (Na ppm), magnesium (Mg ppm), potassium (K ppm), strontium (Sr ppm) and iron (Fe ppm). The relative standard deviation values for the replicates were less than 0.22 % for calcium, less than 0.11 % for phosphorous, less than 0.05 % for magnesium and potassium, less than 0.1 % for sodium and less than 0.01 % for iron and strontium.

4.7 – PYROHYDROLYSIS – ION CHROMATOGRAPHY (P-IC)

4.7.1 – P-IC SPECIMEN PREPARATION DATA COLLECTION AND DATA ANALYSIS

A sub-set of the sample of bone specimens heated to 600 °C was analysed using pyrohydrolysis – ion chromatography (P-IC), carried out by staff at the Natural History Museum, London (see Table 4.1).

The same protocol was adopted for the preparation of each bone specimen. A mass of 200 mg of specimen powder was transferred into a silica glass specimen boat. Care was taken to avoid touching the boat with bare hands and therefore avoid contamination of the specimen. A mass of 300 mg of flux in the form of a 1:1:2 mixture of bismuth oxide (BiO_3): sodium tungsten oxide ($NaWO_4$): vanadium oxide (V_2O_5) was added to the specimen within the boat and thoroughly mixed, ensuring that the mixture was spread across the base of the boat. This was then placed into a pre-heated tube furnace set at a temperature of 950 °C to which steam generator and condenser apparatus were attached as shown in Figure 4.6.

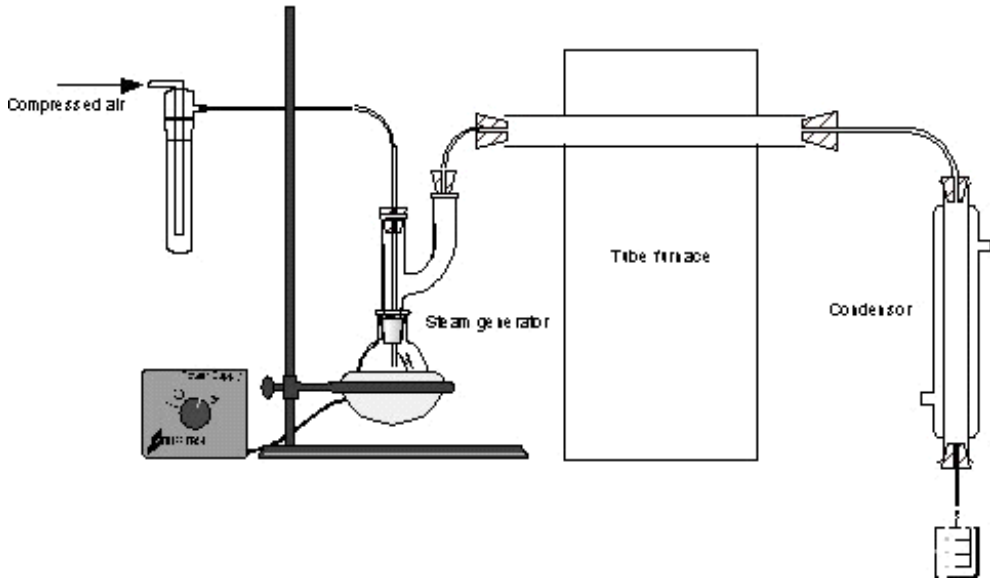

Figure 4.7 – Diagram of pyrohydrolysis apparatus set up for pyrohydrolysis – ion chromatography of bone specimens previously heated to 600 °C (courtesy of Natural History Museum)

The liquid distillation product obtained from the condenser was collected into bottles containing 5 ml of a sodium carbonate (Na_2CO_3) and sodium bicarbonate ($NaHCO_3$) absorption solution and 5 ml of hydrogen peroxide (H_2O_2) solution with a concentration of 30 % weight percentage by volume (w/v). At the end of the distillation, the condenser was washed through with deionised water, the collection bottles were removed and the liquid product specimen was transferred into a 25 ml volumetric flask, made up to volume using deionised water and then transferred back into the collection bottles for storage prior to analysis by ion chromatography. The apparatus was reconnected after the washing of the condenser and the removal of the collection bottles, waste bottles were placed under the condenser and the specimen boats were removed from the tube furnace. Specimen boats were cleaned between each use. The ion chromatography was carried out using a Dionex DX300 instrument and Al450 software. Parts per million values (ppm) were reported for chlorine (Cl ppm), fluorine (F ppm).

4.8 – COMBUSTION – GAS CHROMATOGRAPHY (C-GC)

4.8.1 – C-GC SPECIMEN PREPARATION, DATA COLLECTION AND DATA ANALYSIS

A sub-set of the sample of bone specimens heated to 600 °C was analysed using combustion – gas chromatography (C-GC), carried out by staff at the Natural History Museum, London (see Table 4.1).

The combustion – gas chromatography was carried out using a Thermo Finnigan Flash EA1112 Elemental analyser and Eager 300 software. A mass of 5 – 10 mg of specimen powder was transferred into an 8 x 5 mm tin specimen capsule, loaded onto an autosampler for introduction into the combustion reactor of the Elemental analyser. The analysis conditions included a combustion temperature of 1000 °C, collection of gas products by a helium flow carrier gas and the use of an aspartic acid standard of known concentration (weight percentage of carbon, 36.09 %). Weight percentage values were reported for carbon (C %), nitrogen (N %) and hydrogen (H %).

4.9 – MEASUREMENT OF MASS CHANGE DUE TO HEAT TREATMENT

The mass of each heated bone specimen was recorded before and after heating. For each individual, mass change for bone heated to 600 °C was obtained for a bone specimens heated from room temperature to 600 °C, with a dwell time of two hours and mass change for bone heated to 1400 °C was obtained from a separate bone specimen heated from room temperature to 1400 °C, with a dwell time of two hours (see section 4.3.2).

Mass change was recorded as a percentage of the mass of a bone specimen before heating (see Equation 4.6) and mass after heating was measured after slow cooling of bone specimens within the furnace for a period of approximately 20 hours.

$$\text{Mass change} = \left(\frac{\text{mass before heating - mass after heating}}{\text{mass before heating}} \right) \times 100$$

Equation 4.6 – Calculation of mass change on heating of bone specimens

4.10 – STATISTICAL ANALYSIS OF DATA

Statistical analysis of the results was carried out using the Statistical Package for Social Sciences software (version 16) [242-245].

The descriptive statistics of the mean value, the standard error of the mean (Std. Error), the minimum value (Min) and the maximum value (Max) were obtained for; the data set of all species including human AUS bone specimens, the data set of all species excluding human AUS bone specimens and for, each species group, for each bone mineral characteristic measured.

Kendall's tau correlation co-efficient (τ) (see Equation 4.7) was calculated for each group, for each bone mineral characteristic measured and the significance of each coefficient value was tested, on a two tailed test basis. This co-efficient was used due to the ranked nature of the values obtained for HAP and β-TCP lattice parameters and two tailed tests were used due to uncertainties regarding the negative or positive nature of correlations within the data.

$$\tau = \frac{2(n_c - n_d)}{n(n-1)}$$

n_c = number of concordant pairs

n_d = number of discordant pairs

n = number of pairs of values in data set

Equation 4.7 – Calculation of Kendall's tau correlation co-efficient

One-way analysis of variance (ANOVA) and Bonferroni post-hoc tests were carried out to identify significant differences between species groups for a selection of bone mineral characteristics measured using XRD analysis. ANOVA was deemed to be the most appropriate statistical tool for comparing the means of multiple sample (species) groups and the data held the assumptions of normality and equal variances. The Bonferroni test was used due to its statistical robustness and conservativeness. It was not possible to include monkey and elephant within the ANOVA and Bonferroni tests due to the analysis of bone from only one individual from each species. Significant differences between each of these species and all other species were tested using one sample t-tests for each bone mineral characteristic. Elephant and monkey were not tested against each other and rat was not tested using ANOVA with respect to unheated bone mineral characteristics, due to small sample size or, in the case of rat, no data. The results of these tests are presented in section 5.9.1 in terms of p-values which are the probabilities of obtained results as extreme as the values actually observed, assuming the null hypothesis is true. The levels of $p < 0.01$ and $p < 0.05$ are used to indicate significant results. For example, for the HAP 'a' lattice parameter values

obtained for unheated bone, a result of a p-value less than 0.01 indicates that there is a significant difference between the mean values obtained for two different species and thus leads to the rejection of the null hypothesis that there is no difference between the two species.

CHAPTER 5 – RESULTS

The results presented within this chapter relate to bone specimens from a total of 123 individuals from a range of animal species (see section 4.2). The full data set consisted of three bone specimens per individual; one unheated specimen, one specimen heated to 600 °C and, one specimen heated to 1400 °C, with the exception of the rat bone specimens, for which no unheated specimens were included (see chapter 4). General results are presented for the data set, including and excluding human AUS bone specimens and, when results are presented for species groups, human AUS and human UK are categorised into separate groups.

X-ray diffractograms and IR spectra are presented in the appendix. Results tables relating to the figures presented in section 5.9 and results tables relating to section 5.10.2 are also presented within the appendix.

5.1 – X-RAY DIFFRACTION ANALYSIS OF UNHEATED BONE

The X-ray diffractograms obtained from all unheated bone specimens had broad, overlapping peaks (see appendix). Calcium hydroxylapatite (HAP) was detected in all unheated bone specimens and was the only mineral phase detected. The values obtained for the HAP relative coherence length (HAP <00ℓ>) were all less than 300 Å. In general, the lattice parameter values were above those of stoichiometric HAP; 'a' = 9.420 Å and 'c' = 6.880 Å (see Table 5.1).

		All Species (excl. human AUS)	**All Species** (incl. human AUS)			**All Species** (excl. human AUS)	**All Species** (incl. human AUS)
Number		68	115	**Number**		68	115
HAP %		100 (only HAP detected)	100 (only HAP detected)	**HAP <00ℓ> (Å)**	Mean	238.7	248.6
					Std. Error	2.6	2.1
					Min	175.3	175.3
					Max	281.5	288.0
HAP a (Å)	Stoich.	9.420		**HAP c (Å)**	Stoich.	6.880	
	Mean	9.468	9.462		Mean	6.901	6.902
	Std. Error	0.002	0.001		Std. Error	0.001	0.001
	Min	9.419	9.419		Min	6.888	6.880
	Max	9.493	9.493		Max	6.918	6.921

Table 5.1 – XRD analysis results for HAP %, HAP <00ℓ>, HAP 'a' and HAP 'c' obtained from unheated bone specimens, including all species investigated (unheated rat bone was not investigated using this technique). Data presented as two groups: one that excludes human AUS and one that includes human AUS

5.2 – INDUCTIVELY COUPLED PLASMA – ATOMIC EMISSION SPECTROMETRY OF BONE HEATED TO 600 °C

The results obtained from inductively coupled plasma – atomic emission spectrometry of bone specimens heated to 600 °C were in agreement with those of the X-ray diffraction analysis. Bone specimens had a bulk composition of calcium and phosphorous (see Table 5.2) and this finding is consistent with a HAP mineral structure (see chapter 2). The mean value obtained for the percentage of calcium, by weight, was not significantly different to the stoichiometric calcium hydroxylapatite value of 39.9 %, within one standard error of the mean value. However, lower values, outside two standard error of the mean values, were obtained for approximately 40 % of bone specimens. Approximately 70 % of values obtained for the percentage of phosphorous by weight were greater than the stoichiometric value of 18.5 %, outside two standard error of the mean values. The resultant calculated values of atomic and weight Ca/P ratios were all less than the stoichiometric values of 1.67 (atomic) and 2.16 (weight).

		All Species (excl. human AUS)	All Species (incl. human AUS)			All Species (excl. human AUS)	All Species (incl. human AUS)
Number		15	18	**Number**		15	18
Ca % (weight)	Stoich.	39.9		**Ca/P (atomic)**	Stoich.	1.67	
	Mean	39.7	39.6		Mean	1.57	1.58
	Std. Error	0.4	0.4		Std. Error	0.02	0.02
	Min	38.0	38.0		Min	1.47	1.47
	Max	43.7	43.7		Max	1.66	1.66
P % (weight)	Stoich.	18.5		**Ca/P (weight)**	Stoich.	2.16	
	Mean	19.6	19.5		Mean	2.02	2.04
	Std. Error	0.2	0.2		Std. Error	0.02	0.02
	Min	18.6	17.8		Min	1.90	1.90
	Max	20.6	20.6		Max	2.15	2.15

Table 5.2 – ICP-AES results for Ca % and P %, calculated Ca/P $_{(atomic)}$ and calculated Ca/P $_{(weight)}$ obtained from bone specimens heated to 600 °C, including all species investigated (elephant and rat not investigated using this technique). Data presented as two groups: one that excludes human AUS and one that includes human AUS

The elements; sodium (Na), magnesium (Mg), potassium (K), strontium (Sr) and iron (Fe) were detected in all bone specimens (see Table 5.3). The order of these elements in decreasing amounts detected was Na > Mg > K > Sr > Fe in all cases, with the exception of the chicken bone specimen where Mg > Na.

		All Species (excl. human AUS)	**All Species** (incl. human AUS)			**All Species** (excl. human AUS)	**All Species** (incl. human AUS)
Number		15	18	**Number**		15	18
Na ppm	Mean	8902	8812	**Mg ppm**	Mean	5922	5611
	Std. Error	295	250		Std. Error	289	295
	Min	5878	5878		Min	3717	3685
	Max	10329	10329		Max	7575	7575
K ppm	Mean	1600	1393	**Sr ppm**	Mean	196	186
	Std. Error	355	315		Std. Error	23	20
	Min	389	168		Min	54	54
	Max	5946	5946		Max	351	351
				Fe ppm	Mean	18.8	18.4
					Std. Error	3.6	3.1
					Min	4.3	4.3
					Max	59.6	59.6

Table 5.3 – ICP-AES results for Na ppm, Mg ppm, K ppm, Sr ppm and Fe ppm obtained from bone specimens heated to 600 °C, including all species investigated (elephant and rat not investigated using this technique). Data presented as two groups: one that excludes human AUS and one that includes human AUS

5.3 – PYROHYDROLYSIS – ION CHROMATOGRAPHY OF BONE HEATED TO 600 °C

Fluorine (F) and chlorine (Cl) were detected in all bone specimens (see Table 5.4). The results obtained for the rabbit bone specimen were semi-quantitative due to the small amount of specimen available for analysis and so these results are not presented. In general, the amount of F detected was less than 450 ppm and the amount of Cl detected was greater than that of F for the same bone specimen. However, for the human bone specimens and the dog bone specimen, the F values obtained were all greater than 550 ppm and, in the case of the two human AUS bone specimens, the F values were greater than the Cl values obtained.

		All Species (excl. human AUS)	**All Species** (incl. human AUS)			**All Species** (excl. human AUS)	**All Species** (incl. human AUS)
Number		14	17	**Number**		14	17
F ppm	Mean	256	439	**Cl ppm**	Mean	673	640
	Std. Error	52	130		Std. Error	38	36
	Min	46	46		Min	450	435
	Max	722	2048		Max	967	967

Table 5.4 – P-IC results for F ppm and Cl ppm obtained from bone specimens heated to 600 °C, including all species investigated (elephant and rat not investigated using this technique). Data presented as two groups: one that excludes human AUS and one that includes human AUS

5.4 – COMBUSTION – GAS CHROMATOGRAPHY OF BONE HEATED TO 600 °C

The percentage of nitrogen (N) detected was less than 0.1 % for all bone specimens, with values of less than 0.05 % obtained for 67 % of bone specimens. Less than 1.5 % of carbon (C) was detected in all bone specimens. The expected percentage of hydrogen (H) in stoichiometic HAP is 0.2 % and in general, the percentage values obtained were less than this value (see Table 5.5).

		All Species (excl. human AUS)	**All Species** (incl. human AUS)			**All Species** (excl. human AUS)	**All Species** (incl. human AUS)
Number		15	18	**Number**		15	18
Total N %	Mean	0.034	0.035				
	Std. Error	0.005	0.004				
	Min	0.013	0.013				
	Max	0.062	0.062				
Total C %	Mean	0.873	0.921	**Total H %**	Mean	0.243	0.248
	Std. Error	0.047	0.047		Std. Error	0.010	0.009
	Min	0.470	0.470		Min	0.188	0.188
	Max	1.100	1.230		Max	0.313	0.313

Table 5.5 – C-GC results for C %, N % and H % obtained from bone specimens heated to 600 °C, including all species investigated (elephant and rat not investigated using this technique). Data presented as two groups: one that excludes human AUS and one that includes human AUS

5.5 – INFRARED SPECTROSCOPY OF BONE HEATED TO 600 °C

The presence of carbonate ions (CO_3^{2-}) was detected in all bone specimens analysed using IR spectroscopy. In general, weight percentage values were calculated to be between 1 % and 2 %. Phosphate ion splitting factor values (SF) of 3.5 to 5.6 were obtained for all bone specimens (see Table 5.6).

		All Species (excl. human AUS)	**All Species** (incl. human AUS)			**All Species** (excl. human AUS)	**All Species** (incl. human AUS)
Number		15	15	**Number**		15	15
CO_3 %	Mean	1.53	1.53	**Splitting Factor (SF)**	Mean	4.07	4.07
	Std. Error	0.12	0.12		Std. Error	0.13	0.13
	Min	0.59	0.59		Min	3.53	3.53
	Max	2.27	2.27		Max	5.53	5.53

Table 5.6 – IR spectroscopy results for CO_3 % and *SF* obtained from bone specimens heated to 600 °C, including all species investigated (elephant, rat and human AUS not investigated using this technique)

5.6 – MASS CHANGE ON HEATING

All heated bone specimens lost mass due to heat treatment, within the range of 27 – 60 % of their mass prior to heating (see Table 5.7). The mean percentage mass loss at 1400 °C was greater than that at 600 °C but the mass loss at 1400 °C was not always greater than that at 600 °C for bone from the same individual. The results suggest that the majority of mass loss from bone heated to 1400 °C occurs on heating bone between room temperature and 600 °C and that a gain in mass can occur within the temperature range of 600 °C to 1400 °C. However, these suggestions are tentative as two different bone specimens from the same individual were used to measure mass change on heating to each temperature and mass change was not measured in situ during heating.

		All Species (excl. human AUS)	**All Species** (incl. human AUS)			**All Species** (excl. human AUS)	**All Species** (incl. human AUS)
Number		73	123	**Number**		73	123
Mass Loss % 600 °C	Mean	37.100	37.706	**Mass Loss %** 1400 °C	Mean	39.650	40.991
	Std. Error	0.743	0.476		Std. Error	0.506	0.351
	Min	27.700	27.700		Min	31.878	31.878
	Max	57.542	57.542		Max	51.768	51.768

Table 5.7 – Mass change results for mass change on heating bone specimens to 600 °C and on heating bone specimens to 1400 °C, including all species investigated. Data presented as two groups: one that excludes human AUS and one that includes human AUS

5.7 – X-RAY DIFFRACTION ANALYSIS OF BONE HEATED TO 600 °C

5.7.1 – CALCIUM HYDROXYLAPATITE (HAP)

Calcium hydroxylapatite (HAP) was detected in all heated bone specimens (see Table 5.8). In general, the HAP diffraction peaks from heated bone specimens appeared to be more resolved than those from unheated bone specimens from the same individual (see appendix).

Values of HAP <00ℓ> greater than 200 Å were obtained for all bone specimens heated to 600 °C. These values were therefore all greater than the minimum value of HAP <00ℓ> obtained for unheated bone specimens. Also, the maximum value of HAP <00ℓ> obtained for bone specimens heated to 600 °C was approximately 2.5 times the magnitude of the maximum value obtained for unheated bone specimens. However, in general, there was little difference between the values obtained for unheated and heated bone specimens from the same individual (see Table 5.1 and Table 5.8).

Values of less than 9.420 Å were obtained for HAP ‘a’ for 75 % of the bone specimens heated to 600 °C. All values obtained for HAP ‘c’, for bone specimens heated to 600 °C were above 6.880 Å, with the exception of one chicken bone specimen. In general, values of HAP ‘a’ and HAP ‘c’ obtained from bone specimens heated to 600 °C, were less than values obtained for unheated bone specimens corresponding to the same individual. Also, a smaller

range of values was obtained for heated bone specimens compared to that obtained for unheated bone specimens, for both HAP lattice parameters (see Table 5.1, Table 5.8 and Table 5.10).

		All Species (excl. human AUS)	**All Species** (incl. human AUS)			**All Species** (excl. human AUS)	**All Species** (incl. human AUS)
Number		73	123	**Number**		73	123
HAP %	Mean	98.90	99.35	**HAP a (Å)**	Mean	9.415	9.416
	Std. Error	0.33	0.20		Std. Error	0.001	0.001
	Min	86.08	86.08		Min	9.402	9.402
	Max	100.00	100.00		Max	9.430	9.437
HAP <00ℓ> (nm)	Mean	26.93	25.74	**HAP c (Å)**	Mean	6.886	6.890
	Std. Error	1.06	0.65		Std. Error	0.000	0.000
	Min	20.09	20.09		Min	6.880	6.880
	Max	72.27	72.27		Max	6.897	6.900

Table 5.8 – XRD analysis results for HAP %, HAP <00ℓ>, HAP 'a', and HAP 'c' obtained from bone specimens heated to 600 °C, including all species investigated. Data presented as two groups: one that excludes human AUS and one that includes human AUS

5.7.2 – ADDITIONAL MINERAL PHASES (β-TCP AND MgO)

In general, calcium hydroxylapatite was the only mineral phase detected in bone specimens heated to 600 °C (see Table 5.8 and Table 5.9). Exceptionally, β-tri-calcium phosphate (β-TCP) was detected in 9 % of bone specimens heated to 600 °C and magnesium oxide (MgO) was detected in 2 bone specimens heated to 600 °C (in less than 2% of specimens). The mineral phases of β-TCP and MgO were not detected in the same bone specimens. For bone specimens in which β-TCP was detected, the percentage detected in each specimen was less than 15 % and for those in which MgO was detected, the percentage was less than 1 %.

Magnesium oxide is not routinely reported as a thermal decomposition product of bone mineral [145]. Evidence for the presence of this phase has therefore been presented in Figure 5.1 and a stick representation the expected diffractograms for MgO showing the five most intense peaks is presented in Figure A.36 within the appendix.

		All Species (excl. human AUS)	All Species (incl. human AUS)			All Species (excl. human AUS)	All Species (incl. human AUS)
Number		73	123	**Number**		73	123
β-TCP %	No. Det	11	11	**MgO %**	No. Det	2	2
	Mean	7.15	7.15		Mean	0.77	0.77
	Std. Error	1.01	1.01		Std. Error	0.05	0.05
	Min	3.13	3.13		Min	0.72	0.72
	Max	13.92	13.92		Max	0.82	0.82
β-TCP a (Å)	Mean	10.370	10.370	**β-TCP c (Å)**	Mean	37.167	37.167
	Std. Error	0.003	0.003		Std. Error	0.005	0.005
	Min	10.352	10.352		Min	37.135	37.135
	Max	10.393	10.393		Max	37.193	37.193

Table 5.9 – XRD analysis results for β-TCP and MgO obtained from bone specimens heated to 600 °C, including all species investigated. Data presented as two groups: one that excludes human AUS and one that includes human AUS

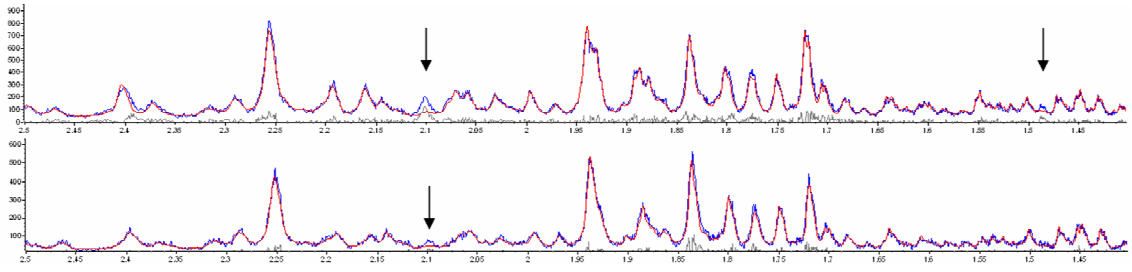

Figure 5.1 – X-ray diffractograms from bone specimens heated to 1400 °C showing evidence for detection of MgO presented using Topas software. XRD data is represented by the blue line, the Rietveld refinement data is represented by the red line. Rietveld refinement has been carried out for all mineral phases except MgO in order to highlight MgO peaks (indicated by arrows). A weight percentage of 0.36 % MgO was obtained from the lower diffractogram (peak at approximately 1.38 d-spacing is not observed due to low weight percentage of MgO) and 1.4 % MgO was obtained from the upper diffractogram

5.8 – X-RAY DIFFRACTION ANALYSIS OF BONE HEATED TO 1400 °C

5.8.1 – CALCIUM HYDROXYLAPATITE (HAP)

HAP was detected in all bone specimens heated to 1400 °C and the percentage detected was greater than 20 % in all cases. However, a percentage of less than 50 % was detected for 80 % of bone specimens (see Table 5.10).

Values of less than 9.420 Å were obtained for HAP ‘a’ for all bone specimens heated to 1400 °C, with the exception of two human AUS bone specimens and one human UK bone specimen. However, the values obtained for HAP ‘c’ were all greater than 6.880 Å (see Table 5.10).

		All Species (excl. human AUS)	All Species (incl. human AUS)			All Species (excl. human AUS)	All Species (incl. human AUS)
Number		73	123	**Number**		73	123
HAP %	Mean	42.48	41.04				
	Std. Error	1.16	0.86				
	Min	22.22	22.22				
	Max	72.33	72.33				
HAP a (Å)	Mean	9.414	9.413	**HAP c (Å)**	Mean	6.888	6.891
	Std. Error	0.000	0.000		Std. Error	0.001	0.000
	Min	9.400	9.400		Min	6.882	6.882
	Max	9.423	9.423		Max	6.900	6.901

Table 5.10 – XRD analysis results for HAP %, HAP 'a' and HAP 'c' obtained from bone specimens heated to 1400 °C, including all species investigated. Data presented as two groups: one that excludes human AUS and one that includes human AUS

5.8.2 – ADDITIONAL MINERAL PHASES (β-TCP AND MgO)

The mineral phases of β-tri-calcium phosphate (β-TCP) and magnesium oxide (MgO) were detected in all bone specimens heated to 1400 °C (Table 5.11). The percentage of MgO detected was less than 1.5 % in each case and was less than 1 % for 80 % of bone specimens. It was therefore identified as a minor phase for all bone specimens.

The percentage of β-TCP detected was at least 8 % for all bone specimens and in general (for 89 % of bone specimens), was between 20 % and 50 %. It was

therefore identified as a major phase for the majority of bone specimens heated to 1400 °C. Also, for bone specimens heated to 600 °C, in which β-TCP was detected, a greater percentage of β-TCP was detected in the bone specimen heated to 1400 °C, corresponding to the same individual. All values obtained for β-TCP 'a' for bone specimens heated to 1400 °C were greater than the maximum value obtained for all bone specimens heated to 600 °C. This was also found to be the case for values of β-TCP 'c' (see Table 5.11).

		All Species (excl. human AUS)	**All Species** (incl. human AUS)			**All Species** (excl. human AUS)	**All Species** (incl. human AUS)
Number		73	123	**Number**		73	123
β-TCP %	Mean	39.91	36.79	**MgO %**	Mean	0.87	0.78
	Std. Error	1.10	0.88		Std. Error	0.03	0.02
	Min	13.37	8.90		Min	0.36	0.36
	Max	60.34	60.34		Max	1.40	1.40
β-TCP a (Å)	Mean	10.440	10.442	**β-TCP c (Å)**	Mean	37.327	37.331
	Std. Error	0.000	0.000		Std. Error	0.001	0.001
	Min	10.428	10.428		Min	37.304	37.304
	Max	10.448	10.450		Max	37.351	37.372

Table 5.11 – XRD analysis results for β-TCP and MgO obtained from bone specimens heated to 1400 °C, including all species investigated. Data presented as two groups: one that excludes human AUS and one that includes human AUS

5.8.3 – ADDITIONAL MINERAL PHASES (TTCP, CaO AND α-TCP)

The mineral phases of tetra-calcium phosphate (TTCP) and calcium oxide (CaO) were detected in the majority of bone specimens heated to 1400 °C (approximately 98 % and 88 % respectively). However, the mineral phase; α-tri-calcium phosphate (α-TCP) was generally not detected in bone specimens heated to 1400 °C; it was detected in only 7 % of bone specimens (see Table 5.12). TTCP ranged from detection as a minor phase (values of < 10 %) to a major phase. However, the percentage of TTCP detected was less than 40 % for all bone specimens. The mineral phase; α-TCP also ranged from detection as a minor phase to a major phase, whereas, CaO was only identified as a minor phase, when detected, as all percentage values obtained were less than 1.5 % (see Table 5.12).

		All Species (excl. human AUS)	All Species (incl. human AUS)			All Species (excl. human AUS)	All Species (incl. human AUS)
Number		73	123	**Number**		73	123
α-TCP %	No. Det	7	9				
	Mean	8.65	7.63				
	Std. Error	2.63	2.15				
	Min	1.43	1.43				
	Max	19.57	19.57				
TTCP %	No. Det	71	121	**CaO %**	No. Det	62	108
	Mean	15.60	20.45		Mean	0.86	0.81
	Std. Error	1.14	0.94		Std. Error	0.03	0.02
	Min	1.96	1.96		Min	0.31	0.31
	Max	39.72	39.72		Max	1.39	1.39

Table 5.12 – XRD analysis results for TTCP, CaO and α-TCP obtained from bone specimens heated to 600 °C, including all species investigated. Data presented as two groups: one that excludes human AUS and one that includes human AUS

5.9 – INTER-SPECIES VARIATION

5.9.1 – STATISTICAL SIGNIFICANCE OF INTER-SPECIES VARIATION

For a selection of bone mineral characteristics measured using X-ray diffraction and, for mass change results, each difference between the mean value of each species group and the mean value of every other species group was tested to determine its statistical significance (see section 4.10). The results of these tests are presented in Figure 5.2 and are referred to throughout this section. Figure 5.2 consists of an array of squares. Each square represents the result of a significance test between two species for a particular bone mineral characteristic. The position of each box within the figure relates to the bone mineral characteristic and the species tested. Where boxes are labelled with an ‘X’, no test was carried out (see section 4.10). Level of significance is indicated by the shading of each box and a black box indicates a significant difference between two species at the level of $p < 0.01$.

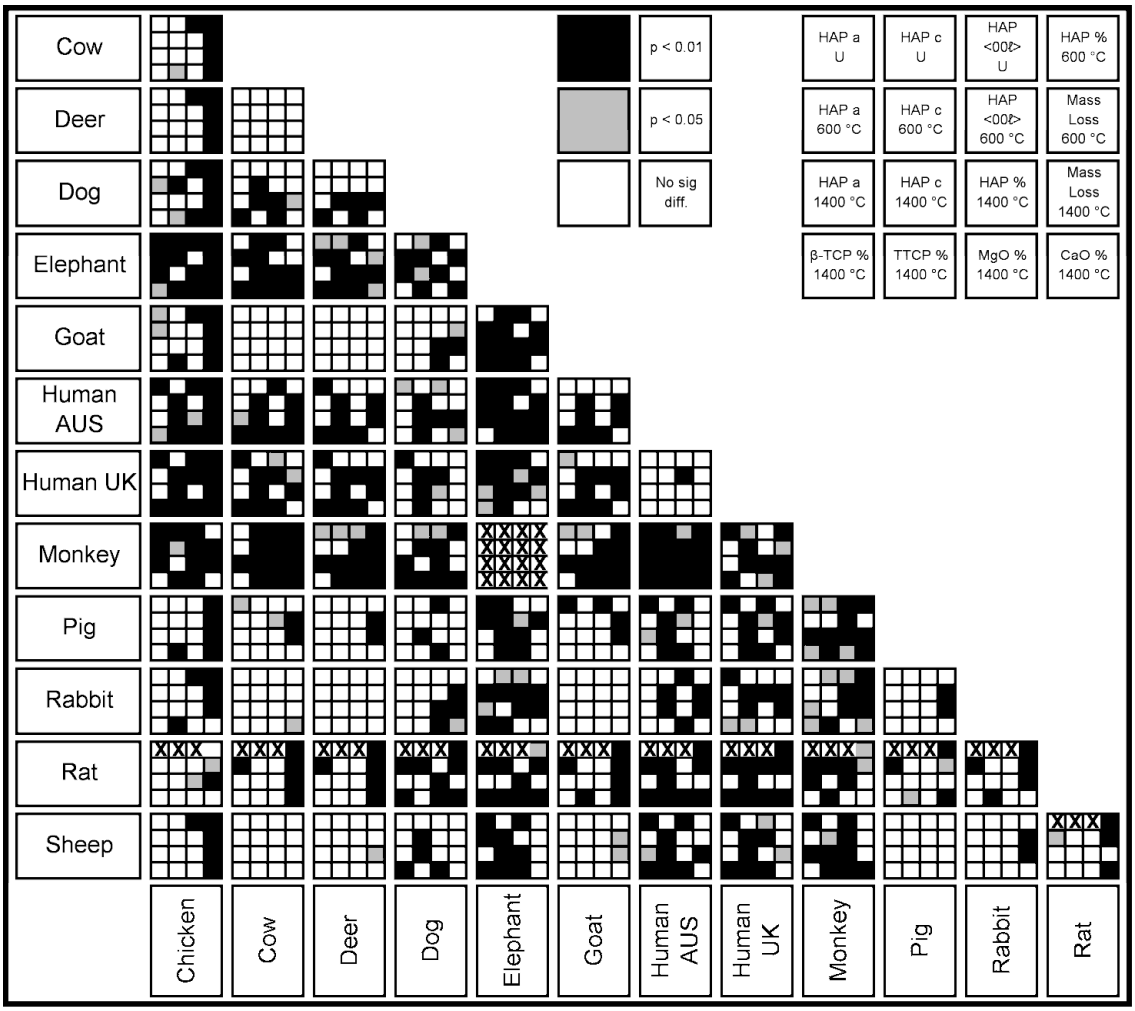

Figure 5.2 – Results of Bonferroni ANOVA post-hoc tests for statistical significance of inter-species variation for a selection of bone mineral characteristics measured using X-ray diffraction analysis and for mass change on heating. Results presented for elephant and monkey represent one individual from each species and one sample t-tests were carried out for these species. An 'X' within a box indicates that no test was carried out for the corresponding species pair for a particular bone mineral characteristic due to absence of data or insufficient data

In general, species groups were significantly different from other species studied, in terms of at least one bone mineral characteristic. Overall, elephant, monkey, human UK and human AUS had a greater number of significant differences at the level of $p < 0.01$ compared to the other species studied. Elephant bone had the highest mean number of significant differences at this level, per species comparison, followed by monkey bone and human bone. However, results for elephant and monkey are based on one individual of each species and so the results may not be significant in terms of larger sample sets of bone specimens from these two species. A greater mean number of significant differences was obtained for human AUS than for human UK. Deer and cow had a smaller number of significant differences than all other species studied. Deer had the lowest mean number of significant differences at the level of $p < 0.01$ per species comparison.

There were several species for which there were no significant differences for any characteristics when compared with another species group, such as cow and goat. Furthermore, no single characteristic was shown to be significantly different for all species comparisons. Neither were groups of characteristics, grouped as unheated, 600 °C and 1400 °C characteristics, shown to be significantly different for all species comparisons at the level of $p < 0.01$. However, there were several comparison pairs of species that were significantly different in terms of all characteristics within a group. For example, human UK was significantly different ($p < 0.01$) to elephant for all unheated bone mineral characteristics.

5.9.2 – X-RAY DIFFRACTION ANALYSIS OF UNHEATED BONE

There was no variation observed in the percentage of HAP detected in unheated bone specimens, as HAP was the only mineral phase detected in all cases. However, inter-species variation was observed for other measured characteristics of the HAP mineral phase.

The values obtained for HAP <00ℓ> for chicken bone specimens were significantly less ($p < 0.01$) than the values obtained for unheated bone specimens from all other species, with the exception of pig (see Figure 5.3). The values obtained for all bone specimens from chicken, pig and elephant were all less than 231 Å whereas values above this were obtained for at least one individual from each species, for all other species studied. Values of HAP <00ℓ> greater than 260 Å were only observed for dog, goat and human and values greater than 280 Å were only observed for human. Furthermore, the range of values obtained for human did not overlap with the ranges of values obtained for chicken and pig. Similar mean values and ranges of values were obtained for HAP <00ℓ> for the human UK and human AUS groups (see Figure 5.3).

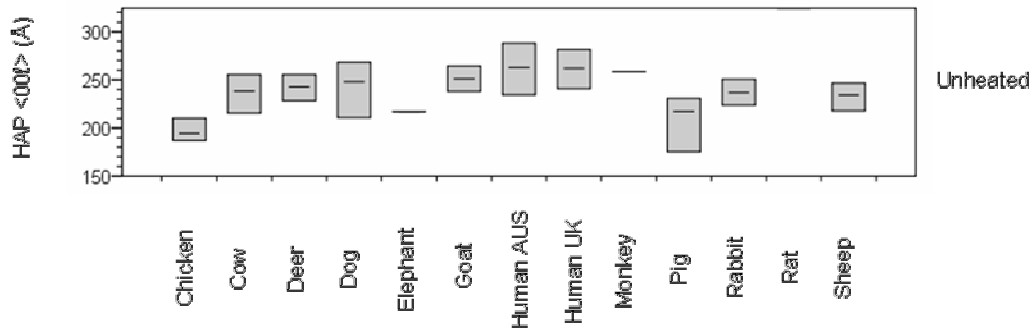

Figure 5.3 – XRD analysis results for HAP <00ℓ> obtained from unheated bone specimens, grouped by species, showing mean (line within a box), minimum (lower limit of a box) and maximum (upper limit of a box) values. Unheated rat bone was not investigated and data presented for elephant and monkey represents one individual from each species

The values obtained for HAP 'a' for chicken, deer, elephant, monkey, pig and sheep were all above 9.46 Å (see Figure 5.4). However, the highest mean values were obtained for chicken and pig. Furthermore, the values obtained for HAP 'a' for chicken and pig were significantly greater ($p < 0.01$) than those obtained for elephant and monkey ($p < 0.05$ for pig and monkey). Values of less than 9.43 Å for HAP 'a' were only obtained for human bone. The values obtained for human UK were significantly less ($p < 0.01$) than those of all other species, with the exceptions of human AUS bone (no significant difference) and goat bone ($p < 0.05$).

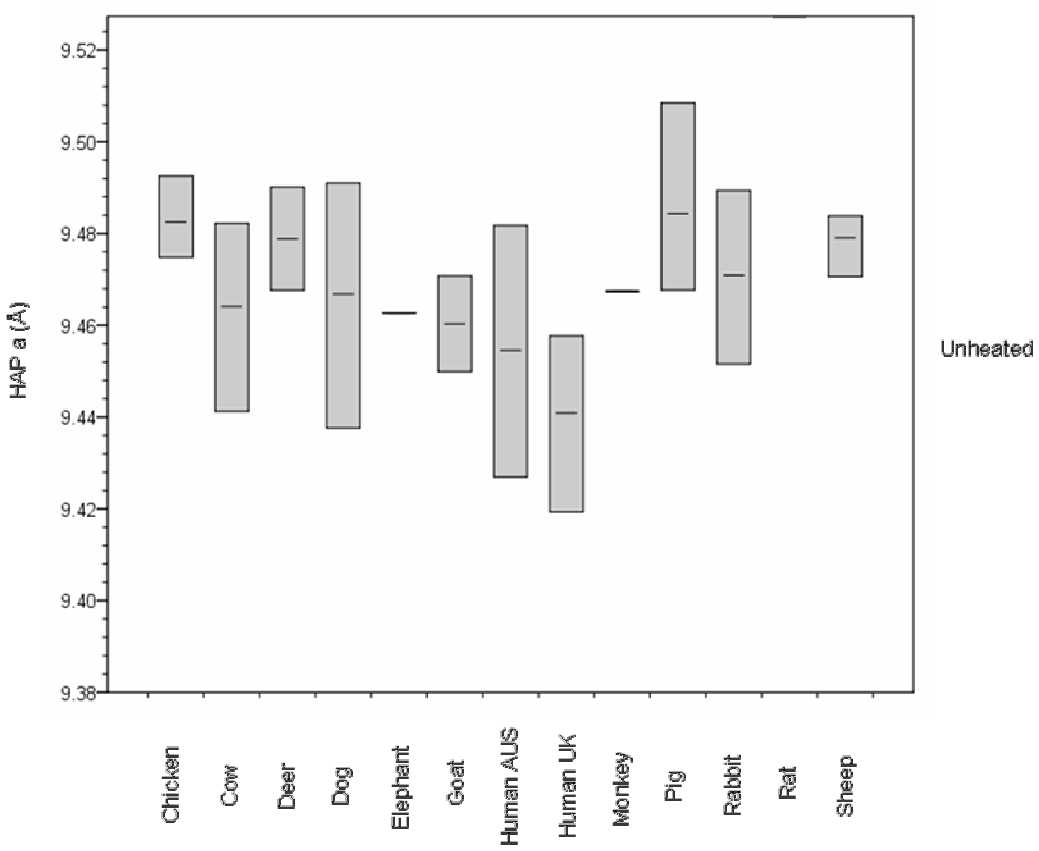

Figure 5.4 – XRD analysis results for HAP 'a' obtained from unheated bone specimens, grouped by species, showing mean (line within a box), minimum (lower limit of a box) and maximum (upper limit of a box) values. Unheated rat bone rat was not investigated and data presented for elephant and monkey represents one individual from each species

There was less variation in the values obtained for HAP 'c' for unheated bone specimens compared to those obtained for HAP 'a' both in terms of the overall range of values obtained and also inter-species variation (see Figure 5.4 and Figure 5.5). The greatest range of values for HAP 'c' was obtained for human AUS. This range encompassed the maximum and minimum values obtained for all bone specimens from all species and was considerably greater than the

range obtained for human UK. The lowest mean value was obtained for chicken and the greatest mean value was obtained for goat, although the values obtained for elephant and monkey were both greater than the goat mean value. The values obtained for HAP ‘c’ for elephant and monkey were significantly greater ($p < 0.01$) than the majority of the other species but there were no other significant differences between species (see Figure 5.2).

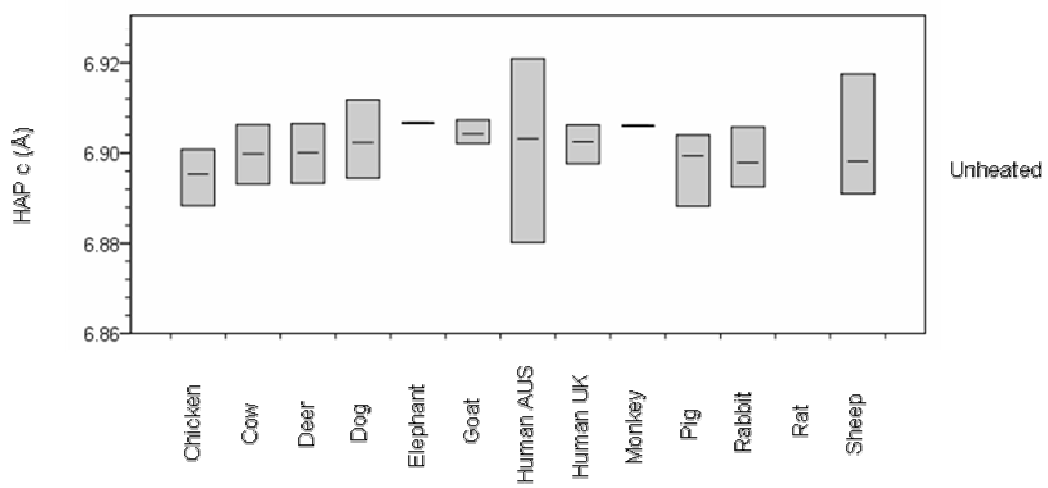

Figure 5.5 – XRD analysis results for HAP ‘c’ obtained from unheated bone specimens, grouped by species, showing mean (line within a box), minimum (lower limit of a box) and maximum (upper limit of a box) values. Unheated rat bone rat was not investigated and data presented for elephant and monkey represents one individual from each species

5.9.3 – INDUCTIVELY COUPLED PLASMA – ATOMIC EMISSION SPECTROMETRY OF BONE HEATED TO 600 °C

A weight percentage of calcium greater than 42 % was obtained for rabbit (see Figure 5.6). Values lower than 42 % were obtained for all other species investigated and the lowest weight percentage value was obtained for dog. The greatest value for the weight percentage of phosphorous was also obtained for rabbit bone. Values of 20 % or greater were only obtained for rabbit, chicken and cow. The relatively high phosphorous and low calcium composition of chicken and cow bone resulted in a lower Ca/P ratio for these species (Ca/P both less than 1.55), compared to the other species investigated (Ca/P all greater than 1.55). Due to the combined measure nature of Ca/P values, there was less inter-species variation for this characteristic compared with the variation observed for each ratio component.

Values obtained for the weight percentage of sodium were greater than 7500 ppm for all species; with the exception of chicken for which a much lower value was obtained. The next lowest value was obtained for sheep bone. The highest value obtained was for human UK bone. However, there were differences of approximately 2000 ppm between the human UK value and those obtained for human AUS bone.

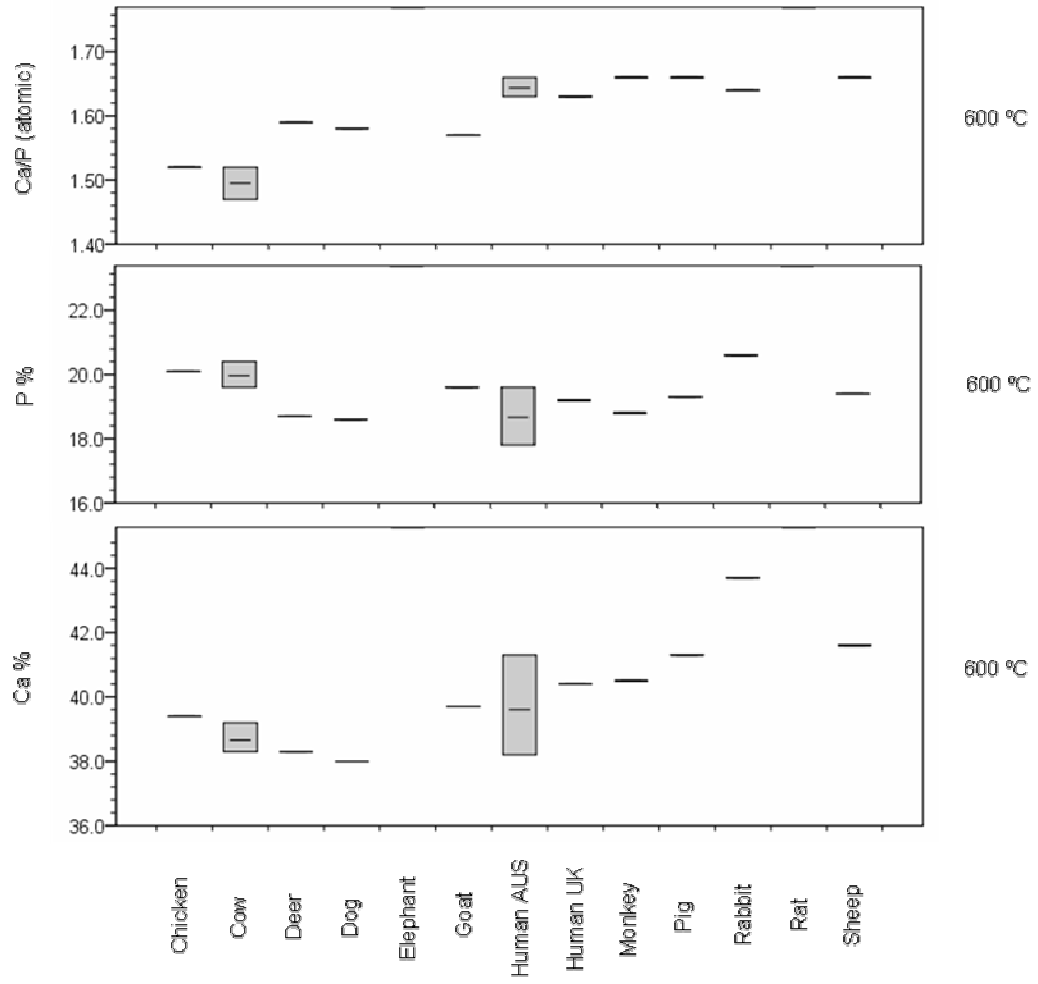

Figure 5.6 – ICP-AES results for Ca %, P % and calculated Ca/P $_{(atomic)}$ obtained from bone specimens heated to 600 °C, grouped by species. Data for one individual from each species presented with the exception of cow and human AUS (mean (line within a box), minimum (lower limit of a box) and maximum (upper limit of a box) values shown for these species) and elephant and rat which were not investigated using this technique

The values obtained for the weight percentage of magnesium appear, from Figure 5.7, to be in general, negatively correlated with corresponding values obtained for the weight percentage of sodium. Chicken and sheep, which had the lowest sodium values, had the greatest magnesium values and the human UK bone specimen, which had the greatest sodium value, had one of the lowest magnesium values. However, exceptions to this general trend are evident. The magnesium values obtained for cow and goat were greater than would be expected based on the observed trend whereas values obtained for human AUS and dog were less than would be expected.

Similar to the results obtained for the weight percentage values of magnesium, the greatest values obtained for the weight percentage of potassium were for chicken and sheep. The value obtained for chicken was approximately twice the value that was obtained for sheep and was approximately 3 – 6 times greater than the values obtained for all other species. The values obtained for human bone were less than those obtained for any other species.

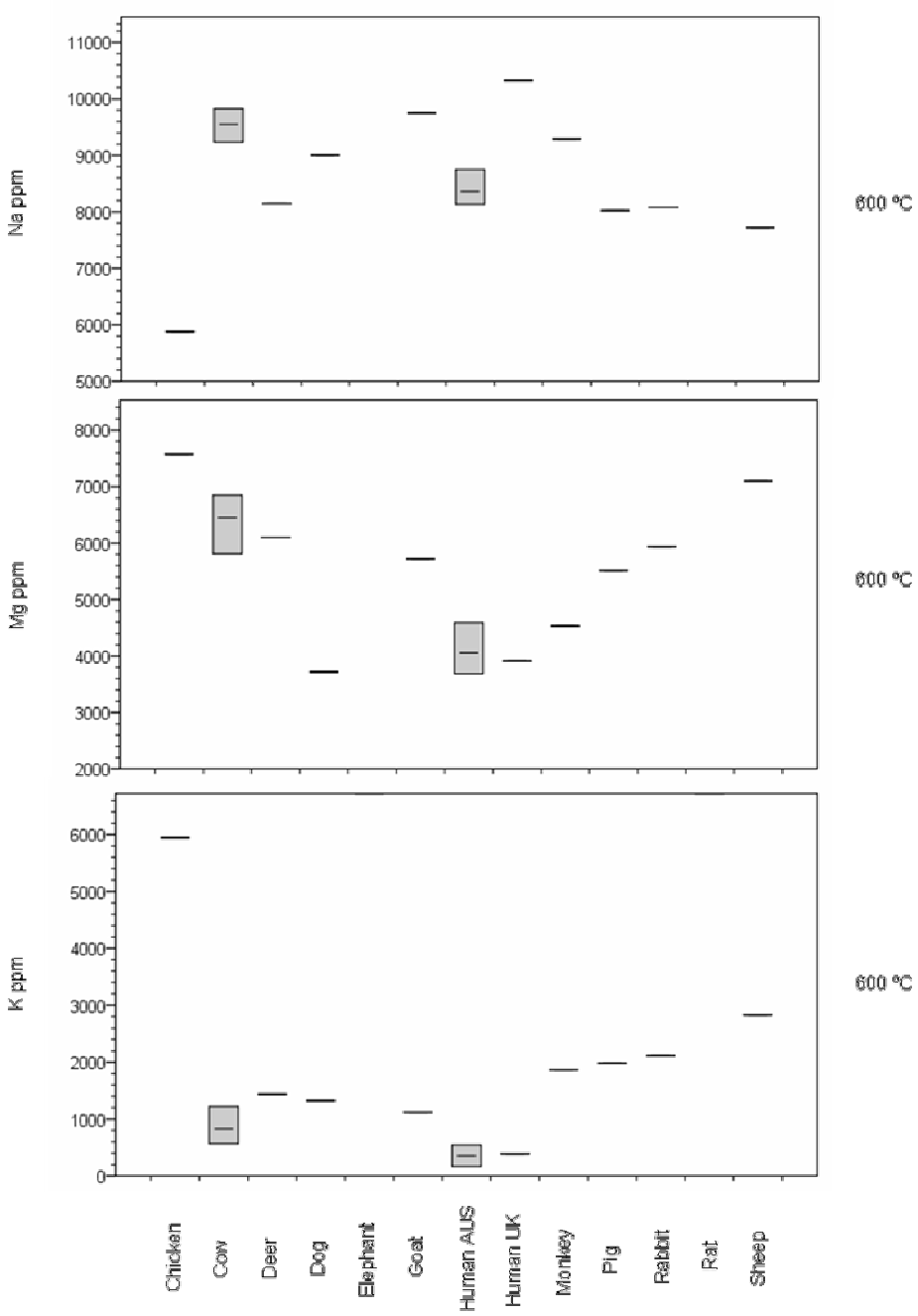

Figure 5.7 – ICP-AES results for K ppm, Mg ppm and Na ppm obtained from bone specimens heated to 600 °C, grouped by species. Data for one individual from each species presented with the exception of cow and human AUS (mean (line within a box), minimum (lower limit of a box) and maximum (upper limit of a box) values shown for these species) and elephant and rat which were not investigated using this technique

Two groups of species were apparent in terms of the values obtained for the weight percentage of strontium (see Figure 5.8). Values greater than 200 ppm were obtained for chicken, cow, deer, goat and rabbit whilst values less than this were obtained for all other species. However, a relatively large intra-species range of variation was observed for cow, for which the highest value was obtained but also, for which values less than 200 ppm were also obtained.

The greatest value for the weight percentage of iron was obtained for chicken and the lowest value was obtained for pig (see Figure 5.8). Although similar results were obtained for chicken and sheep in terms of the values obtained for sodium, magnesium and potassium compared to those for other species, these two species were dissimilar in terms of values obtained for strontium and iron. Relatively low values were obtained for sheep whereas relatively high values were obtained for chicken.

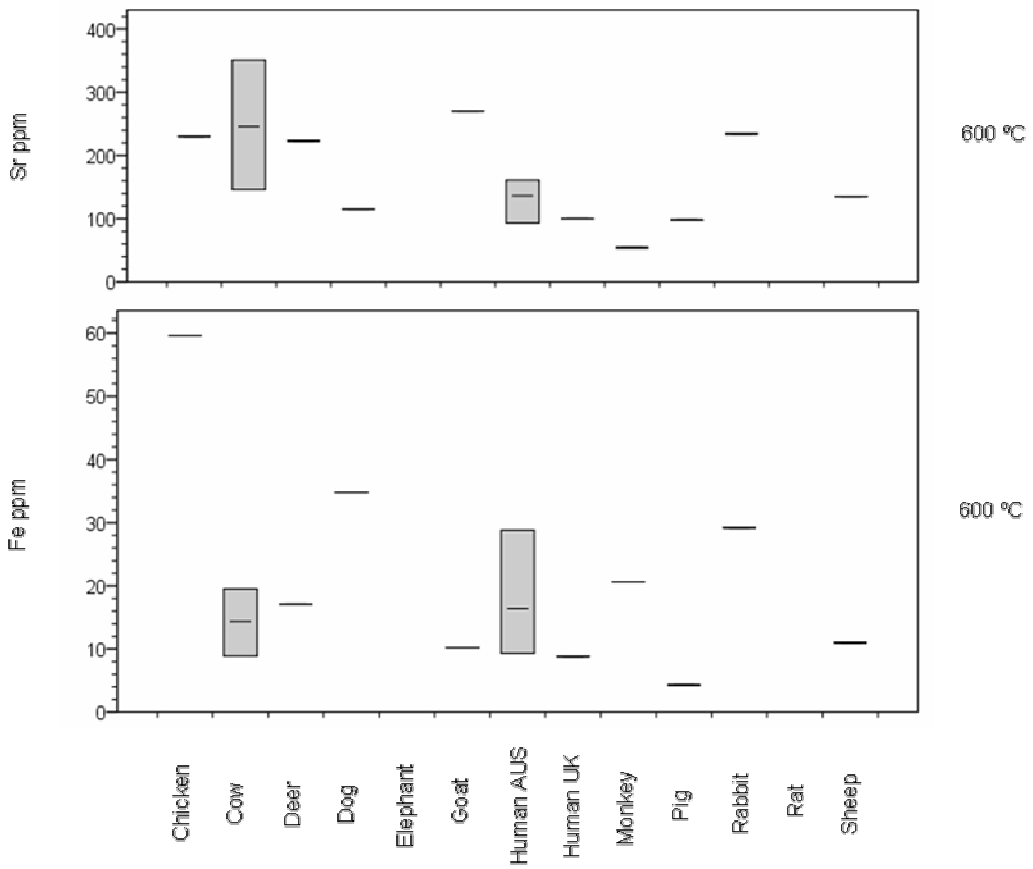

Figure 5.8 – ICP-AES results for Fe ppm and Sr ppm obtained from bone specimens heated to 600 °C, grouped by species. Data for one individual from each species presented with the exception of cow and human AUS (mean (line within a box), minimum (lower limit of a box) and maximum (upper limit of a box) values shown for these species) and elephant and rat which were not investigated using this technique

5.9.4 – PYROHYDROLYSIS – ION CHROMATOGRAPHY OF BONE HEATED TO 600 °C

The highest values for the percentage of fluorine detected were obtained for human and dog (see Figure 5.9). Values greater than 750 ppm were only obtained for human AUS. The lowest value was obtained for pig. The highest value for the percentage of chlorine was obtained for goat and the lowest values were obtained for human AUS and deer. A relatively low value was obtained for pig and the intra-species range obtained for cow was large. However, there was little variation between any other species; all other values were within the range of 700 – 750 ppm.

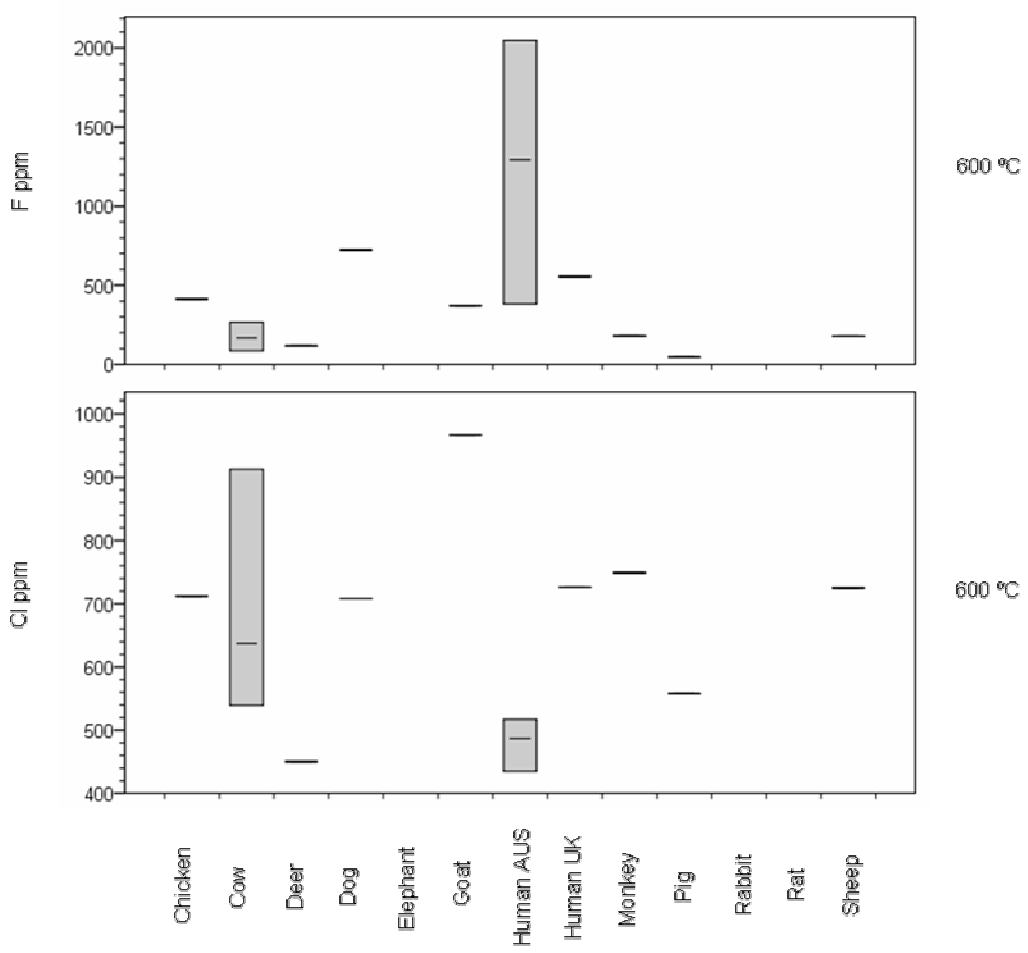

Figure 5.9 – P-IC results for Cl ppm and F ppm obtained from bone specimens heated to 600 °C, grouped by species. Data for one individual from each species presented with the exception of cow and human AUS (mean (line within a box), minimum (lower limit of a box) and maximum (upper limit of a box) values shown for these species), elephant and rat which were not investigated using this technique and rabbit, for which semi-quantitative results were obtained

5.9.5 – COMBUSTION – GAS CHROMATOGRAPHY OF BONE HEATED TO 600 °C

The lowest value for the weight percentage of carbon was obtained for chicken (see Figure 5.10). This value was less than 0.5 % and values greater than 0.5 % were obtained for all other species. A relatively low value was also obtained for sheep and values greater than 1 % were only obtained for human, cow and dog. The lowest value for the weight percentage of nitrogen was obtained for rabbit. However, overall there was little inter-species variation in the values obtained. Cow and human AUS were distinctive from all other species for the high values obtained and were the only species for which values greater than 0.3 % were obtained. Similar to the results obtained for the weight percentage of nitrogen, the greatest values for the weight percentage of hydrogen were obtained for cow, human AUS and dog. The lowest values (less than 0.2%) were obtained for monkey, human UK and rabbit. Differences between human UK and human AUS are evident, from Figure 5.10, in terms of the weight percentage values obtained for nitrogen, carbon and hydrogen, with greater values obtained for human AUS for each characteristic.

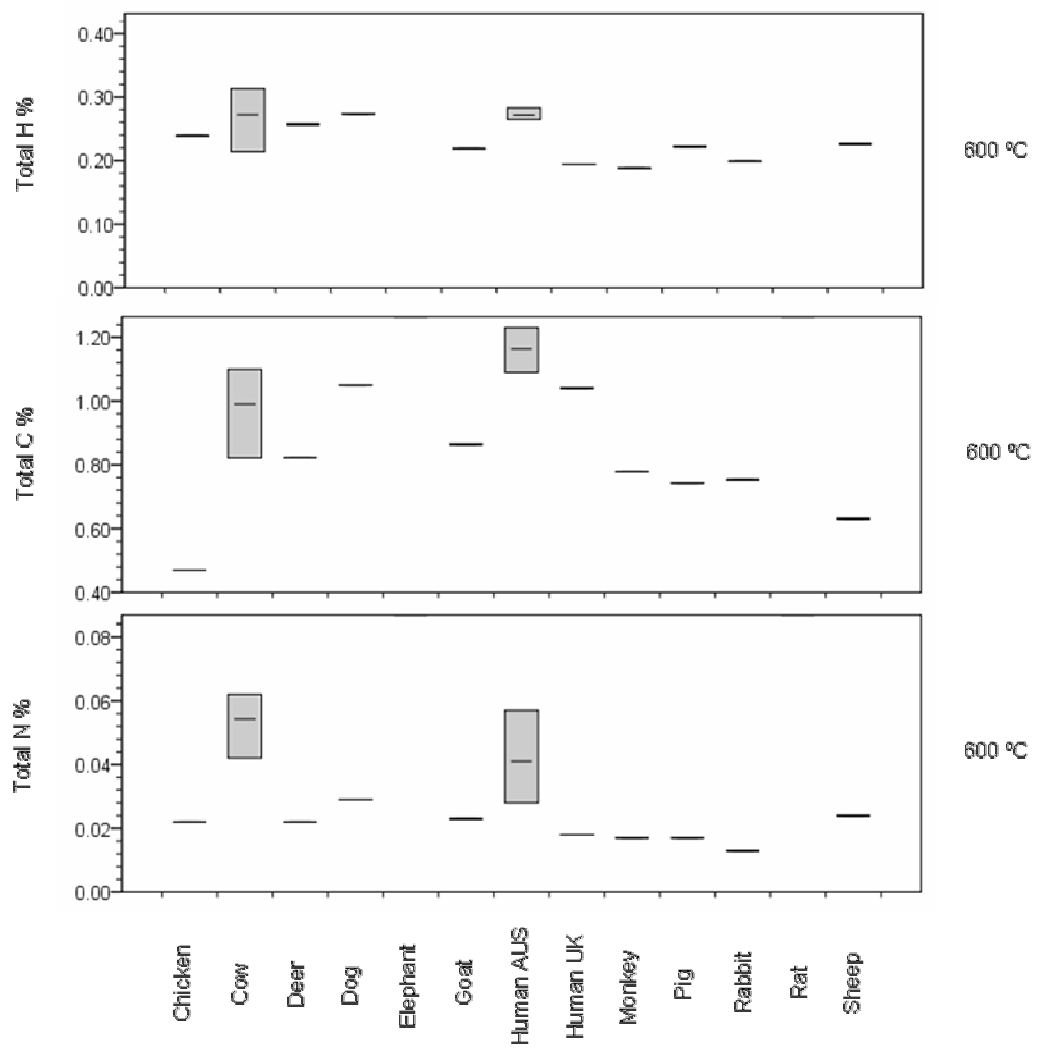

Figure 5.10 – C-GC results for N %, C % and H % obtained from bone specimens heated to 600 °C, grouped by species. Data for one individual from each species presented with the exception of cow and human AUS (mean (line within a box), minimum (lower limit of a box) and maximum (upper limit of a box) values shown for these species) and elephant and rat which were not investigated using this technique

5.9.6 – INFRARED SPECTROSCOPY OF BONE HEATED TO 600 °C

The highest value for the weight percentage of carbonate ions was obtained for cow, followed by relatively high values obtained for monkey, rabbit and dog (see Figure 5.11). Pig was the only species, for which a value less than 0.8 % was obtained. The highest value for the phosphate ion splitting factor was obtained for monkey (see Figure 5.12). This value was greater than 5.0, whereas values less than 5.0 were obtained for all other species. The lowest value was obtained for cow.

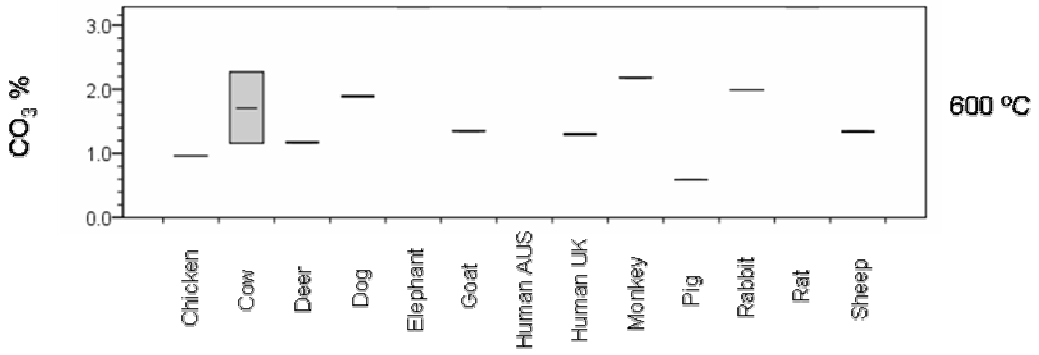

Figure 5.11 – IR spectroscopy results for CO_3 % obtained from bone specimens heated to 600 °C, grouped by species. Data for one individual from each species presented with the exception of cow (mean (line within a box), minimum (lower limit of a box) and maximum (upper limit of a box) values shown for this species) and elephant, human AUS and rat which were not investigated using this technique

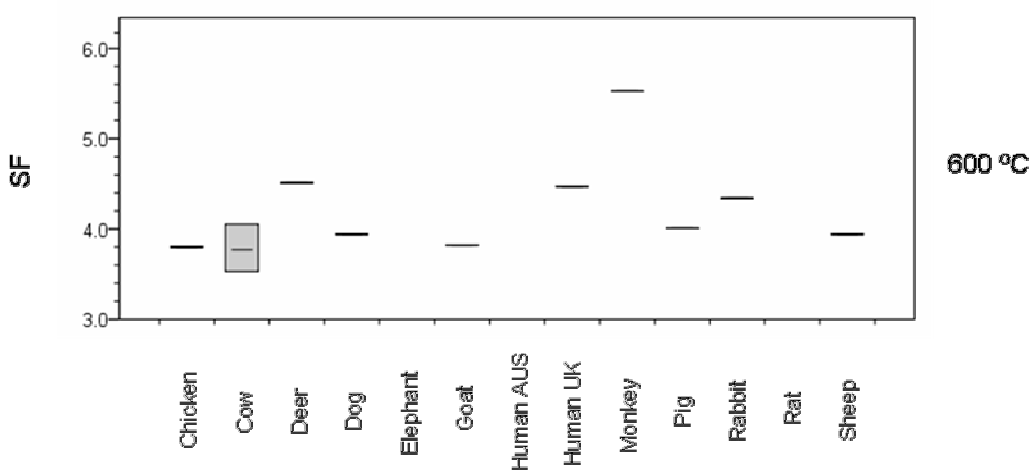

Figure 5.12 – IR spectroscopy results for phosphate splitting factor (*SF*) obtained from bone specimens heated to 600 °C, grouped by species. Data for one individual from each species presented with the exception of cow (mean (line within a box), minimum (lower limit of a box) and maximum (upper limit of a box) values shown for this species) and elephant, human AUS and rat which were not investigated using this technique

5.9.7 – MASS CHANGE ON HEATING

All chicken bone specimens heated to 600 °C lost over 49 % of their mass on heating. The mass loss from bone specimens from all other species was less than 47 %, with the exception of one rat and one human AUS bone specimen. Only deer, goat and rabbit species had bone specimens which lost less than 30 % of their mass, on heating. Rabbit had the lowest mean mass loss value and the range obtained for rabbit did not overlap with the range obtained for the majority of the other species (see Figure 5.13)

The relative inter-species distribution of mass loss values for bone heated to 1400 °C was similar to that observed for mass loss values for bone heated to 600 °C (see Figure 5.13 and Figure 5.14). For example, the relative inter-species trend of mass loss values for chicken, cow, deer and dog bone specimens heated to 600 °C was also observed for bone specimens heated to 1400 °C for these species. However, there was less intra-species variation observed for mass loss values for bone heated to 1400 °C compared to the variation observed for bone heated to 600 °C. Furthermore, mass loss values for bone heated to 1400 °C that were less than the corresponding value obtained for the same individual for bone heated to 600 °C, for chicken, rat, pig, sheep and human AUS, suggestive of mass gain on heating for these individuals (see Figure 5.14).

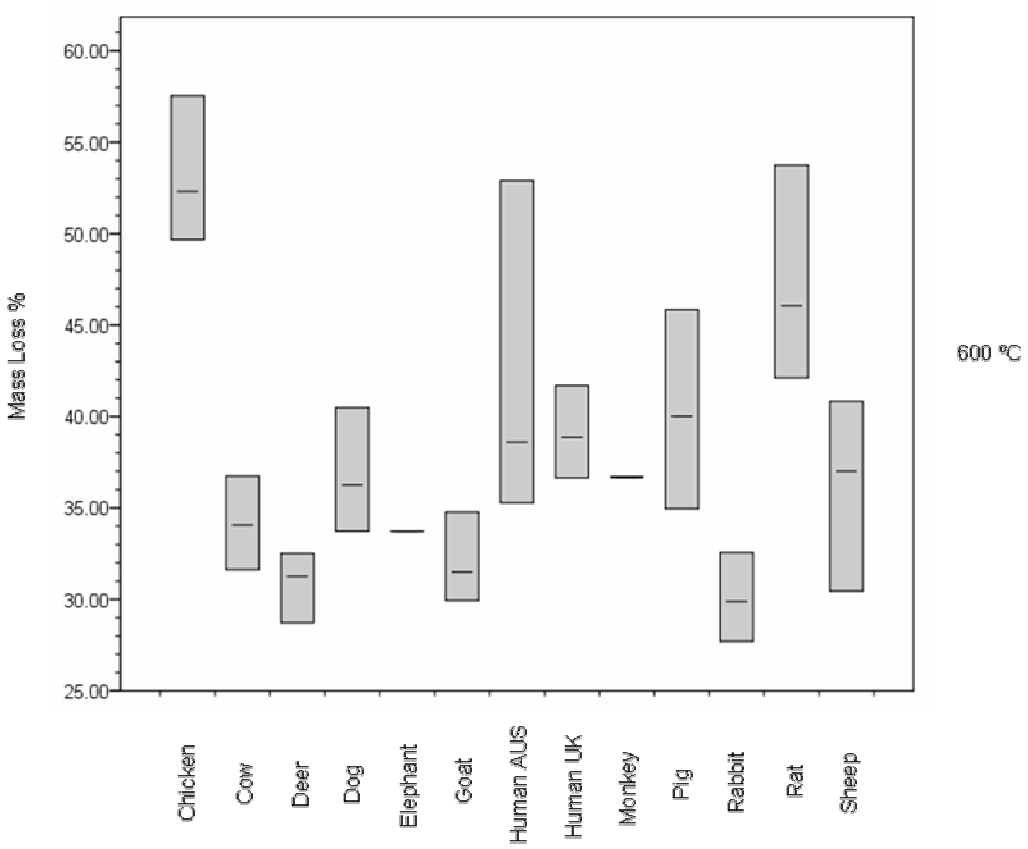

Figure 5.13 – Mass change results for mass change on heating bone specimens to 600 °C, grouped by species, showing mean (line within a box), minimum (lower limit of a box) and maximum (upper limit of a box) values. Data presented for elephant and monkey represents one individual from each species

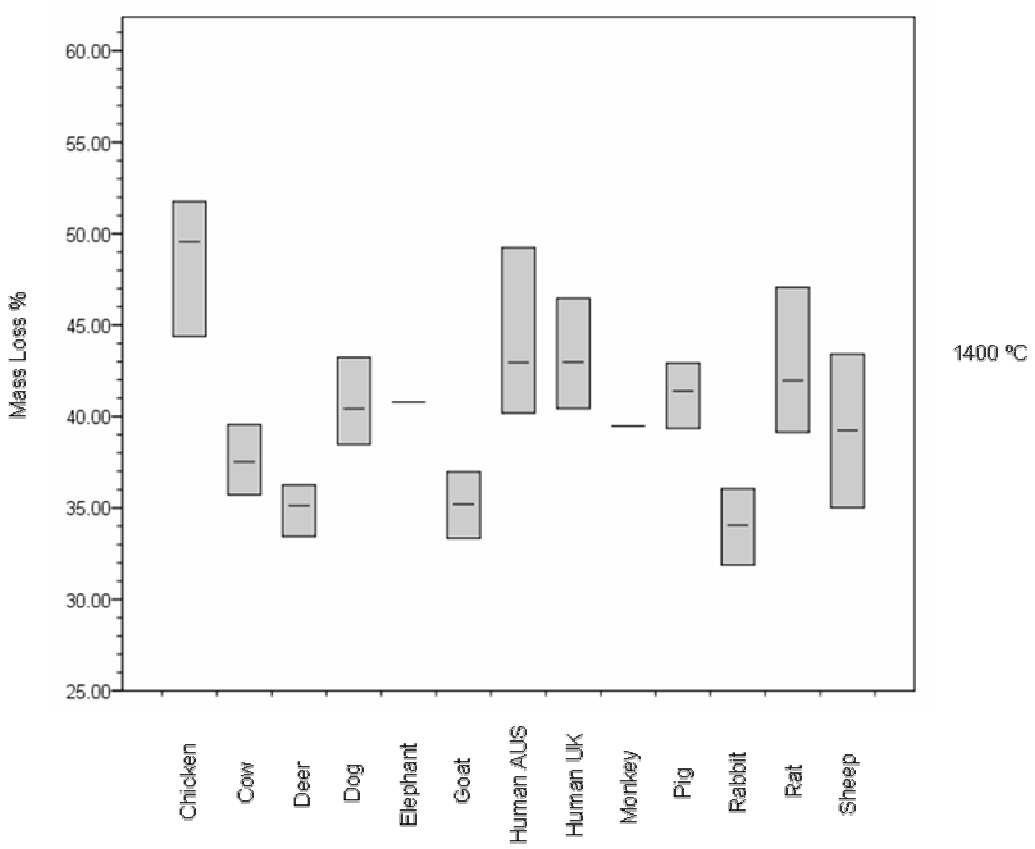

Figure 5.14 – Mass change results for mass change on heating bone specimens to 1400 °C, grouped by species, showing mean (line within a box), minimum (lower limit of a box) and maximum (upper limit of a box) values. Data presented for elephant and monkey represents one individual from each species

5.9.8 – X-RAY DIFFRACTION ANALYSIS OF BONE HEATED TO 600 °C

Values of HAP <00ℓ> greater than 300 Å were obtained for human, monkey, pig and goat for bone heated to 600 °C (see Figure 5.15). Values greater than 500 Å were only obtained for human UK and monkey and the values obtained for these two species were significantly greater than the values obtained for all other species. Although, relatively high values were obtained for pig, a large intra-species range of values was obtained for this species, with values less than 210 Å also obtained. The only other species for which values less than 210 Å obtained were chicken, cow and dog. Unlike the values obtained for human UK, all values obtained for human AUS were less than 350 Å.

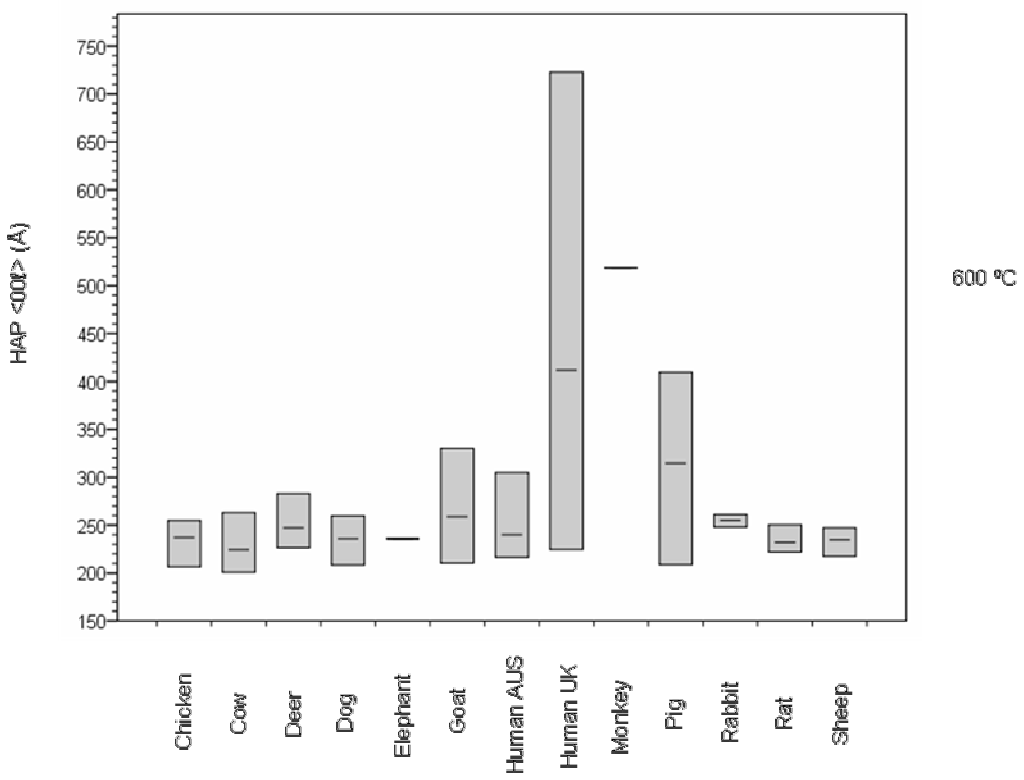

Figure 5.15 – XRD analysis results for HAP <00ℓ> obtained from bone specimens heated to 600 °C, grouped by species, showing mean (line within a box), minimum (lower limit of a box) and maximum (upper limit of a box) values. Data presented for elephant and monkey represents one individual from each species

Rat was the only species for which all values obtained for HAP ‘a’ were greater than 4.92 Å, for bone heated to 600 °C (see Figure 5.16). However, values greater than 4.92 Å were also obtained for chicken, dog, human and sheep. The lowest value was obtained for elephant. A large intra-species range was obtained for human AUS compared with those of other species. This range encompassed the ranges of values obtained for all other species, with the exception of elephant. All values obtained for rat and chicken for HAP ‘c’ for bone heated to 600 °C were 6.885 Å or less and all values obtained for elephant and human were 6.89 Å or greater (see Figure 5.17).

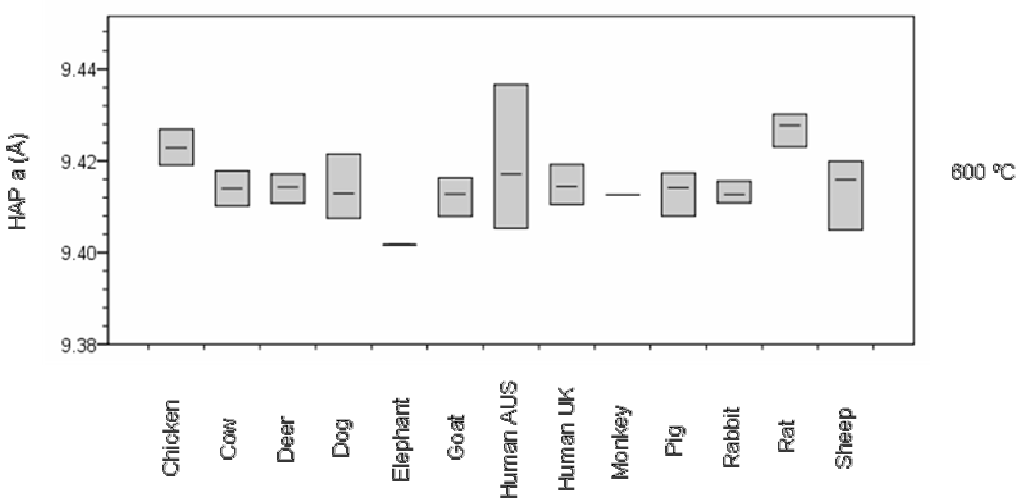

Figure 5.16 – XRD analysis results for HAP ‘a’ obtained from bone specimens heated to 600 °C, grouped by species, showing mean (line within a box), minimum (lower limit of a box) and maximum (upper limit of a box) values. Data presented for elephant and monkey represents one individual from each species

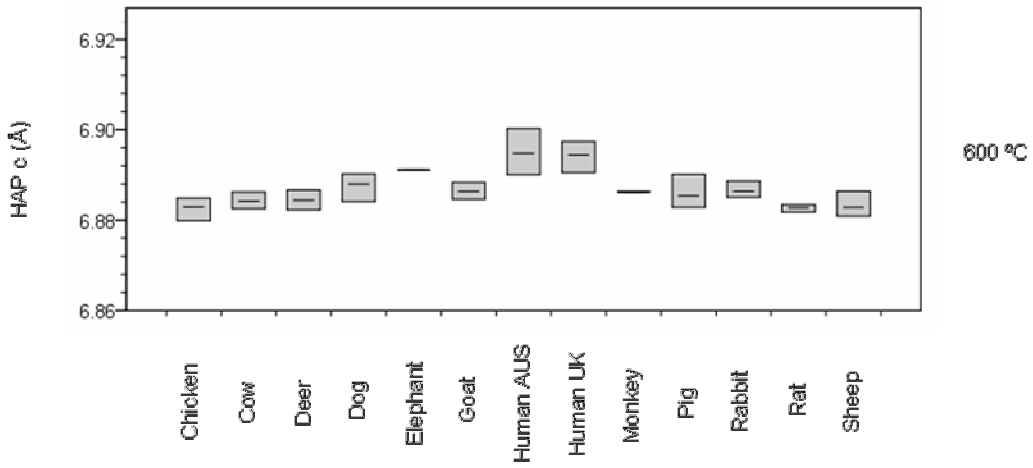

Figure 5.17 – XRD analysis results for HAP 'c' obtained from bone specimens heated to 600 °C, grouped by species, showing mean (line within a box), minimum (lower limit of a box) and maximum (upper limit of a box) values. Data presented for elephant and monkey represents one individual from each species

The mineral phase; β-TCP was detected in all chicken and rat bone specimens and in one sheep bone specimen, heated to 600 °C. It was not detected in bone specimens, heated to 600 °C, from any other species studied. The percentage of β-TCP detected was less than 15 % for chicken, rat and sheep bone specimens but the range of values obtained for rat bone specimens was greater than that obtained for chicken bone specimens (see appendix). MgO was detected in one monkey bone specimen and one human UK bone specimen heated to 600 °C and the percentage detected was less than 1 % in each case (see appendix).

For those species for which β-TCP was detected in bone specimens heated to 600 °C, the value obtained for sheep for β-TCP ‘a’ was less than 10.36 Å whereas, values greater than this were obtained for all chicken and rat specimens. A large intra-species range of values was obtained for chicken for β-TCP ‘c’ compared to that obtained for rat and all values obtained for rat and sheep were encompassed within the range obtained for chicken (see appendix).

5.9.9 – X-RAY DIFFRACTION ANALYSIS OF BONE HEATED TO 1400 °C

The only species for which values of less than 25 % were obtained for the weight percentage of HAP detected within bone heated to 1400 °C were elephant and monkey. However, all the values obtained for cow, deer, goat, rabbit and rat were less than 50 %. The highest value was obtained for dog and all values obtained for dog and chicken were greater than 40 % (see Figure 5.18).

Both the highest and lowest values of HAP ‘a’ for bone heated to 1400 °C were obtained for human, for which the largest intra-species ranges of values were obtained. However, human was also the only species for which values outside the range of 4.05 – 4.92 Å, were obtained (see Figure 5.19). The lowest values of HAP ‘c’ for bone heated to 1400 °C were obtained for cow, deer, rabbit and sheep. The highest values were obtained for human and values greater than 6.89 Å were only obtained for dog, human and rat (see Figure 5.20).

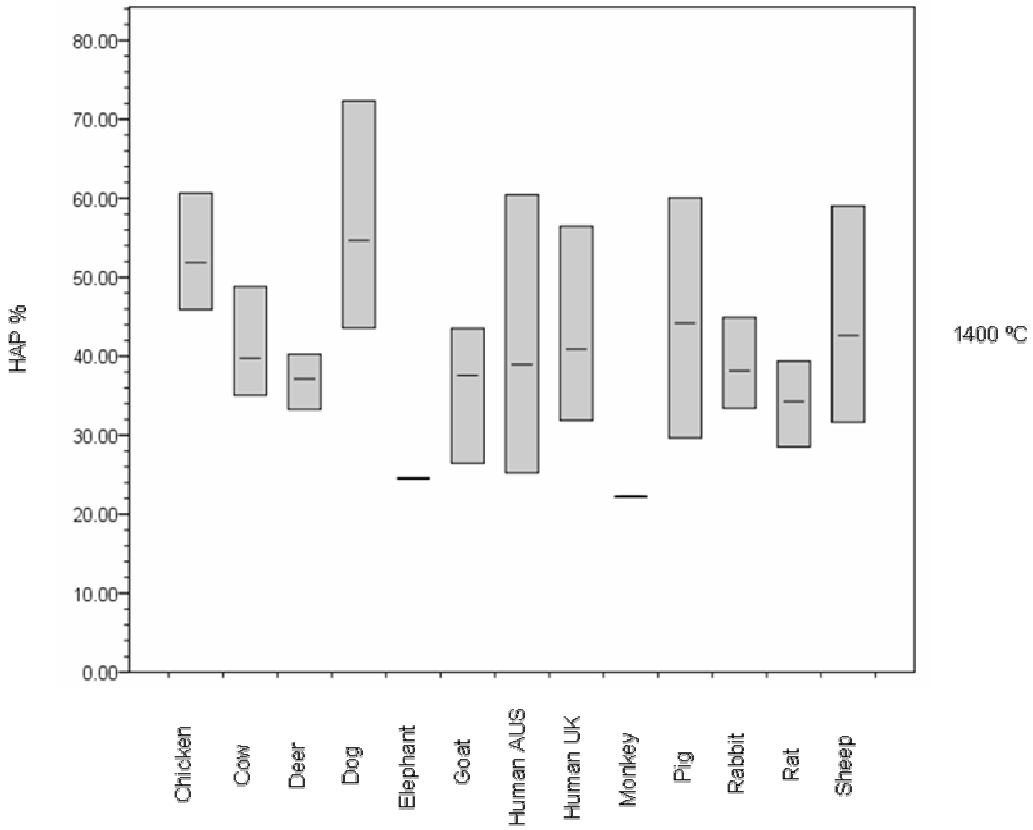

Figure 5.18 – XRD analysis results for HAP % obtained from bone specimens heated to 1400 °C, grouped by species, showing mean (line within a box), minimum (lower limit of a box) and maximum (upper limit of a box) values. Data presented for elephant and monkey represents one individual from each species

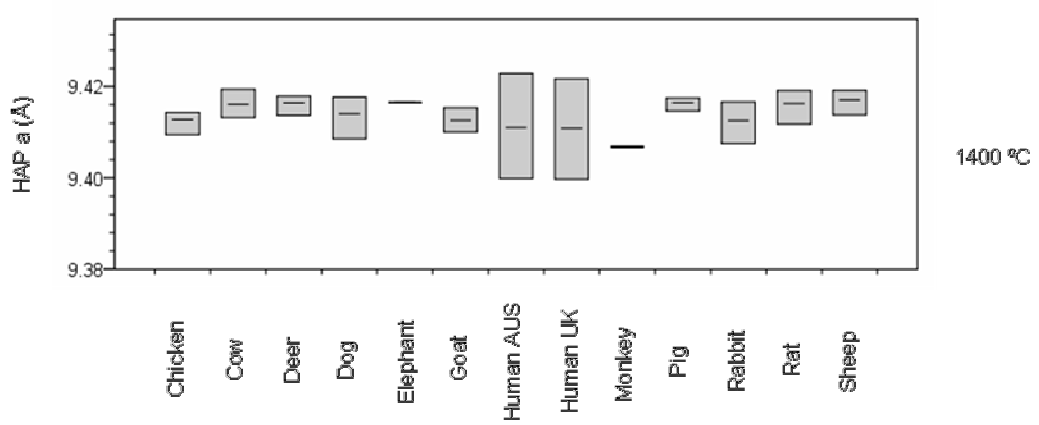

Figure 5.19 – XRD analysis results for HAP 'a' obtained from bone specimens heated to 1400 °C, grouped by species, showing mean (line within a box), minimum (lower limit of a box) and maximum (upper limit of a box) values. Data presented for elephant and monkey represents one individual from each species

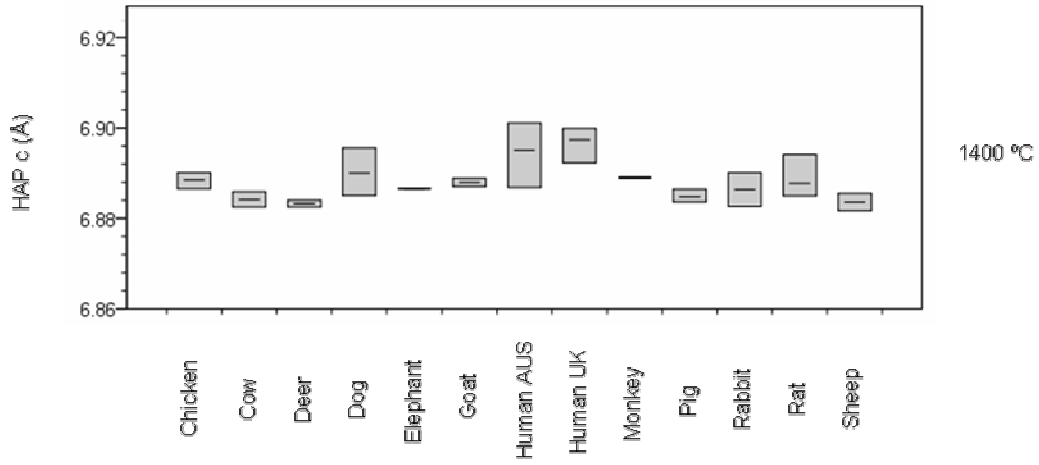

Figure 5.20 – XRD analysis results for HAP 'c' obtained from bone specimens heated to 1400 °C, grouped by species, showing mean (line within a box), minimum (lower limit of a box) and maximum (upper limit of a box) values. Data presented for elephant and monkey represents one individual from each species

Percentage values of β-TCP, of less than 30 % were only obtained for dog and human bone heated to 1400 °C. However, only for cow, deer, monkey and rat were all values obtained greater than 40 % (see Figure 5.21). The value obtained for β-TCP ‘a’ for chicken and rat were significantly lower than those obtained for all other species and the values obtained for human were significantly greater than those obtained for all other species (see Figure 5.22). Values greater than 37.34 Å for β-TCP ‘c’ were only obtained for human and rat. However, relatively low values were also obtained for human, whereas all values obtained for rat were greater than 37.33 Å (see Figure 5.23).

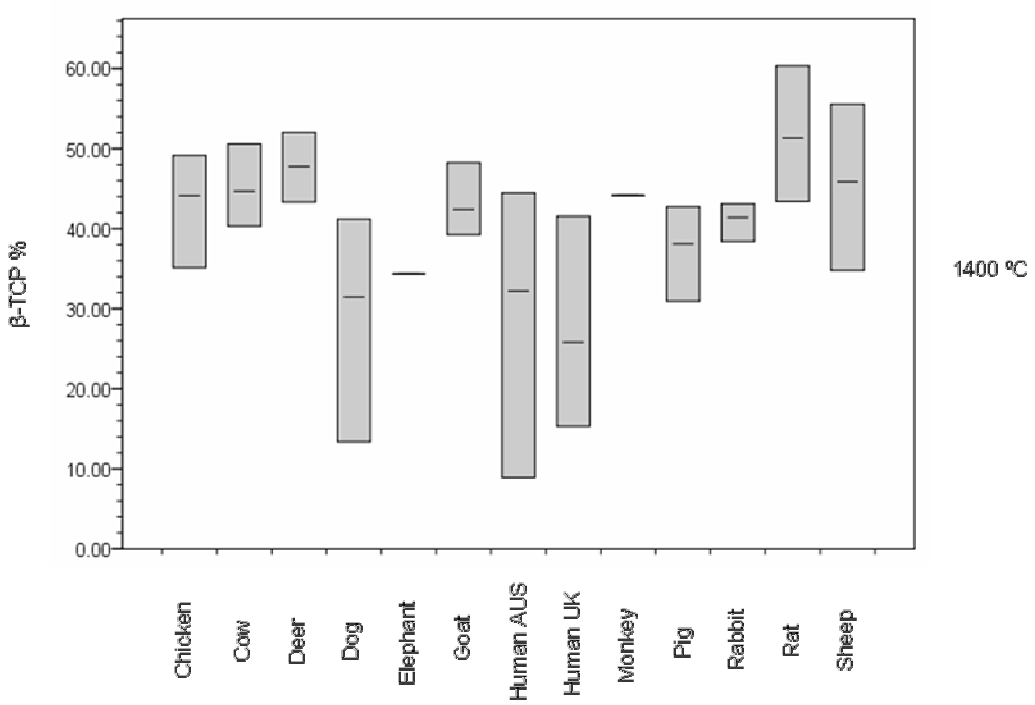

Figure 5.21 – XRD analysis results for β-TCP % obtained from bone specimens heated to 1400 °C, grouped by species, showing mean (line within a box), minimum (lower limit of a box) and maximum (upper limit of a box) values. Data presented for elephant and monkey represents one individual from each species

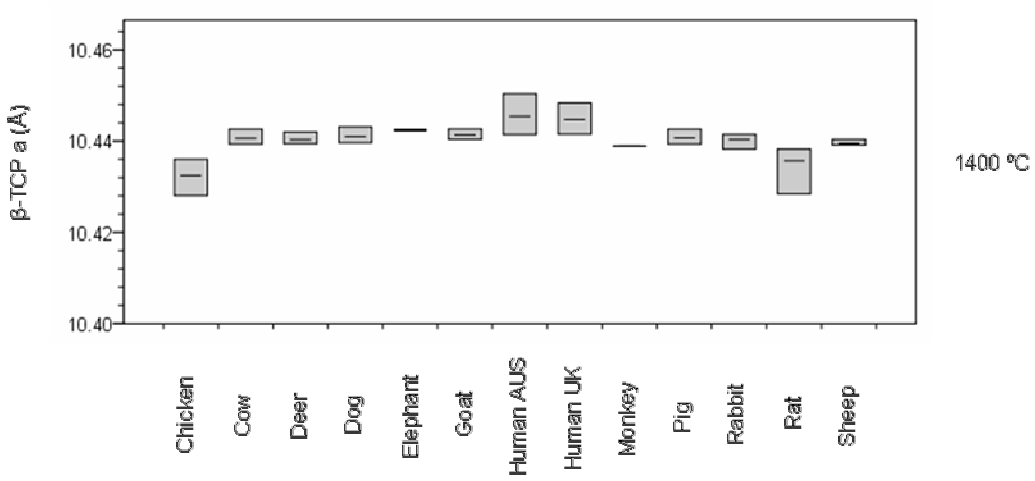

Figure 5.22 – XRD analysis results for β-TCP 'a' obtained from bone specimens heated to 1400 °C, grouped by species, showing mean (line within a box), minimum (lower limit of a box) and maximum (upper limit of a box) values. Data presented for elephant and monkey represents one individual from each species

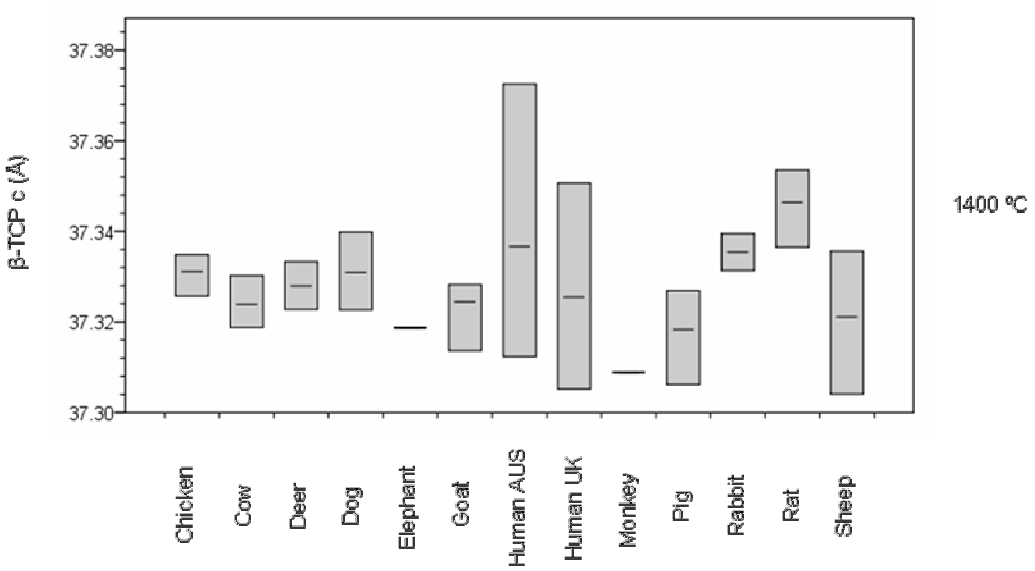

Figure 5.23 – XRD analysis results for β-TCP 'c' obtained from bone specimens heated to 1400 °C, grouped by species, showing mean (line within a box), minimum (lower limit of a box) and maximum (upper limit of a box) values. Data presented for elephant and monkey represents one individual from each species

The mineral phase; α-TCP was detected in chicken, human AUS and rat bone heated to 1400 °C but was not detected for bone of any other species (see Figure 5.24). It was detected in 3 out of 5 chicken bone specimens, 4 out of 5 rat bone specimens and 2 out of 50 human AUS bone specimens. The percentage of α-TCP detected in the chicken and human AUS bone specimens was less than 7 % in each case was between 7 % and 20 % for all rat bone specimens. TTCP was not detected in two chicken bone specimens heated to 1400 °C. However, it was detected in all other bone specimens from all species. The highest weight percentage value was obtained for elephant and values greater than 30 % were also obtained for human and monkey. All values obtained for chicken and rat were less than 4 % whereas values greater than this were obtained for all bone specimens from all other species.

The lowest values for the weight percentage of MgO detected in bone heated to 1400 °C were obtained for dog, elephant and human (see Figure 5.25). The highest value was obtained for rabbit, although the intra-species range that was obtained for rabbit encompassed the ranges obtained for the majority of the other species. The mineral phase CaO was not detected for any rat or monkey bone specimens. It was not detected for the majority of chicken bone specimens, 4 out of 50 human AUS bone specimens and one rabbit bone specimen. However, it was detected in all bone specimens from all other species. The lowest value was obtained for chicken and the largest value was obtained for human. However, the intra-species range obtained for human encompassed those obtained for all other species except chicken and rabbit.

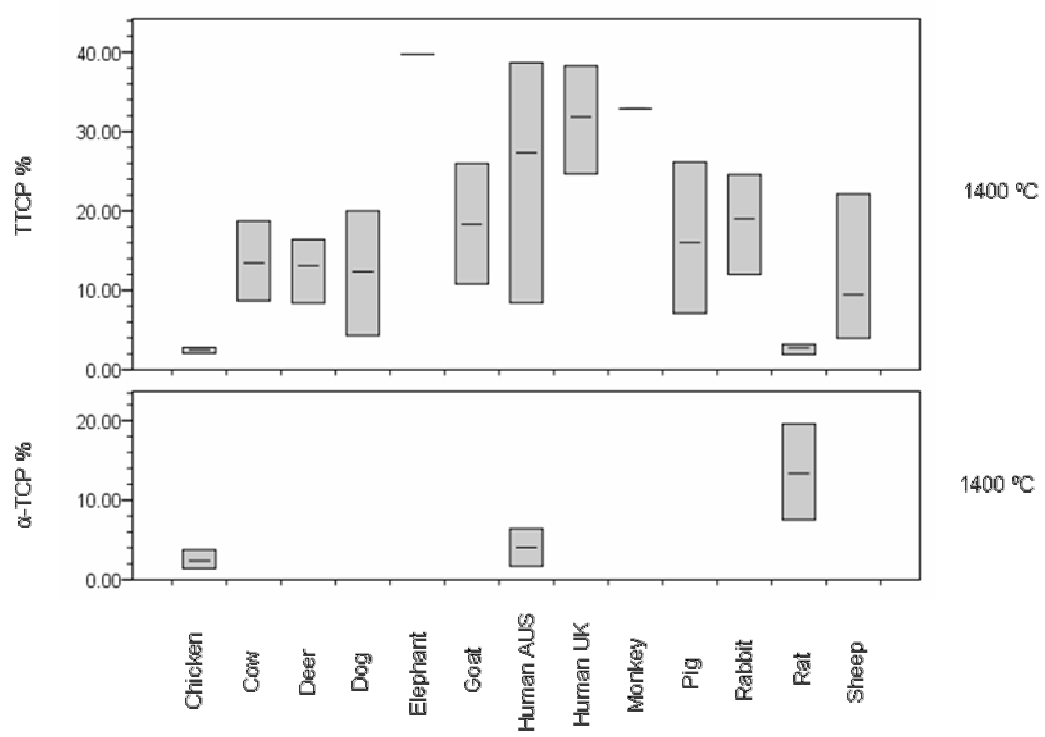

Figure 5.24 – XRD analysis results for α-TCP % and TTCP % obtained from bone specimens heated to 1400 °C, grouped by species, showing mean (line within a box), minimum (lower limit of a box) and maximum (upper limit of a box) values. Data presented for elephant and monkey represents one individual from each species. The phase α-TCP was only detected in chicken, human AUS and rat bone specimens. Data for individuals for which mineral phase weight percentage was equal to zero are not presented and not included in calculation of mean values

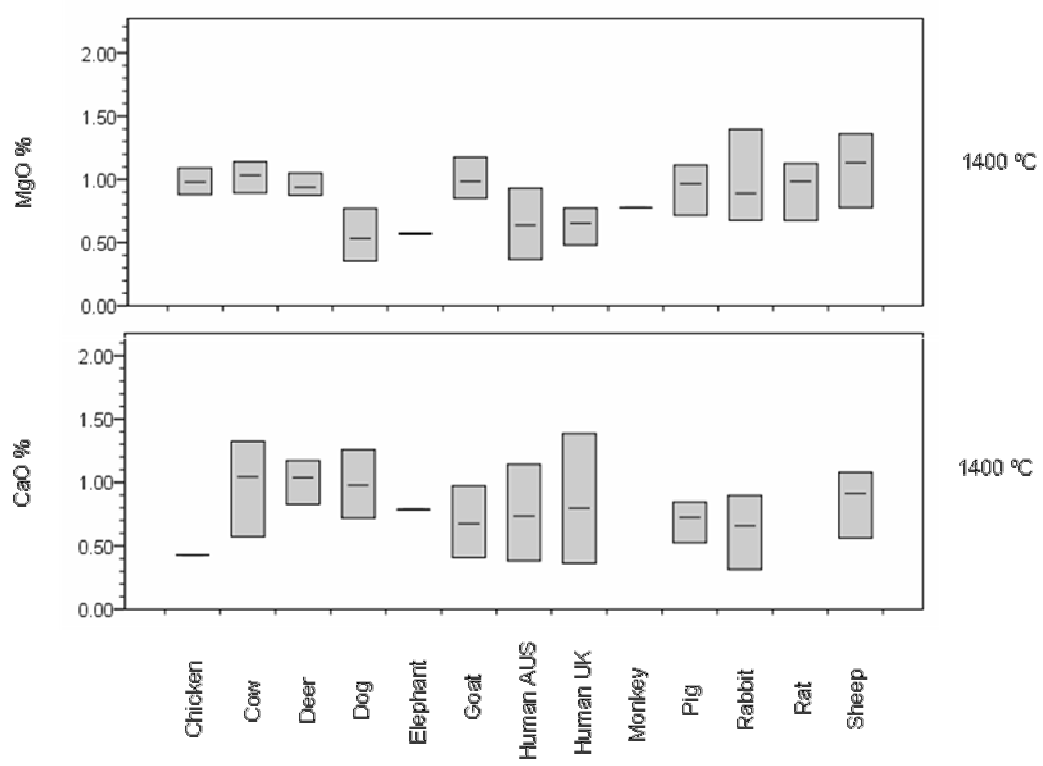

Figure 5.25 – XRD analysis results for CaO % and MgO % obtained from bone specimens heated to 1400 °C, grouped by species, showing mean (line within a box), minimum (lower limit of a box) and maximum (upper limit of a box) values. Data presented for elephant and monkey represents one individual from each species. The phase CaO was not detected in monkey and rat bone specimens. Data for individuals for which mineral phase weight percentage was equal to zero are not presented and not included in calculation of mean values

5.10– KENDALL'S TAU CORRELATIONS OF BONE MINERAL CHARACTERISTICS

5.10.1 – GENERAL CORRELATIONS (ALL SPECIES)

The results of tests for general correlations within the data from all species investigated are presented in Table 5.13 through to Table 5.15. The tables are an array of 'boxes', each containing two values. The upper value within each box is the Kendall's Tau correlation coefficient (τ) and the lower values indicate the sample size used for each test. The shading of each box indicates the significance of the coefficient value it contains. No shading indicates that the result was not significant, grey shading indicates a significance of $p < 0.05$ and black shading indicates a significance of $p < 0.01$.

In general, characteristics were found to be poorly correlated with each other and all correlation coefficients were less than 0.80. However, coefficients, greater than 0.60, were obtained. Also, in general, characteristics were significantly correlated ($p < 0.05$) with at least one other characteristic.

For unheated bone, the values obtained for HAP <00ℓ> were significantly correlated to the values of both HAP lattice parameters. They were negatively correlated with HAP 'a' values and positively correlated with HAP 'c' values. However, the magnitude of correlation coefficients was less than 0.35 in each case (see Table 5.13). Values of HAP <00ℓ> for unheated bone were significantly correlated to values of percentage of magnesium and percentage

of fluorine. They were negatively correlated with magnesium values and positively correlated with fluorine values (see Table 5.14).

HAP ‘c’ values obtained for unheated bone were not correlated to any of the values obtained for any elemental or IR characteristics (see Table 5.14). However, values of HAP ‘a’ were significantly correlated (at least to the level of $p < 0.05$) to values obtained for the percentage of carbon, potassium and sodium.

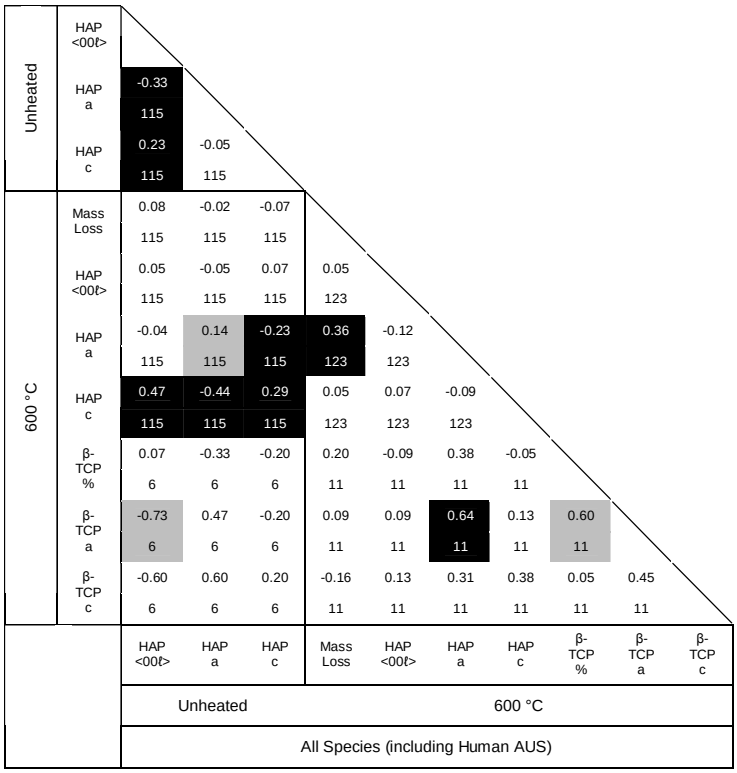

Table 5.13 – Kendall's Tau correlation results for HAP <00ℓ>, HAP 'a' and HAP 'c' obtained from XRD analysis of unheated bone specimens, HAP <00ℓ>, HAP 'a', HAP 'c', β-TCP %, β-TCP 'a' and β-TCP 'c' obtained from XRD analysis of bone specimens heated to 600 °C and mass change results for bone specimens heated to 600 °C, tested against each other. Data presented includes all species investigated with the exception of tests involving data from unheated bone specimens for which rat was not included and tests for β-TCP %, β-TCP 'a' and β-TCP 'c' obtained from bone specimens heated to 600 °C for which only rat, chicken and sheep were included. In each test result 'box' the correlation coefficient is presented above the number of individuals used for the test

		All Species (including Human AUS)														
		600 °C														
		Ca %	P %	Atomic Ca/P	Total N %	Total C %	Total H %	Fe ppm	K ppm	Mg ppm	Na ppm	Sr ppm	F ppm	Cl ppm	CO3 %	SF
Unheated	HAP <00*l*>	-0.05	-0.33	0.09	0.02	0.34	0.02	-0.11	-0.33	-0.42	0.16	-0.19	0.40	0.16	0.34	0.19
		18	18	18	18	18	18	18	18	18	18	18	17	17	15	15
	HAP a	0.16	0.19	0.06	-0.21	-0.46	-0.09	0.08	0.54	0.31	-0.38	0.00	-0.30	0.04	-0.11	0.08
		18	18	18	18	18	18	18	18	18	18	18	17	17	15	15
	HAP c	-0.17	-0.12	0.03	0.04	0.16	-0.02	0.04	-0.10	-0.26	-0.01	0.08	0.21	-0.21	0.05	0.22
		18	18	18	18	18	18	18	18	18	18	18	17	17	15	15
600 °C	Mass Loss	0.20	-0.37	0.35	-0.16	-0.02	-0.01	-0.19	-0.05	-0.16	-0.28	-0.37	0.25	0.07	-0.23	0.00
		18	18	18	18	18	18	18	18	18	18	18	17	17	15	15
	HAP <00*l*>	0.19	-0.35	0.46	-0.56	-0.15	-0.41	-0.10	0.15	-0.46	-0.16	-0.36	0.29	0.15	-0.04	0.67
		18	18	18	18	18	18	18	18	18	18	18	17	17	15	15
	HAP a	0.24	0.10	0.05	-0.11	-0.34	-0.27	-0.14	0.14	0.23	-0.15	-0.01	-0.03	0.26	-0.54	0.19
		18	18	18	18	18	18	18	18	18	18	18	17	17	15	15
	HAP c	-0.02	-0.43	0.34	-0.22	0.35	-0.01	-0.02	-0.27	-0.70	-0.08	-0.20	0.38	-0.21	0.19	0.38
		18	18	18	18	18	18	18	18	18	18	18	17	17	18	18
1400 °C	Mass Loss	0.14	-0.26	0.22	-0.09	0.02	-0.01	-0.11	-0.10	-0.11	-0.28	-0.32	0.25	0.04	-0.27	0.02
		18	18	18	18	18	18	18	18	18	18	18	17	17	15	15
	HAP %	-0.05	0.07	-0.23	0.14	0.05	0.36	0.01	-0.01	0.29	-0.19	0.06	0.21	0.00	-0.19	-0.38
		18	18	18	18	18	18	18	18	18	18	18	17	17	15	15
	HAP a	-0.14	0.06	-0.19	0.14	-0.09	0.19	-0.11	-0.02	0.36	-0.07	0.12	-0.41	-0.03	-0.15	-0.38
		18	18	18	18	18	18	18	18	18	18	18	17	17	15	15
	HAP c	0.13	-0.21	0.24	-0.14	0.32	-0.03	0.06	-0.27	-0.57	0.02	-0.18	0.65	-0.06	0.15	0.06
		18	18	18	18	18	18	18	18	18	18	18	17	17	15	15
	β-TCP %	-0.05	0.22	-0.23	0.06	-0.31	-0.07	0.01	0.36	0.45	-0.06	0.16	-0.60	0.07	0.02	-0.06
		18	18	18	18	18	18	18	18	18	18	18	17	17	15	15
	β-TCP a	-0.07	-0.13	0.05	0.11	0.47	0.15	-0.19	-0.62	-0.35	0.14	-0.03	0.13	-0.25	0.02	-0.17
		18	18	18	18	18	18	18	18	18	18	18	17	17	15	15
	β-TCP c	0.03	0.11	0.03	-0.06	0.03	0.10	0.15	0.03	-0.01	-0.41	-0.01	0.09	-0.29	-0.08	-0.06
		18	18	18	18	18	18	18	18	18	18	18	17	17	15	15
	TTCP %	0.16	-0.31	0.43	-0.30	0.22	-0.22	0.03	-0.13	-0.71	0.00	-0.28	0.42	-0.10	0.27	0.27
		17	17	17	17	17	17	17	17	17	17	17	16	16	14	14
	CaO %	-0.15	0.09	-0.23	0.10	-0.18	0.02	0.05	0.17	0.37	-0.02	0.15	-0.16	-0.03	-0.14	0.01
		16	16	16	16	16	16	16	16	16	16	16	15	15	13	13
	MgO %	-0.10	0.27	-0.33	0.20	-0.20	0.07	0.01	0.18	0.61	0.02	0.40	-0.43	0.25	-0.33	-0.36
		18	18	18	18	18	18	18	18	18	18	18	17	17	15	15

Table 5.14 – Kendall's Tau correlation results for bone mineral characteristics obtained from ICP-AES, P-IC, C-GC and IR spectroscopy of bone specimens heated to 600 °C tested against characteristics obtained from XRD analysis of unheated bone specimens, bone specimens heated to 600 °C and to 1400 °C and for mass change results for 600 °C and 1400 °C. Data includes all species investigated with the exception of tests involving data from unheated bone for which rat was not included and tests for β-TCP %, β-TCP 'a' and β-TCP 'c' obtained from bone specimens heated to 600 °C for which only rat, chicken and sheep were included. In each test result 'box' the correlation coefficient is presented above the number of individuals used for the test

Values obtained for HAP <00ℓ> for bone heated to 600 °C were not correlated to values obtained for unheated bone for HAP <00ℓ>, HAP ‘a’ or HAP ‘c’ (see Table 5.13). They were however, significantly correlated ($p < 0.01$) to values obtained for the atomic Ca/P ratio (+ 0.46), the phosphate ion splitting factor (+ 0.67) and, the percentage of nitrogen (- 0.56) and magnesium (- 0.46) (see Table 5.14).

For bone heated to 600 °C, values obtained for HAP ‘a’ and HAP ‘c’ were significantly correlated to those obtained for unheated bone. However, a coefficient of a magnitude of at least 0.4 was only obtained for HAP ‘c’ (600 °C) and HAP ‘a’ (unheated) (see Table 5.13). Values of HAP ‘a’ obtained for bone heated to 600 °C, were significantly correlated ($p < 0.01$) to values obtained for carbonate percentage. They were not significantly correlated to values of any other elemental or IR spectroscopy characteristics. HAP ‘c’ (600 °C) was significantly negatively correlated ($p < 0.01$, $\tau < 0.6$) to values obtained for percentage of magnesium (see Table 5.14).

The percentage of β-TCP detected in bone heated to 600 °C was not significantly correlated to any measured HAP characteristics of unheated bone or, bone heated to 600 °C. However, coefficients greater than 0.30, in magnitude, were obtained for the correlations of percentage of β-TCP to; HAP ‘a’ (unheated) and to, HAP ‘a’ (600 °C). Also, the values obtained for β-TCP ‘a’ were significantly correlated to values obtained for percentage of β-TCP and to those obtained for HAP ‘a’ (600 °C) (see Table 5.13).

In general, values obtained for characteristics of bone heated to 1400 °C were significantly correlated to those obtained for HAP characteristics (unheated and 600 °C). However, coefficients were, in general, less than 0.4 in magnitude. Coefficients greater than 0.4 were only obtained for correlations between; HAP ‘a’ (1400 °C) and HAP <00ℓ> (unheated), HAP ‘a’ (1400 °C) and HAP ‘a’ (unheated), β-TCP ‘a’ (1400 °C) and HAP <00ℓ> (unheated) and, TTCP ‘a’ (1400 °C) and HAP ‘a’ (unheated bone) (see Table 5.15).

All coefficients obtained for correlations between values of percentage of HAP (1400 °C) and any unheated bone characteristics or, those of bone heated to 600 °C were less than 0.25 in magnitude. However, values obtained for HAP ‘c’ (600 °C) were significantly correlated ($p < 0.01$, $\tau > 0.5$) to values obtained for HAP ‘c’ (1400 °C), percentage of β-TCP (1400 °C), β-TCP ‘a’ (1400 °C) and percentage of TTCP (1400 °C) (see Table 5.15).

Values obtained for the percentage of α-TCP detected in bone heated to 1400 °C were not significantly correlated to any characteristics of unheated bone or bone heated to 600 °C. However, a coefficient greater than 0.4, was obtained for the correlation of percentage of α-TCP to the percentage of β-TCP (600 °C). The coefficients obtained for correlations between percentage of CaO (1400 °C) and any characteristic of unheated bone or bone heated to 600 °C, were less than 0.3 in magnitude (see Table 5.15).

		All Species (including Human AUS)										
		1400 °C										
		Mass Loss	HAP %	HAP a	HAP c	β-TCP %	β-TCP a	β-TCP c	α-TCP %	TTCP %	CaO %	MgO %
Unheated	HAP <00ℓ>	0.19	-0.08	-0.24	0.43	-0.31	0.45	0.22	0.20	0.37	-0.12	-0.35
		115	115	115	115	115	115	115	5	113	105	115
	HAP a	-0.09	0.10	0.37	-0.48	0.36	-0.35	-0.06	-0.40	-0.46	0.14	0.32
		115	115	115	115	115	115	115	5	113	105	115
	HAP c	0.02	-0.06	-0.16	0.25	-0.26	0.20	-0.05	-0.40	0.32	-0.11	-0.27
		115	115	115	115	115	115	115	5	113	105	115
600 °C	Mass Loss	0.68	0.14	0.00	0.15	-0.10	0.07	0.20	-0.06	-0.06	-0.05	-0.01
		123	123	123	123	123	123	123	9	121	108	123
	HAP <00ℓ>	-0.02	0.08	-0.14	0.11	-0.20	-0.04	-0.20	-0.11	0.13	-0.02	-0.06
		123	123	123	123	123	123	123	9	121	108	123
	HAP a	0.26	-0.07	0.19	-0.07	0.25	0.03	0.35	0.33	-0.25	0.01	0.18
		123	123	123	123	123	123	123	9	121	108	123
	HAP c	0.23	-0.10	-0.35	0.65	-0.53	0.64	0.17	-0.28	0.60	-0.23	-0.46
		123	123	123	123	123	123	123	9	121	108	123
	β-TCP %	0.16	-0.20	-0.42	0.60	-0.27	-0.45	0.27	0.43	-0.39	------	-0.27
		11	11	11	11	11	11	11	7	9	2	11
	β-TCP a	0.05	-0.24	-0.09	0.27	-0.24	-0.27	0.09	0.43	-0.50	------	-0.60
		11	11	11	11	11	11	11	7	9	2	11
	β-TCP c	0.09	-0.13	0.09	-0.05	-0.27	-0.09	-0.02	0.14	-0.39	------	-0.56
		11	11	11	11	11	11	11	7	9	2	11

Table 5.15 – Kendall's Tau correlation results for bone mineral characteristics obtained from XRD analysis of bone specimens heated to 600 °C and mass change results for bone specimens heated to 600 °C tested against bone mineral characteristics obtained from XRD analysis of bone specimens heated to 1400 °C and mass change results for bone specimens heated to 1400 °C. Data presented includes all species investigated with the exception of tests involving data from unheated bone specimens for which rat was not included, tests for β-TCP %, β-TCP 'a' and β-TCP 'c' obtained from bone specimens heated to 600 °C for which only rat, chicken and sheep were included and tests for α-TCP % for which only chicken, human AUS and rat were included. In each test result 'box' the correlation coefficient is presented above the number of individuals used for the test

The values for percentage of magnesium were significantly correlated ($p < 0.01$, $\tau > 0.6$) to values of percentage of TTCP and percentage of MgO (1400 °C). They were also correlated ($p < 0.01$) to values obtained for HAP ‘c’, and the percentage of β-TCP (1400 °C). The values obtained for the percentage of fluorine were significantly negatively correlated to values obtained for the percentage of β-TCP and significantly positively correlated to those obtained for HAP ‘c’. Also values obtained for the percentage of potassium were significantly negatively correlated to values obtained for β-TCP ‘a’ (1400 °C) (see Table 5.14).

5.10.2 – SPECIES-SPECIFIC CORRELATIONS

Table A.13 through to Table A.31 in the appendix present correlation test results, grouped by species. In general, a larger proportion of coefficients were greater than 0.6 in magnitude, for each species group, compared to the results obtained for all species. However, inter-species variation was encountered, in terms of correlation test results obtained for each species individually and, the results for individual species were not always fully consistent with the general correlations observed for all species, as one group.

CHAPTER 6 – DISCUSSION

The results presented within this thesis represent a body of research with a sample size and range of animal species that is believed to be considerably larger and more extensive than any X-ray diffraction based study previously published. A large number of results were obtained from the data collected. This has provided characteristic information about the crystal structure of unheated bone. It has also provided characteristic information about the mass loss, crystal structure and mineral phase composition of heated bone and, the response of bone to heat treatment. These results were presented, in chapter 5 and in the appendix, both in terms of general characteristics of unheated bone and heated bone and also, in terms of inter-species variation.

6.1 – GENERAL COMPOSITION AND STUCTURE OF BONE MINERAL

The results obtained from X-ray diffraction analysis of unheated bone demonstrate that the mineral component of bone, for all species investigated, has the composition and structure of a poorly crystalline, non-stoichiometric form of calcium hydroxylapatite (HAP) and consists of no other mineral phases. The results of ICP-AES, P-IC, C-GC and IR spectroscopy corroborate the XRD results. They demonstrate that calcium and phosphorous are the major compositional components of bone mineral but that sodium, magnesium, potassium, strontium, iron, fluorine and chlorine, nitrogen, hydrogen, carbon

and carbonate ions, are also consistently present in bone, of all species investigated.

The findings of this study are consistent with those of many previous researchers and the currently accepted general model of bio-apatite (b-HAP) for bone mineral composition and structure. Therefore, they enable the acceptance of all hypotheses associated with the first aim of this study (see section 4.1.1). Moreover, they provide support for the acceptance of a further hypothesis that; bone from all species that possess an internal skeleton has the same general mineral composition and structure.

The cause of non-stoichiometric values of HAP lattice parameters is the presence of lattice defects such as ion substitutions and ion vacancies. The values obtained for HAP ‘a’ and HAP ‘c’ for unheated bone were consistently larger than the stoichiometric values. This finding suggests that the net effect of lattice defects in bone mineral is the expansion of unit cell volume. Based on the results of this study and the work of previous researchers [154], it is proposed that the ion substitutions within bone mineral include; sodium, magnesium, potassium, strontium, iron, chlorine, fluorine and, carbonate ions. However, it is acknowledged that this list does not represent all ion substitutions of bone mineral, as many other ions have previously been reported to be present in bone [79, 196, 246].

6.2 – BIOLOGICAL CONTROL OF COMPOSITION AND STRUCTURE

Bone mineral HAP crystals were shown to be of nanometre dimensions in the <00ℓ> direction, for all species. The HAP <00ℓ> results also suggest that the HAP crystallites have considerable lattice strain. This is supported by the evidence that ions known to substitute within the HAP lattice are present in bone and the non-stoichiometric values obtained for HAP lattice parameters. It is widely accepted that crystallinity (size and strain) is controlled *in vivo* and that maintaining a bone mineral component of small, strained crystals is essential to the fulfilment of functional roles of bone [59, 107]. For example, smaller strained crystals have a relatively large surface area and high reactivity, including solubility, compared to larger, less defective crystals. These properties are important for bone turnover mechanisms *in vivo*. The defects within a crystal lattice and ions located on crystal surfaces determine crystallite size and strain. In bone, it is also proposed that the organic collagen matrix imposes a physical restriction on crystallite size of HAP crystals.

The second aim of this thesis was to demonstrate that biological control of the general composition and structure of bone mineral is similar for all species. Mechanisms of biological control were investigated through the testing of hypothesis 2 (a) through to 2 (c).

The values obtained for HAP <00ℓ> were significantly correlated to values obtained for HAP lattice parameters. These results show that crystallinity is biologically controlled *in vivo* and, that this control, in terms of lattice contents, is similar for all species investigated.

The physiological importance of sodium, magnesium and potassium within a variety of biological functional roles is widely recognised [79, 150]. A consistent order of the percentages of these ions in bone was demonstrated. This finding, along with that of an expanded unit cell volume, for all species, is further evidence in support of the proposal that there is systematic control of bone mineral composition and structure, *in vivo* and that this applies to all species. The same consistent order of percentage of sodium, magnesium and potassium has been recognised by other researchers [79, 247]. However, there has not previously been the demonstration that this consistency exists across species groups and extends to the ions of strontium, iron, fluorine and chlorine.

Magnesium within bone is reported to play a role in the restriction of crystallite morphology and stability [79, 150, 240]. The significant negative correlation obtained for values of HAP <00ℓ> and percentage of magnesium, across all species, supports this proposal. However, whether the restriction of crystallinity by magnesium is achieved through a lattice or surface ion mechanism, or both, has yet to be fully determined [152, 240].

Contrary to the effect of magnesium on HAP crystallinity, there is evidence within the literature for the proposal that fluorine substitution has a stabilising influence on HAP crystals and enhances crystallite size and perfection [79, 107, 166, 207, 248]. Such a proposal is supported by the results of this study; a significant positive correlation was obtained for the relationship between HAP <00ℓ> values and percentage of fluorine.

The results have enabled the acceptance of each of the hypotheses associated with the second aim of this thesis. However, whilst similar biological control of bone mineral composition and structure has been demonstrated. The inter-species variation in the results for correlations between HAP lattice parameters and HAP <00ℓ> suggest that variation exists between species in the combined application of control mechanisms.

6.3 – GENERAL RESPONSE OF BONE TO HEAT TREATMENT

The analysis of heated bone has achieved the aim of demonstrating a measurable, general response of bone to heat treatment, when heat treatment conditions are standardised (see section 4.1.3). The general response identified by this study included; mass loss from bone and, recrystallisation, contraction of unit cell volume and thermal decomposition of the HAP phase. This response is consistent with that described in section 2.5 and, therefore with general consensus within the published literature.

The finding of mass loss on heating for all bone specimens is consistent with the accepted understanding of the processes of combustion of the organic component of bone and the evolution of gases from the bone mineral crystal lattice. The majority of mass loss on heating bone to 600 °C and 1400 °C is attributed to the removal of the organic component. However, there is evidence within the literature to suggest that the majority of the organic component will have been removed on heating bone specimens to 600 °C under the conditions of this study. Differences between mass change results for bone specimens from the same individual heated to 600 °C and 1400 °C should therefore be indicative of changes to the bone mineral and decomposition product crystal surfaces and lattices. The results from this study suggest that the changes for some bone specimens cause a gain in mass and that these changes may be species specific. Alternatively, an explanation for a gain in mass is the adsorption of water on cooling. Different decomposition products may have different affinities for water adsorption and therefore different proportions of decomposition products within bone specimens heated to 1400 °C could result in mass change differences due to differential adsorption of water.

Recrystallisation on heating was confirmed by the observation of greater resolution of diffraction peaks, obtained from heated bone compared with those from unheated bone. A decrease in peak broadening is indicative of an increase in crystallite size and perfection. However, the values obtained for HAP <00ℓ> for bone heated to 600 °C and for unheated bone demonstrate that, in general, recrystallisation of HAP in the <00ℓ> direction, does not occur to any great

extent, on heating bone to 600 °C. Therefore, hypothesis 3 (b), proposed in section 4.1.3, cannot be accepted based on the results of this study.

The results do enable hypothesis 3 (c) to be accepted. The HAP lattice parameters do, in general, tend towards stoichiometric values on heating bone to 600 °C and 1400 °C. The lattice parameter results correspond to a general contraction of the unit cell volume. However, the results show that contraction of HAP ‘a’ values extends beyond the stoichiometric value of 9.42 Å. Changes to the unit cell contents on heating bone are restricted to the exchange of ions with the atmosphere. The amount of ions such as calcium, sodium, magnesium, and phosphate is assumed to be fixed within HAP, until thermal decomposition occurs. It is also proposed that, on decomposition of HAP, not all foreign ions are incorporated into the decomposition products. Therefore, although on heating bone, HAP lattice parameters tend towards stoichiometry, the most stable structure for the non-stoichiometric contents consists of a contracted unit cell.

In general, the HAP mineral phase did not undergo thermal decomposition on heating bone to 600 °C. This finding is consistent with the majority of the published literature. The temperature range for the thermal decomposition of the HAP mineral phase of bone is generally quoted as 800 °C – 1000 °C. However, the detection of β-TCP in chicken, rat and sheep bone heated to 600 °C is a result that demands the rejection of hypothesis 3 (d) as thermal decomposition of bone mineral does occur at this temperature.

The results obtained from X-ray diffraction analysis of bone specimens heated to 1400 °C are indicative of a mineral component of bone that consists of HAP and also several other mineral phases. They demonstrate that thermal decomposition occurs on heating bone to 1400 °C but also, that full decomposition of the HAP phase does not occur. Consistently, the decomposition products included β-tri-calcium phosphate (β-TCP) and in general, they also included tetra-calcium phosphate (TTCP) and calcium oxide (CaO). Therefore, the results are consistent with decomposition pathways that involve the formation of oxyapatite and follow the equations proposed in section 2.5.3.

Magnesium oxide (MgO) was also consistently detected in bone heated to 1400 °C. In general, the detection of this phase is not reported in studies of bone heated to high temperatures [89, 145, 154]. This is likely to be due to its presence in relatively small weight percentage values resulting in a lack of detection. Thus, a mechanism for the formation of MgO in heated bone has not previously been proposed. The formation of MgO may be the result of the presence of a greater amount of magnesium than can be accommodated within the HAP, β-TCP and, perhaps, TTCP crystal lattices, on heating bone to 1400 °C. It is proposed that the capacity of HAP and β-TCP to accommodate magnesium ions is reduced by the competitive substitution of sodium and potassium ions. This is supported by evidence within the results for the significant positive correlation of percentage of β-TCP with percentage of

potassium. Furthermore, significant correlations were obtained for β-TCP lattice parameter values with percentages of potassium and sodium. It is proposed here, that the consistent formation of MgO in bone heated to 1400 °C occurs in place of the formation of CaO as a thermal decomposition product of HAP.

6.4 – CHEMICAL BASIS FOR VARIATION IN RESPONSE OF BONE TO HEAT TREATMENT

The results of the analysis of heated bone demonstrate that the response of bone mineral to heat treatment is related to the compositional and structural characteristics of unheated bone mineral. The weight percentage values of β-TCP, TTCP and MgO, obtained for bone heated to 1400 °C, were significantly correlated to the characteristics of unheated bone, measured using X-ray diffraction.

However, the percentages of HAP, CaO and α-TCP phases were not significantly correlated to unheated bone mineral characteristics. Previous researchers have demonstrated that the thermal stability of HAP is dependent on the hydroxyl and acid phosphate content of bone mineral and, atmospheric conditions. The results of this study, obtained for the percentage of hydrogen and mass loss support the proposal that hydrogen content and atmospheric conditions have a greater influence on the stability of HAP compared with other characteristics of composition and structure. The results obtained for CaO and α-TCP support the proposals that CaO is involved in formation of TTCP as a

secondary decomposition product and the formation of α-TCP occurs through the conversion of β-TCP.

In general, α-TCP was not detected in bone specimens heated to 1400 °C. This is consistent with literature evidence for the stabilisation of β-TCP in the presence of magnesium [249] and, the increase of the temperature at which the thermal conversion of β-TCP to α-TCP occurs [154]. However, the absence of α-TCP is possibly due to the conversion of α-TCP into β-TCP on slow cooling of bone specimens after heat treatment which is also believed to be promoted by the presence of magnesium [154, 162].

The results have also shown that the response of bone mineral to heat treatment is related to the compositional characteristics of bone, measured using elemental analyses and IR spectroscopy. They have demonstrated that magnesium, potassium, sodium, strontium and fluorine each exert a significant influence on the thermal decomposition of HAP.

The presence of magnesium was shown to influence the percentages of β-TCP, TTCP, MgO and CaO formed on heating bone to 1400 °C. The results suggest that magnesium favours the formation of β-TCP, MgO and CaO but that the formation of TTCP is unfavourable in the presence of magnesium. Furthermore, the results also suggest that β-TCP formation is favoured in the presence of potassium ions.

The results for the percentage of strontium and fluorine in bone suggest that the presence of strontium favours the stabilisation of the MgO decomposition product whereas the presence of fluorine does not favour the formation of MgO and β-TCP. However, the results also suggest the presence of fluorine favours the formation of TTCP. Fluorine has been shown to stabilise the mineral phase of HAP by substituting in place of hydroxyl ions within the crystal lattice. It is proposed here that fluorine may stabilise TTCP by substituting in place of oxide ions within the lattice that are not associated with any phosphate ions and that oxide ion vacancies maintain charge balance within the lattice.

There are no previous reports of the detection of β-TCP or MgO in bone heated to 600 °C. This is likely to be due to a combination of the following reasons. The methods of phase identification employed have not been sensitive enough to detect the presence of either of the two phases and, temperatures other than 600 °C are more commonly used in studies of heated bone. Furthermore, chicken bone, in particular, is rarely investigated.

The formation of β-TCP in bone heated to 600 °C is attributed to a much reduced thermal decomposition temperature of the HAP mineral phase. However, the thermal decomposition of HAP is not a satisfactory explanation for the formation of MgO. No other decomposition products were detected in association with MgO in bone heated to 600 °C. Therefore, it is proposed that the mechanism for its formation differs from the mechanism proposed for bone heated to 1400 °C. One possible explanation is the formation of MgO from

magnesium ions contained within the organic component and as a result of the combustion of the organic component. MgO would therefore be formed on heating bone that has a relatively high amount of magnesium within the organic component. This explanation is consistent with the lack of detection of associated decomposition products. However, another explanation for the formation of MgO from magnesium located on the HAP crystal surfaces is also plausible. The detection of MgO was found for bone specimens with relatively high values of HAP <00ℓ> when heated to 600 °C. It is proposed that recrystallisation on heating results in the stabilisation of HAP crystals beyond the point that enables the incorporation of surface bound magnesium ions within the lattice and therefore, necessitates the formation of MgO. It is not possible to unequivocally establish the mechanism for MgO formation in bone heated to 600 °C, based on the results of this study. Further investigation of its formation is therefore recommended.

Although, in general it was found that recrystallisation of HAP crystals in the <00ℓ> direction did not occur to any great extent on heating bone to 600 °C, a distinctive exception to this general finding was human UK bone. Human bone had significantly greater values to those obtained for all other species. Furthermore, the variation in HAP <00ℓ> values for unheated bone was the only significant difference found between human UK and human AUS bone for the characteristics measured using XRD. It is widely acknowledged that an increase in crystallintity of the HAP, on heating bone, coincides with the loss of the organic component through the process of combustion. However, the physical

restriction imposed by the organic component, on the increase in HAP <00ℓ> values has not previously been directly demonstrated. The percentages of nitrogen, carbon and hydrogen for human AUS bone were greater than those obtained for human UK. Also, the maximum value obtained for the percentage of mass loss for human AUS bone specimens heated to 600 °C was significantly greater than the maximum value obtained for human UK bone speciemens. Thus, it is proposed that a greater amount of the organic component was present in human AUS bone heated to 600 °C and that this had the effect of restricting the increase in HAP <00ℓ> values on heating. However, similar values to human UK were obtained for the percentages of nitrogen, carbon and hydrogen for other species but similar increases in HAP <00ℓ> values did not occur. It is therefore also proposed that the presence of the organic component is only one of several factors that inhibit the increase in crystallinity of the HAP phase on heating bone.

6.5 – INTER-SPECIES VARIATION IN COMPOSTITION AND STRUCTURE

The results have demonstrated that significant inter-species differences exist, in terms of the structure and composition of bone mineral. The HAP <00ℓ> values of unheated chicken bone were significantly less than those of the majority of other species. Whereas HAP <00ℓ> values of unheated human AUS bone were significantly greater than the majority of other species and HAP <00ℓ> values of unheated human UK bone were significantly greater than 50 % of the other species. These results suggest that there are inter-species differences in

biological requirements for the crystallinity of bone mineral. The reasons behind a need for small size and/or highly strained crystals in chicken but larger size and/or less strained crystals in human bone have yet to be fully determined. However, possible explanations include a need for a higher bone turnover rate and a greater need for quickly accessible ions in chicken.

Compared to the differences observed for HAP <00ℓ>, there were fewer significant differences between species in terms of the HAP lattice parameters obtained for unheated bone. The only significant differences between species in terms of HAP ‘c’ were between elephant and other species and between monkey and other species. However, chicken bone was notable for high values obtained for HAP ‘a’ and low values obtained for HAP ‘c’. In general, values of HAP ‘a’ obtained for human bone were significantly lower than those obtained for other species.

Inter-species variation was evident within the general correlations of HAP <00ℓ> and each of the HAP lattice parameters, for unheated bone. Significant positive correlations were obtained for deer and pig species in terms of HAP ‘a’ and HAP <00ℓ>. Negative correlations were obtained for rabbit, chicken and sheep species, although these were not significant.

6.6 – INTER-SPECIES VARIATION IN RESPONSE TO HEAT TREATMENT

The results have demonstrated that significant inter-species differences exist, in terms of the general response of bone to heat treatment. In particular, chicken and rat were distinctive from all other species due to the consistent formation of β-TCP in bone heated to 600 °C and the low percentage values, or absence, of TTCP in bone heated to 1400 °C. They were also distinctive due to the low values obtained for β-TCP ‘a’ for bone heated to 1400 °C.

Human bone was also distinctive from all other species in terms of β-TCP ‘a’, for the high values obtained. Also, values obtained for HAP ‘c’ for human bone heated to 600 °C were significantly greater than those obtained for all other species. Human, dog and elephant were significantly different from the majority of other species, in terms of the percentage of MgO formed on heating bone to 1400 °C.

However, there were species which could not be distinguished from each other based on the characteristics measured within this study, for example cow and goat (see section 5.9). The proposal that dietary differences are the underlying cause for the variation observed between species within this study potentially offers a plausible explanation for these findings. This is supported by the similarity of the characteristics measured for ruminant species and rabbit bone (see section 6.7).

6.7 – SPECIES IDENTIFICATION

The potential for the development of a new method of species identification based on bone mineral characteristics, measured using X-ray diffraction is evaluated here, through the testing of the hypotheses listed in section 4.1.7.

Hypothesis 7 (a) proposed that human bone can be distinguished from bone of all other species, based on the extent of inter-species variation in bone mineral characteristics of unheated and heated bone. The hypothesis can be accepted, based on the results of this study. Human bone was shown to be significantly distinct from the bone of all other species investigated in terms of its structure and composition and also, its response to heat treatment.

It is proposed here that human bone can be identified from non-human bone when the characteristics of a bone specimen meet all of the following criteria:

The HAP <00ℓ> value obtained for unheated bone is greater than 230 Å. No β-TCP is detected in bone heated to 600 °C but is detected in bone heated to 1400 °C, with a weight percentage of less than 50 %. The mineral phases TTCP, MgO and CaO are all detected in bone heated to 1400 °C and the percentage of MgO detected is less than 1 %. The value obtained for HAP ‘c’ for bone heated to 600 °C is greater than 6.89 Å and the value obtained for β-TCP ‘a’ for bone heated to 1400 °C is greater than 10.44 Å. Mass loss from bone heated to 1400 °C is between 40- 50 % of the mass prior to heating.

Hypothesis 7 (b) proposed that sheep bone can be distinguished from goat bone. The only significant differences found between sheep and goat were mass loss characteristics. Therefore, the hypothesis cannot be accepted based on the results of this study. However, despite non-significant results, HAP <00ℓ> values obtained for unheated goat bone were clearly greater than values obtained for unheated sheep bone and, HAP ‘a’ values for sheep were greater than those obtained for goat. Furthermore, the percentage of carbon in bone heated to 600 °C was shown to be greater for goat than for sheep and, the two species differ in terms of the percentage of sodium, magnesium, potassium, strontium and chlorine in bone. It is proposed that additional characteristics are investigated for sheep and goat bone to further explore the variation between the two species.

The ruminant species investigated within this study were not significantly different from each other in terms of the characteristics of unheated and heated bone measured using XRD. They were each significantly different from the majority of other species. However, rabbit could not be distinguished from any of the ruminant species and there were few significant differences between each of ruminant species and pig. Rabbit bone did however tend to have, lower mass loss values, lower values for the percentage of β-TCP and greater values of β-TCP ‘c’ for bone heated to 1400 °C, and lower values for the percentage of CaO. Also, rabbit bone had a greater percentage of calcium than any other species and a greater percentage of iron compared to ruminant species.

Therefore, hypothesis 7 – (c) can be accepted; bone from ruminant species can be distinguished from the bone of non-ruminant species.

The results obtained from this study have clearly demonstrated the considerable potential for the development of a new method of species identification based on bone mineral characteristics, measured using X-ray diffraction. The development of such a method for the purpose of distinguishing human from non-human bone and ruminant from non-ruminant species is therefore recommended. The development of a method of distinguishing sheep from goat bone is also recommended. However, it is acknowledged any development must involve the investigation of additional characteristics in order to improve identification power.

CHAPTER 7 – CONCLUSIONS

7.1 – RESEARCH CONCLUSIONS

This thesis has demonstrated that bone mineral has a general composition and structure that is common to all the individuals of all species investigated. It provides strong support for the acceptance of the further hypothesis that bone from all species that possess an internal skeleton has the same general mineral composition and structure. It has also provided evidence that the general biological control of bone mineral composition and structure is similar for all species investigated. Control of crystallinity through variation in HAP lattice defects has been demonstrated. In particular, magnesium and fluorine in bone have been shown to influence HAP crystallinity and there is biological control over the amount of each ion, relative to other ions, within bone.

The investigation of heated bone has shown that there is a measurable, general response of bone to heat treatment, when heat treatment conditions are standardised. The general response includes a reduction in HAP unit cell volume and the consistent formation of β-tri-calcium phosphate and magnesium oxide as thermal decomposition products of the calcium hydroxylapatite mineral phase.

The study of heated bone from a range of species has also demonstrated that there is variation in the general response of bone to heat treatment. Characteristics of heated bone have been shown to exhibit significant inter-species variation. Furthermore, an underlying chemical basis for the variation has been demonstrated. An evaluation of the inter-species variation in the measured characteristics of unheated and heated bone have resulted in the conclusion that there is considerable potential for the development of a new method of species identification, using X-ay diffraction analysis of bone.

7.2 – CONTRIBUTION TO KNOWLEDGE

This thesis makes a significant contribution to knowledge of bone mineral chemistry, its response to heat treatment and the extent of variation in bone mineral characteristics of unheated and heated bone. It is the largest published study of X-ray diffraction analysis of bone that has been conducted to date, in terms of the range and numbers of individuals of each species.

This study is the first to demonstrate significant differences between species in terms of bone mineral characteristics, measured using X-ray diffraction analysis. Furthermore, the results obtained from this research provide clear foundation boundaries for knowledge of the extent of variation in bone mineral characteristics. The research approach that was adopted for this study provides a robust means of testing these boundaries in future work (see section 7.3).

It is also the first quantitative comparative study of the thermal decomposition products of bone mineral. The direct influence of the organic component of bone on the recrystallisation of bone mineral on heating has not previously been demonstrated. Furthermore, this study is the first to present evidence for inter-species variation of the biological control mechanisms imposed on bone mineral composition and structure.

The results of this study are of wide-scale relevance to bone mineral research fields and have considerable potential value to a large number of practical applications. To forensic science, archaeology and other allied research fields, it demonstrates the value of research into bone mineral chemistry, using X-ray diffraction, particularly in terms of the development of a new method of species identification. This study is the first to provide data that enables species discrimination based on bone mineral characteristics. To bio-medical and bio-materials science, this thesis demonstrates the value of establishing a better understanding of the extent of inter-species variation in bone mineral characteristics. This is of particular importance for research that involves the choice of appropriate animal models as analogues for human bone. Furthermore, to all these research fields, it clearly shows the benefits of an interdisciplinary perspective towards bone mineral research and assists in bridging current subject gaps.

7.3 – FUTURE WORK

The expansion and development of knowledge of bone mineral chemistry, its response to heat treatment and, the extent of variation in bone mineral characteristics of unheated and heated bone, marked by the contributions of this thesis should be continued through further research in the future.

There are many factors that affect the observed variation in bone mineral characteristics of unheated and heated bone and the nature and extent of their influence should be investigated. Future studies should, for example, investigate the bone mineral characteristics of archaeological bone, bone affected by disease and bone heated under a variety of heat treatment conditions. Although, diagenetic factors (changes due to burial) are known to cause an increase in bone mineral crystallinity, the extent of this and knowledge of other diagenetic effects on bone mineral chemistry are not well established. Similarly, although bone disease such as osteoporosis, is known to cause a loss of bone mineral density, its effect on bone mineral crystal quality is to-date, poorly defined.

The experimental approach adopted for the research yielded many results from the collected data for bone mineral characteristics additional to those presented within this thesis. Further work should consider and discuss these results, with reference to the findings of this thesis. In addition, future studies should develop the experimental approach used in this study, to incorporate the investigation of crystal lattice site occupancy, using Rietveld refinement. Principal component

analysis should also be applied to the data set of this study and those of future studies.

This study has provided a baseline for variation in bone mineral characteristics through the strict control of heat treatment conditions. Future studies should investigate the effect of systematic variation of heat treatment conditions on the response of bone to heat treatment, controlling for species and potential confounding factors such as age. Future work should also explore the response of bone to heat treatment through in situ analysis.

An investigation into inter-species variation in terms of crystallite size and strain of unheated bone and how these characteristics change due to heat treatment of bone should be conducted. Further investigations of the formation mechanism of magnesium oxide in bone heated to 600 °C and the influence of the organic component on HAP crystal morphology should also be carried out.

Research that specifically focuses on further investigating inter-species variation in bone mineral characteristics using infrared spectroscopy and a range of elemental analytical techniques should be conducted. The knowledge of the processes of thermal decomposition of calcium hydroxylapatite should be expanded and developed, using synthetic calcium hydroxylapatites to supplement bone mineral studies and, through the employment of techniques such as thermo-gravimetric analysis and mass spectrometry.

REFERENCES

1. Bass, W.M., *Human Osteology: A Laboratory and Field Manual*. 4 ed. 1995: Missouri Archaeological Society Inc.
2. Buikstra, J.E. and D.H. Ubelaker, eds. *Standards for Data Collection from Human Skeletal Remains*. 1994.
3. Cornwall, I.W., *Determination of Species from Bones*. Bones for the Archaeologist, London: Phoenix House Ltd.
4. Brothwell, D.R., *II: 2: The Differentiation of Human from Other Larger Mammal Bones*, in *Digging Up Bones*. 1981, Cornell University Press. p. 36-43.
5. Cattaneo, C., *Forensic Anthropology: Developments of a Classical Discipline in the New Millenium.* Forensic Science International, 2007. **165**(2-3): p. 185 - 193.
6. Imaizumi, K., et al., *Identification of Fragmented Bones Based on Anthropological and DNA Analyses: Case Report.* Legal Medicine, 2002. **4**: p. 251 - 256.
7. Andrews, P., *Experiments in Taphonomy.* Journal of Archaeological Science, 1995. **22**: p. 147 - 153.
8. Ambrose, S.H. and J. Krigbaum, *Bone Chemistry and Bioarchaeology.* Journal of Anthropological Archaeology, 2003. **22**: p. 193 - 199.
9. Bonnichsen, R. and M.H. Sorg, eds. *Bone Modification*. Center for the Study of the First Americans, Peopling of the Americas Publications. 1989, Thompson-Shore Inc.: Dexter.
10. Lambert, J.B. and J.M. Weydert-Homeyer, *The Fundamental Relationship Between Ancient Diet and the Inorganic Constituents of Bone as Derived from Feeding Experiments.* Archaeometry, 1993. **35**(2): p. 279 - 294.
11. Caulier, H., et al., *The Effect of Ca-P Plasma-sprayed Coatings on the Initial Bone Healing of Oral Implants: An Experimental Study in the Goat.* Journal of Biomedical Materials Research, 1997. **34**: p. 121 - 128.
12. Lambert, J.B., X. Liang, and J.E. Buikstra, *Inorganic Analysis of Excavated Human Bone after Surface Removal.* Journal of Archaeological Science, 1991. **18**: p. 363 - 383.
13. Castellano, M.A., E.C. Villanueva, and R. von Frenckel, *Estimating the Date of Bone Remains: A Multivariate Study.* Journal of Forensic Sciences, 1984. **29**(2): p. 527 - 534.
14. Whyte, T.R., *Distinguishing remains of human cremations from burned animal bones.* J. Field Archaeol., 2001. **28**: p. 437 - 448.
15. Hedges, R.E.M., *Bone Diagenesis: An Overview of Processes.* Archaeometry, 2002. **44**(3): p. 319 - 328.
16. Munro, L.E., F.J. Longstaffe, and C.D. White, *Burning and Boiling of Modern Deer Bone: Effects on Crystallinity and Oxygen Isotope*

Comparison of Bioapatite Phosphate. Palaeogeography, Palaeoclimatology, Palaeoecology, 2007. **249**: p. 90 - 102.
17. Person, A., et al., *Early Diagenetic Evolution of Bone Phosphate: An X-ray Diffractometry Analysis.* Journal of Archaeological Science, 1995. **22**: p. 211 - 221.
18. Pijoan, C.M., et al., *Thermal alterations in archaeological bones.* Archaeometry, 2007. **4**: p. 713 - 727.
19. Stiner, M.C., et al., *Differential burning, recrystallization, and fragmentation of archaeological bone.* J. Arch. Sci., 1995. **22**: p. 223 - 237.
20. Bollongino, R. and J.-D. Vigne, *Temperature Monitoring in Arcaheological Animal Bone Samples in the Near East Arid Area, Before, Durning and After Excavation.* Journal of Archaeological Science, 2008. **35**(4): p. 873 - 881.
21. Staiti, N., D. Di Martino, and L. Saravo, *A Novel Approach in Personal Identification from Tissue Samples Undergone Different Processes Through STR Typing.* Forensic Science International, 2004. **146S**: p. S171 - S173.
22. Pfeiffer, I., J. Burger, and B. Brenig, *Diagnostic Polymorphisms in the Mitochondrial Cytochrome b Gene Allow Discrimination Between Cattle, Sheep, Goat, Roe buck and Deer by PCR-RFLP.* Biomed Central Genetics, 2004. **5**(30): p. 1 - 5.
23. Enlow, D.H. and S.O. Brown, *A Comparative Histological Study of Fossil and Recent Bone Tissues. Part II.* Texas Journal of Science, 1957. **9**: p. 186 - 214.
24. Jowsey, J., *Age Changes in Human Bone.* Clinical Orthopaedics and Related Research, 1960. **17**: p. 210 - 217.
25. Jowsey, J., *Studies of Haversian Systems in Man and Some Animals.* Journal of Anatomy, 1966. **100**(4): p. 857 - 864.
26. Enlow, D.H. and S.O. Brown, *A Comparative Histological Study of Fossil and Recent Bone Tissues. Part I.* Texas Journal of Science, 1957. **7**: p. 405 - 443.
27. Enlow, D.H. and S.O. Brown, *A Comparative Histological Study of Fossil and Recent Bone Tissues. Part III.* Texas Journal of Science, 1958. **10**: p. 187 - 230.
28. Hillier, M.L. and L.S. Bell, *Differentiating human bone from animal bone: a review of histological methods.* J. Forensic Sci., 2007. **52**(2): p. 249 - 263.
29. Cuijpers, A.G.F.M., *Histological identification of bone fragments in archaeology: telling humans apart from horses and cattle.* Int. J. Osteoarchaeol., 2006. **16**: p. 465 - 480.
30. Martiniakova, M., et al., *Differences among species in compact bone tissue microstructure of mammalian skeleton: use of a discriminant function analysis for species identification.* J. Forensic Sci., 2006. **51**(6): p. 1235 - 1239.
31. Cattaneo, C., et al., *Differential Survival of Albumin in Ancient Bone.* Journal of Archaeological Science, 1995. **22**: p. 271 - 276.

32. Cattaneo, C., et al., *Determining the human origin of fragments of burnt bone: a comparative study of histological, immunological and DNA techniques.* Forensic Sci. Int., 1999. **102**: p. 181 - 191.
33. Lowenstein, J.M., et al., *Identification of Animal Species by Protein Radioimmunoassay of Bone Fragments and Bloodstained Stone Tools.* Forensic Science International, 2006. **159**(2 - 3): p. 182 - 188.
34. Ferllini, R., *Silent Witness: How Forensic Anthropology is Used to Solve the World's Toughest Crimes*. 1 ed. 2002: Firefly Books Ltd.
35. Bergslien, E.T., M. Bush, and P.J. Bush, *Identification of cremains using X-ray diffraction spectroscopy and a comparison to trace element analysis.* Forensic Sci. Int., 2008. **175**(2): p. 218 - 226.
36. Brooks, T., et al., *Elemental Analysis of Human Cremains Using ICP-OES to Classify Legitimate and Contaminated Cremains.* Journal of Forensic Science, 2006. **51**(5): p. 967 - 1004.
37. Scheuer, L., *Application of Osteology to Forensic Medicine.* Clinical Anatomy, 2002. **15**: p. 297 - 312.
38. Thompson, T.J.U., *Heat-induced Dimensional Changes in Bone and their Consequences for Forensic Anthropology.* Journal of Forensic Science, 2005. **50**(5): p. 1 - 8.
39. Owsley, D.W., A.M. Mires, and M.S. Keith, *Case involving differentiation of deer and human bone fragments.* J. Forensic Sci., 1985. **30**(2): p. 572 - 578.
40. Parson, W., et al., *Species Identification by Means of the Cytochrome b Gene.* International Journal of Legal Medicine, 2000. **144**: p. 23 - 28.
41. Driver, J.C., *Identification, classification and zooarchaeology.* Circaea, 1992. **9**(1): p. 35 - 47.
42. Gilmore, R.M., *The Identification and Value of Mammal Bones from Archaeologic Excavations.* Journal of Mammalogy, 1949. **30**(2): p. 163 - 169.
43. Baker, B.W. and B.S. Shaffer, *Assumptions about Species: A Case Study of Tortoise Bones from SE Texas.* Journal of Field Archaeology, 1999. **26**(1): p. 69 - 74.
44. Balasse, M. and S.H. Ambrose, *Distinguishing Sheep and Goats Using Dental Morphology and Stable Carbon Isotopes in C4 Grassland Environments.* Journal of Archaeological Science, 2005. **32**: p. 691 - 702.
45. Bond, J.M., *Burnt Offerings: Animal Bone in Anglo-Saxon Cremations.* World Archaeology, 1996. **28**(1: Zooarchaeology: New Approaches and Theory): p. 76 - 88.
46. Outram, A.K., et al., *Understanding Complex Fragmented Assemblages of Human and Animal Remains: A Fully Integrated Approach.* Journal of Archaeological Science, 2005. **32**: p. 1699 - 1710.
47. Knusel, C.J. and A.K. Outram, *Fragmentation: The Zonation Method Applied to Fragmented Human Remains from Archaeological and Forensic Contexts.* Environmental Archaeology, 2004. **9**: p. 85 - 97.
48. Choyke, A.M., *Patterns in the Use of Cattle and Sheep/Goat Metapodials in Bronxze Age Hungary*. Animals and Archaeology: 4. Husbandry in Europe, ed. C. Grigson and J. Clutton-Brock. 1984: BAR International Series 227

57 - 65.
49. Ryder, M.L., *Animal Bones in Archaeology*. 1969: Blackwell Scientific Publications.
50. Bokonyi, S., *A New Method for the Determination of the Number of Individuals in Animal Bone Material.* American Journal of Archaeology, 1970. **74**(3): p. 291 - 292.
51. Wan, Q.-H. and S.-G. Fang, *Application of Species-specific Polymerase Chain Reaction in the Forensic Identification of Tiger Species.* Forensic Science International, 2003. **131**: p. 75 - 78.
52. Karlsson, A.O. and G. Holmlund, *Identification of Mammal Species Using Species-Specific DNA Pyrosequencing.* Forensic Science International, 2007. **173**: p. 16 - 20.
53. Wetton, J.H., et al., *An Extremely Sensitive Species-specific ARMS PCR Test for the Presence of Tiger Bone DNA.* Forensic Science International, 2002. **126**: p. 137 - 144.
54. Verma, S.K. and L. Singh, *Novel Universal Primers Establish Identity of an Enormous Number of Animal Species for Forensic Application.* Molecular Ecology Notes, 2003. **3**: p. 28 - 31.
55. Aarts, H.J.M., et al., *Detection of Bovine Meat and Bone Meal in Animal Feed at a Level of 0.1%.* Agricultural Materials, 2006. **89**(6): p. 1443 - 1446.
56. Colgan, S., et al., *Development of a DNA-based Assay for Species Identification in Meat and Bone Meal.* Food Research International, 2001. **34**: p. 409 - 414.
57. van Raamsdonk, L.W.D., et al., *New developments in the detection and identification of processed animal proteins in feeds.* Animal Feed Sci. Technol., 2007. **133**: p. 63 - 83.
58. Einhorn, T., *Bone Strength: The Bottom Line.* Calcified Tissue International, 1992. **51**: p. 333 - 339.
59. Boskey, A., *Mineralization of Bones and Teeth.* Elements, 2007. **3**: p. 385 - 391.
60. Nafte, M., *4: The Human Skeleton - A Beginner's Guide*, in *Flesh and Bone: An Introduction to Forensic Anthropology*. 2000, Carolina Academic Press. p. 51 - 54.
61. Rho, J.-Y., L. Kuhn-Spearing, and P. Zioupos, *Mechanical Properties and the Hierarchical Structure of Bone.* Medical Engineering and Physics, 1998. **20**: p. 92 - 102.
62. Elliott, J.C., *The Problems of the Composition and Structure of the Mineral Components of the Hard Tissues.* Clinical Orthopaedics and Related Research, 1973. **93**: p. 313 - 344.
63. Betts, F., N.C. Blumenthal, and A.S. Posner, *Bone Mineralization.* Journal of Crystal Growth, 1981. **53**: p. 63 - 73.
64. Brown, W.E. and L.C. Chow, *Chemical Properties of Bone Mineral.* Annu. Rev. Materials Science, 1976. **6**: p. 213 - 236.
65. Posner, A.S., *Crystal Chemistry of Bone Mineral.* Physiological Reviews, 1969. **49**(4): p. 760 - 792.

66. Bale, W.F., H.C. Hodge, and S.L. Warren, *Roentgen-ray Diffraction Studies of Enamel and Dentine.* American Journal of Roetgenol Radium Therapy, 1934. **32**(3): p. 369 - 376.
67. Mathew, M. and S. Takagi, *Structures of Biological Minerals in Dental Research.* Journal of Research of the National Institute of Standards and Technology, 2001. **106**: p. 1035 - 1044.
68. Beckett, S., M. Hatton, and K. Rogers, *The Discovery and Analysis of a Urinary Calculus from an Anglo-Saxon Burial in Sedgeford, Norfolk.* Norfolk Archaeology, 2008. **XLV**: p. 397 - 409.
69. Dorozhkin, S.V. and M. Epple, *Biological and medical significance of calcium phosphates.* Angew. Chem. Int. Ed., 2002. **41**: p. 3130 - 3146.
70. van Raemdonck, W., P. Ducheyne, and P. de Meester, *Calcium Phosphate Ceramics*. Metal and Ceramic Biomaterials Volume II: Strength and Surface, ed. P. Ducheyne and G.W. Hastings, Florida: CRC Press Inc.
71. Wenk, H.-R. and A. Bulakh, *Minerals, their constitution and origin*. Vol. 1. 2004: Cambridge University Press.
72. Rey, C., *Apatite Channels and Zeolite-Like Properties*. Hydroxyapatite and Related Materials, ed. P.W. Brown and B. Constantz. Vol. 1. 1994: CRC Press. 257 - 262.
73. Elliott, J.C., R.M. Wilson, and S.E.P. Dowker, *Apatite Structures.* Adv. X-ray Anal., 2002. **45**: p. 172 - 181.
74. Young, R.A., *Biological apatite vs hydroxyapatite at the atomic level.* Clin. Orthop. Relat. Res., 1975. **113**: p. 249 - 262.
75. Elliott, J.C., P.E. Mackie, and R.A. Young, *Monoclinic Hydroxyapatite.* Science, 1973. **180**(4090): p. 1055 - 1057.
76. Elliott, J.C., *Recent Progress in the Chemistry, Crystal Chemistry and Structure of the Apatites.* Calcified Tissue Research, 1969. **3**: p. 293 - 307.
77. LeGeros, R.Z., *Apatites in biological systems.* Prog. Cryst. Growth Charact., 1981. **4**: p. 1 - 45.
78. Brown, P.W. and B. Constantz, eds. *Hydroxyapatites and Related Materials*. 1994, CRC Press.
79. LeGeros, R.Z., *Biological and Synthetic Apatites*. Hydroxyapatite and Related Materials, ed. P.W. Brown and B. Constantz. Vol. 1. 1994: CRC Press. 3 - 28.
80. Antonakos, A., E. Liarokapis, and T. Leventouri, *Micro-Raman and FTIR Studies of Synthetic and Natural Apatites.* Biomaterials, 2007. **28**: p. 3043 - 3054.
81. Bale, W.F., *A Comparative Roentgen-ray Diffraction Study of Several Natural Apatites and the Apatite-like Constituent of Bone and Tooth Substance.* American Journal of Roentgenol Radium Therapy, 1940. **43**(5): p. 735 - 747.
82. Baxter, J.D., R.M. Biltz, and E.D. Pellegrino, *The Physical State of Bone Carbonate: A Comparative Infra-red Study in Several Mineralized Tissues.* Jale Journal of Biology and Medicine, 1966. **38**: p. 456 - 470.

83. Berry, E.E., *The Structure and Composition of Some Calcium-deficient Apatites.* Bulletin Societe Chimique de France, 1968. **Special Issue**: p. 1765 - 1770.
84. Berry, E.E., *The Structure and Composition of Some Calcium-deficient Apatites.* J. Inorg. Nucl. Chem., 1967. **29**: p. 317 - 327.
85. Berry, E.E., *The Structure and Composition of Some Calcium-deficient Apatites. II.* Journal of Inorganic Nucl. Chemistry, 1967. **29**: p. 1585 - 1590.
86. Dykes, E. and J.C. Elliott, *The Occurence of Chloride Ions in the Apatite Lattice of Holly Springs Hydroxyapatite and Dental Enamel.* Calcified Tissue International, 1971. **7**: p. 241 - 248.
87. Young, R.A. and D.W. Holcomb, *Variability of Hydroxyapatite Preparations.* Calcified Tissue International, 1982. **34**: p. S17 - S32.
88. Wopenka, B. and J.D. Pasteris, *A mineralogical perspective on the apatite in bone.* Mater. Sci. Eng. C, 2005. **25**: p. 131 - 143.
89. Chakraborty, S., et al., *Structural and microstructural characterization of bioapatites and synthetic hydroxyapatite using X-ray powder diffraction and fourier transform infrared techniques.* J. Appl. Cryst., 2006. **39**: p. 385 - 390.
90. Pasteris, J.D., et al., *Lack of OH in Nanocrystalline Apatite as a Function of Degree of Atomic Order: Implications for Bone and Biomaterials.* Biomaterials, 2004. **25**: p. 229 - 238.
91. Posner, A.S., *The Mineral of Bone.* Clinical Orthopaedics and Related Research, 1985. **200**: p. 87 - 99.
92. Termine, J.D., *Mineral Chemistry and Skeletal Biology.* Clinical Orthopaedics and Related Research, 1972. **85**: p. 207 - 241.
93. Neuman, W.F. and M.W. Neuman, *The Nature of the Mineral Phase of Bone.* Chem. Rev., 1953. **53**: p. 1 - 45.
94. Astala, R. and M.J. Stott, *First Principles Investigation of Mineral Component of Bone: CO3 Substitutions in Hydroxyapatite.* Chem. Materials, 2005. **17**: p. 4125 - 4133.
95. Hendricks, S.B. and W.L. Hill, *The Nature of Bone and Phosphate Rock.* Proceedings of the National Academy of Sciences of the United States of America, 1950. **36**(12): p. 731 - 737.
96. Armstrong, W.D. and L. Singer, *Composition and Constitution of the Mineral Phase of Bone.* Clinical Orthopaedics and Related Research, 1965. **38**: p. 179 - 190.
97. Balmain, N., J.P. LeGeros, and G. Bonel, *X-ray diffraction of calcined bone tissue:a reliable method for the determination of bone Ca/P molar ratio.* Calcif. Tissue Int., 1982. **34**: p. S93 - S98.
98. LeGeros, R., N. Balmain, and G. Bonel, *Age-related changes in mineral of rat and bovine cortical bone.* Calcif. Tissue Int., 1987. **41**: p. 137 - 144.
99. McConnell, D., *The Crystal Chemistry of Carbonate Apatites and Their Relationship to the Composition of Calcified Tissues.* Journal of Dental Research, 1952. **31**: p. 53 - 63.
100. Ravaglioli, A., et al., *Mineral evolution of bone.* Biomaterials, 1996. **17**: p. 617 - 622.

101. Rischak, G., G. Lenart, and J. Pinter, *Comparative crystallographic analysis of different bones with X-ray diffractometry.* Acta Biochim. et Biophys. Acad. Sci. Hung., 1971. **6**(2): p. 157 - 164.
102. Aerssens, J., et al., *Interspecies differences in bone composition, density, and quality: potential implications for in vivo bone research.* Endo., 1998. **139**(2): p. 663 - 670.
103. Danilchenko, S.N., et al., *Carbonate location in bone tissue mineral by X-ray diffraction and temperature-programmed desorption mass spectrometry.* Crystal. Res. Technol., 2005. **40**(7): p. 692 - 697.
104. Ellies, L.G., D.G.A. Nelson, and J.D.B. Featherstone, *Crystallographic Structure and Surface Morphology of Sintered Carbonated Apatites.* Journal of Biomedical Materials Research, 1988. **22**: p. 541 - 553.
105. Currey, J.D., *The Mechanical Consequences of Variation in the Mineral Content of Bone.* Journal of Biomechanics, 1969. **2**: p. 1 - 11.
106. Handschin, R.G. and W.B. Stern, *X-ray Diffraction Studies on the Lattice Perfection of Human Bone Apatite (Crista Iliaca).* Bone, 1995. **16**(4): p. 355S - 363S.
107. Boskey, A., *Bone Mineral Crystal Size.* Osteoporosis International, 2003. **14**(S5): p. S16 - S21.
108. Bloebaum, R.D., et al., *Determining mineral content variations in bone using backscattered electron imaging.* Bone, 1997. **20**(5).
109. Bonar, L.C., et al., *X-ray Diffraction Studies of the Crystallinity of Bone Mineral in Newly Synthesized and Density Fractionated Bone.* Calcified Tissue International, 1983. **35**: p. 202 - 209.
110. Burnell, J.M., E.J. Teubner, and A.G. Miller, *Normal Maturational Changes in Bone Matrix, Mineral, and Crystal Size in the Rat.* Calcified Tissue International, 1980. **31**: p. 13 - 19.
111. Currey, J.D., *Some Effects of Ageing in Human Haversian Systems.* Journal of Anatomy, 1964. **98**(1): p. 69 - 75.
112. Woodard, H.Q., *The Composition of Human Cortical Bone: Effect of Age and Some Abnormalities.* Clinical Orthopaedics and Related Research, 1964. **37**: p. 187 - 193.
113. Muller, S.A., A.S. Posner, and H.E. Firschein, *Effect of Vitamin D Deficiency ont he Crystal Chemistry of Bone Mineral.* Proceedings of the Society for Experimental Biology and Medicine, 1966. **121**: p. 844 - 846.
114. Quinaux, N. and L.J. Richelle, *X-ray Diffraction and Infrared Analysis of Bone Specific Gravity Fractions in the Growing Rat.* Israel Journal of Medical Sciences, 1967. **3**: p. 77 - 90.
115. Fisher, L.W., et al., *Two Bovine Models of Osteogenesis Imperfecta Exhibit Decreased Apatite Crystal Size.* Calcified Tissue International, 1987. **40**: p. 282 - 285.
116. Gedalia, I., et al., *Calcium and Phosphate Content of Ash of Bones and Teeth of Human Fetuses in Relation to Fluoride Content of Drinking Water.* Proceedings of the Society of Experimental Biology in Medicine, 1965. **119**: p. 694 - 697.
117. Ioannidou, E., *Taphonomy of Animal Bones: Species, Sex, Age, and Breed Variability of Sheep, Cattle and Pig Bone Density.* Journal of Archaeological Science, 2003. **30**: p. 355 - 365.

118. Menczel, J., A.S. Posner, and R.A. Harper, *Age Changes in the Crystallinity of Rat Bone Apatite.* Israel Journal of Medical Sciences, 1965. **1**(2): p. 251 - 252.
119. Mkukuma, L.D., et al., *Thermal Stability and Structure of Canellous Bone Mineral from the Femoral Head of Patients with Osteoarthritis or Osteoporosis.* Ann. Rheum. Dis., 2005. **64**: p. 222 - 225.
120. Parkins, F.M., et al., *Relationships of Human Plasma Fluoride and Bone Fluoride to Age.* Calcified Tissue International, 1974. **16**: p. 335 - 338.
121. Posner, A.S., R.A. Harper, and S.A. Muller, *Age Changes in the Crystal Chemistry of Bone Apatite.* Annals of New York Academy of Science, 1965. **131**: p. 373 - 742.
122. Paschalis, E.P., et al., *FTIR Microspectroscopic Analysis of Human Iliac Crest Biopsies from Untreated Osteoporotic Bone.* Calcified Tissue International, 1997. **61**: p. 487 - 492.
123. Sobel, A.E., M. Rockenmacher, and B. Kramer, *Carbonate Content of Bone in Relation to the Composition of Blood and Diet.* Journal of Biological Chemistry, 1945. **158**: p. 475 - 489.
124. Thomson, D.D., *Age Changes in Bone Mineralization, Cortical Thickness, and Haversian Canal Area.* Calcified Tissue International, 1980. **31**: p. 5 - 11.
125. Rey, C., et al., *Fourier Transform Infrared Spectroscopic Study of the Carbonate Ions in Bone Mineral During Aging.* Calcified Tissue International, 1991. **49**: p. 251 - 258.
126. Wang, X., J.D. Mabrey, and C.M. Agrawal, *An Interspecies Comparison of Bone Fracture Properties.* Bio-Medical Materials and Engineering, 1998. **8**: p. 1 - 9.
127. Termine, J.D. and A.S. Posner, *Infrared Analysis of Rat Bone: Age Dependency of Amorphous and Crystalline Mineral Fractions.* Science, 1966. **153**(3743): p. 1523 - 1525.
128. Vetter, U., et al., *Changes in Apatite Crystal Size in Bones of Patients with Osteogenesis Imperfecta.* Calcified Tissue International, 1991. **49**: p. 248 - 250.
129. Biltz, R.M. and E.D. Pellegrino, *The chemical anatomy of bone: I. a comparative study of bone composition in sixteen vertebrates.* J. Bone Joint Surg. Am., 1969. **51**(3): p. 456 - 466.
130. Biltz, R.M. and E.D. Pellegrino, *The Nature of Bone Carbonate.* Clinical Orthopaedics and Related Research, 1977. **129**: p. 279 - 292.
131. Webster, A.V., et al., *The Properties of Milled Bone.* British Ceramic Trans. Journal, 1987. **86**: p. 91 - 98.
132. Buchanan, D.L. and A. Nakao, *Studies on the Nature of Bone Carbonate.* Archives of Biochemistry and Biophysics, 1958. **77**: p. 168 - 180.
133. Chickerur, N.S., M.S. Tung, and B.W. E., *A Mechanism for Incorporation of Carbonate into Apatite.* Calcified Tissue International, 1980. **32**: p. 55 - 62.
134. Catanese, J., J.D.B. Featherstone, and T.M. Keaveny, *Characterization of the Mechanical and Ultrastructural Properties of Heat-treated Cortical Bone for use as a Bone Substitute.* Journal of Biomedical Materials Research, 1999. **45**: p. 327 - 336.

135. Etok, S.E., et al., *Structural and Chemical Changes of Thermally Treated Bone Apatite.* Journal of Materials Science, 2007. **42**: p. 9807 - 9816.
136. Thompson, T.J.U., *Recent advances in the study of burned bone and their implications for forensic anthropology.* Forensic Sci. Int., 2004. **146S**: p. S203 - S205.
137. Walker, P.L., K.W.P. Miller, and R. Richman, *Time, Temperature, and Oxygen Availability: An Experimental Study of the Effects of Environmental Conditions on the Colour and Organic Content of Cremated Bone*, in *The Analysis of Burned Human Remains*, C.W. Schmidt and S.A. Symes, Editors. 2008, Academic Press.
138. Holden, J.L., *Heat-induced physical, chemical and structural alterations to human bone*, in *Department of Physics*. 1995, Monash University: Melbourne.
139. Bradtmiller, B. and J.E. Buikstra, *Effects of Burning on Human Bone Microstructure: A Preliminary Study.* Journal of Forensic Sciences, 1984. **29**(2): p. 535 - 540.
140. Ramrakhiani, M., D. Pal, and S.C. Datta, *Effect fo Heating on the Hardness of Human Bone.* Acta Analytica, 1980. **108**: p. 316 - 320.
141. Rogers, K.D. and P. Daniels, *An X-ray diffraction study of the effects of heat treatment on bone mineral microstructure.* Biomaterials, 2002. **23**: p. 2577 - 2585.
142. Carlstrom, D. and J.B. Finean, *X-ray Diffraction Studies on the Ultrastructure of Bone.* Biochimica et Biophysica Acta, 1954. **13**(2): p. 183 - 191.
143. Holden, J.L., J.G. Clement, and P.P. Phakey, *Age and temperature related changes to the ultrastructure and composition of human bone mineral.* J. Bone Min. Res., 1995. **10**(9): p. 1400 - 1407.
144. Hiller, J.C., et al., *Bone mineral change during experimental heating: an X-ray scattering investigation.* Biomaterials, 2003. **24**: p. 5091 - 5097.
145. Danilchenko, S.M., et al., *Thermal behaviour of biogenic apatite crystals in bone: an X-ray diffraction study.* Cryst. Res. Technol., 2006. **41**(3): p. 268 - 275.
146. Enzo, S., et al., *A study by thermal treatment and X-ray powder diffraction on burnt fragmented bones from tombs II, IV and IX belonging to the hypogeic necropolis of "Sa Figu" near Ittiri, Sassari (Sardinia, Italy).* J. Arch. Sci., 2007. **34**: p. 1731 - 1737.
147. Legros, R., N. Balmain, and G. Bonel, *Structure and Composition of the Mineral Phase of Periosteal Bone.* Journal of Chemical Research, 1986. **(S)**: p. 8 - 9.
148. Wheeler, E.J. and D. Lewis, *An X-ray Study of the Paracrystalline Nature of Bone Apatite.* Calcified Tissue Research, 1977. **24**: p. 243 - 248.
149. Amprino, R., *Investigations on Some Physical Properties of Bone Tissue.* Acta Anatomica, 1958. **34**(3): p. 161 - 186.
150. Barinov, S.M., et al., *Carbonate Loss from Two Magnesium-substituted Carbonated Apatites Prepared by Different Synthesis Techniques.* Materials Research Bulletin, 2006. **41**: p. 485 - 494.
151. Haberko, K., et al., *Natural hydroxyapatite - its behaviour during heat treatment.* J. Euro. Ceram.Soc., 2006. **26**: p. 537 - 542.

152. Neuman, W.F. and B.J. Mulryan, *Synthetic Hydroxyapatite Crystals.* Calcified Tissue Research, 1971. **7**: p. 133 - 138.
153. LeGeros, R.Z., et al., *Apatite Crystallites: Effects of Carbonate on Morphology.* Science, 1987. **155**: p. 1409 - 1411.
154. Baravelli, S., et al., *Thermal behaviour of bone and synthetic hydroxyapatites submitted to magnesium interaction in aqueous medium.* J. Inorg. Biochem., 1984. **20**: p. 1 - 12.
155. Shipman, P., G. Foster, and M. Schoeninger, *Burnt Bones and Teeth: an Experimental Study of Color, Morphology, Crystal Structure and Shrinkage.* Journal of Archaeological Science, 1984. **11**: p. 307 - 325.
156. Mkukuma, L.D., et al., *Effect of the proportion of organic material in bone on thermal decomposition of bone mineral: an investigation of a variety of bones from different species using thermogravimetric analysis coupled to mass spectrometry, high-temperature X-ray diffraction, and fourier transform infrared spectroscopy.* Calcif. Tissue Int., 2004. **75**: p. 321 - 328.
157. Ooi, C.Y., M. Hamdi, and S. Ramesh, *Properties of hydroxyapatite produced by annealing of bovine bone.* Ceram. Int., 2007. **33**: p. 1171 - 1177.
158. Bett, J.A.S., L.G. Christner, and W.K. Hall, *Studies of the Hydrogen Held by Solids. XII Hydroxyapatite Catalysts.* Journal of the American Chemical Society, 1967. **89**(22): p. 5535 - 5541.
159. Gross, K.A., et al., *Oxyapatite in Hydroxyapatite Coatings.* Journal of Materials Science, 1998. **33**: p. 3985 - 3991.
160. Barralet, J., et al., *Thermal Decomposition of Synthesised Carbonate Hydroxyapatite.* Journal of Materials Science: Materials in Medicine, 2002. **13**: p. 529 - 533.
161. Chen, J., et al., *Effect of Atmosphere on Phase Transformation in Plasma-Sprayed Hydroxyapatite Coatings During Heat Treatment.* Journal of Biomedical Materials Research, 1997. **34**: p. 15 - 20.
162. Ando, J., *Tricalcium phosphate and its variation.* Bull. Chem. Soc. Jpn., 1958. **31**: p. 196 - 201.
163. Haberko, K., et al., *Transformation of Bone Origin Hydroxyapatite at Elevated Temperatures and in Selected Atmospheres.* Advanced Materials Research, 2007. **29 - 30**: p. 231 - 234.
164. Lee, K.M., et al., *Development of a Method for the Determination of Heavy Metals in Calcified Tissues by Inductively Coupled Plasma-Mass Spectrometry.* Fresenius Journal Anal. Chem., 1999. **364**: p. 245 - 248.
165. Ostergard, M., *X-ray Diffractometer Investigations of Bones from Domestic and Wild Animals.* American Antiquity, 1980. **45**(1): p. 59 - 63.
166. Eanes, E.D., et al., *Small Angle X-ray Diffraction Analysis of the Effect of Fluoride on Human Bone Apatite.* Archives of Oral Biology, 1965. **10**: p. 161 - 173.
167. Bertelsen, P.K., J.G. Clement, and C.D.L. Thomas, *A Morphometric Study of the Cortex of the Human Femur from Early Childhood to Advanced Old Age.* Forensic Science International, 1995. **74**: p. 63 - 77.

168. Cartier, P., *Les Constituants Mineraux des Tissus Calcifies. II La Structure Moleculaire du Sel de l'Os.* Bulletin Societe Chimique Biologique, 1948. **30**: p. 73 - 81.
169. Chambers, E., *PIXE and Paleodiet: Reconstructing Subsistence of Florida's Middle Archaic Using a New Method of Trace Element Analysis.* Journal of Undergraduate Research, 2004. **5**(6): p. 1 - 9.
170. Chenery, S., et al., *Determination of Rare Earth Elements in Biological and Mineral Apatite by EPMA and LAMP-ICP-MS.* Mikrochim. Acta, 1996. **13**(S): p. 259 - 269.
171. De Leeuw, N.H., J.R. Bowe, and J.A.L. Rabone, *A Computational Investigation of Stoichiometric and Calcium-Deficient Oxy- and Hydroxy-apatites.* Faraday Discussions, 2007. **134**: p. 195 - 214.
172. Eanes, E.D., L. Powers, and J.L. Costa, *Extended X-ray Absorption Fine Structure (EXAFS) Studies on Calcium in Crystalline and Amorphous Solids of Biological Interest.* Cell Calcium, 1981. **2**(3): p. 251 - 262.
173. Horvath, A.L., *Solubility of Structurally Complicated Materials: II - Bone.* Journal of Physical and Chemical Reference Data, 2006. **35**(4): p. 1653 - 1668.
174. Outridge, P.M., R.J. Hughes, and R.D. Evans, *Determination of Trace Metals in Teeth and Bones by Solution Nebulization ICP-MS.* Atomic Spectroscopy, 1996. **17**(1): p. 1 - 8.
175. Sillen, A. and R. LeGeros, *Solubility Profiles of Synthetic Apatites and of Modern and Fossil Bones.* Journal of Archaeological Science, 1991. **18**: p. 385 - 397.
176. De Jong, W.F., *La Substance Minerale Dans Les Os.* Recueil des Travaux Chimiques, 1962. **45**: p. 445 - 448.
177. Glimcher, M.J., et al., *Recent Studies of Bone Mineral: Is the Amorphous Calcium Posphate Theory Valid?* Journal of Crystal Growth, 1981. **53**: p. 100 - 119.
178. Joschek, S., et al., *Chemical and physicochemical characterization of porous hydroxyapatite ceramics made of natural bone.* Biomaterials, 2000. **21**: p. 1645 - 1658.
179. Jokl, P. and H.C.W. Skinner, *Fluoride-Indiced Changes in Ashed Bone Mineral of Growing Sheep: An X-ray Diffraction Analysis.* The Journal of Bone and Joint Surgery, 1973. **55 (A)**(4): p. 761 - 770.
180. Larsen, M.J., O. Fejerskov, and S.J. Jensen, *Effects of Fluoride, Caclium, and Phosphate Administration on Mineralization in Rats.* Calcified Tissue International, 1980. **31**: p. 225 - 230.
181. Larsen, M.J., E.I.F. Pearce, and G. Ravnholt, *The Effectiveness of Bone Char in the Defluoridation of Water in Relation to its Crystallinity, Carbon Content and Dissolution Pattern".* Archives of Oral Biology, 1994. **39**(9): p. 807 - 816.
182. MacGregor, J. and B.E.C. Nordin, *Equilibrium Studies with Human Bone Powder.* The Journal of Biological Chemistry, 1960. **235**(4): p. 1215 - 1218.
183. Piga, G., et al., *A new method of the XRD technique for the study of archaeological burned human remains.* J. Arch. Sci., 2008. **35**: p. 2171 - 2178.

184. Posner, A.S. and S.R. Stephenson, *Crystallographic Investigation of Tricalcium Phosphate Hydrate.* Journal of Dental Research, 1952. **31**: p. 371 - 382.
185. Seltzer, M.D., V.A. Lance, and R.M. Elsey, *Laser Ablation ICP-MS Analysis of the Radial Distribution of Lead in the Femur of Alligator mississippiensis.* Science of the Total Environment, 2006. **363**: p. 245 - 252.
186. Soejoko, D.S. and M.O. Tjia, *Infrared Spectroscopy and X-ray Diffraction Study on the Morphological Variations of Carbonate and Phosphate Compounds in Giant Prawn (Macrobrachium rosenbergii) Skeletons During its Moulting Period.* Journal of Materials Science, 2003. **38**: p. 2087 - 2093.
187. Roberts, N.B., et al., *Determination of Elements in Human Femoral Bone Using Inductively Coupled Plasma Atomic Emission Spectrometry and Inductively Coupled Plasma Mass Spectrometry.* Journal of Analytical Atomic Spcetrometry, 1996. **11**: p. 133 - 138.
188. Rindby, A., P. Voglis, and P. Engstrom, *Microdiffraction Studies of Bone Tissues Using Synchrotron Radiation.* Biomaterials, 1998. **19**: p. 2083 - 2090.
189. Reinhard, K.J. and A.M. Ghazi, *Evaluation of Lead Concentrations in 18th-Century Omaha Indian Skeletons Using ICP-MS.* American Journal of Physical Anthropology, 1992. **89**: p. 183 - 195.
190. Turner, I.G. and G.M. Jenkins, *The Spatial Arrangement of Bone Mineral by Ion Bombardment.* Biomaterials, 1981. **2**: p. 234 - 238.
191. Tadic, D. and M. Epple, *A Thorough Physicochemical Characterisation of 14 Calcium Phosphate-based Substitution Materials in Comparison to Natural Bone.* Biomaterials, 2004. **25**: p. 987 - 994.
192. Raynaud, S., et al., *Determination of calcium/phosphorous ratio of calcium phosphate apatites using X-ray diffractometry.* J. Am. Ceram. Soc., 2001. **84**(2): p. 359 - 366.
193. Wilson, E.E., et al., *Highly Ordered Interstitial Water Observed in Bone by Nuclear Magnetic Resonance.* Journal of Bone and Mineral Research, 2005. **20**(4): p. 625 - 634.
194. Zlateva, B., R. Djingova, and I. Kuleff, *On the Possibilities of ICP-AES for Analysis of Archaeological Bones.* Central European Jounral of Chemistry, 2003. **3**: p. 201 - 221.
195. Yoshinaga, J., *Isotope Ratio Analysis of Lead in Biological Materials by Inductively Coupled Plkasma Mass Spectrometry.* Tohoku J. Exp. Med., 1996. **178**: p. 37 - 47.
196. Barnes, R.M., *Advances in Inductively Coupled Plasma Mass Spectrometry: Human Nutrition and Toxicology.* Analytica Chimica Acta, 1993. **283**: p. 115 - 130.
197. Cullity, B.D., *Diffraction I: Directions of Diffracted Beams*. 2 ed. Elements of X-ray Diffraction, ed. B.D. Cullity. 1978: Addison-Wesley Publishing Company Inc.
198. Jenkins, R. and R.L. Snyder, *Introduction to X-ray powder diffractometry*. A Series of Monographs on Analytical Chemistry and Its Appications, ed. J.D. Winefordner. Vol. 138. 1996: John Wiley & Sons, Inc.

199. Rouessac, F. and A. Rouessac, *Chemical Analysis: Modern Instrumentation Methods and Techniques*. English 1 ed. 2000.
200. Buldini, P.L., S. Cavalli, and A. Trifiro, *State-of the art ion chromatographic determination of inorganic ions in food.* Journal of Chromatography A, 1997. **789**(1-2): p. 529 -548.
201. Roseberry, A.B. Hastings, and J.K. Morse, *X-ray Analysis of Bone and Teeth.* Journal of Biological Chemistry, 1931. **90**: p. 395 - 408.
202. Clark, J.H., *A Study of Tendons, Bones and Other Forms of Connective Tissue by Means of X-ray Diffraction Patterns.* American Journal of Physiology, 1936. **98**: p. 328 - 337.
203. Dalconi, M.C., et al., *Structure of Bioapatite in Human Foetal Bones: An X-ray Diffraction Study.* Nuclear Instruments and Methods in Physics Research B, 2003. **200**: p. 406 - 410.
204. Young, R.A. and D.W. Holcomb, *Role of Acid Phosphate in Hydroxyapatite Lattice Expansion.* Calcified Tissue International, 1984. **36**: p. 60 - 63.
205. Nelson, D.G.A. and J.D.B. Featherstone, *Preparation, Analysis, and Characterization of Carbonated Apatites.* Calcified Tissue International, 1982. **34**(Supplement): p. S69 - S81.
206. Finean, J.B. and A. Engstrom, *The Low-Angle Scatter of X-rays from Bone Tissue.* Biochimica and Biophysica Acta, 1953. **11**: p. 178 - 189.
207. Frazier, P.D., I. Zipkin, and L.F. Mills, *X-ray Diffraction Study of Human Bone - Direct Methods of Estimating Changes in Line Broadening.* Archives of Oral Biology, 1967. **12**: p. 73 - 78.
208. Fernandez-Moran, H. and A. Engstrom, *Electron Microscopy and X-ray Diffraction of Bone.* Biochimica and Biophysica Acta, 1957. **23**: p. 260 - 264.
209. Carlstrom, D. and J.E. Glas, *The Size and Shape of the Apatite Crystallites in Bone as Determined from Line-Broadening Measurements on Oriented Specimens.* Biochimica et Biophysica Acta, 1959. **35**: p. 46 - 53.
210. Harper, R.A. and A.S. Posner, *Measurement of Non-Crystalline Calcium Phosphate in Bone Mineral.* Proceedings of the Society of Experimental Biology in Medicine, 1966. **122**: p. 137 - 142.
211. Termine, J.D. and A.S. Posner, *Amorphous/Crystalline Interrelationships in Bone Mineral.* Calcified Tissue Research, 1967. **1**: p. 8 - 23.
212. Roufosse, A.H., et al., *Identification of Brushite in Newly Deposited Bone Mineral from Embryonic Chicks.* Journal of Ultrastructure Research, 1979. **68**: p. 235 - 255.
213. Grynpas, M.D., L.C. Bonar, and M.J. Glimcher, *Failure to Detect an Amorphous Calcium-Phosphate Solid Phase in Bone Mineral: A Radial Distribution Function Study.* Calcified Tissue International, 1984. **36**: p. 291 - 301.
214. Bonar, L.C., M.D. Grynpas, and M.J. Glimcher, *Failure to Detect Crystalline Brushite in Embryonic Chick and Bovine Bone by X-ray Diffraction.* Journal of Ultrastructure Research, 1984. **86**: p. 93 - 99.
215. Rietveld, H.M., *A profile refinement method for nuclear and magnetic structures.* J. Appl. Cryst., 1969. **2**: p. 65 - 71.

216. Pritzkow, W. and H. Rentsch, *Stucture Refinement with X-ray Powder Diffraction Data for Synthetic Calcium Hydroxyapatite by Rietveld Method.* Crystal Research Technology, 1985. **20**: p. 857 - 960.
217. Holden, J.L. 1995.
218. Menghini, C., et al., *Rietveld Refinement on X-ray Diffraction Patterns of Bioapatite in Human Fetal Bones.* Biophysical Journal, 2003. **84**(3): p. 2021 - 2029.
219. Perdikatsis, B., *X-ray Powder Diffraction Study of Francolite by the Rietveld Method.* Materials Science Forum, 1991. **79 - 82**: p. 809 - 814.
220. Badraoui, B., et al., *Physicochemical Properties and Structural Refinement of Strontium-Lead Hydroxyapatites.* European Journal of Inorganic Chemistry, 2002: p. 1864 - 1870.
221. El Feki, H., J.M. Savariault, and A.B. Salah, *Structure Refinements by the Reitveld Method of Partially Substituted Hydroxyapatite: Ca9Na0.5(PO4)4.5(CO3)1.5(OH)2.* Journal of Alloys and Compounds, 1999. **287**: p. 114 - 120.
222. Ivanova, T.I., et al., *Crystal Structure of Calcium-Deficient Carbonated Hydroxyapatite. Thermal Decomposition.* Journal of Solid State Chemistry, 2001. **160**: p. 340 - 349.
223. Jackson, S.A., A.G. Cartwright, and D. Lewis, *The Morphology of Bone Mineral Crystals.* Calcified Tissue Research, 1978. **25**: p. 217 - 222.
224. Reid, J.W. and J.A. Hendry, *Rapid, accurate phase quantification of multiphase calcium phosphate materials using Reitveld refinement.* J. Appl. Cryst., 2006. **39**: p. 536 - 543.
225. Wilson, R.M., et al., *Reitveld Refinements and Spectroscopic Studies of the Structures of Ca-deficient Apatite.* Biomaterials, 2005. **26**: p. 1317 - 1327.
226. Young, R.A. and D.B. Wiles, *Profile Shape Functions in Rietveld Refinements.* Journal of Applied Crystallography, 1982. **15**: p. 430 - 438.
227. Paschalis, E.P., et al., *FTIR Microspectroscopic Analysis of Normal Human Cortical and Trabecular Bone.* Calcified Tissue International, 1997. **61**: p. 480 - 486.
228. Rey, C., et al., *The Carbonate Environment in Bone Mineral: A Resolution-Enhanced Fourier Transform Infrared Spectroscopy Study.* Calcified Tissue International, 1989. **45**: p. 157 - 164.
229. Emerson, W.H. and E.E. Fischer, *The Infra-red Absorption Spectra of Carbonate in Calcified Tissues.* Archives of Oral Biology, 1962. **7**: p. 671 - 683.
230. Gadaleta, S.J., et al., *Fourier Transform Infrared Spectroscopy of the Solution-Mediated Conversion of Amorphous Calcium Phosphate to Hydroxyapatite: New Correlations Between X-ray Diffraction and Infrared Data.* Calcified Tissue International, 1996. **58**: p. 9 - 16.
231. LeGeros, R.Z., *Effect of Carbonate on the Lattice Parameters of Apatite.* Nature, 1965. **206**: p. 403 - 404.
232. Paschalis, E.P., et al., *FTIR Microspectroscopic Analysis of Human Osteonal Bone.* Calcified Tissue International, 1996. **59**: p. 480 - 487.

233. Featherstone, J.D.B., S. Pearson, and R.Z. LeGeros, *An Infrared Method for Quantification of Carbonate in Carbonated Apatites.* Caries Research, 1984. **18**: p. 63 - 66.
234. Miller, L.M., et al., *In Situ Analysis of Mineral Content and Crystallinity in Bone Using Infrared Micro-spectroscopy of the v4 PO43- Vibration.* Biochimica et Biophysica Acta, 2001. **1527**: p. 11 - 19.
235. Pleshko, N., A.L. Boskey, and R. Mendelsohn, *Novel Infrared Spectroscopic Method for the Determination of Crystallinity of Hydroxyapatite Minerals.* Biophysical Journal, 1991. **60**: p. 786-793.
236. Blumenthal, N.C., A.S. Posner, and J.M. Holmes, *Effect of Preparation Conditions on the Properties and Transformation of Amorphous Calcium Phosphate* Materials Research Bulletin, 1972. **7**: p. 1181 - 1190.
237. Hiller, J.C., et al., *Small-angle X-ray Scattering: a High-Throughput Technique for Investigating Archaeological Bone Preservation.* Journal of Archaeological Science, 2004. **31**: p. 1349 - 1359.
238. Thompson, T.J.U., M. Gauthier, and M. Islam, *The application of a new method of Fourier Transform Infrared Spectroscopy to the analysis of burned bone.* Journal of Archaeological Science, 2009. **36**: p. 910 - 914.
239. Kuo, H.W., et al., *Determination of 14 Elements in Taiwanese Bones.* The Science of the Total Environment, 2000. **255**: p. 45 - 54.
240. Aoba, T., E.C. Moreno, and S. Shimoda, *Competitive Adsorption of Magnesium and Calcium Ions onto Synthetic and Biological Apatites.* Calcified Tissue International, 1992. **51**: p. 143 - 150.
241. Langford, J.I., *The Use of the Voigt Function in Determining Microstructural Properties from Diffraction Data by means of Pattern Decomposition.* Accuracy in Powder Diffraction II, 1992. **2**: p. 110 - 126.
242. Kim, H., et al., *Control of Phase Composition in Hydroxyapatite/Tetracalcium phosphate Biphasic Thin Coatings for Biomedical Applications.* Journal of Materials Science: Materials in Medicine, 2005. **16**: p. 961 - 966.
243. Huizingh, E., *Applied Statistics with SPSS*. 1 ed. 2007: Sage Publications Ltd.
244. Harper, W.M., *Statistics*. 6 ed. 1991: Pearson Education Ltd.
245. Salkind, N.J., *Statistics for People Who (Think They) Hate Statistics*. 1 ed. 2000: Sage Publications Ltd.
246. Benes, B., et al., *Determination of Thirty-Two Elements in Human Autopsy Tissue.* Biological Trace Element Research, 2000. **75**(1 - 3): p. 195 - 203.
247. Lacout, J.L., *Calcium Phosphate as Bioceramics.* Biomaterials: Hard Tissue Repair and Replacement, 1992: p. 81 - 95.
248. Posner, A.S., et al., *X-ray diffraction analysis of the effect of fluoride on human bone apatite.* Arch. Oral Biol., 1963. **8**: p. 549 - 570.
249. Dickens, B., L.W. Schroeder, and W.E. Brown, *Crystallographic Studies of the Role of Mg as a Stabilizing Impurity in β-Ca3(PO4)2. I The Crystal Structure of Pure β-Ca3(PO4)2.* Journal of Solid State Chemistry, 1974. **10**: p. 232 - 248.

A – APPENDIX

A.2 – X-RAY DIFFRACTOGRAMS

The X-ray diffractograms presented within this section relate to the results presented in chapter 5 and discussed in chapter 6. They represent X-ray diffraction data obtained from bone specimens corresponding to a total of 123 individuals, from a range of animal species. Details of the data collection conditions are reported within chapter 4.

Each figure is comprised of several diffractograms. These have been stacked for clarity. The y – axis of each figure represents relative intensity, normalized to the highest peak for all diffractograms and so no units are presented. The x – axis of each figure represents d – spacing, with a scale measurement in Ångströms (Å). Each figure is labelled to identify the species presented within the figure. The caption relating to each figure indicates whether the presented diffractograms were obtained from unheated or heated bone specimens and, for heated bone specimens, the temperature of heat treatment.

The stacking order is consistent within each species, across unheated and heated sets of bone specimens, in terms of the individuals represented. For example, diffractograms at the base of each stack in Figure A.2, Figure A.3 and Figure A.4 represent bone specimens from the same individual. Data was not collected for unheated rat bone specimens and so is not presented.

Stick representations of diffractograms for several relevant mineral phases are presented in Figure A.36.

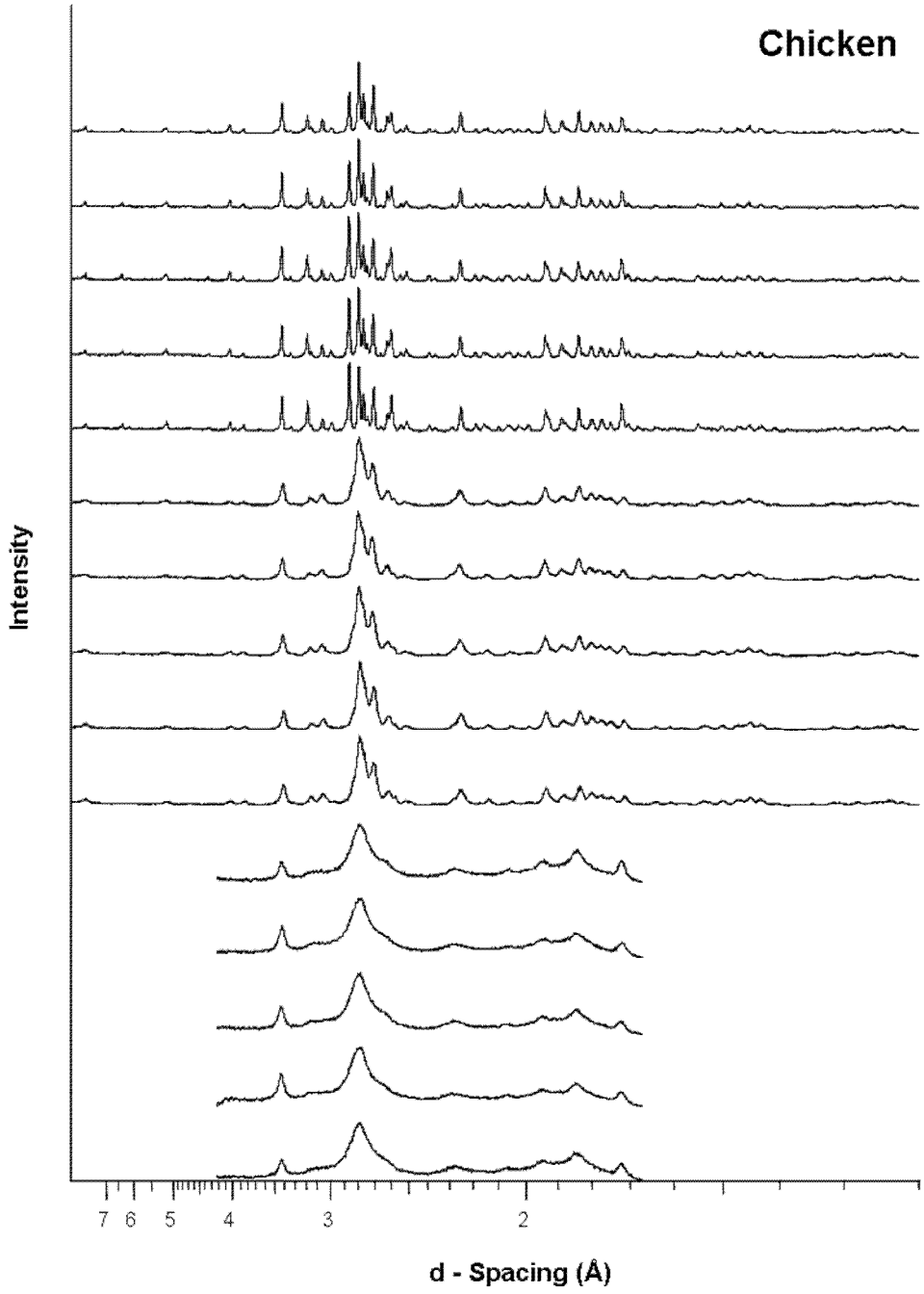

Figure A.1 – Diffractograms obtained from chicken bone specimens from five individuals. Lower five: unheated bone specimens, middle five; bone specimens heated to 600 °C, upper five; bone specimens heated to 1400 °C

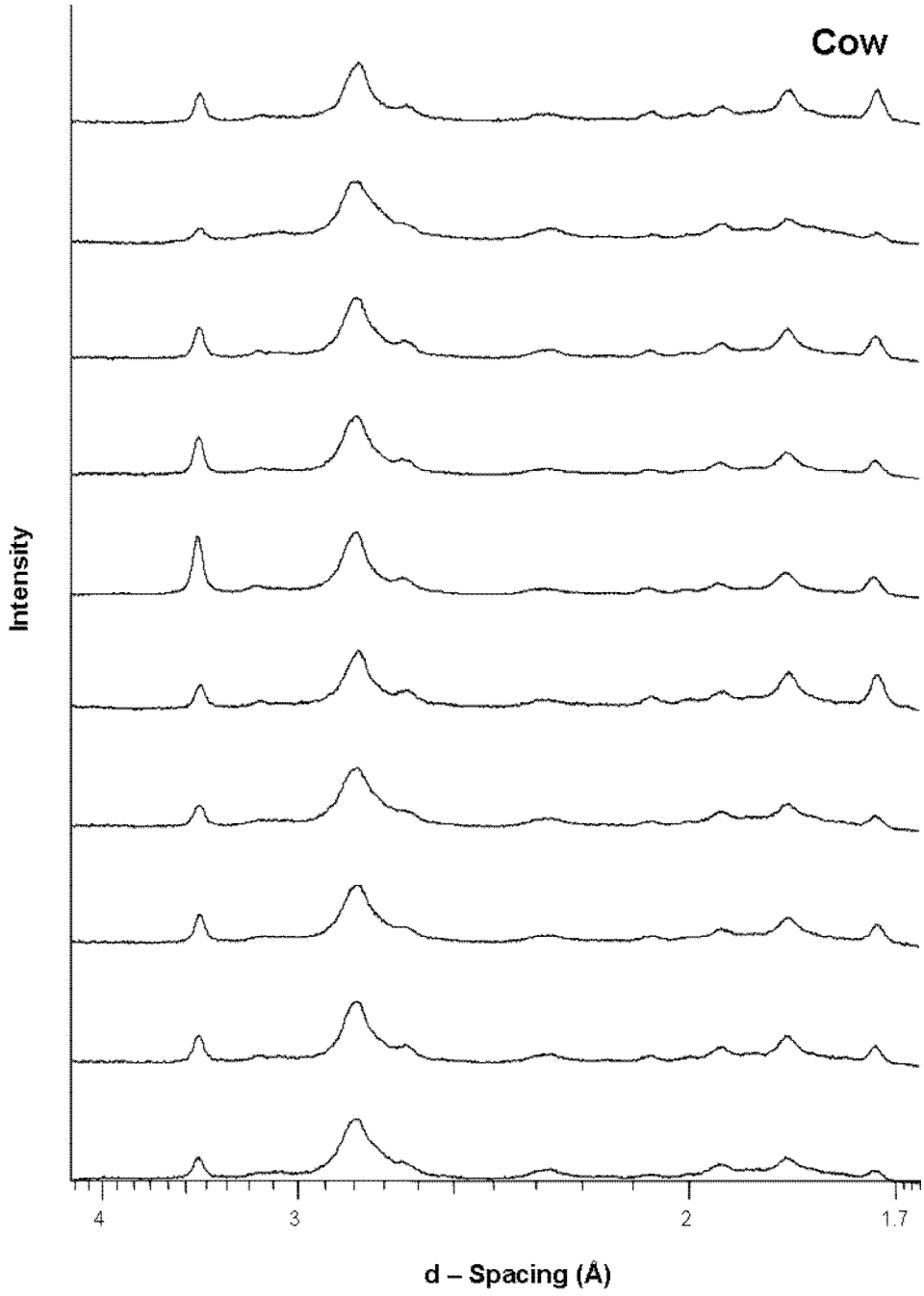

Figure A.2 – Diffractograms obtained from unheated cow bone specimens from ten individuals

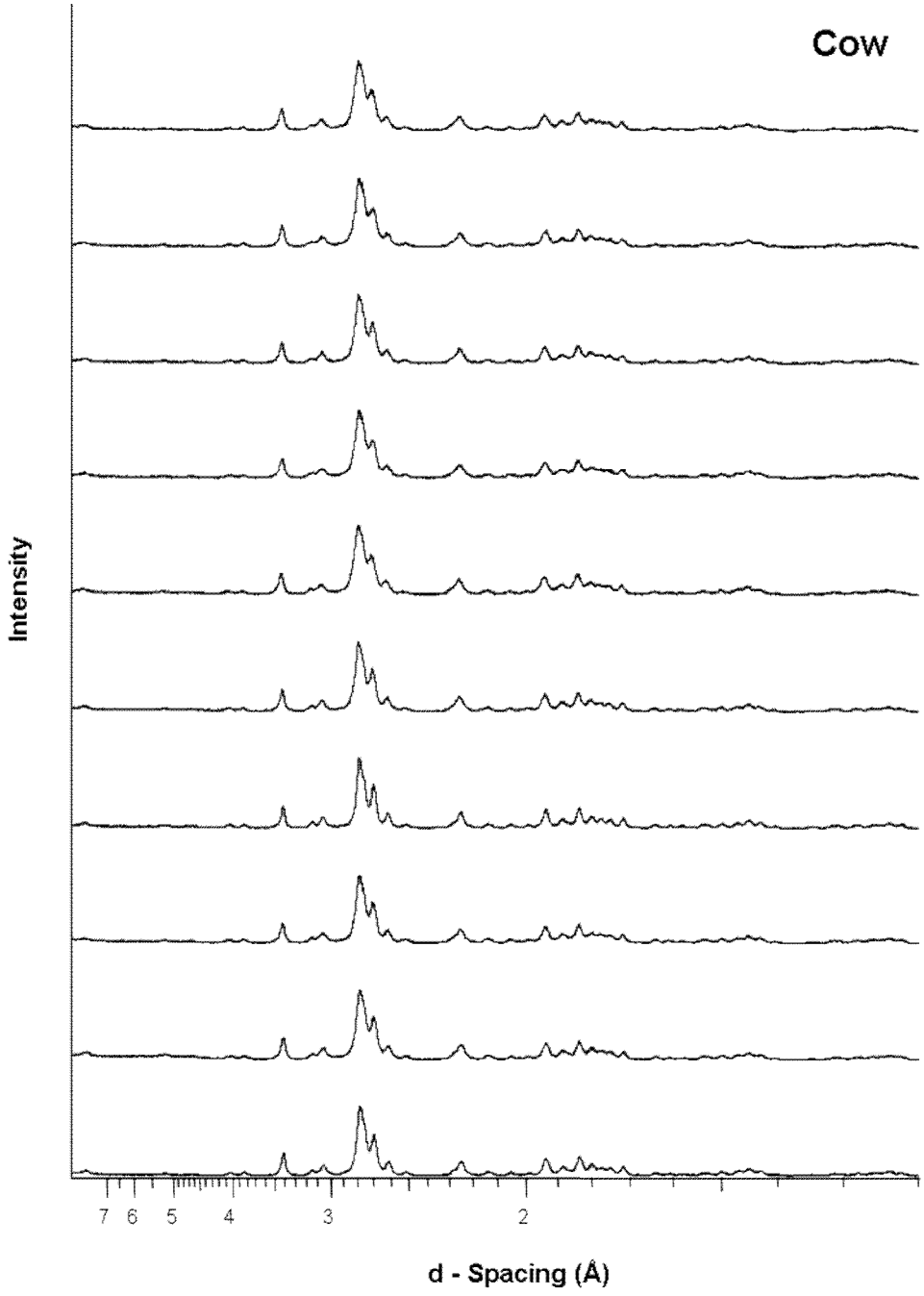

Figure A.3 – Diffractograms obtained from cow bone specimens from ten individuals. All bone specimens heated to 600 °C.

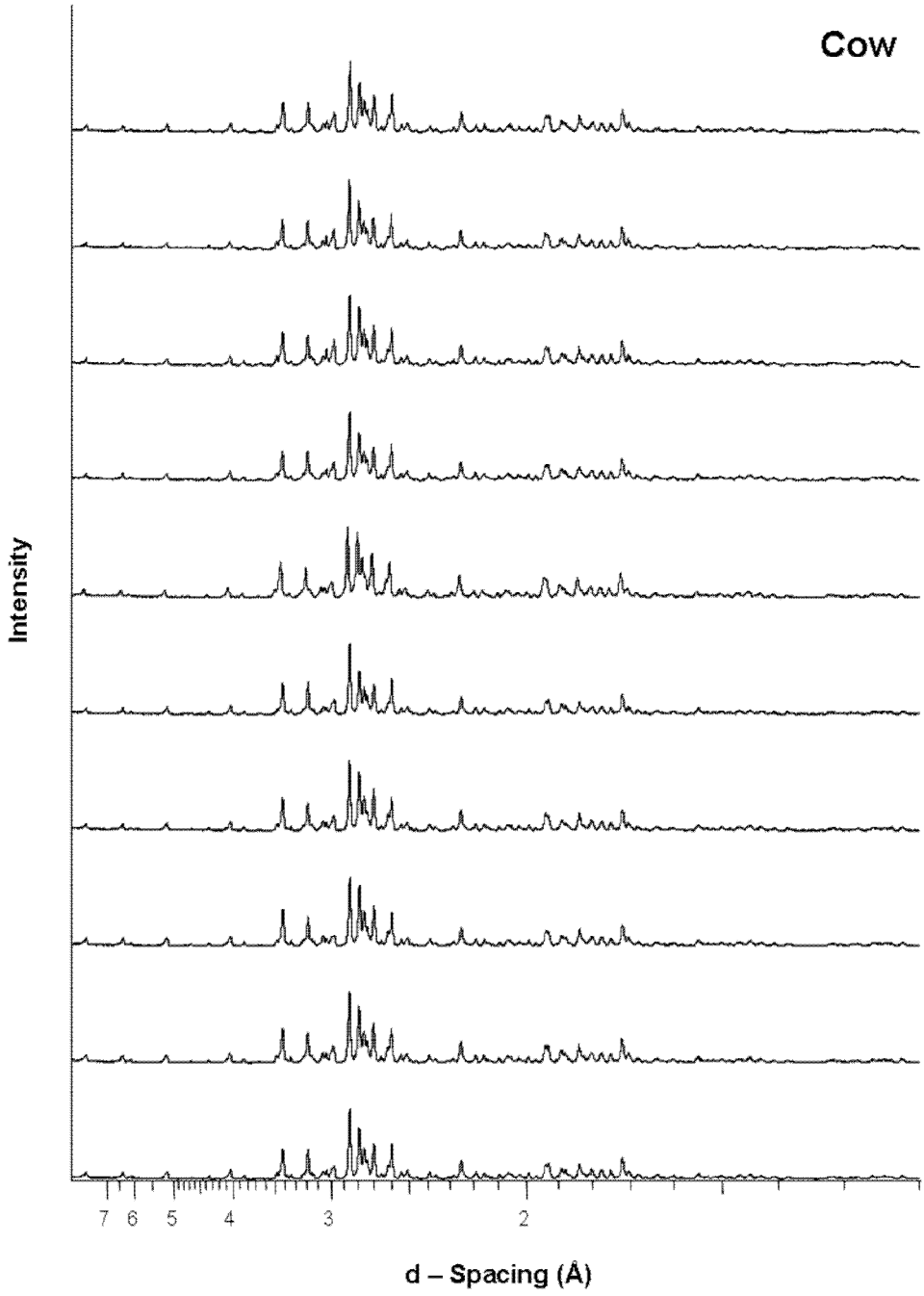

Figure A.4 – Diffractograms obtained from cow bone specimens from ten individuals. All bone specimens heated to 1400 °C.

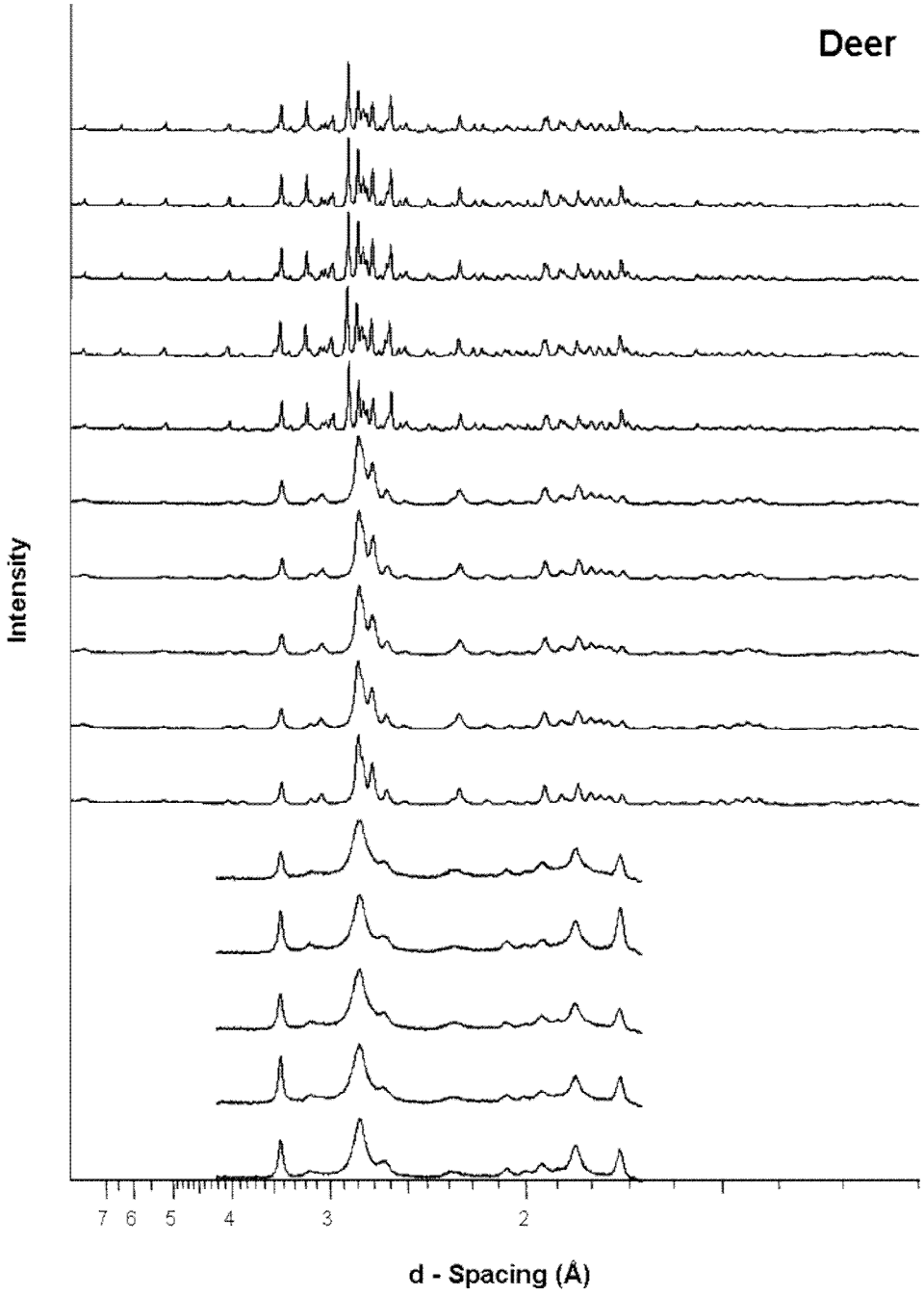

Figure A.5 – Diffractograms obtained from deer bone specimens from five individuals. Lower five; unheated bone specimens, middle five; bone specimens heated to 600 °C, upper five; bone specimens heated to 1400 °C.

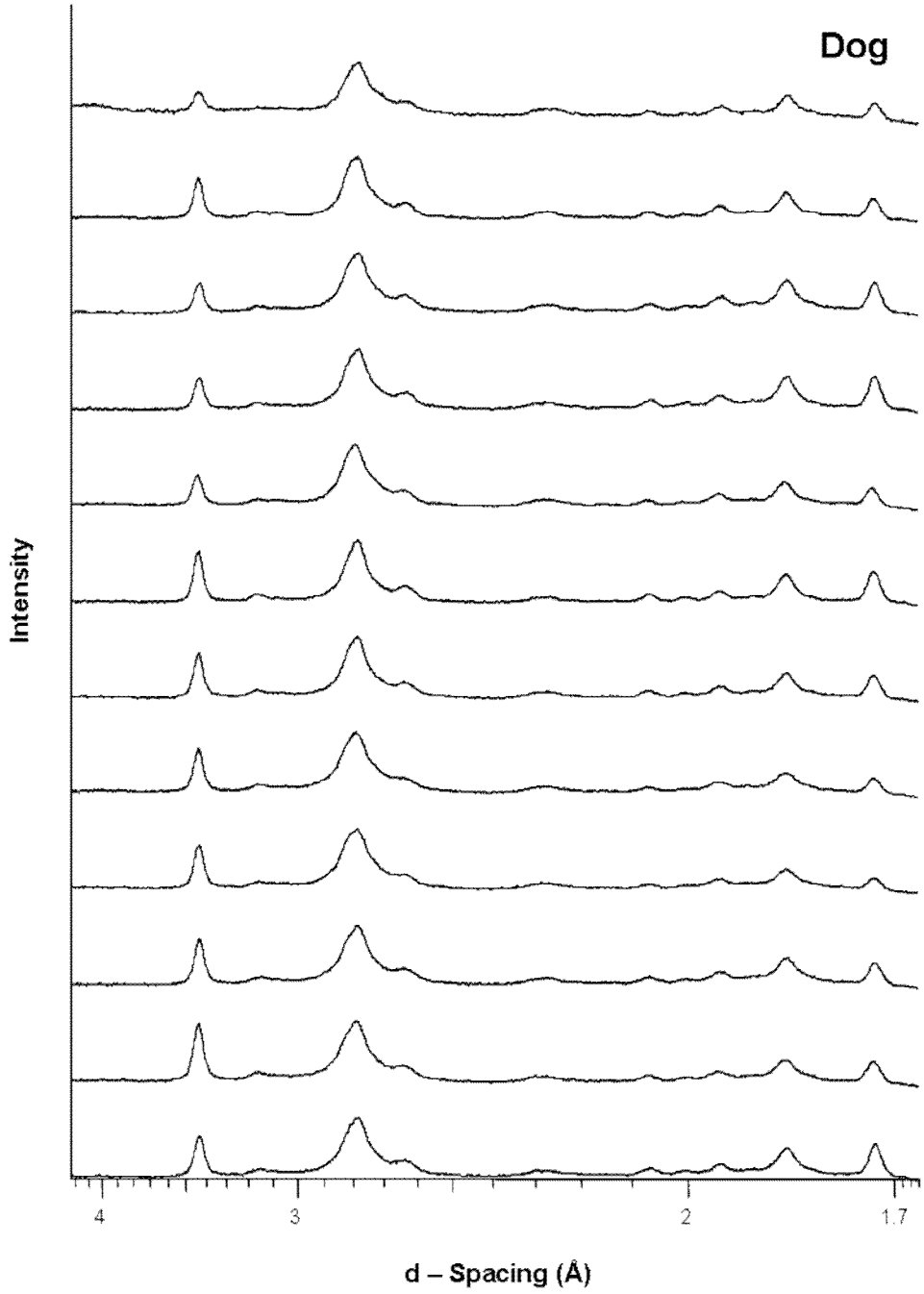

Figure A.6 – Diffractograms obtained from unheated dog bone specimens from twelve individuals.

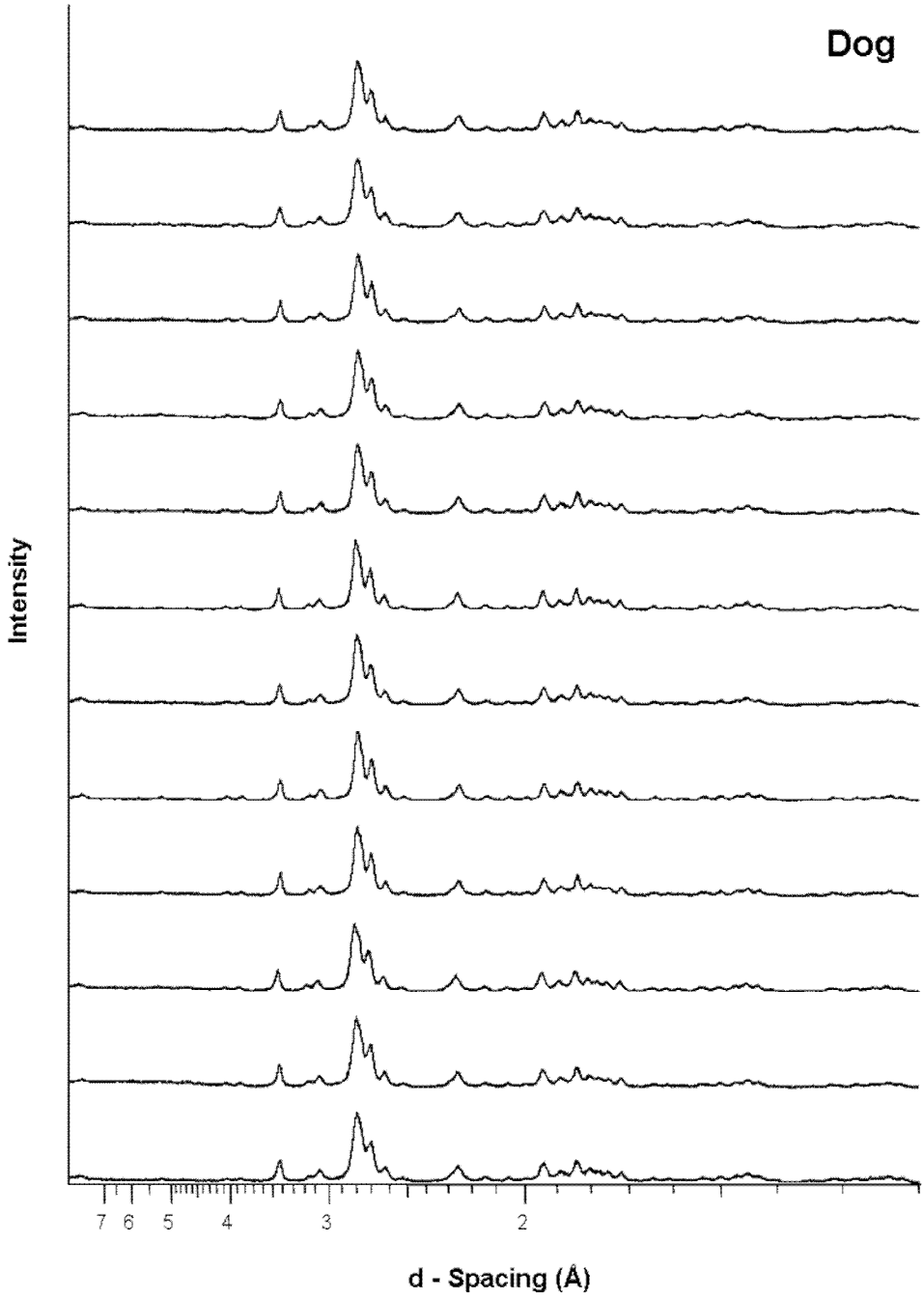

Figure A.7 – Diffractograms obtained from dog bone specimens from twelve individuals. All bone specimens heated to 600 °C.

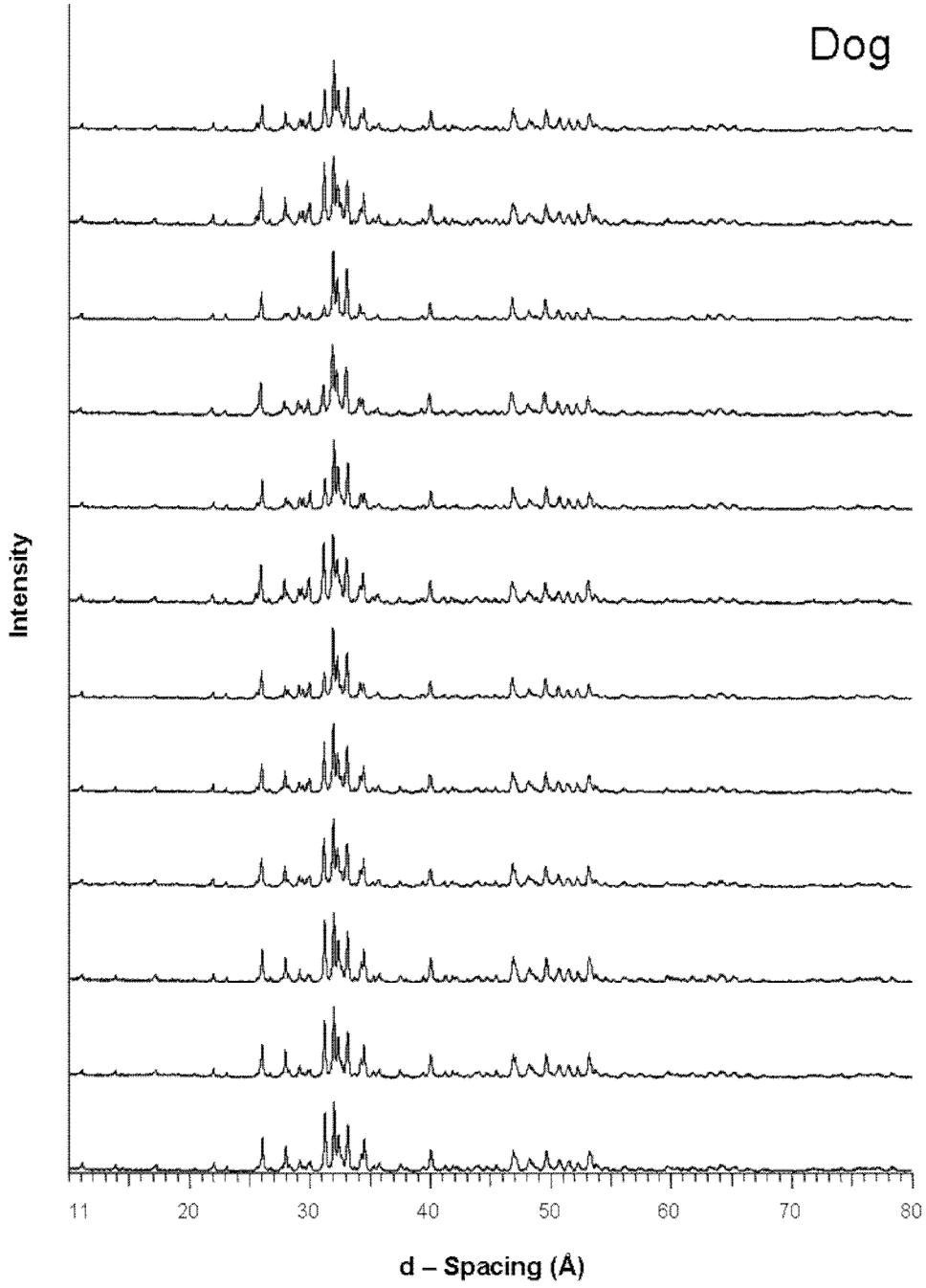

Figure A.8 – Diffractograms obtained from dog bone specimens from twelve individuals. All bone specimens heated to 1400 °C.

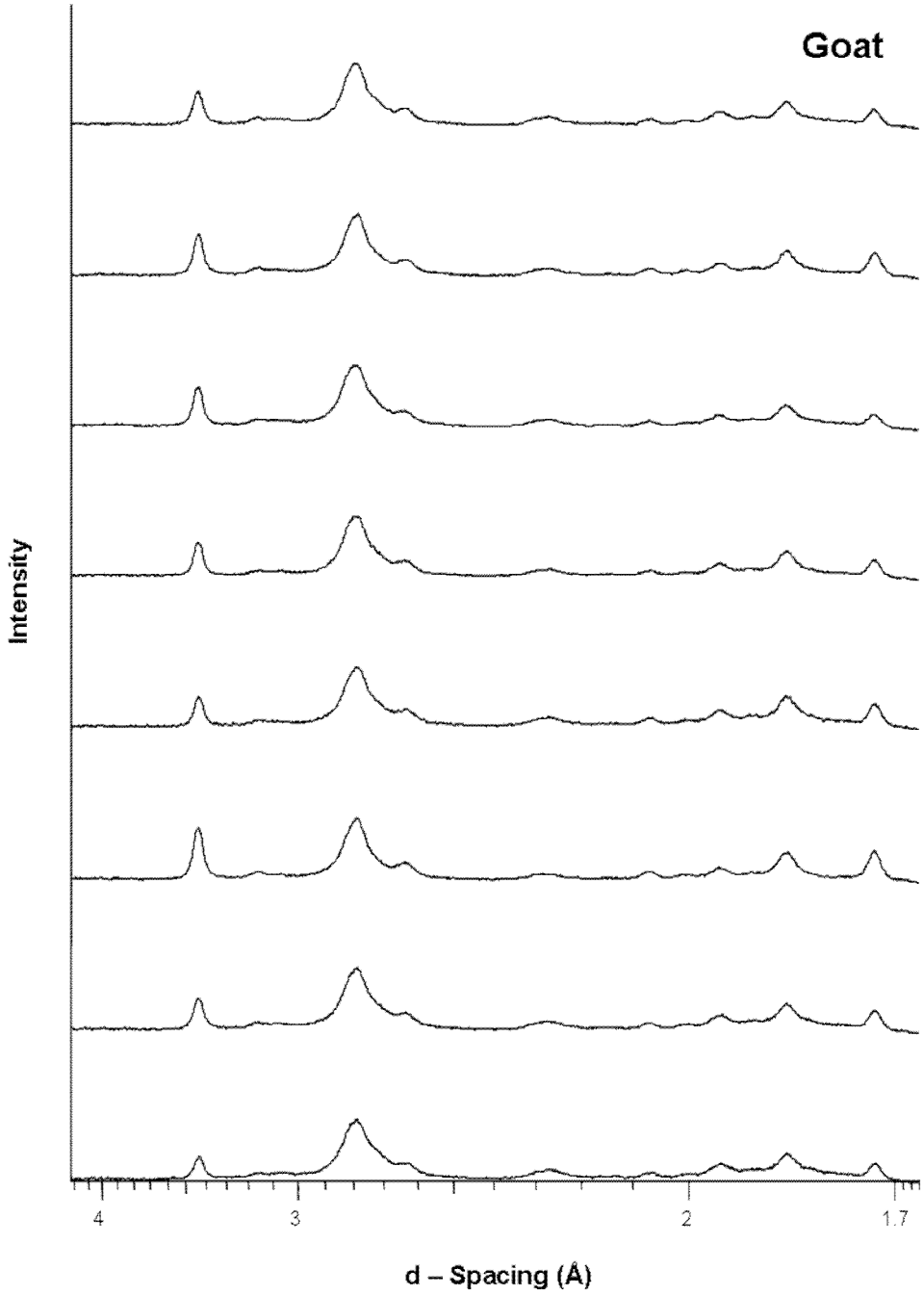

Figure A.9 – Diffractograms obtained from unheated goat bone specimens from eight individuals.

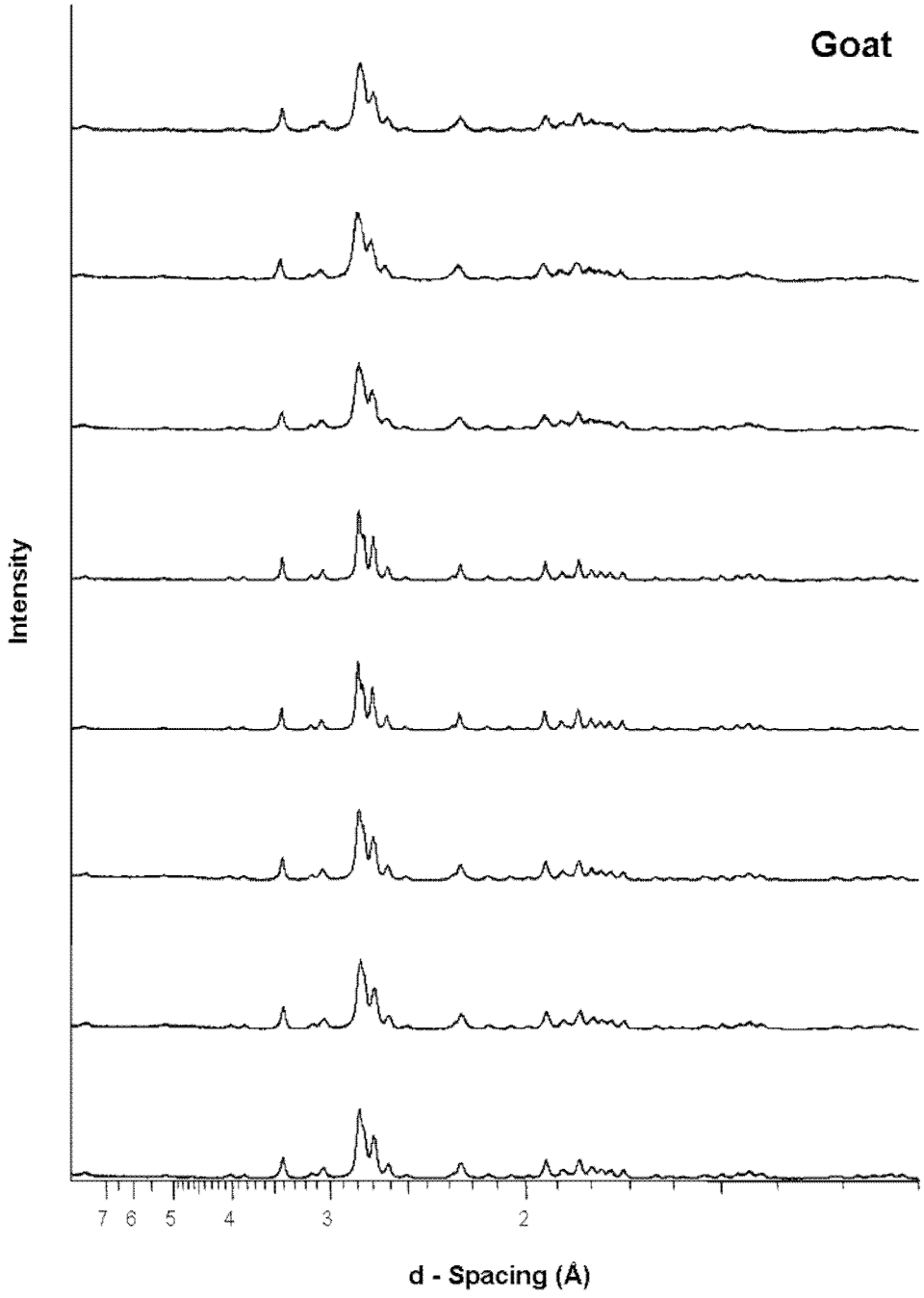

Figure A.10 – Diffractograms obtained from goat bone specimens from eight individuals. All bone specimens heated to 600 °C.

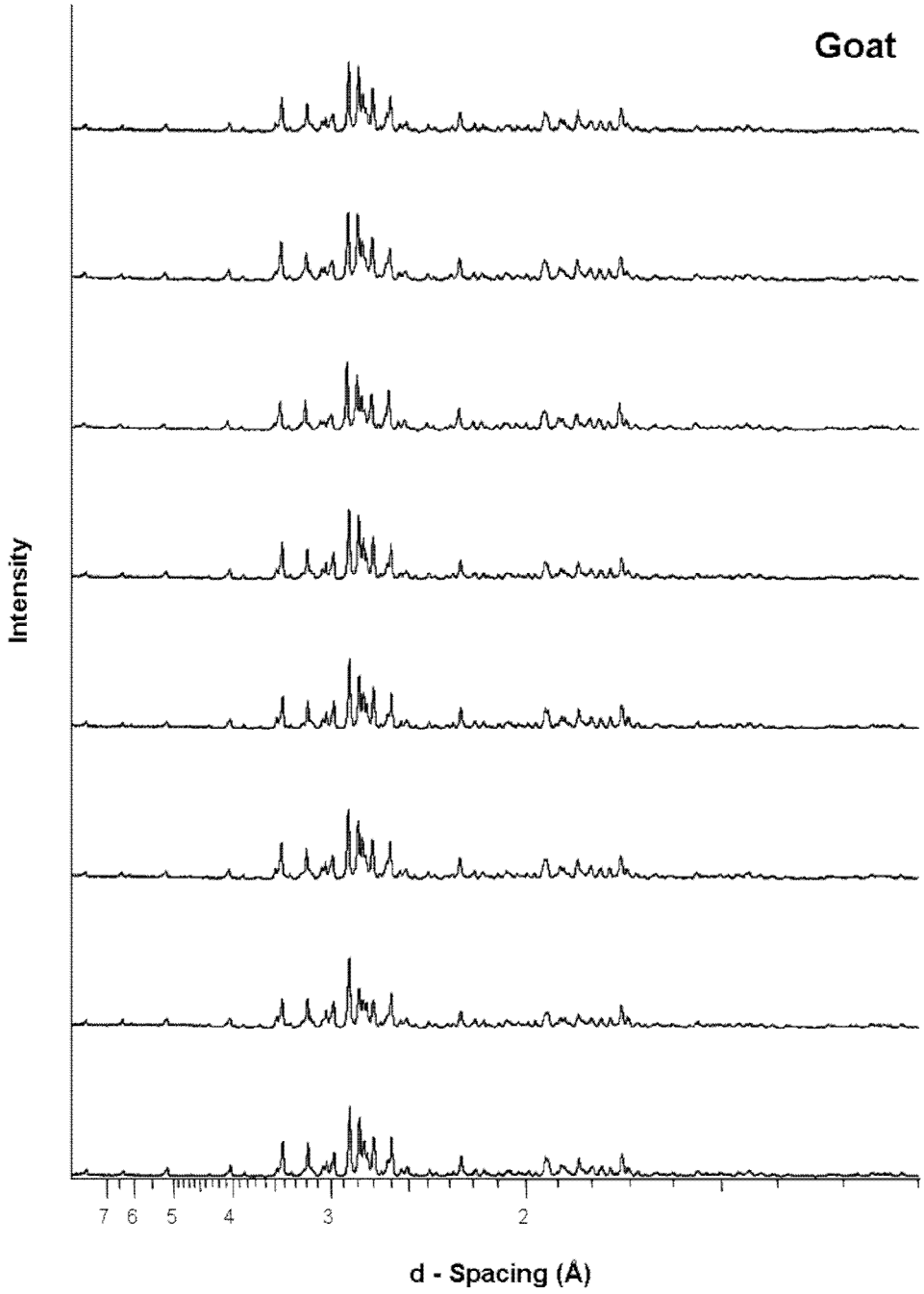

Figure A.11 – Diffractograms obtained from goat bone specimens from eight individuals. All bone specimens heated to 1400 °C.

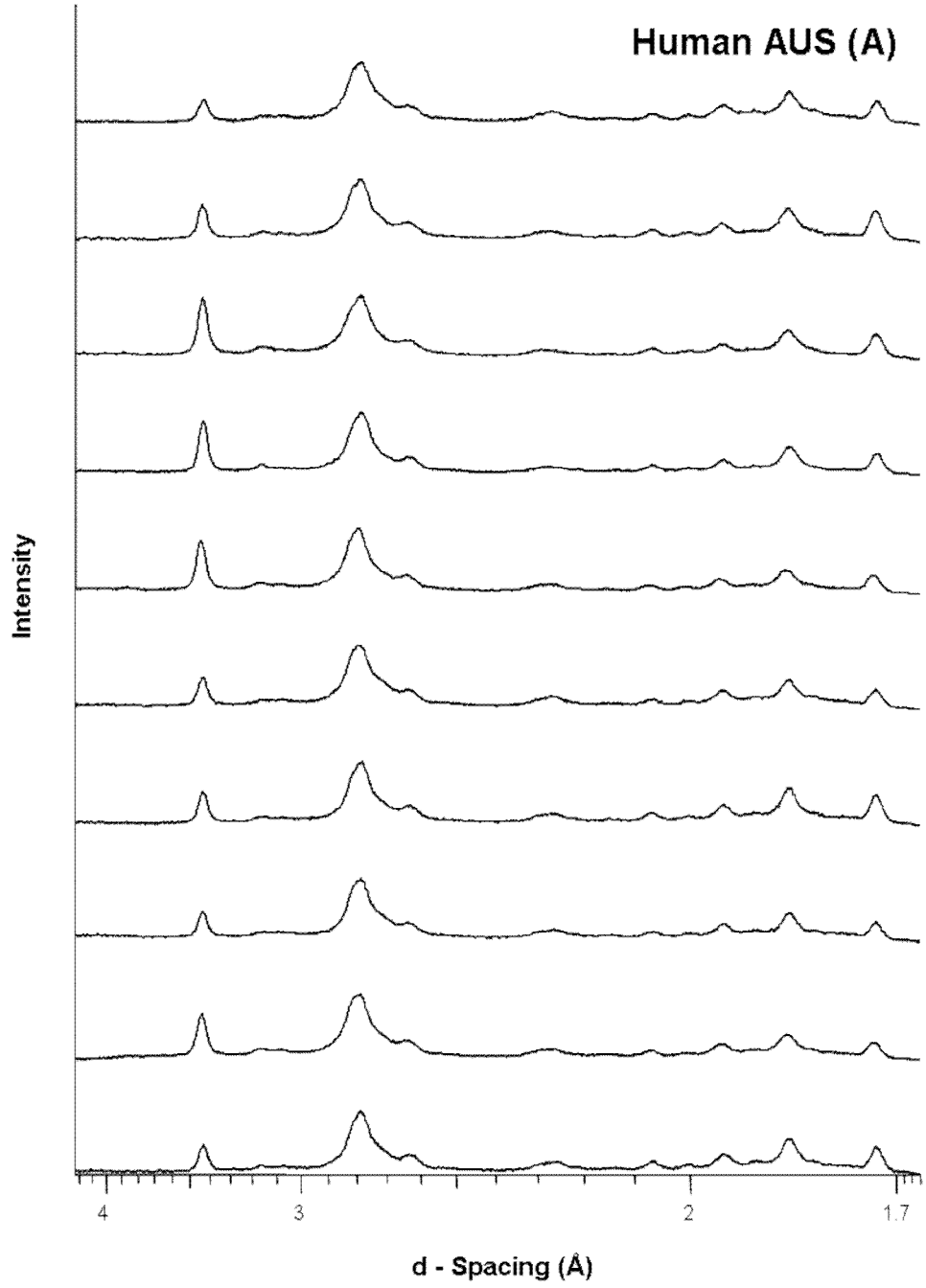

Figure A.12 – Diffractograms obtained from unheated human AUS bone specimens from ten individuals. Group A, of groups A – E (a total of 50 individuals).

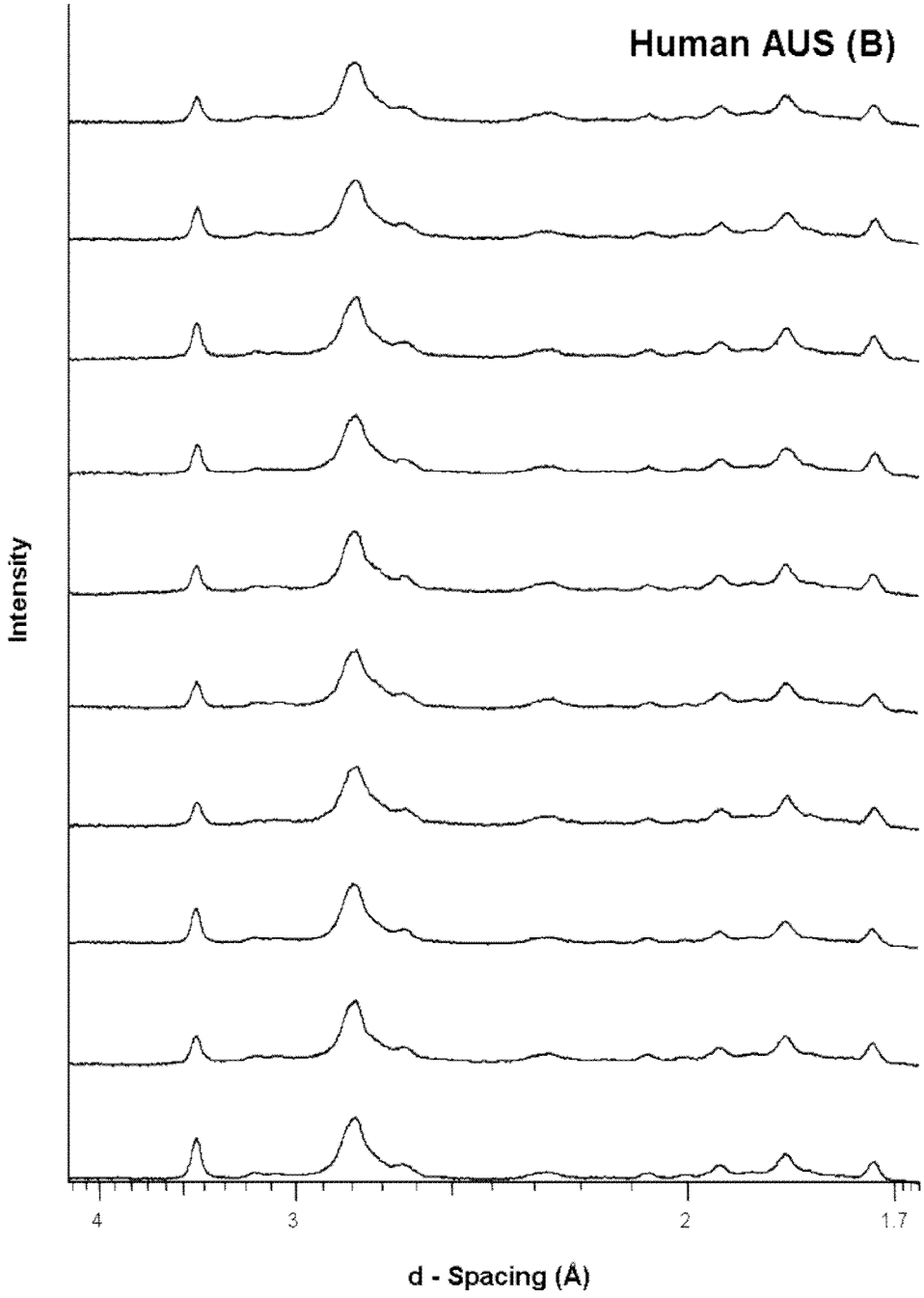

Figure A.13 – Diffractograms obtained from unheated human AUS bone specimens from ten individuals. Group B, of groups A – E (a total of 50 individuals).

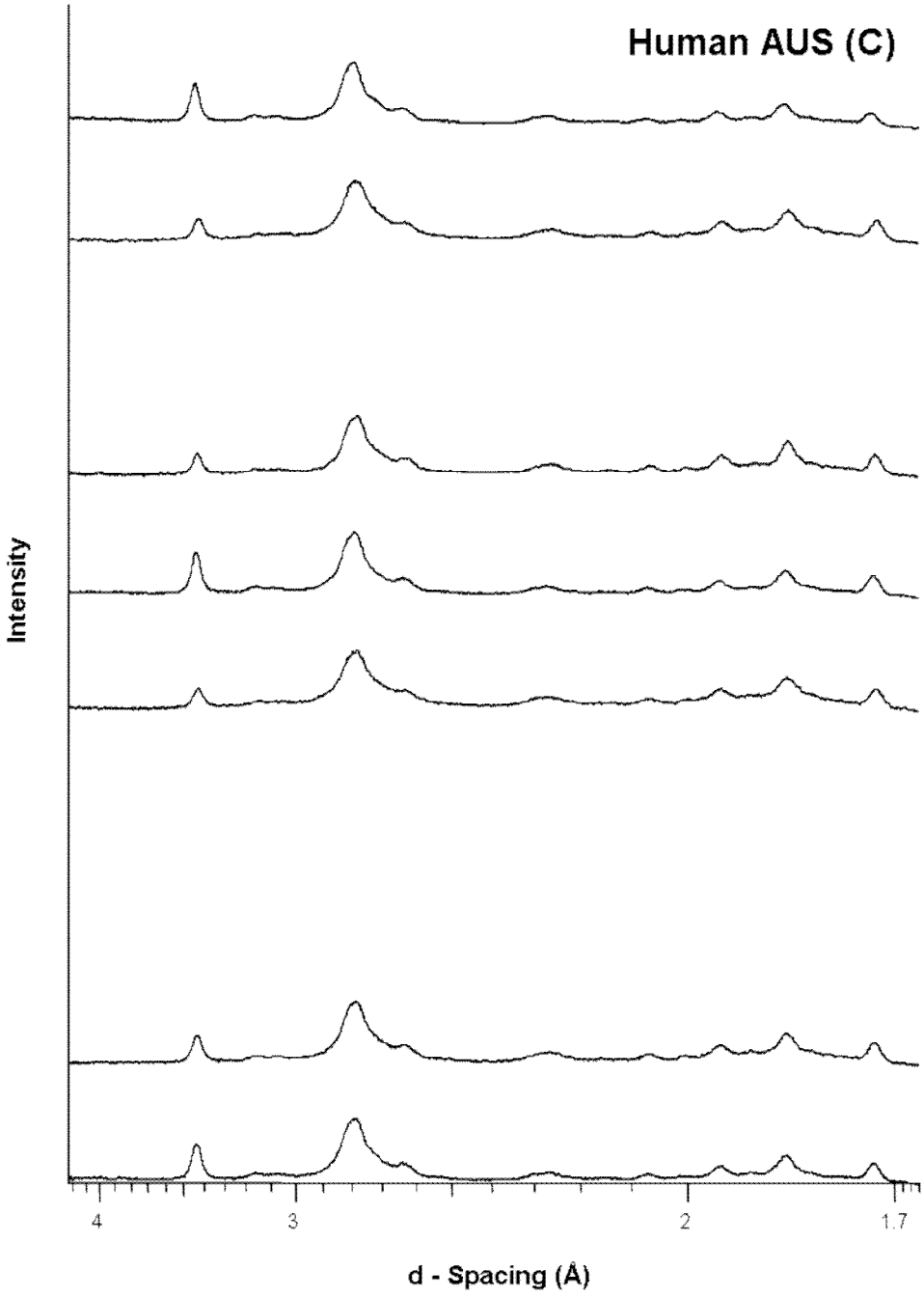

Figure A.14 – Diffractograms obtained from unheated human AUS bone specimens from seven individuals. Group C, of groups A – E (a total of 50 individuals). Unheated bone specimen data was not collected for three of the ten individuals within group C.

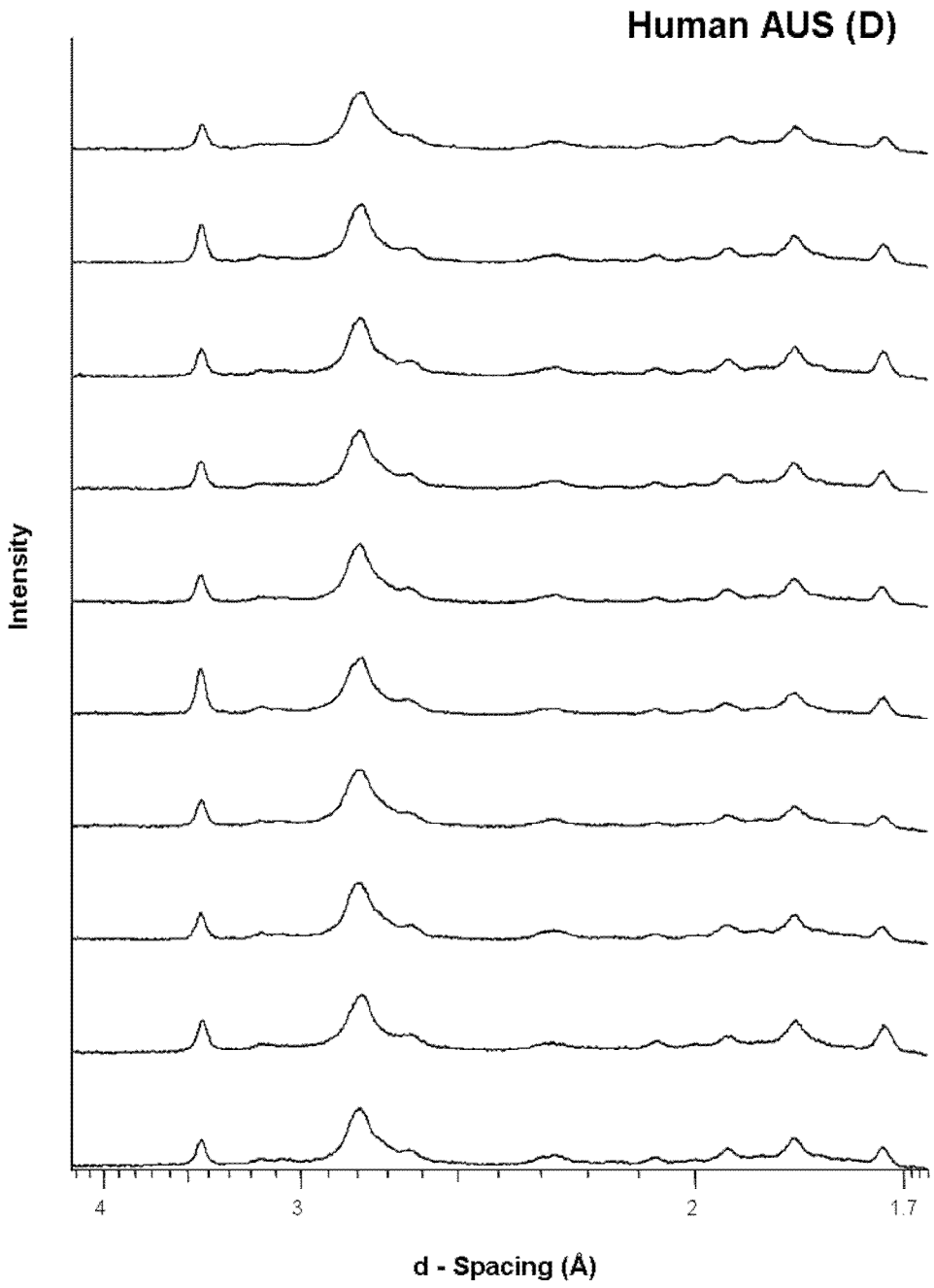

Figure A.15 – Diffractograms obtained from unheated human AUS bone specimens from ten individuals. Group D, of groups A – E (a total of 50 individuals).

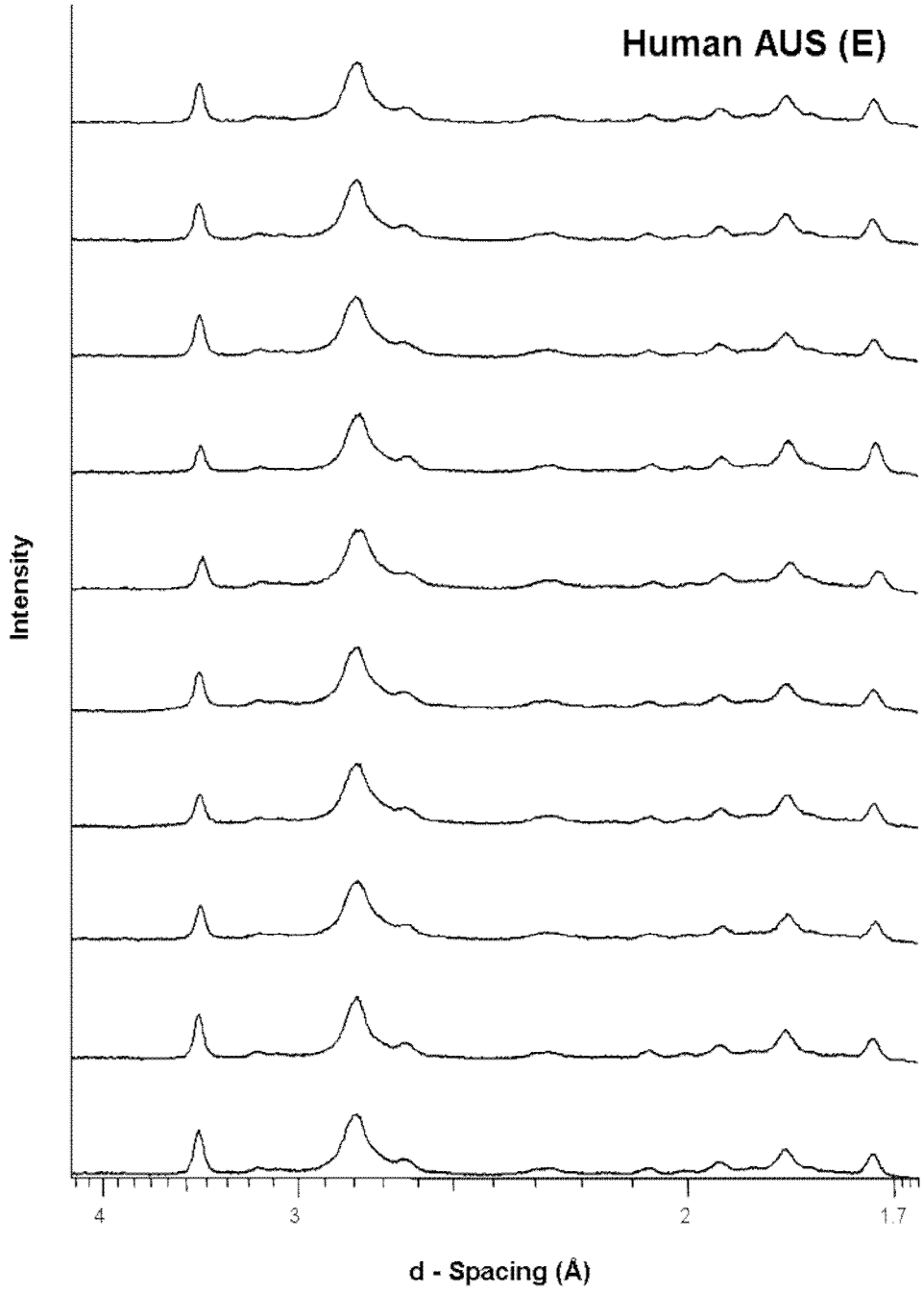

Figure A.16 – Diffractograms obtained from unheated human AUS bone specimens from ten individuals. Group E, of groups A – E (a total of 50 individuals).

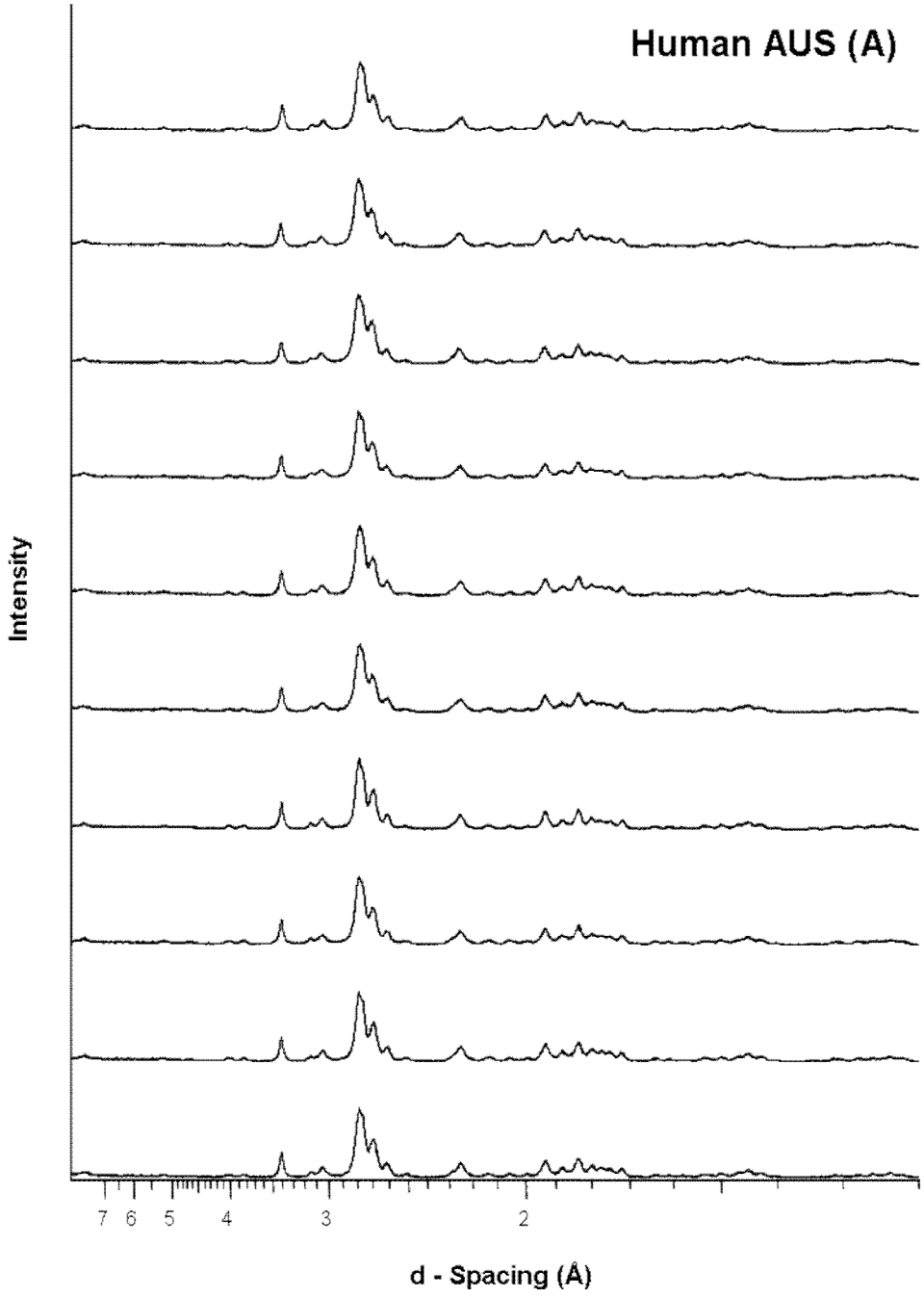

Figure A.17 – Diffractograms obtained from human AUS bone specimens from ten individuals. Group A, of groups A – E (a total of 50 individuals). All bone specimens heated to 600 °C.

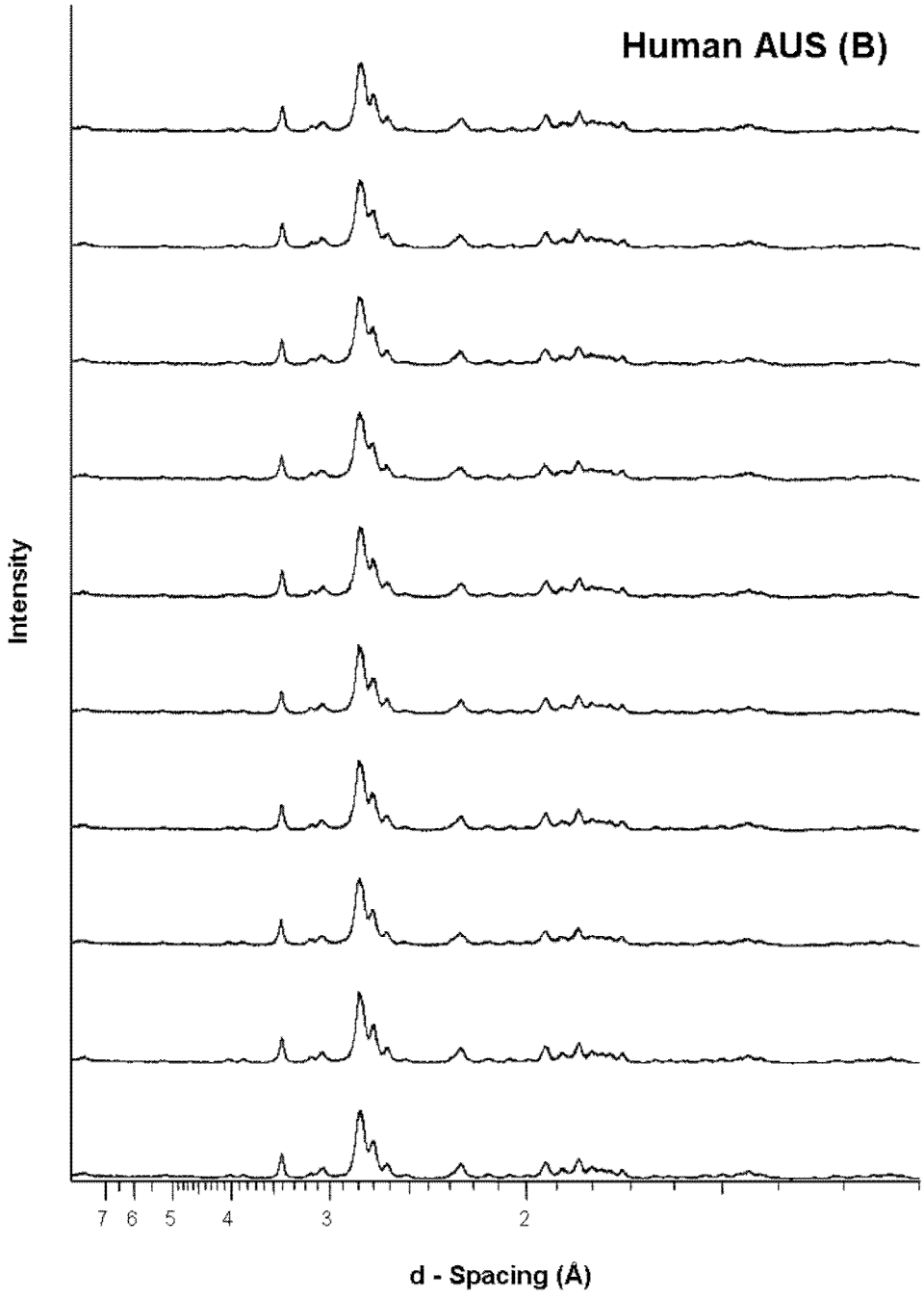

Figure A.18 – Diffractograms obtained from human AUS bone specimens from ten individuals. Group B, of groups A – E (a total of 50 individuals). All bone specimens heated to 600 °C.

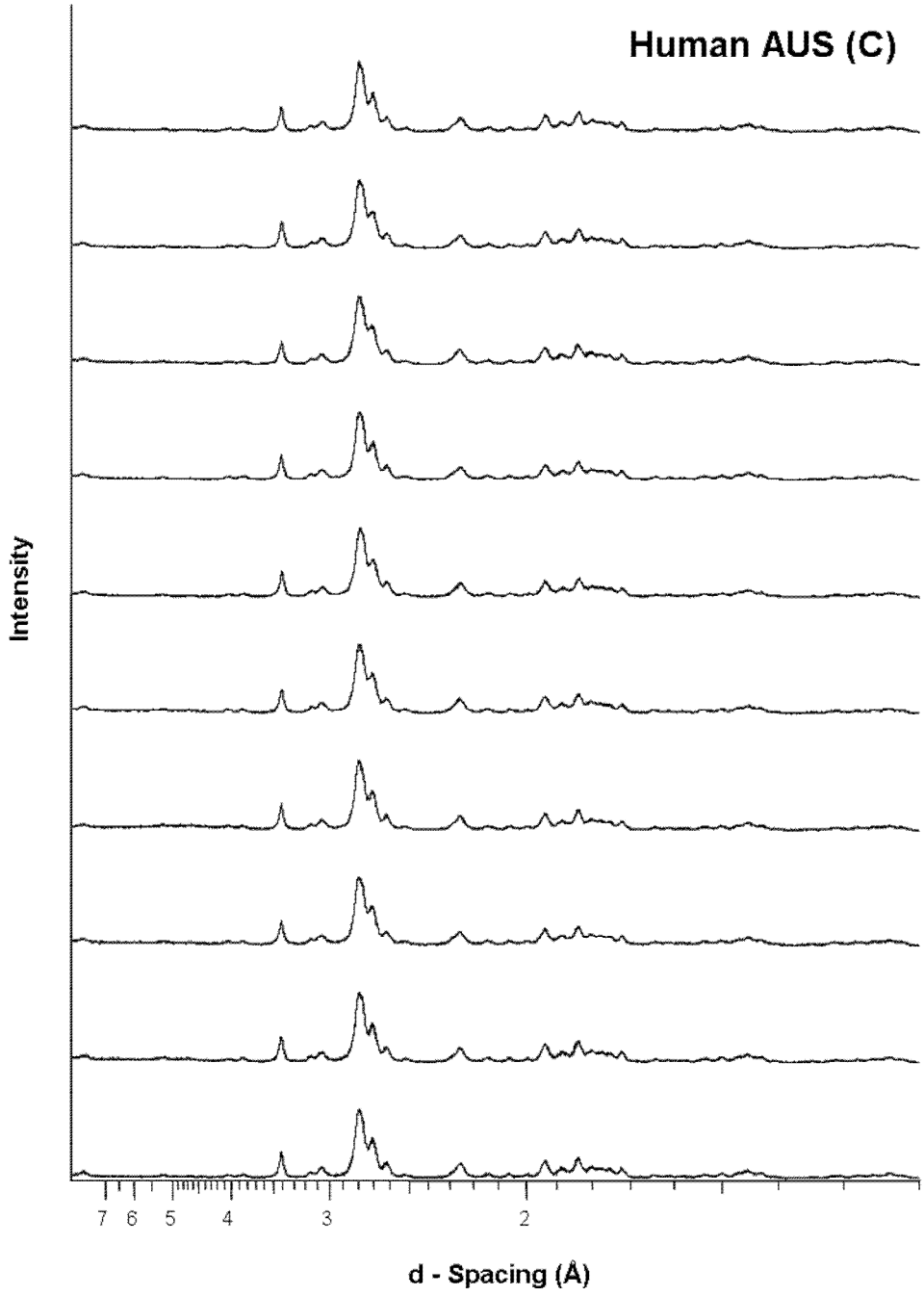

Figure A.19 – Diffractograms obtained from human AUS bone specimens from ten individuals. Group C, of groups A – E (a total of 50 individuals). All bone specimens heated to 600 °C.

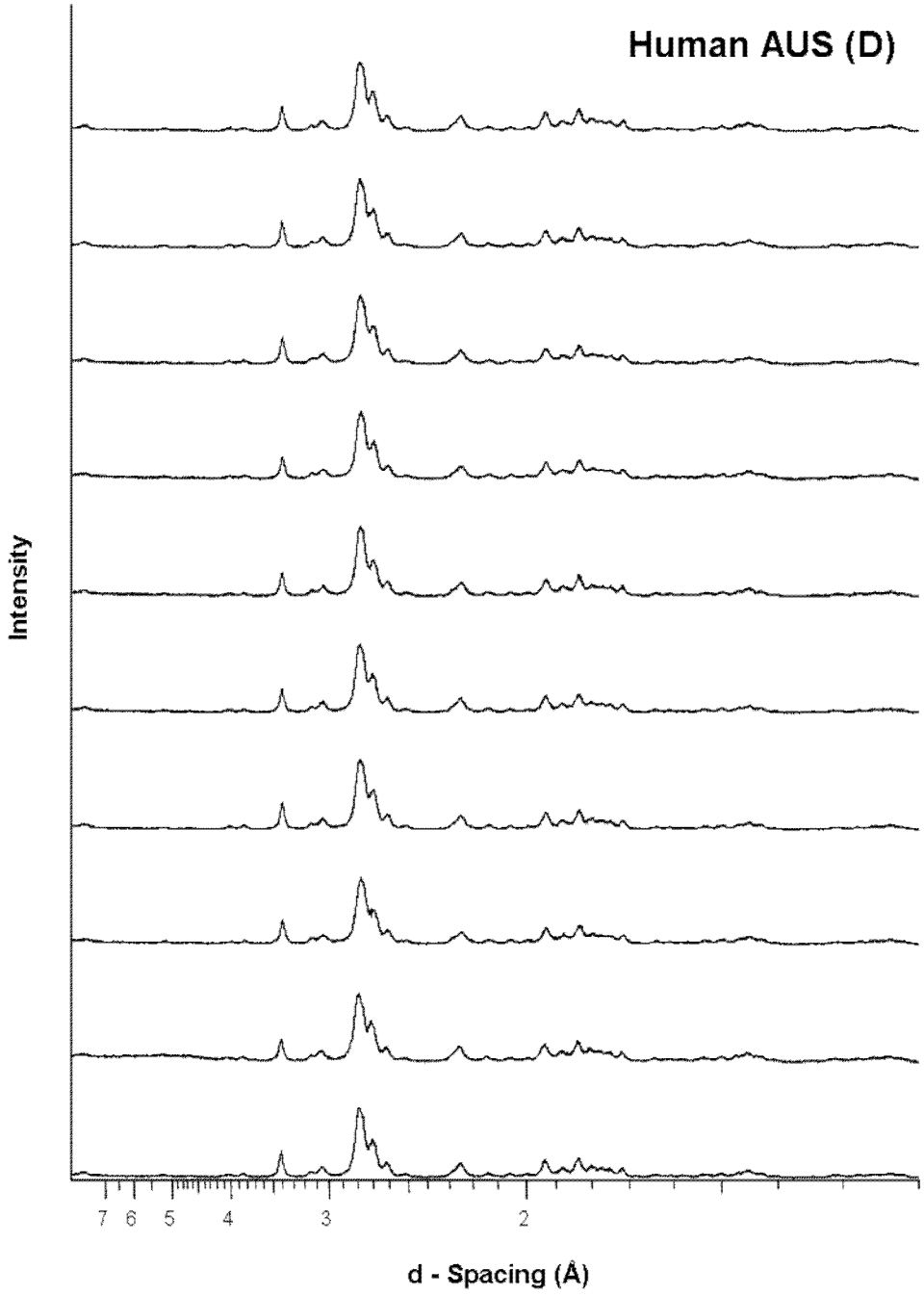

Figure A.20 – Diffractograms obtained from human AUS bone specimens from ten individuals. Group D, of groups A – E (a total of 50 individuals). All bone specimens heated to 600 °C.

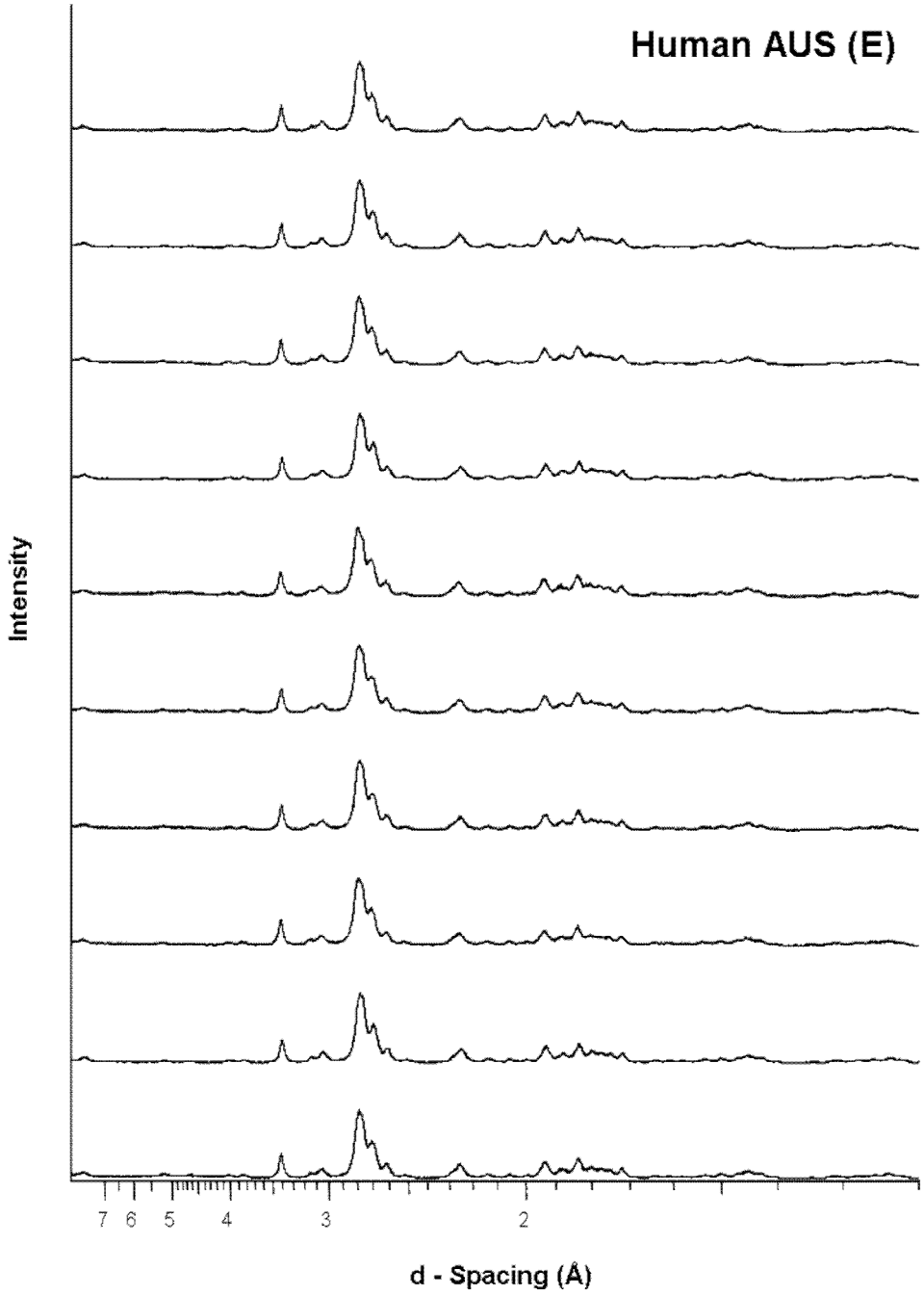

Figure A.21 – Diffractograms obtained from human AUS bone specimens from ten individuals. Group E, of groups A – E (a total of 50 individuals). All bone specimens heated to 600 °C.

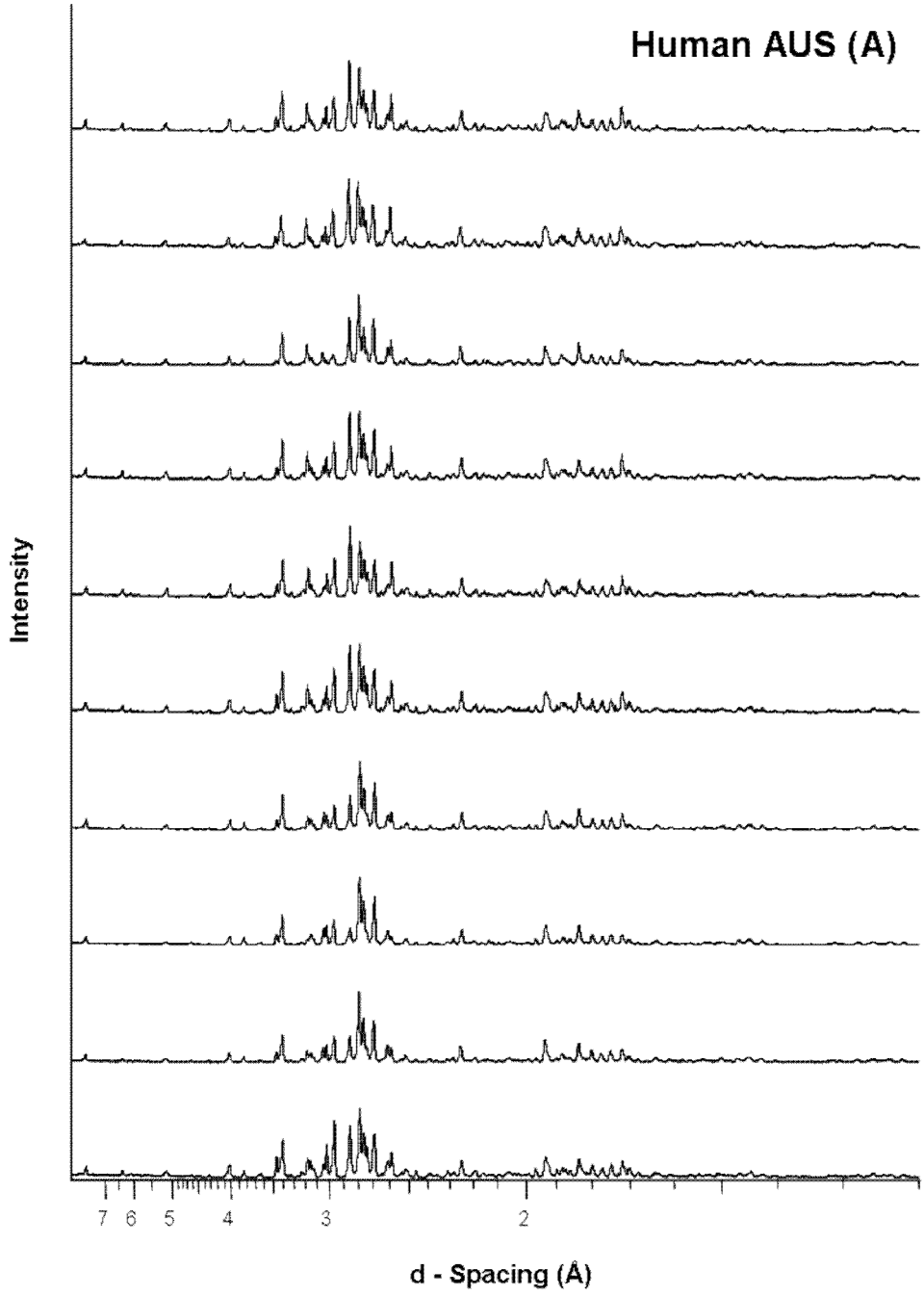

Figure A.22 – Diffractograms obtained from human AUS bone specimens from ten individuals. Group A, of groups A – E (a total of 50 individuals). All bone specimens heated to 1400 °C

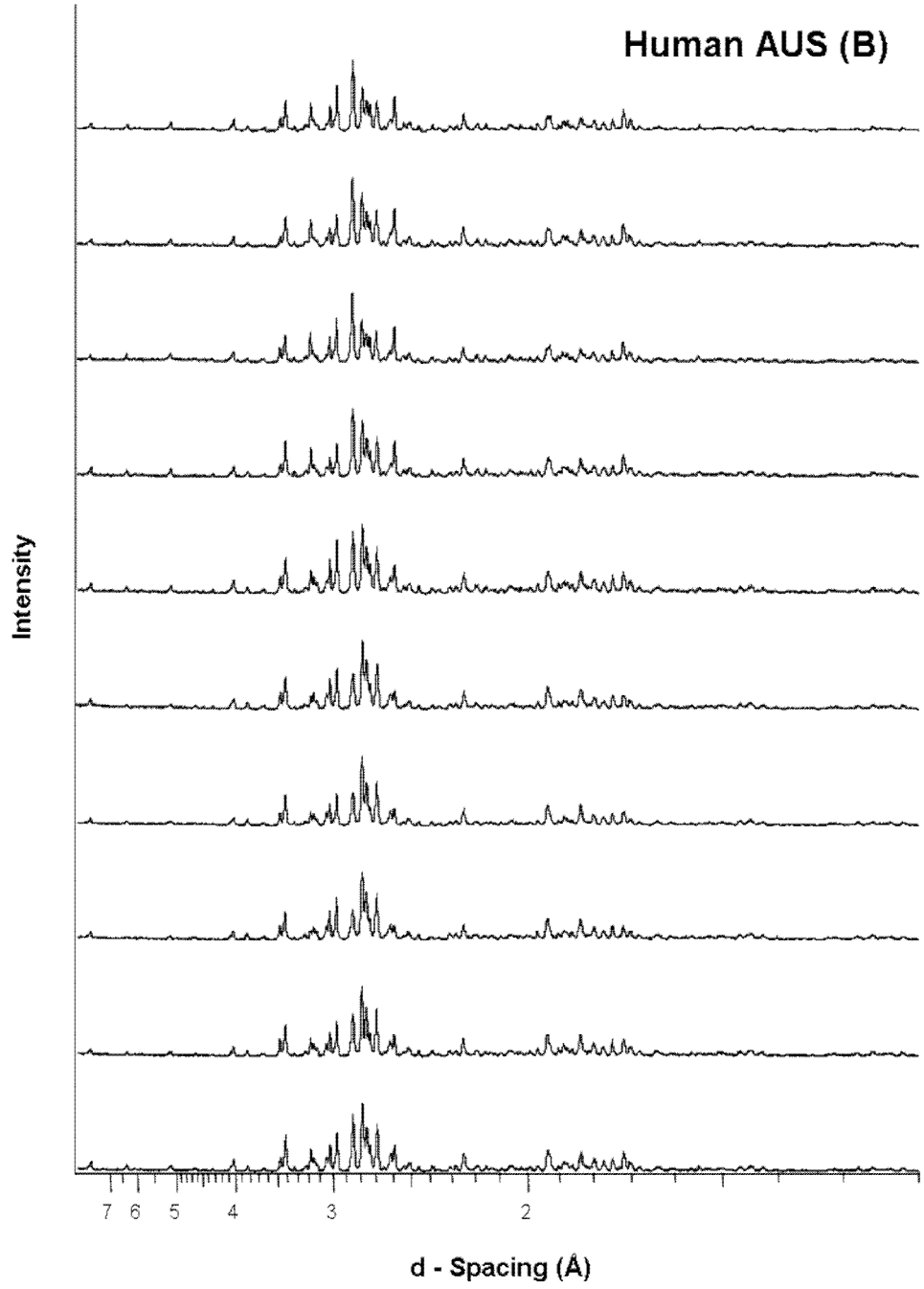

Figure A.23 – Diffractograms obtained from human AUS bone specimens from ten individuals. Group B, of groups A – E (a total of 50 individuals). All bone specimens heated to 1400 °C

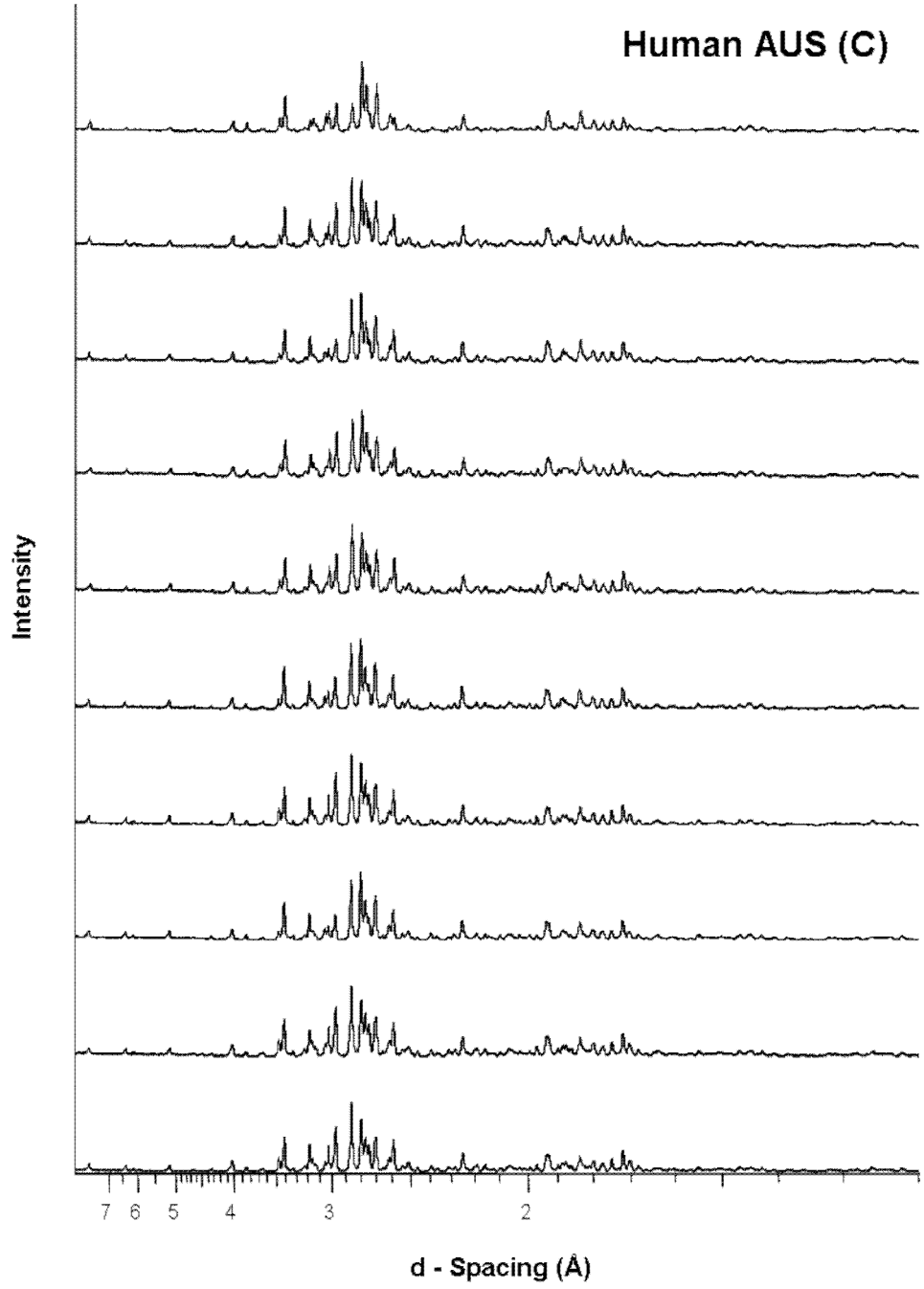

Figure A.24 – Diffractograms obtained from human AUS bone specimens from ten individuals. Group C, of groups A – E (a total of 50 individuals). All bone specimens heated to 1400 °C

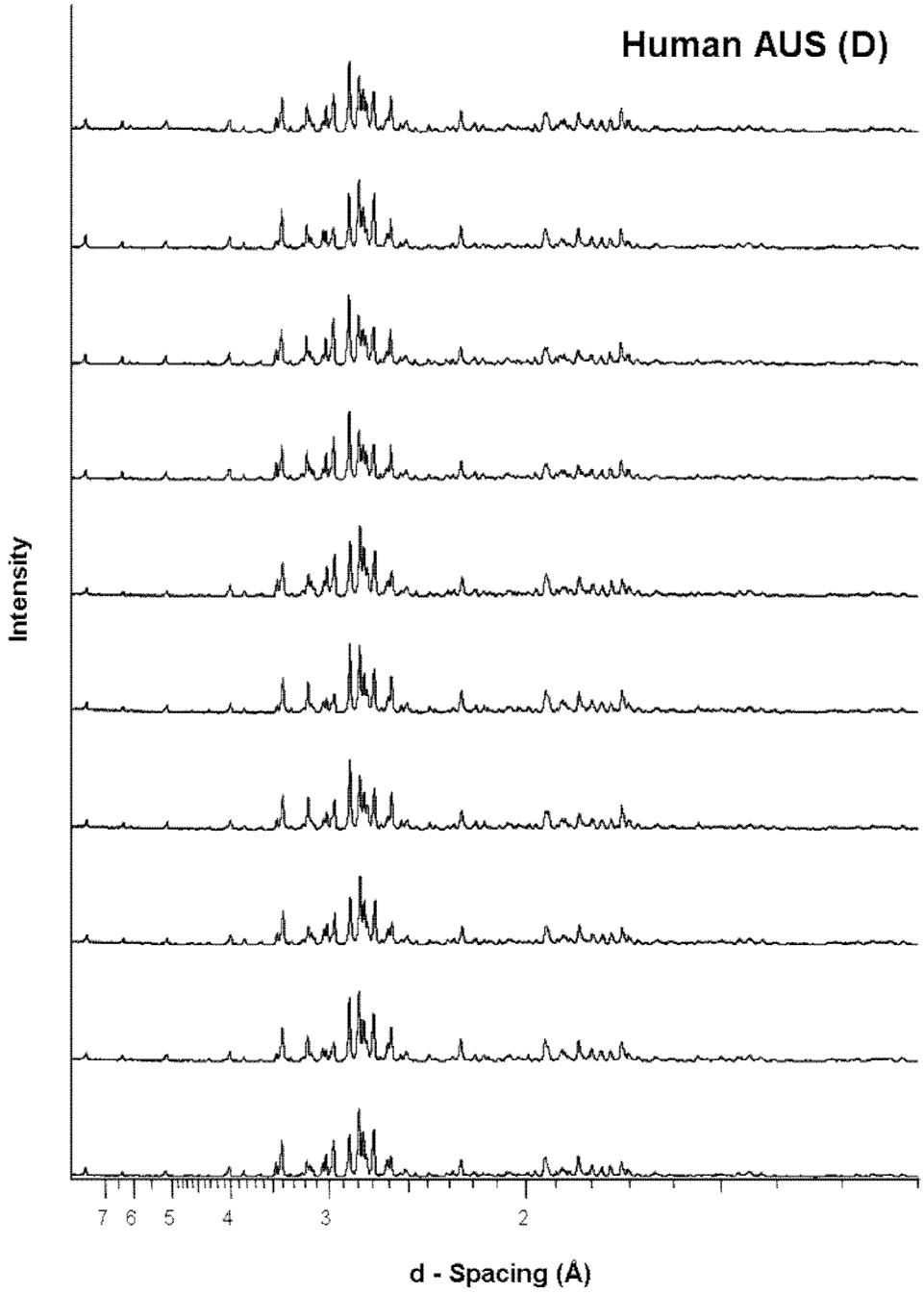

Figure A.25 – Diffractograms obtained from human AUS bone specimens from ten individuals. Group D, of groups A – E (a total of 50 individuals). All bone specimens heated to 1400 °C

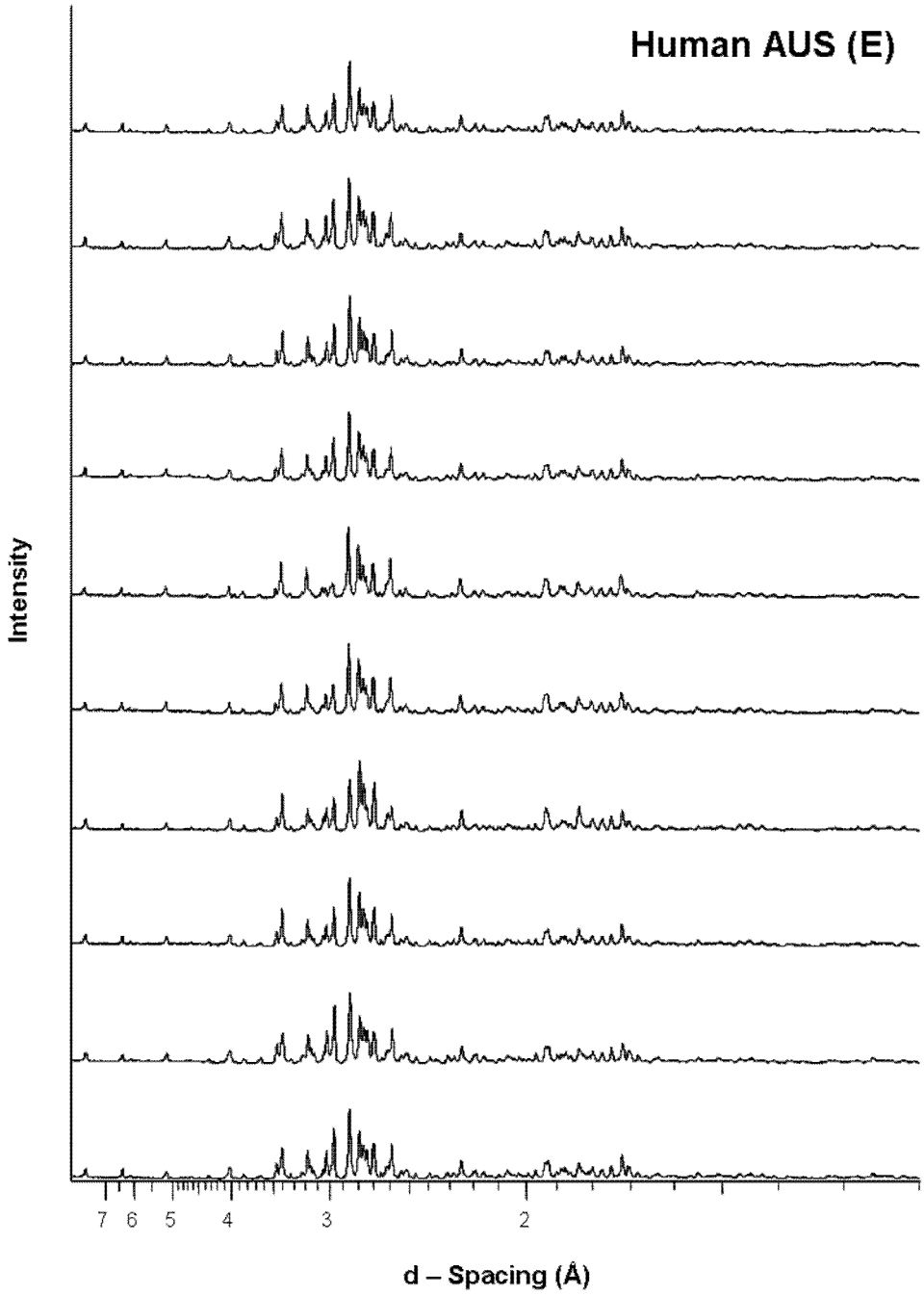

Figure A.26 – Diffractograms obtained from human AUS bone specimens from ten individuals. Group E, of groups A – E (a total of 50 individuals). All bone specimens heated to 1400 °C

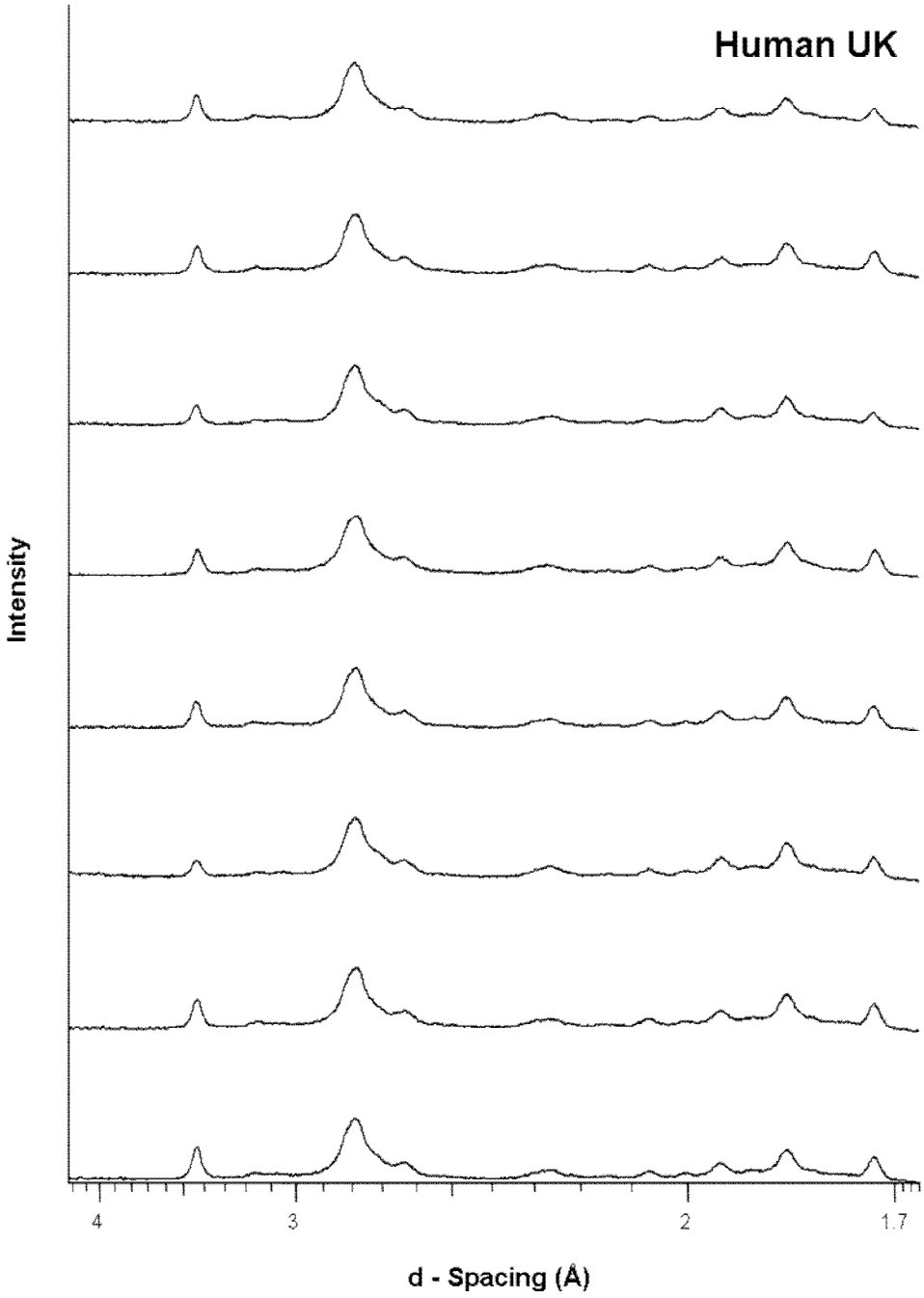

Figure A.27 – Diffractograms obtained from unheated human UK bone specimens from eight individuals.

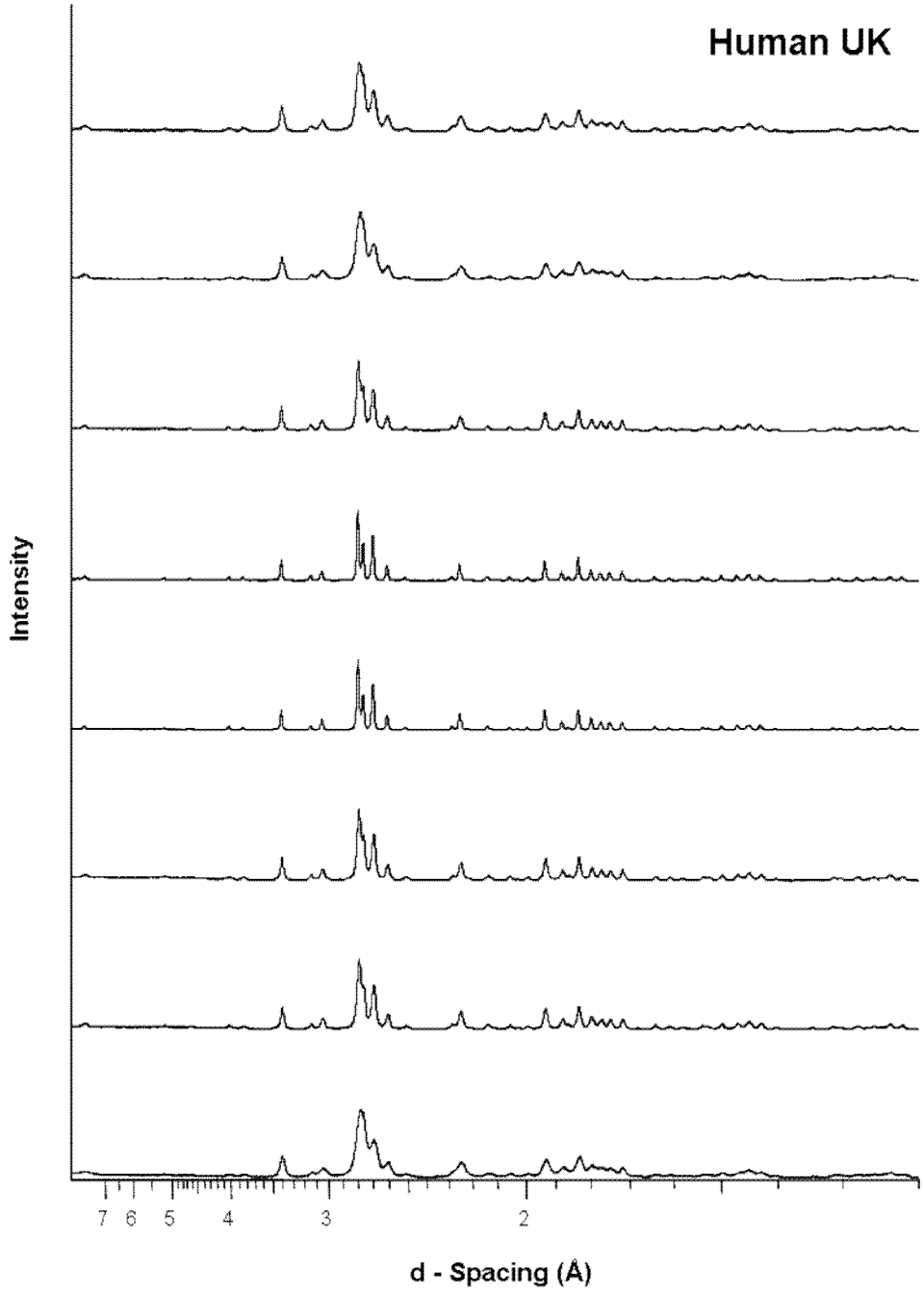

Figure A.28 – Diffractograms obtained from human UK bone specimens from eight individuals. All bone specimens heated to 600 °C.

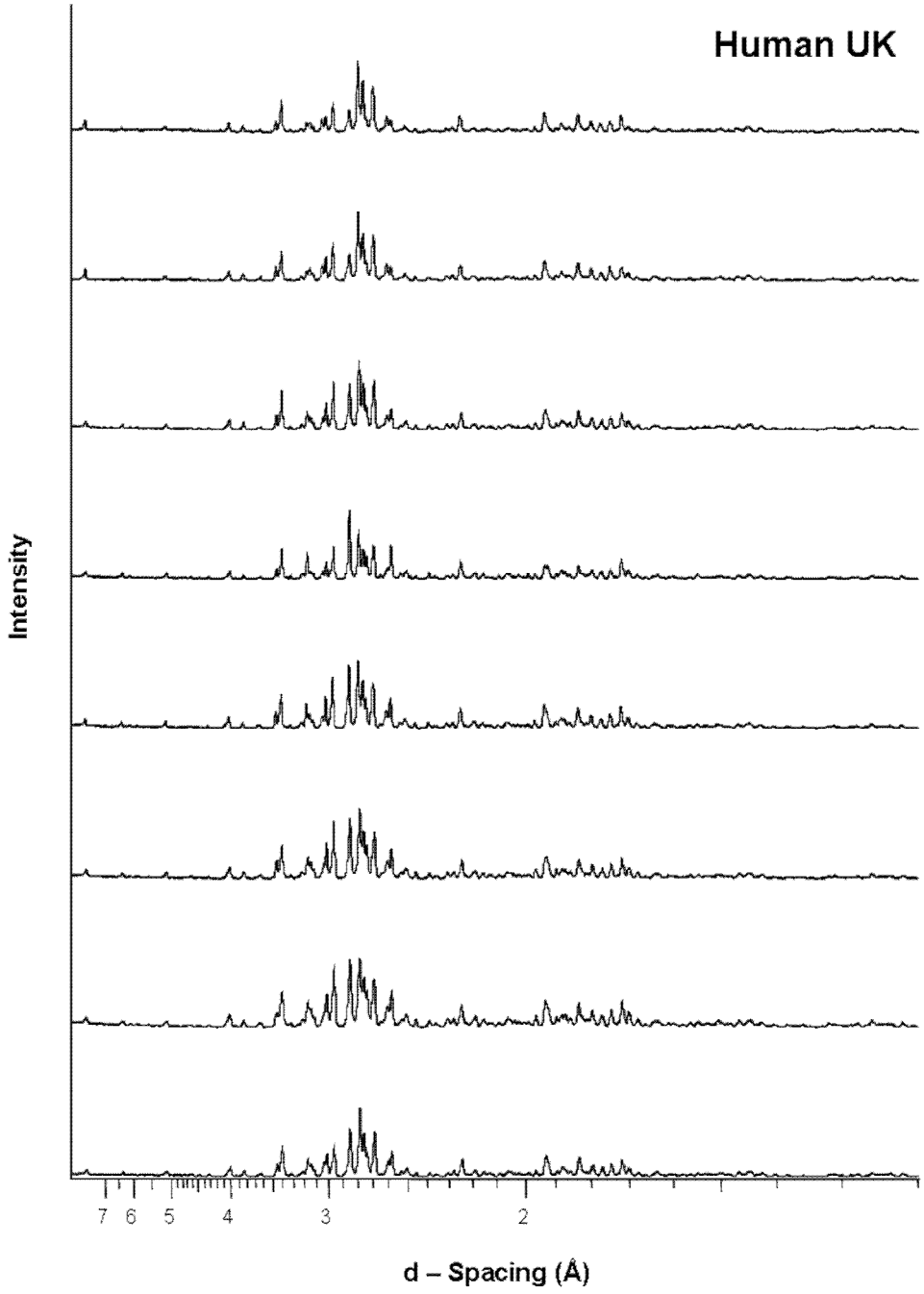

Figure A.29 – Diffractograms obtained from human UK bone specimens from eight individuals. All bone specimens heated to 1400 °C.

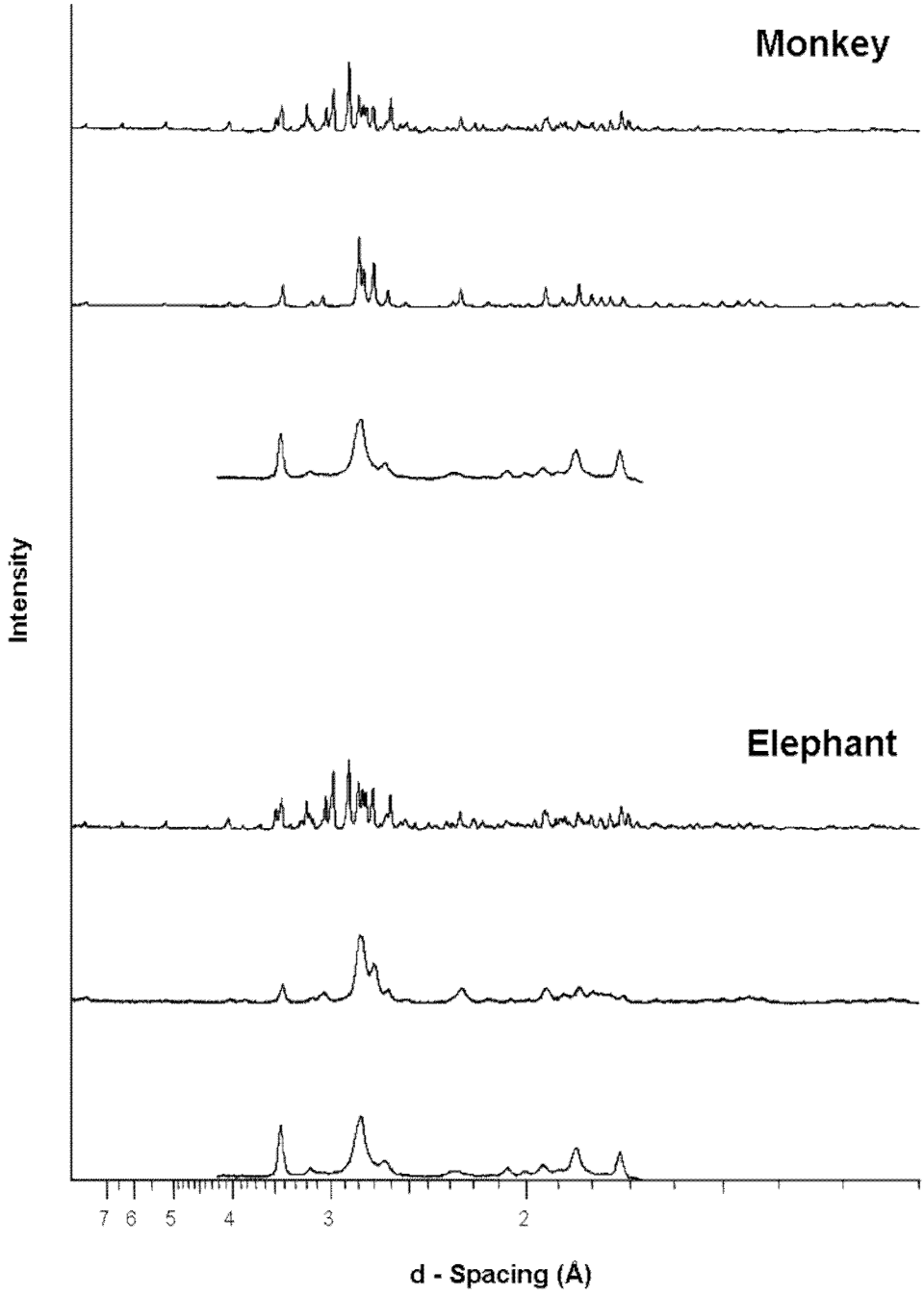

Figure A.30 – Diffractograms obtained from elephant and monkey bone specimens, from one individual from each species. Within each set of three diffractograms: lower profile; unheated bone specimen, middle profile; bone specimen heated to 600 °C, upper profile; bone specimen heated to 1400 °C.

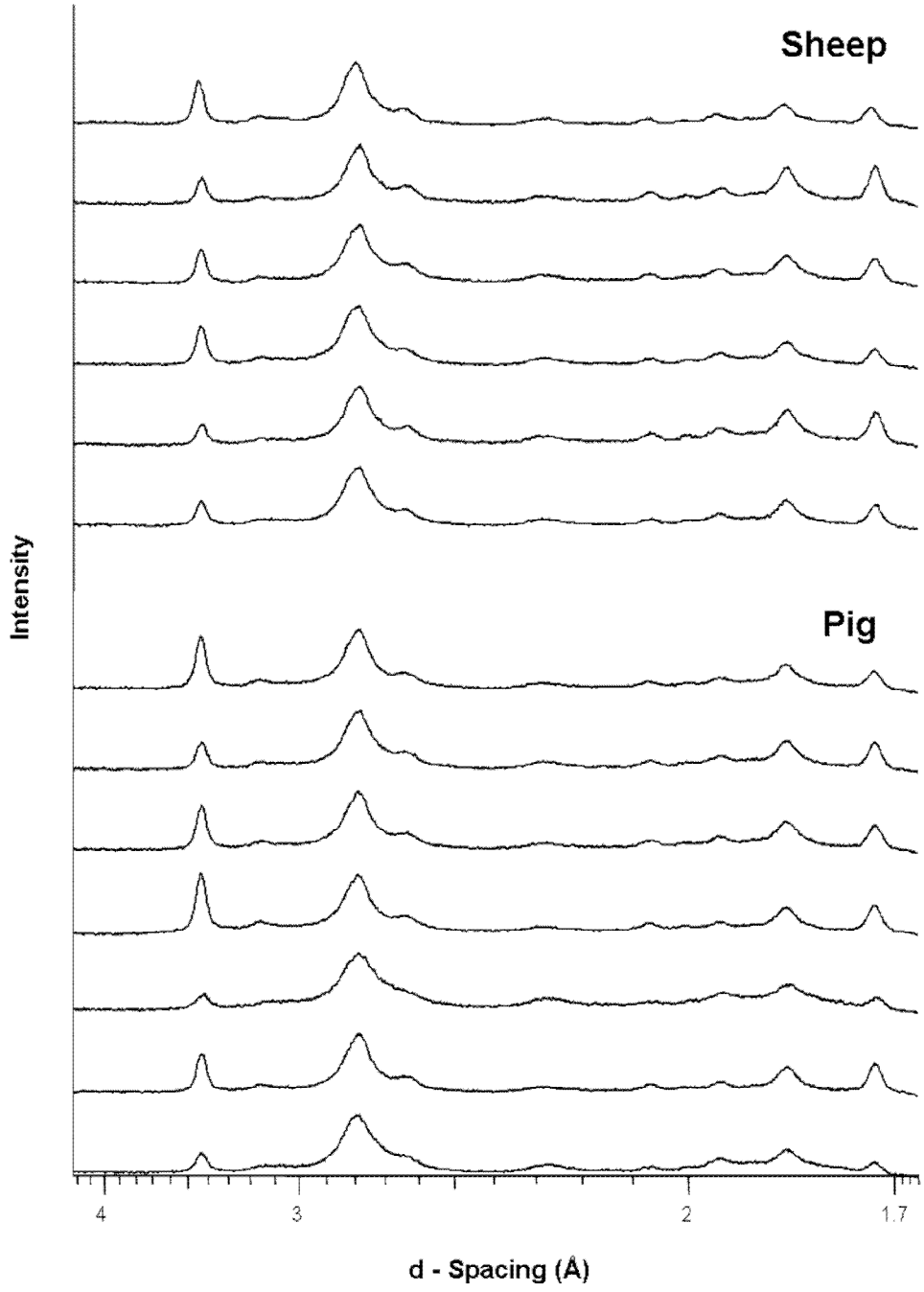

Figure A.31 – Diffractograms obtained from unheated pig bone specimens from seven individuals and from unheated sheep bone specimens from six individuals.

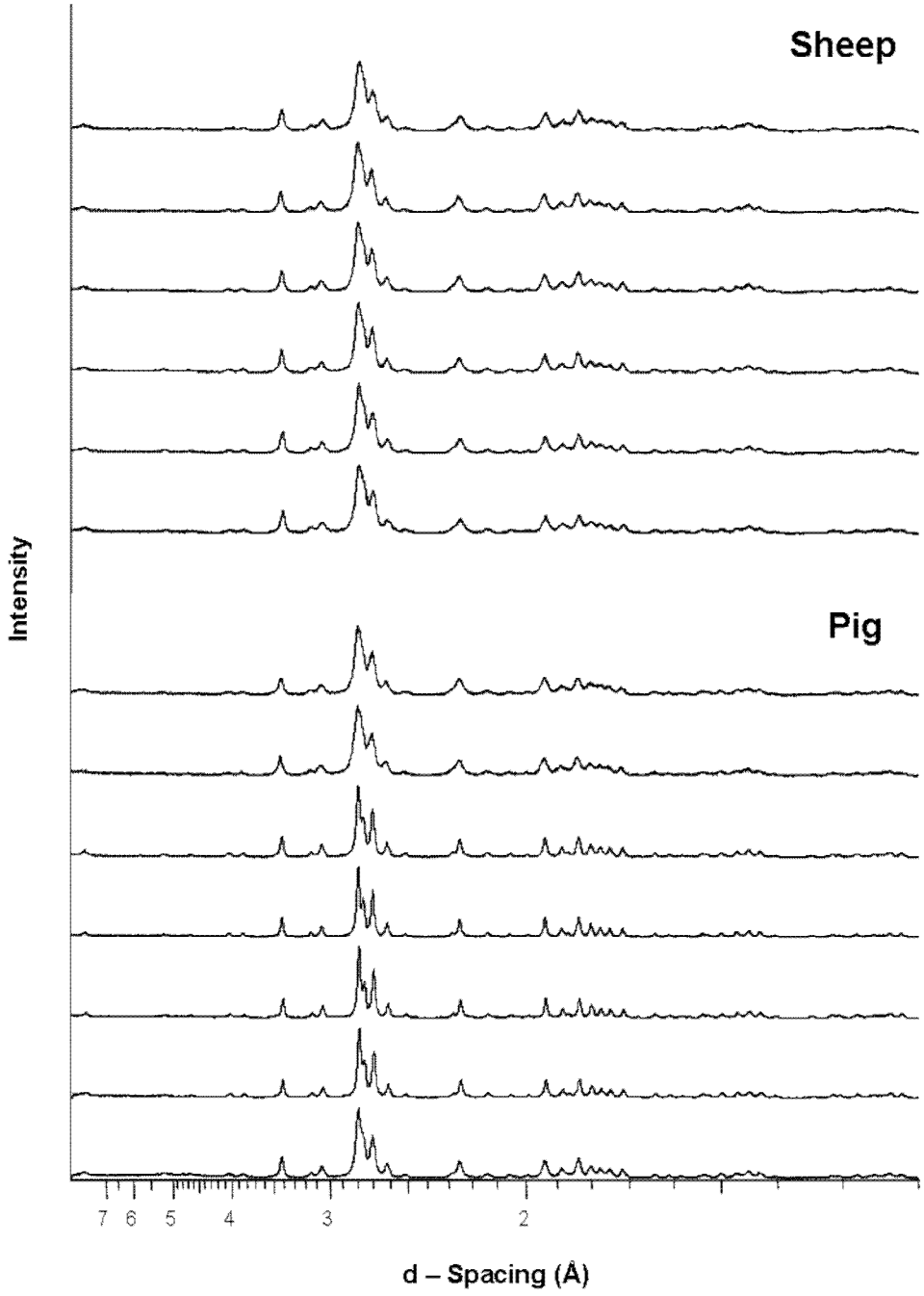

Figure A.32 – Diffractograms obtained from pig bone specimens from seven individuals and from sheep bone specimens from six individuals. All bone specimens heated to 600 °C.

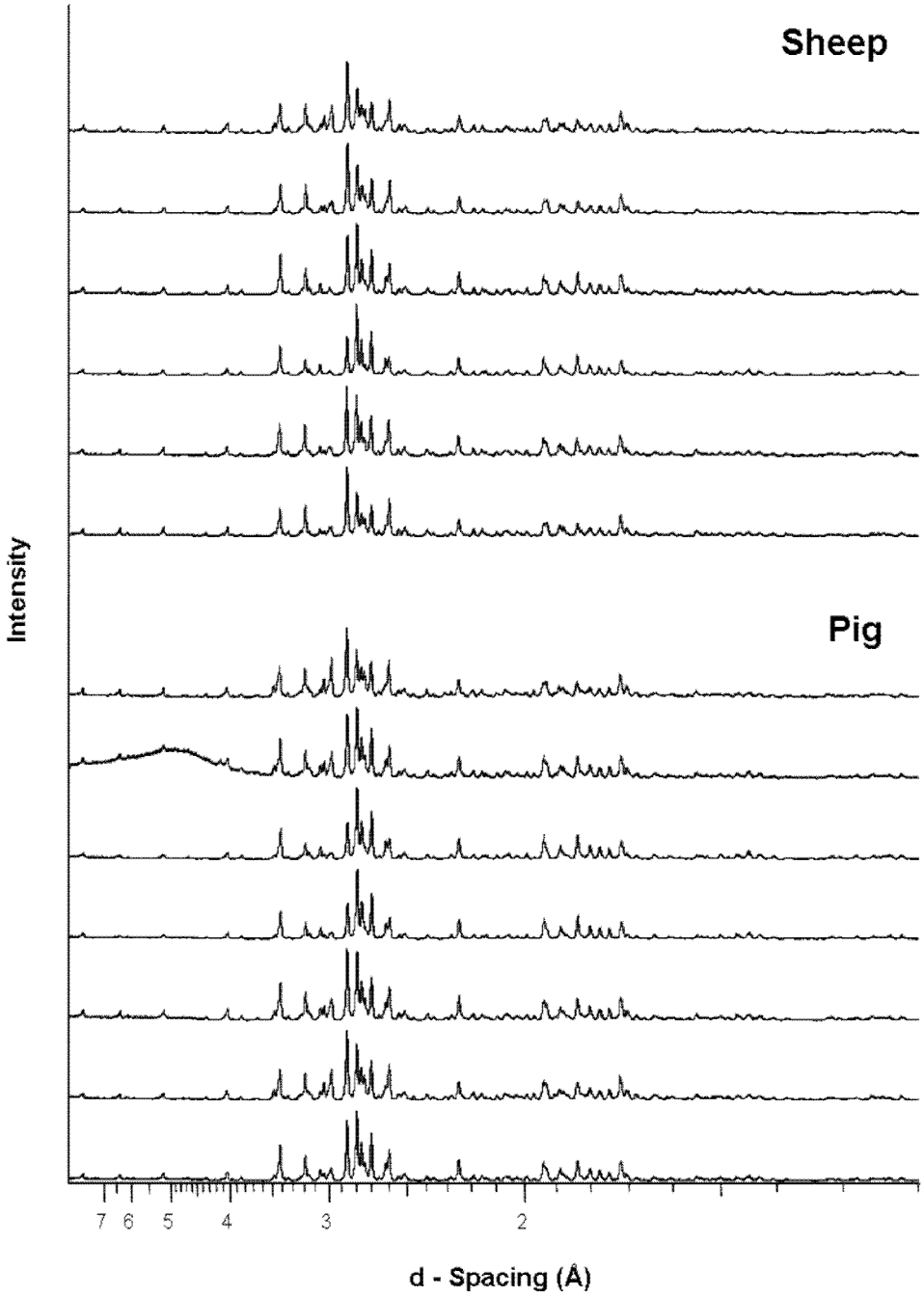

Figure A.33 – Diffractograms obtained from pig bone specimens from seven individuals and from sheep bone specimens from six individuals. All bone specimens heated to 1400 °C.

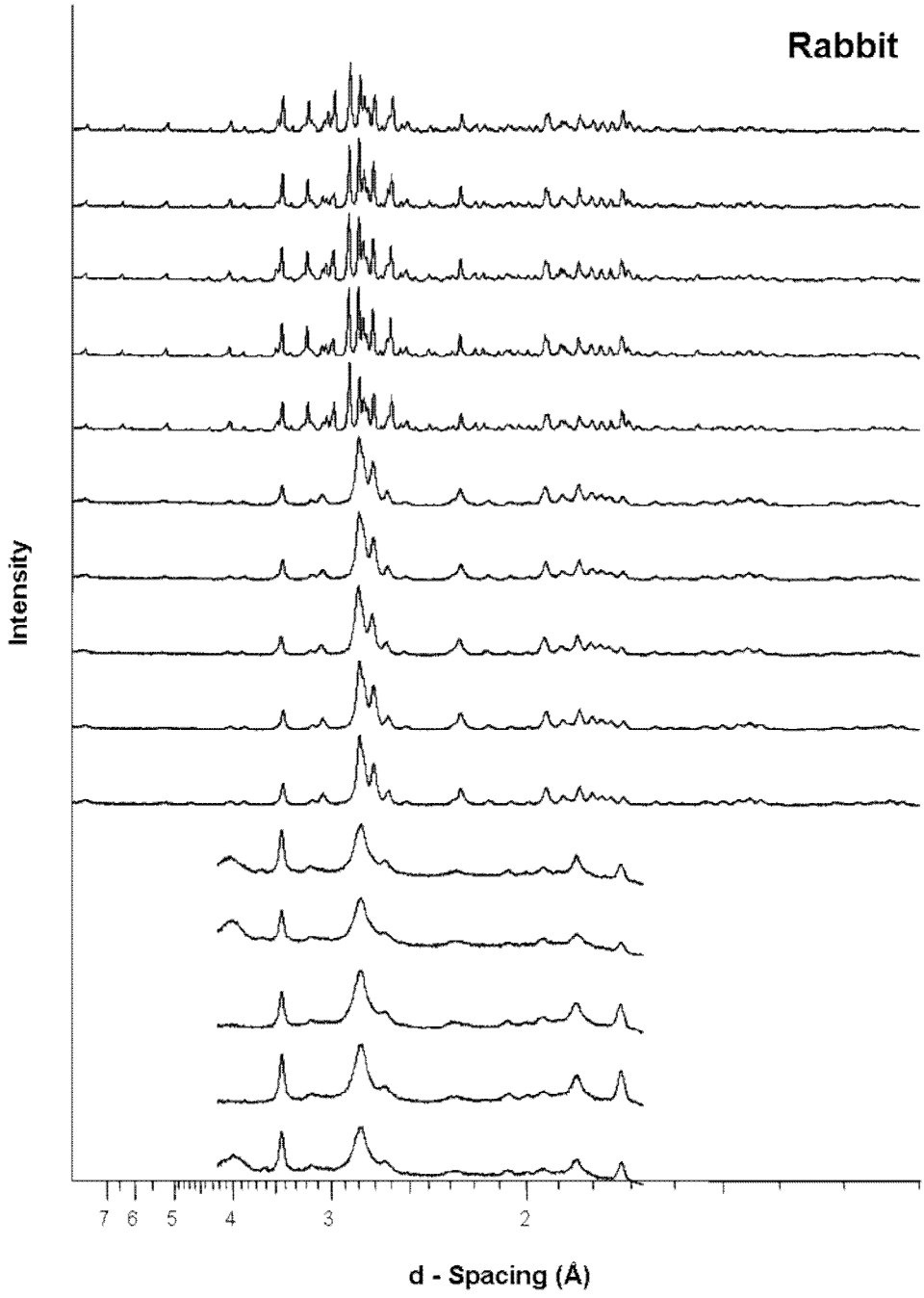

Figure A.34 – Diffractograms obtained from rabbit bone specimens from five individuals. Lower five; unheated bone specimens, middle five; bone specimens heated to 600 °C, upper five; bone specimens heated to 1400 °C.

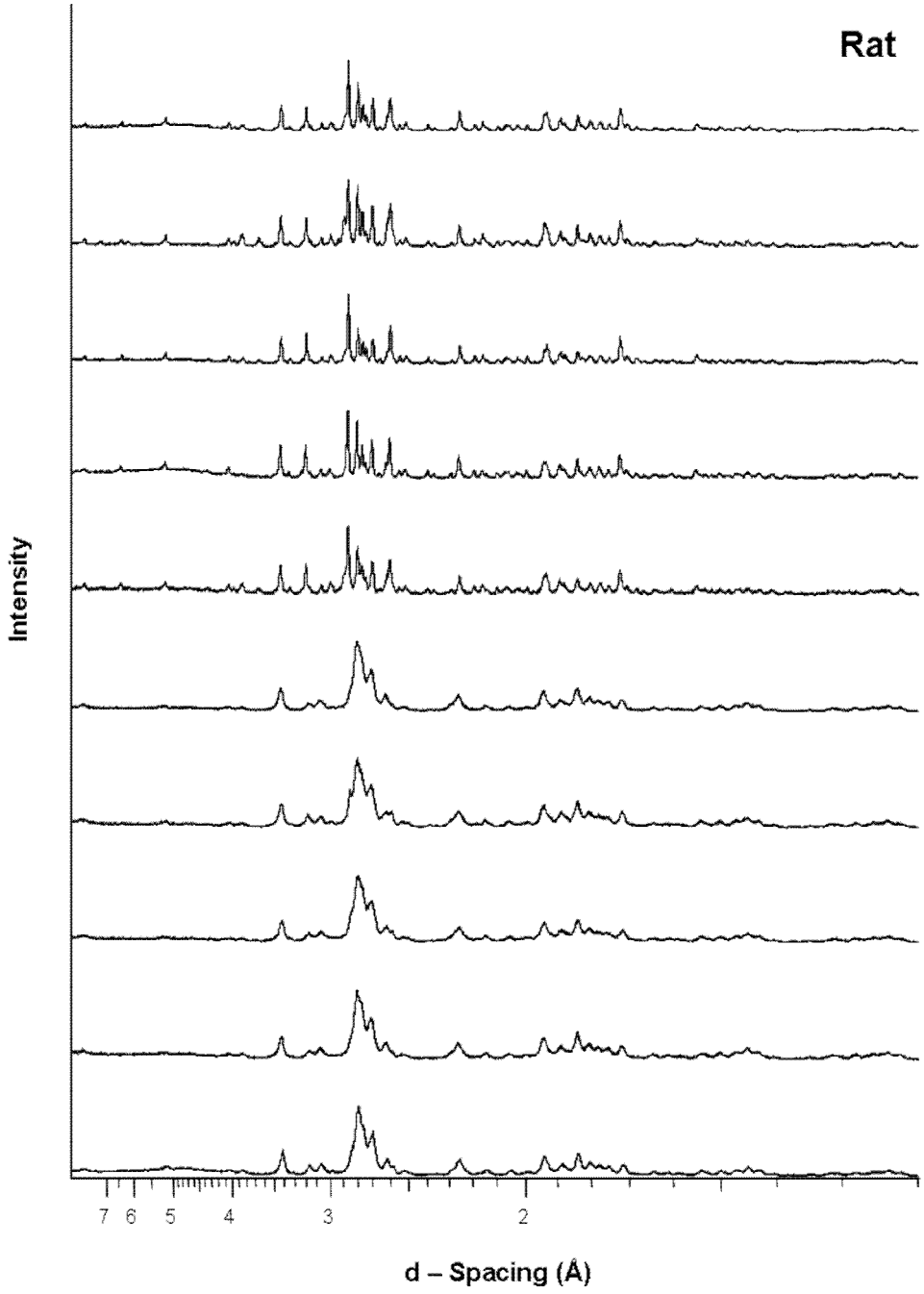

Figure A.35 – Diffractograms obtained from rat bone specimens from five individuals. Lower five; bone specimens heated to 600 °C, upper five; bone specimens heated to 1400 °C.

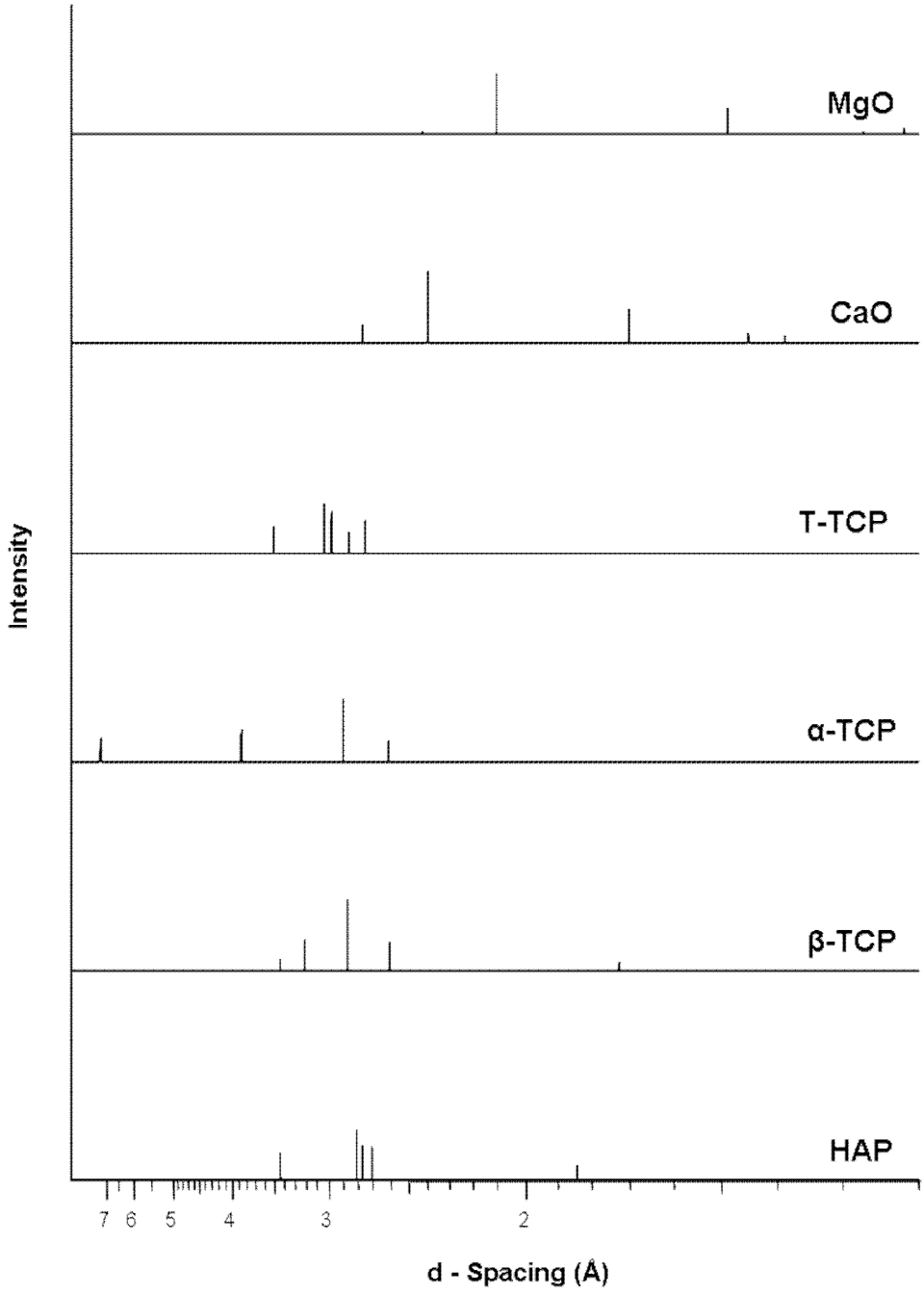

Figure A.36 – Stick representations of diffractograms for several mineral phases. The five highest intensity peaks are presented for each phase. Data obtained from International Centre for Diffraction Data, Powder Diffraction Files: HAP (9-432), β-TCP (9-169), α-TCP (29-359), TTCP (25-1137), CaO (37-1497), MgO (45-946)

A.3 – INFRARED SPECTRA

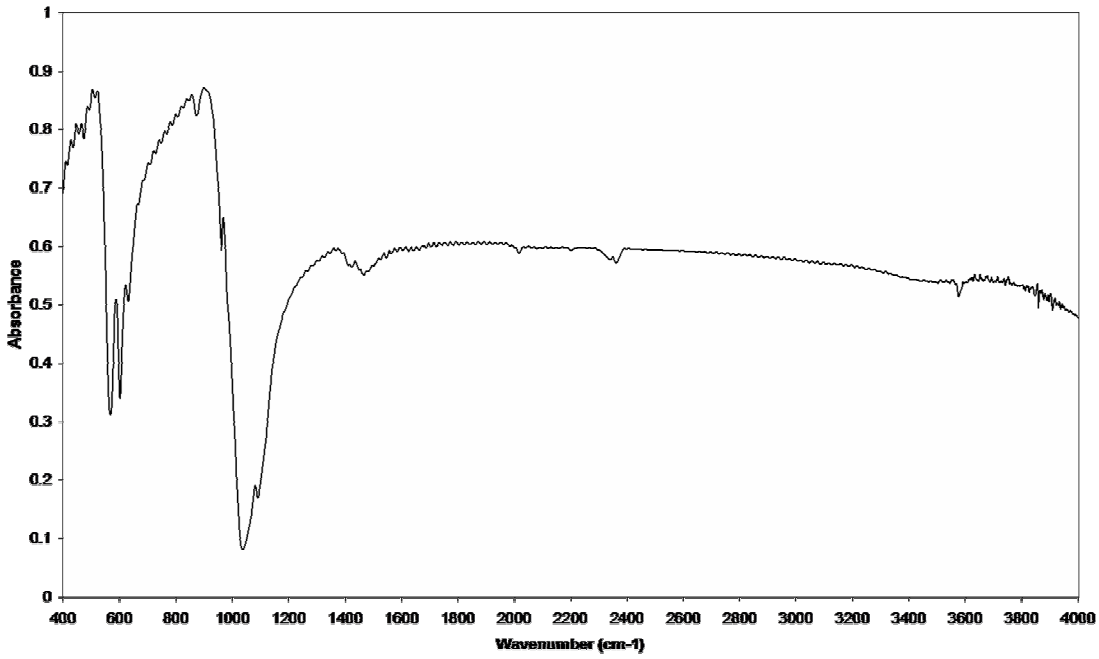

Figure A.37 – Infrared spectrum obtained from a chicken bone specimen (J01) heated to 600 °C

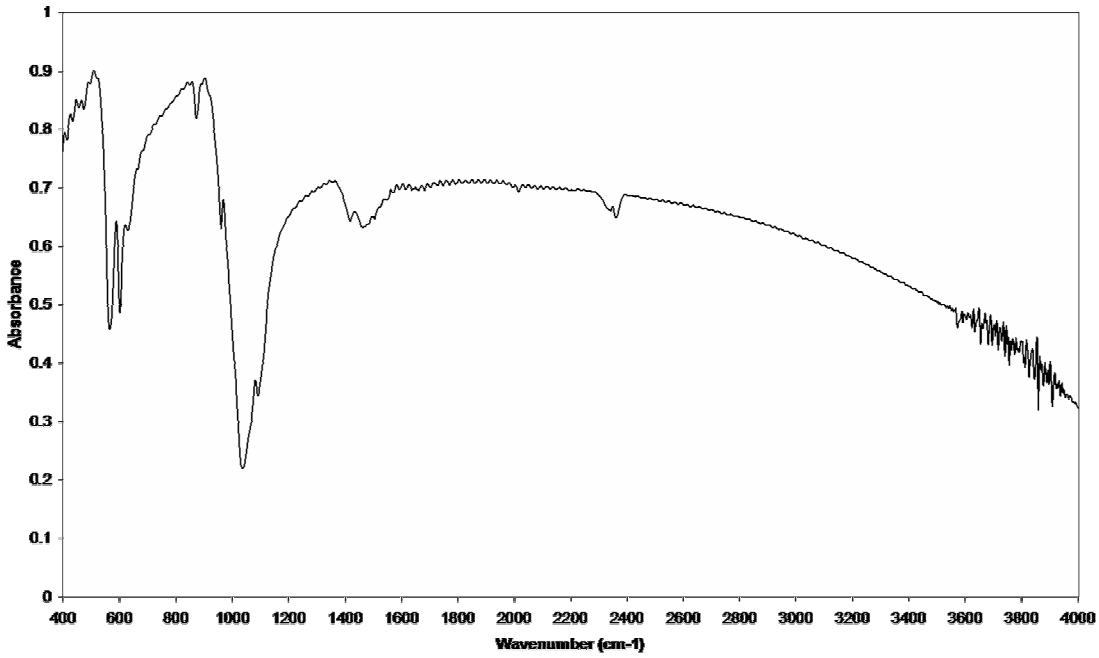

Figure A.38 – Infrared spectrum obtained from a cow bone specimen (C02) heated to 600 °C

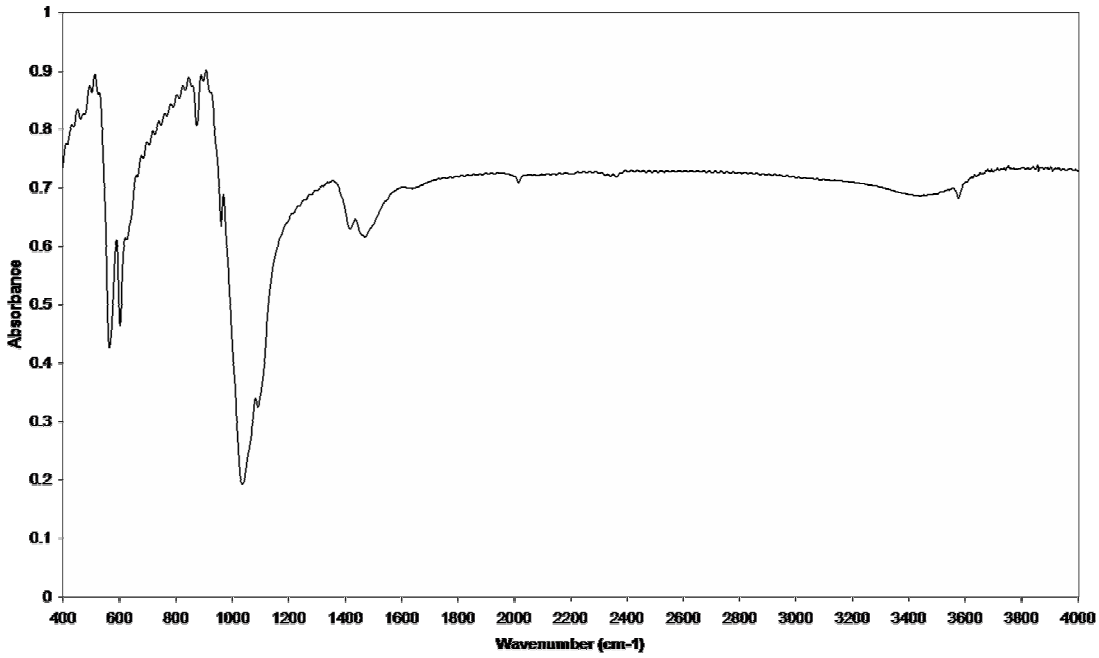

Figure A.39 – Infrared spectrum obtained from a cow bone specimen (C11) heated to 600 °C

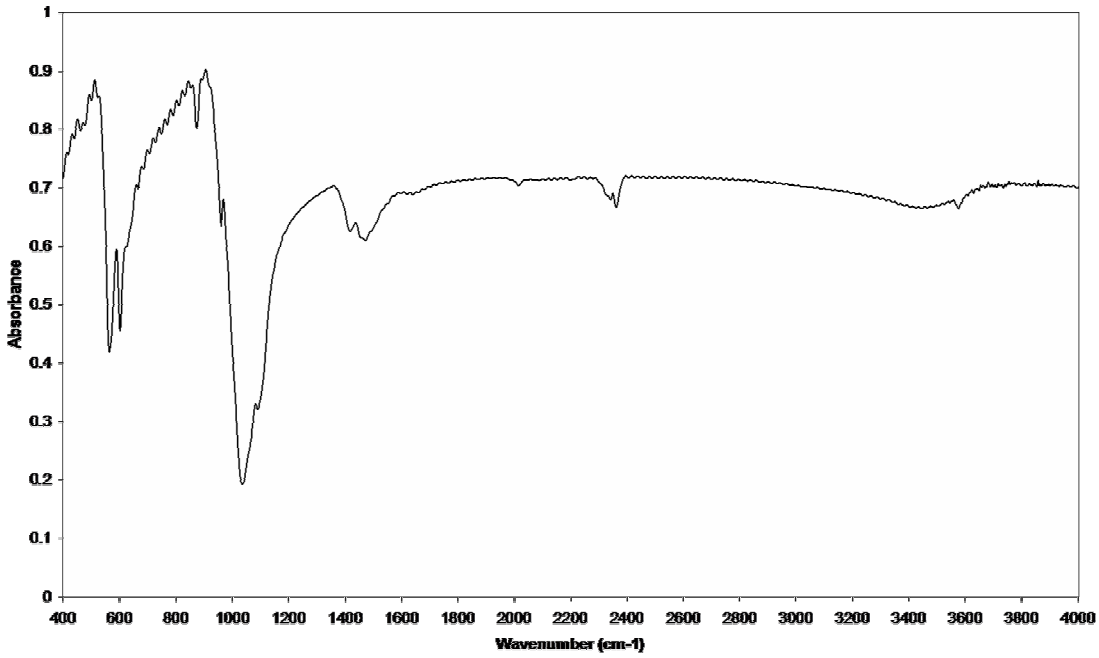

Figure A.40 – Infrared spectrum obtained from a cow bone specimen (C12) heated to 600 °C

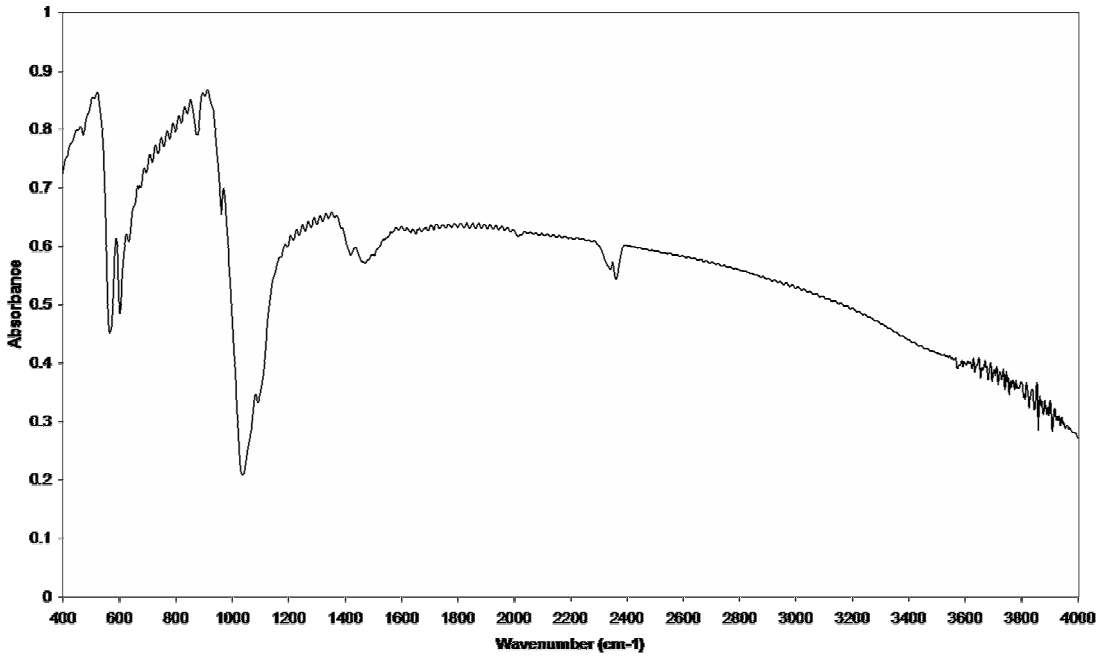

Figure A.41 – Infrared spectrum obtained from a cow bone specimen (C13) heated to 600 °C

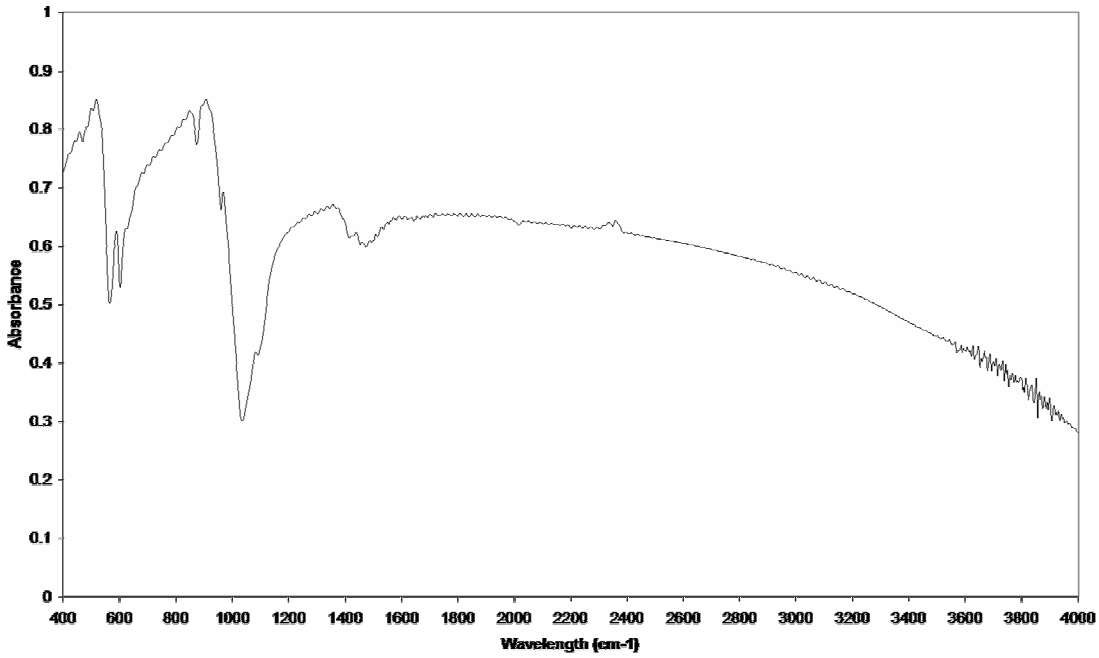

Figure A.42 – Infrared spectrum obtained from a cow bone specimen (C14) heated to 600 °C

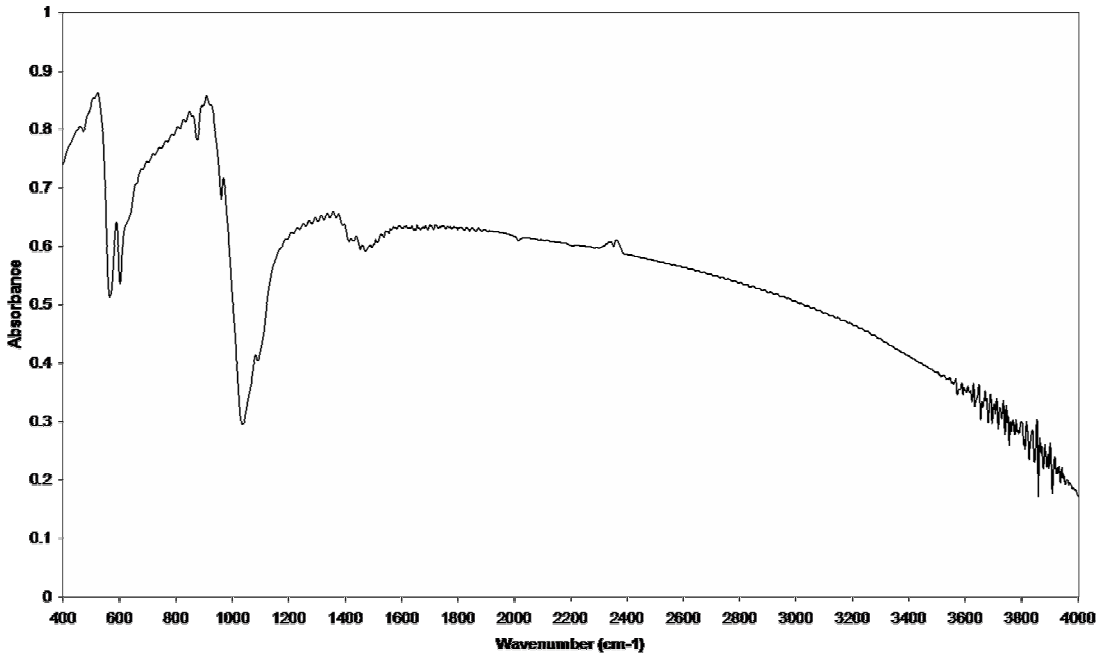

Figure A.43 – Infrared spectrum obtained from a cow bone specimen (C15) heated to 600 °C

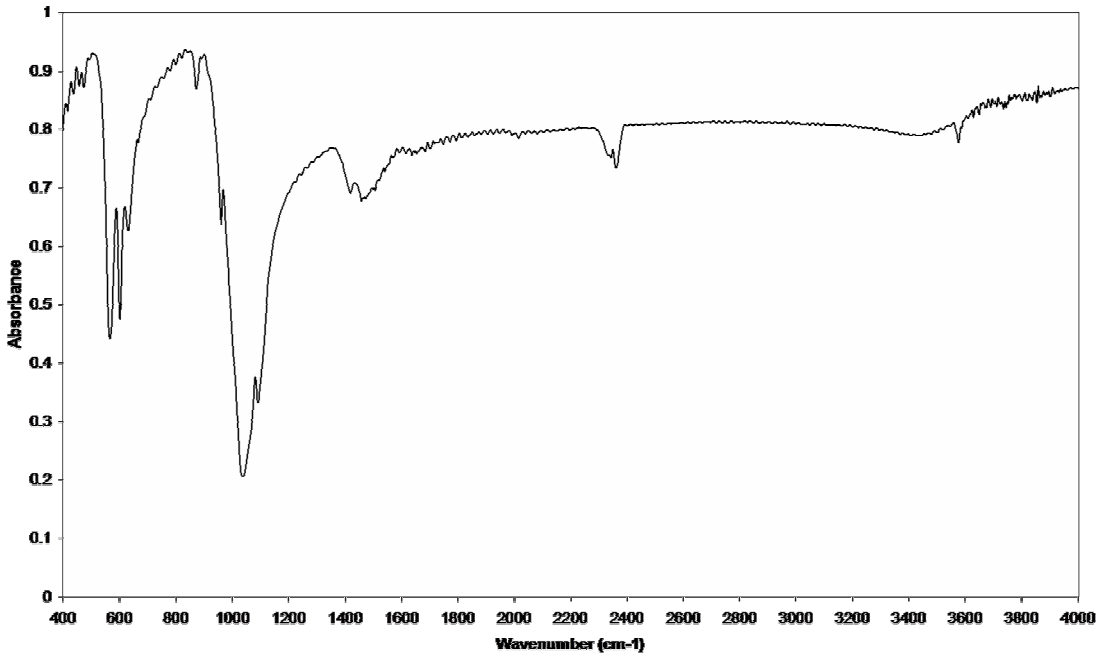

Figure A.44 – Infrared spectrum obtained from a deer bone specimen (K01) heated to 600 °C

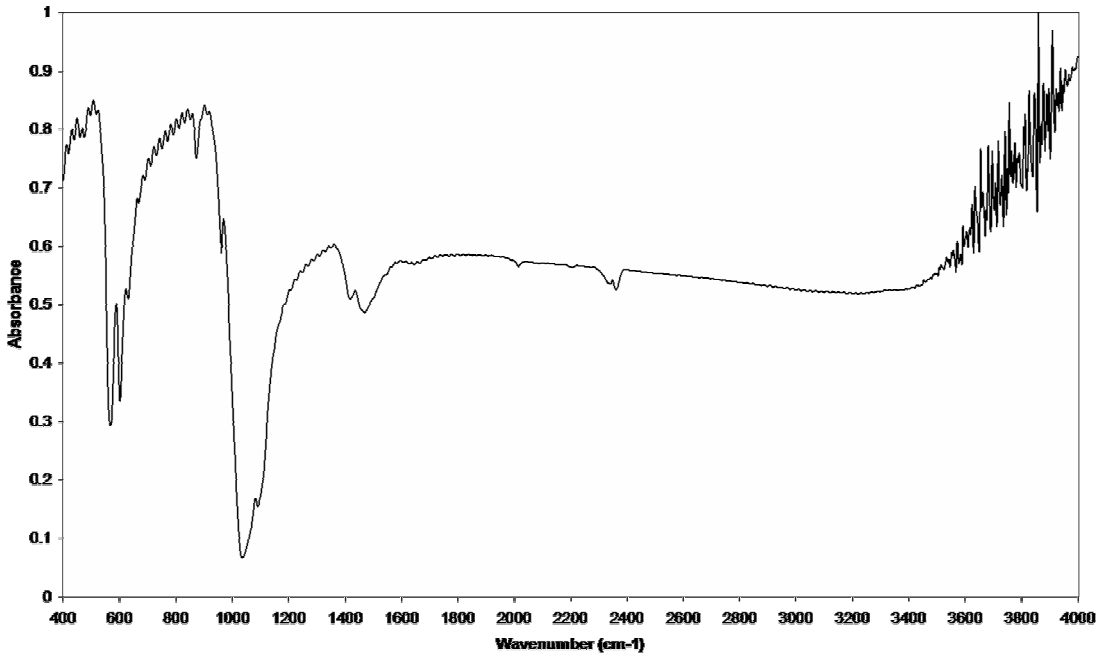

Figure A.45 – Infrared spectrum obtained from a dog bone specimen (D01) heated to 600 °C

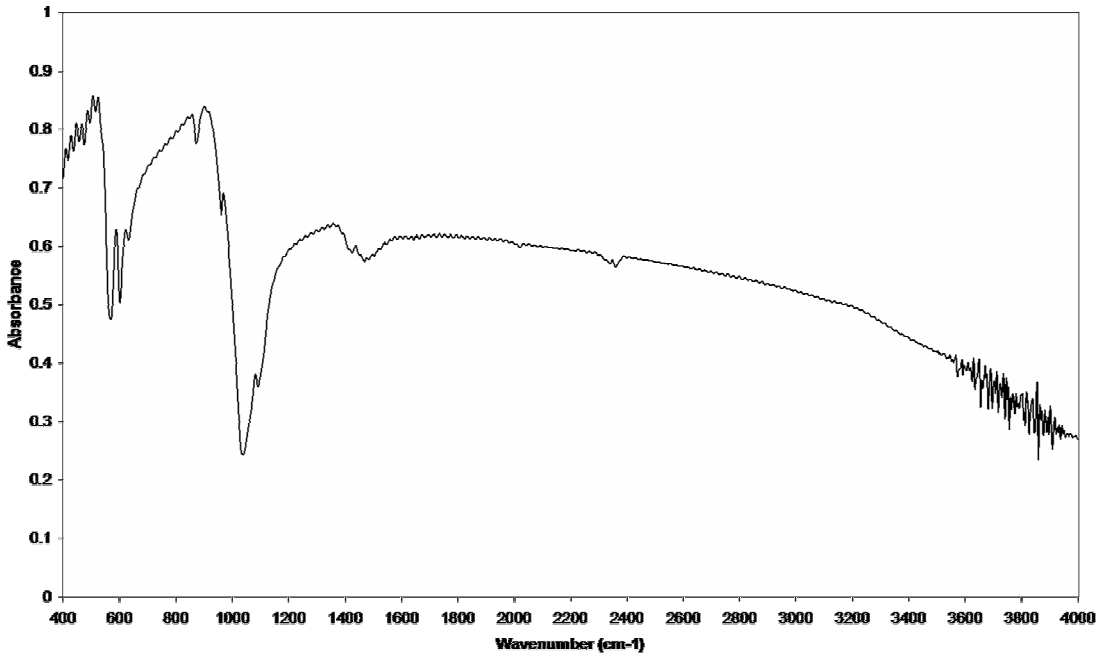

Figure A.46 – Infrared spectrum obtained from a goat bone specimen (G01) heated to 600 °C

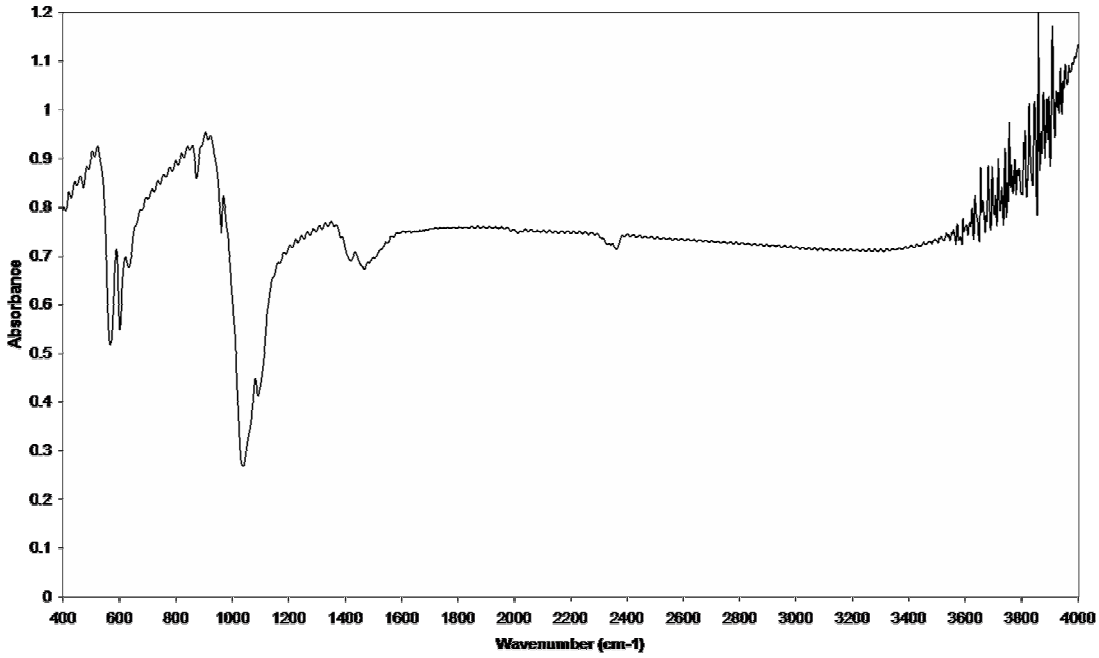

Figure A.47 – Infrared spectrum obtained from a human UK bone specimen (H02) heated to 600 °C

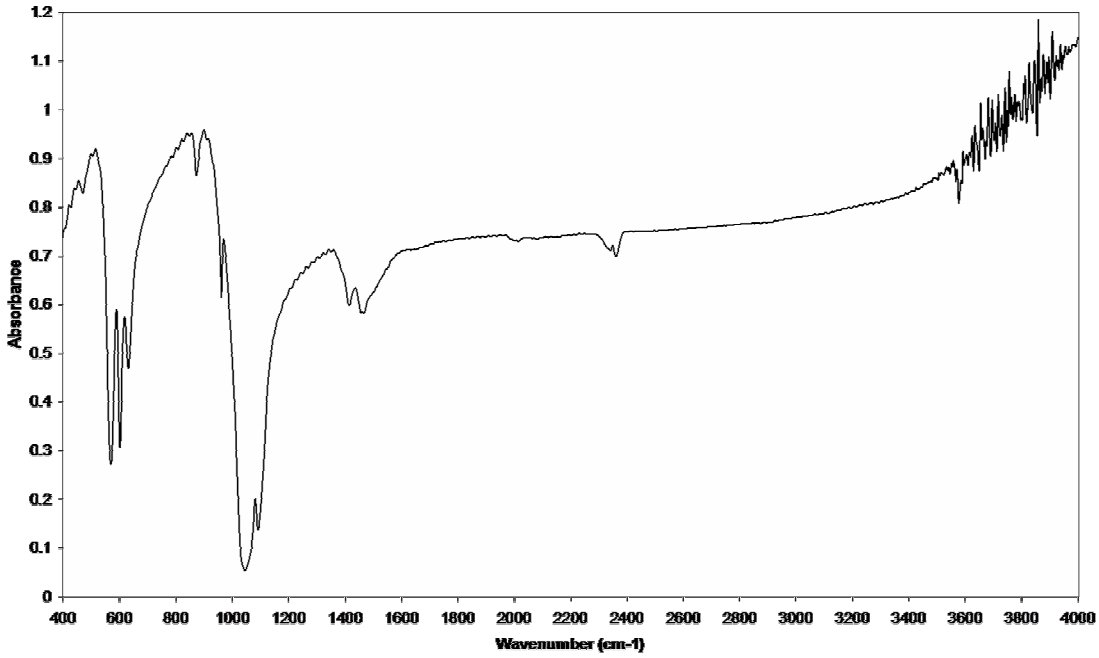

Figure A.48 – Infrared spectrum obtained from a monkey bone specimen (M01) heated to 600 °C

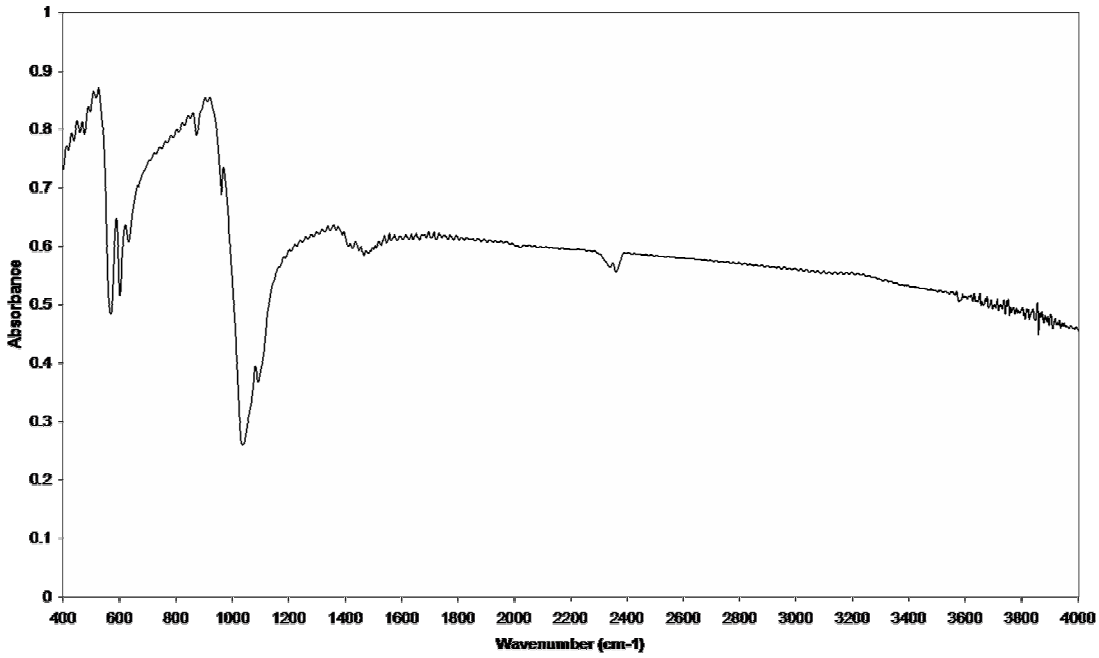

Figure A.49 – Infrared spectrum obtained from a pig bone specimen (P02) heated to 600 °C

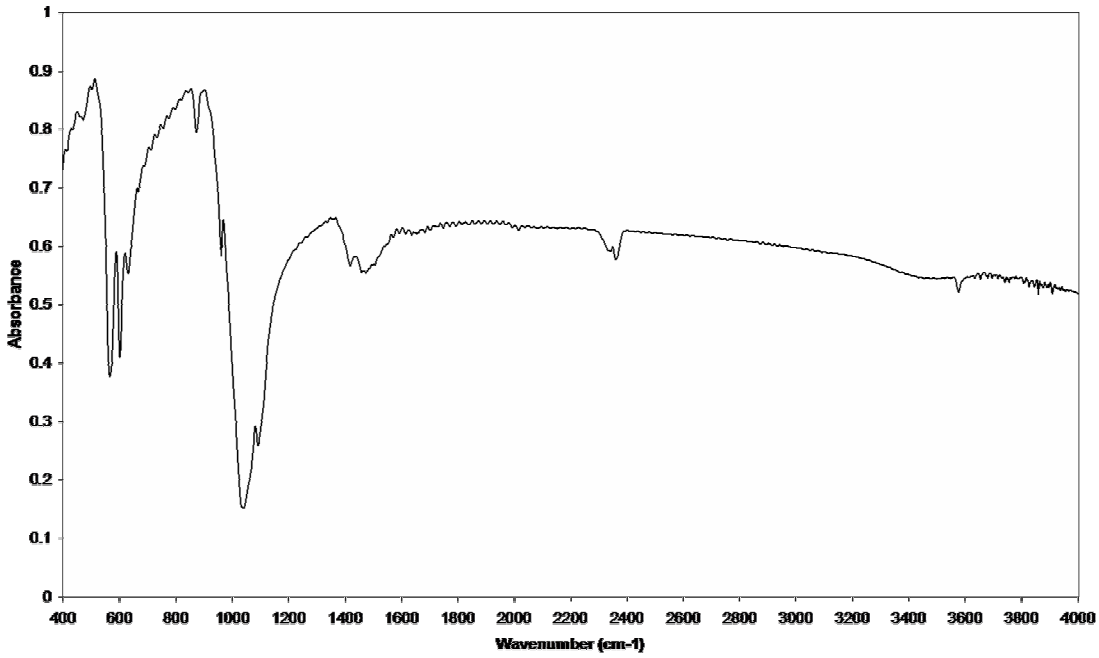

Figure A.50 – Infrared spectrum obtained from a rabbit bone specimen (L03) heated to 600 °C

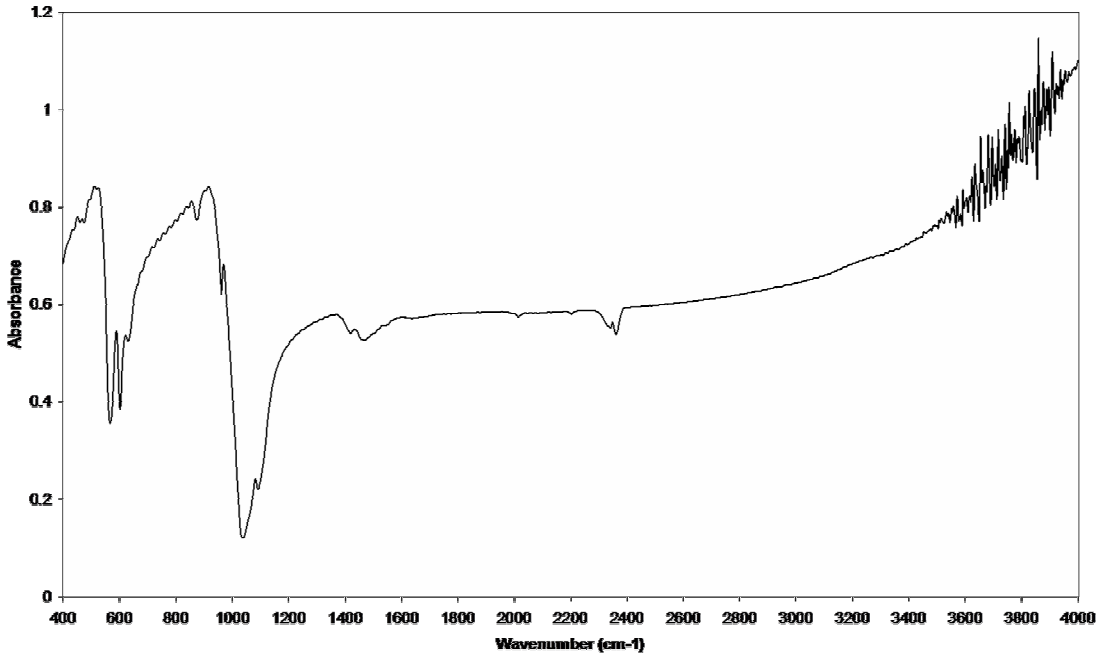

Figure A.51 – Infrared spectrum obtained from a sheep bone specimen (S02) heated to 600 °C

A.4 – DESCRIPTIVE STATISTICS (GROUPED BY SPECIES)

A.4.1 – X-RAY DIFFRACTION ANALYSIS OF UNHEATED BONE

Species		Chicken	Cow	Deer	Dog	Elephant	Goat	Human AUS	Human UK	Monkey	Pig	Rabbit	Rat	Sheep
Number		5	10	5	12	1	8	47	8	1	7	5	0	6
HAP %		100	100	100	100	100	100	100	100	100	100	100	---	100
HAP <00ℓ> (Å)	Mean	194.4	238.3	242.7	247.9	216.9	251.0	263.0	262.0	258.4	217.3	236.7	---	234.4
	Std. Error	4.2	4.2	4.8	4.2	…	3.2	2.0	4.7	…	7.4	5.0	---	4.2
	Min	187.1	215.2	228.3	210.8	…	237.9	234.5	240.7	…	175.3	223.6	---	217.7
	Max	210.2	255.3	255.2	268.3	…	264.5	288.0	281.5	…	230.8	250.6	---	246.5
HAP a (Å)	Mean	9.482	9.464	9.479	9.467	9.463	9.460	9.455	9.441	9.467	9.484	9.471	---	9.479
	Std. Error	0.003	0.004	0.004	0.004	…	0.002	0.002	0.004	…	0.005	0.007	---	0.002
	Min	9.475	9.441	9.468	9.438	…	9.450	9.427	9.419	…	9.468	9.452	---	9.471
	Max	9.493	9.482	9.490	9.491	…	9.471	9.482	9.458	…	9.508	9.489	---	9.484
HAP c (Å)	Mean	6.895	6.900	6.900	6.902	6.907	6.904	6.903	6.902	6.906	6.899	6.898	---	6.898
	Std. Error	0.002	0.001	0.002	0.002	…	0.001	0.001	0.001	…	0.002	0.002	---	0.004
	Min	6.888	6.893	6.893	6.894	…	6.902	6.880	6.898	…	6.888	6.892	---	6.891
	Max	6.901	6.906	6.906	6.912	…	6.907	6.921	6.906	…	6.904	6.906	---	6.918

Table A.1 – XRD analysis results for HAP %, HAP <00ℓ>, HAP 'a' and HAP 'c' obtained from unheated bone specimens, grouped by species. For elephant and monkey the 'mean' values represent data from one individual from each species and so no standard error of the mean, minimum or maximum values are presented. Unheated rat bone was not investigated using this technique

A.4.2 – INDUCTIVELY COUPLED PLASMA – ATOMIC EMISSION SPECTROMETRY

Species		Chicken	Cow	Deer	Dog	Elephant	Goat	Human AUS	Human UK	Monkey	Pig	Rabbit	Rat	Sheep
Number		1	6	1	1	0	1	3	1	1	1	1	0	1
Ca %	Mean	39.4	38.7	38.3	38.0	---	39.7	39.6	40.4	40.5	41.3	43.7	---	41.6
	Std. Error	...	0.1	...	...	---	...	0.9	...	...	...	...	---	...
	Min	...	38.3	...	...	---	...	38.2	...	...	...	...	---	...
	Max	...	39.2	...	...	---	...	41.3	...	...	...	...	---	...
P %	Mean	20.1	20.0	18.7	18.6	---	19.6	18.7	19.2	18.8	19.3	20.6	---	19.4
	Std. Error	...	0.1	...	...	---	...	0.5	...	...	...	...	---	...
	Min	...	19.6	...	...	---	...	17.8	...	...	...	...	---	...
	Max	...	20.4	...	...	---	...	19.6	...	...	...	...	---	...
Ca/P atomic	Mean	1.52	1.50	1.59	1.58	---	1.57	1.64	1.63	1.66	1.66	1.64	---	1.66
	Std. Error	...	0.01	...	...	---	...	0.01	...	...	...	...	---	...
	Min	...	1.47	...	...	---	...	1.63	...	...	...	...	---	...
	Max	...	1.52	...	...	---	...	1.66	...	...	...	...	---	...
Ca/P weight	Mean	1.96	1.94	2.05	2.04	---	2.03	2.13	2.11	2.15	2.14	2.12	---	2.14
	Std. Error	...	0.01	...	...	---	...	0.01	...	...	...	...	---	...
	Min	...	1.90	...	...	---	...	2.11	...	...	...	...	---	...
	Max	...	1.97	...	...	---	...	2.15	...	...	...	...	---	...

Table A.2 – ICP-AES results for Ca % and P %, calculated Ca/P $_{(atomic)}$ and calculated Ca/P $_{(weight)}$ obtained from bone specimens heated to 600 °C, grouped by species. For all species except cow, human AUS and rat the 'mean' values represent data from one individual from each species and so no standard error of the mean, minimum or maximum values are presented. Rat bone was not investigated using this technique

Species		Chicken	Cow	Deer	Dog	Elephant	Goat	Human AUS	Human UK	Monkey	Pig	Rabbit	Rat	Sheep
Number		1	6	1	1	0	1	3	1	1	1	1	0	1
Na ppm	Mean	5878	9551	8149	9005	---	9752	8360	10329	9292	8021	8081	---	7721
	Std. Error	…	86	…	…	---	…	197	…	…	…	…	---	…
	Min	…	9237	…	…	---	…	8136	…	…	…	…	---	7721
	Max	…	9831	…	…	---	…	8752	…	…	…	…	---	…
Mg ppm	Mean	7575	6452	6101	3717	---	5717	4060	3912	4534	5517	5938	---	7103
	Std. Error	…	148	…	…	---	…	271	…	…	…	…	---	…
	Min	---	5814	---	---	---	---	3685	---	---	---	---	---	---
	Max	…	6848	…	…	---	…	4586	…	…	…	…	---	…
K ppm	Mean	5946	832	1437	1329	---	1117	358	389	1863	1982	2115	---	2828
	Std. Error	…	98	…	…	---	…	108	…	…	…	…	---	…
	Min	---	565	---	---	---	---	168	---	---	---	---	---	---
	Max	…	1220	…	…	---	…	543	…	…	…	…	---	…
Sr ppm	Mean	230	246	223	115	---	270	136	100	54	98	234	---	135
	Std. Error	…	35	…	…	---	…	22	…	…	…	…	---	…
	Min	---	146	---	---	---	---	93	---	---	---	---	---	---
	Max	…	351	…	…	---	…	161	…	…	…	…	---	…
Fe ppm	Mean	59.6	14.3	17.1	34.8	---	10.2	16.4	8.8	20.6	4.3	29.2	---	11.0
	Std. Error	…	1.6	…	…	---	…	6.2	…	…	…	…	---	…
	Min	---	8.9	---	---	---	---	9.3	---	---	---	---	---	---
	Max	…	19.5	…	…	---	…	28.8	…	…	…	…	---	…

Table A.3 – ICP-AES results for Na ppm, Mg ppm, K ppm, Sr ppm and Fe ppm obtained from bone specimens heated to 600 °C, grouped by species. For all species except cow, human AUS and rat the 'mean' values represent data from one individual from each species and so no standard error of the mean, minimum or maximum values are presented. Rat bone was not investigated using this technique

A.4.3 – PYROHYDROLYSIS – ION CHROMATOGRAPHY

Species		Chicken	Cow	Deer	Dog	Elephant	Goat	Human AUS	Human UK	Monkey	Pig	Rabbit	Rat	Sheep
Number		1	6	1	1	0	1	3	1	1	1	0	0	1
F ppm	Mean	413	167	118	722	---	370	1293	554	179	46	…	---	178
	Std. Error	…	28	…	…	---	…	487	…	…	…	…	---	…
	Min	…	85	…	…	---	…	382	…	…	…	…	---	…
	Max	…	266	…	…	---	…	2048	…	…	…	…	---	…
Cl ppm	Mean	712	638	450	708	---	967	487	726	749	558	…	---	725
	Std. Error	…	56	…	…	---	…	26	…	…	…	…	---	…
	Min	…	539	…	…	---	…	435	…	…	…	…	---	…
	Max	…	913	…	…	---	…	517	…	…	…	…	---	…

Table A.4 – P-IC results for F ppm and Cl ppm obtained from bone specimens heated to 600 °C, grouped by species. For all species except cow, human AUS and rat the 'mean' values represent data from one individual from each species and so no standard error of the mean, minimum or maximum values are presented. Rat bone was not investigated using this technique. Data obtained for rabbit was semi-quantitative and so is not presented

A.4.4 – COMBUSTION – GAS CHROMATOGRAPHY

Species		Chicken	Cow	Deer	Dog	Elephant	Goat	Human AUS	Human UK	Monkey	Pig	Rabbit	Rat	Sheep
Number		1	6	1	1	0	1	3	1	1	1	1	0	1
Total N %	Mean	0.022	0.054	0.022	0.029	---	0.023	0.041	0.018	0.017	0.017	0.013	---	0.024
	Std. Error	…	0.003	…	…	---	…	0.009	…	…	…	…	---	…
	Min	…	0.042	…	…	---	…	0.028	…	…	…	…	---	…
	Max	…	0.062	…	…	---	…	0.057	…	…	…	…	---	…
Total C %	Mean	0.470	0.990	0.822	1.050	---	0.864	1.163	1.040	0.778	0.742	0.753	---	0.631
	Std. Error	…	0.042	…	…	---	…	0.041	…	…	…	…	---	…
	Min	…	0.821	…	…	---	…	1.090	…	…	…	…	---	…
	Max	…	1.100	…	…	---	…	1.230	…	…	…	…	---	…
Total H %	Mean	0.239	0.272	0.257	0.273	---	0.219	0.271	0.194	0.188	0.222	0.199	---	0.226
	Std. Error	…	0.014	…	…	---		0.006	…	…	…	…	---	…
	Min	…	0.214	…	…	---	…	0.265	…	…	…	…	---	…
	Max	…	0.313	…	…	---	…	0.283	…	…	…	…	---	…

Table A.5 – C-GC results for N %, C % and H % obtained from bone specimens heated to 600 °C, grouped by species. For all species except cow, human AUS and rat the 'mean' values represent data from one individual from each species and so no standard error of the mean, minimum or maximum values are presented. Rat bone was not investigated using this technique

A.4.5 – INFRARED SPECTROSCOPY

Species		Chicken	Cow	Deer	Dog	Elephant	Goat	Human AUS	Human UK	Monkey	Pig	Rabbit	Rat	Sheep
Number		1	6	1	1	0	1	0	1	1	1	1	0	1
CO_3 %	Mean	0.96	1.71	1.17	1.89	---	1.35	---	1.30	2.18	0.59	1.99	---	1.34
	Std. Error	…	0.17	…	…	---	---	---	…	…	…	…	---	…
	Min	…	1.16	…	…	---	…	---	…	…	…	…	---	…
	Max	…	2.27	…	…	---	---	---	…	…	…	…	---	…
SF	Mean	3.80	3.77	4.51	3.94	---	3.82	---	4.47	5.53	4.01	4.34	---	3.94
	Std. Error	…	0.09	…	…	---		---	…	…	…	…	---	…
	Min	…	3.53	…	…	---	…	---	…	…	…	…	---	…
	Max	…	4.05	…	…	---		---	…	…	…	…	---	…

Table A.6 – IR spectroscopy results for CO_3 % and SF obtained from bone specimens heated to 600 °C, grouped by species. For all species except cow, human AUS, elephant and rat the 'mean' values represent data from one individual from each species and so no standard error of the mean, minimum or maximum values are presented. Rat, human AUS and elephant bone were not investigated using this technique

A.4.6 – MASS CHANGE ON HEATING

Species		Chicken	Cow	Deer	Dog	Elephant	Goat	Human AUS	Human UK	Monkey	Pig	Rabbit	Rat	Sheep
Number		5	10	5	12	1	8	50	8	1	7	5	5	6
Mass Loss % 600 °C	Mean	52.307	34.059	31.255	36.246	33.717	31.492	38.590	38.867	36.683	40.009	29.873	46.048	37.004
	Std. Error	1.379	0.54	0.672	0.665	…	0.605	0.417	0.721	…	1.519	0.820	2.097	1.704
	Min	49.664	31.618	28.713	33.728	…	29.930	35.281	36.650	…	34.959	27.700	42.105	30.447
	Max	57.542	36.740	32.517	40.491	…	34.772	52.894	41.691	…	45.833	32.558	53.750	40.824
Mass Loss % 1400 °C	Mean	49.550	37.523	35.122	40.420	40.779	35.204	42.950	42.970	39.474	41.381	34.051	41.962	39.238
	Std. Error	1.338	0.403	0.470	0.521	…	0.505	0.270	0.693	…	0.505	0.683	1.529	1.256
	Min	44.371	35.713	33.438	38.462	…	33.333	40.187	40.433	…	39.353	31.878	39.130	35.018
	Max	51.768	39.556	36.242	43.229	…	36.976	49.237	46.463	…	42.918	36.058	47.059	43.411

Table A.7 – Mass change results obtained from bone specimens heated to 600 °C and 1400 °C, grouped by species. For elephant and monkey the 'mean' values represent data from one individual from each species and so no standard error of the mean, minimum or maximum values are presented

A.4.7 – X-RAY DIFFRACTION ANALYSIS OF BONE HEATED TO 600 °C

Species		Chicken	Cow	Deer	Dog	Elephant	Goat	Human AUS	Human UK	Monkey	Pig	Rabbit	Rat	Sheep
Number		5	10	5	12	1	8	50	8	1	7	5	5	6
HAP %	Mean	93.10	100	100	100	100	100	100	99.91	99.18	100	100	91.79	99.48
	Std. Error	0.45	…	…	…	…	…	…	0.09	…	…	…	2.07	0.52
	Min	91.76	…	…	…	…	…	…	99.28	…	…	…	86.08	96.87
	Max	94.08	…	…	…	…	…	…	100.00	…	…	…	96.41	100.00
HAP <00ℓ> (Å)	Mean	237.16	224.38	247.24	235.90	235.90	258.71	240.03	411.62	518.50	314.67	255.04	231.94	234.70
	Std. Error	8.17	5.95	9.48	4.38	…	15.81	2.33	63.58	…	31.62	2.84	5.52	4.20
	Min	206.50	200.90	226.40	208.30	…	210.30	216.40	224.50	…	208.70	248.10	222.10	217.40
	Max	254.80	263.00	282.80	259.60	…	330.30	304.80	722.70	…	409.60	261.10	250.30	247.30
HAP a (Å)	Mean	9.423	9.414	9.414	9.413	9.402	9.413	9.417	9.414	9.413	9.414	9.413	9.428	9.416
	Std. Error	0.001	0.001	0.001	0.001	…	0.001	0.001	0.001	…	0.001	0.001	0.001	0.002
	Min	9.419	9.410	9.411	9.407	…	9.408	9.405	9.410	…	9.408	9.411	9.423	9.405
	Max	9.427	9.418	9.417	9.421	…	9.416	9.437	9.419	…	9.417	9.416	9.430	9.420
HAP c (Å)	Mean	6.883	6.884	6.884	6.888	6.891	6.886	6.895	6.894	6.886	6.885	6.886	6.883	6.883
	Std. Error	0.001	0.000	0.001	0.001	…	0.000	0.000	0.001	…	0.001	0.001	0.000	0.001
	Min	6.880	6.883	6.882	6.884	…	6.885	6.890	6.891	…	6.883	6.885	6.882	6.881
	Max	6.885	6.886	6.887	6.890	…	6.888	6.900	6.897	…	6.890	6.889	6.883	6.886

Table A.8 – XRD analysis results for HAP %, HAP <00ℓ>, HAP 'a' and HAP 'c' obtained from bone specimens heated to 600 °C, grouped by species. For elephant and monkey the 'mean' values represent data from one individual from each species and so no standard error of the mean, minimum or maximum values are presented

Species		Chicken	Cow	Deer	Dog	Elephant	Goat	Human AUS	Human UK	Monkey	Pig	Rabbit	Rat	Sheep
Number		5	10	5	12	1	8	50	8	1	7	5	5	6
β-TCP %	No. Det	5	0	0	0	0	0	0	0	0	0	0	5	1
	Mean	6.90	…	…	…	…	…	…	…	…	…	…	8.21	3.13
	Std. Error	0.45	…	…	…	…	…	…	…	…	…	…	2.07	…
	Min	5.92	…	…	…	…	…	…	…	…	…	…	3.59	…
	Max	8.24	…	…	…	…	…	…	…	…	…	…	13.92	…
β-TCP a (Å)	Mean	10.369	…	…	…	…	…	…	…	…	…	…	10.376	10.352
	Std. Error	0.002	…	…	…	…	…	…	…	…	…	…	0.006	…
	Min	10.361	…	…	…	…	…	…	…	…	…	…	10.361	…
	Max	10.372	…	…	…	…	…	…	…	…	…	…	10.393	…
β-TCP c (Å)	Mean	37.166	…	…	…	…	…	…	…	…	…	…	37.169	37.156
	Std. Error	0.010	…	…	…	…	…	…	…	…	…	…	0.005	…
	Min	37.135	…	…	…	…	…	…	…	…	…	…	37.153	…
	Max	37.193	…	…	…	…	…	…	…	…	…	…	37.183	…
MgO %	No. Det	0	0	0	0	0	0	0	1	1	0	0	0	0
	Mean	…	…	…	…	…	…	…	0.72	0.82	…	…	…	…
	Std. Error	…	…	…	…	…	…	…	…	…	…	…	…	…
	Min	…	…	…	…	…	…	…	…	…	…	…	…	…
	Max	…	…	…	…	…	…	…	…	…	…	…	…	…

Table A.9 – XRD analysis results for XRD analysis results for β-TCP and MgO obtained from bone specimens heated to 600 °C, grouped by species. For elephant and monkey the 'mean' values represent data from one individual from each species and so no standard error of the mean, minimum or maximum values are presented. The phase β-TCP was only detected in chicken, rat and sheep and MgO was only detected in human UK and monkey bone specimens

A.4.8 – X-RAY DIFFRACTION ANALYSIS OF BONE HEATED TO 1400 °C

Species		Chicken	Cow	Deer	Dog	Elephant	Goat	Human AUS	Human UK	Monkey	Pig	Rabbit	Rat	Sheep
Number		5	10	5	12	1	8	50	8	1	7	5	5	6
HAP %	Mean	51.85	39.77	37.14	54.67	24.56	37.59	38.95	40.91	22.22	44.21	38.15	34.28	42.64
	Std. Error	2.82	1.39	1.35	2.21	…	1.83	1.21	3.14	…	4.39	2.43	1.72	4.19
	Min	45.94	35.06	33.27	43.57	…	26.47	25.24	31.88	…	29.66	33.42	28.55	31.65
	Max	60.66	48.82	40.26	72.33	…	43.52	60.45	56.47	…	60.04	44.95	39.37	59.02
HAP a (Å)	Mean	9.413	9.416	9.416	9.414	9.417	9.413	9.411	9.411	9.407	9.416	9.413	9.416	9.417
	Std. Error	0.001	0.001	0.001	0.001	…	0.001	0.001	0.002	…	0.000	0.002	0.001	0.001
	Min	9.409	9.413	9.414	9.409	…	9.410	9.400	9.400	…	9.415	9.408	9.412	9.414
	Max	9.414	9.419	9.418	9.418	…	9.415	9.423	9.422	…	9.417	9.417	9.419	9.419
HAP c (Å)	Mean	6.888	6.884	6.883	6.890	6.887	6.888	6.895	6.897	6.889	6.885	6.886	6.888	6.884
	Std. Error	0.001	0.000	0.000	0.001	…	0.000	0.000	0.001	…	0.000	0.001	0.002	0.001
	Min	6.887	6.882	6.883	6.885	…	6.887	6.887	6.892	…	6.884	6.883	6.885	6.882
	Max	6.890	6.886	6.884	6.896	…	6.889	6.901	6.900	…	6.886	6.890	6.894	6.886

Table A.10 – XRD analysis results for HAP %, HAP 'a' and HAP 'c' obtained from bone specimens heated to 1400 °C, grouped by species. For elephant and monkey the 'mean' values represent data from one individual from each species and so no standard error of the mean, minimum or maximum values are presented

Species		Chicken	Cow	Deer	Dog	Elephant	Goat	Human AUS	Human UK	Monkey	Pig	Rabbit	Rat	Sheep
Number		5	10	5	12	1	8	50	8	1	7	5	5	6
β-TCP %	Mean	44.15	44.70	47.78	31.46	34.36	42.42	32.23	25.79	44.16	38.09	41.41	51.31	45.86
	Std. Error	2.63	0.93	1.45	2.67	…	1.11	1.17	2.92	…	1.75	0.86	3.16	2.78
	Min	35.12	40.33	43.33	13.37	…	39.26	8.90	15.33	…	30.91	38.41	43.43	34.80
	Max	49.15	50.60	52.05	41.20	…	48.26	44.50	41.58	…	42.77	43.11	60.34	55.55
β-TCP a (Å)	Mean	10.432	10.441	10.440	10.441	10.442	10.441	10.445	10.445	10.439	10.441	10.440	10.436	10.440
	Std. Error	0.002	0.000	0.000	0.000	…	0.000	0.000	0.001	…	0.000	0.001	0.002	0.000
	Min	10.428	10.439	10.439	10.440	…	10.440	10.441	10.442	…	10.439	10.438	10.428	10.439
	Max	10.436	10.443	10.442	10.443	…	10.443	10.450	10.448	…	10.443	10.441	10.438	10.440
β-TCP c (Å)	Mean	37.331	37.324	37.328	37.331	37.319	37.324	37.337	37.325	37.309	37.318	37.335	37.346	37.321
	Std. Error	0.002	0.001	0.002	0.002	…	0.002	0.002	0.006	…	0.003	0.002	0.003	0.004
	Min	37.326	37.319	37.323	37.323	…	37.314	37.312	37.305	…	37.306	37.331	37.337	37.304
	Max	37.335	37.330	37.333	37.340	…	37.328	37.372	37.351	…	37.327	37.339	37.354	37.336
MgO %	Mean	0.98	1.03	0.94	0.53	0.57	0.98	0.64	0.65	0.78	0.97	0.89	0.98	1.13
	Std. Error	0.03	0.02	0.03	0.03	…	0.03	0.02	0.04	…	0.05	0.13	0.08	0.08
	Min	0.88	0.89	0.88	0.36	…	0.85	0.37	0.48	…	0.72	0.68	0.67	0.78
	Max	1.09	1.14	1.05	0.77	…	1.18	0.93	0.77	…	1.11	1.40	1.13	1.36

Table A.11 – XRD analysis results for β-TCP and MgO obtained from bone specimens heated to 1400 °C, grouped by species. For elephant and monkey the 'mean' values represent data from one individual from each species and so no standard error of the mean, minimum or maximum values are presented

Species		Chicken	Cow	Deer	Dog	Elephant	Goat	Human AUS	Human UK	Monkey	Pig	Rabbit	Rat	Sheep
Number		5	10	5	12	1	8	50	8	1	7	5	5	6
α-TCP %	No. Det	3	0	0	0	0	0	2	0	0	0	0	4	0
	Mean	2.38	…	…	…	…	…	4.06	…	…	…	…	13.34	…
	Std. Error	0.70	…	…	…	…	…	2.36	…	…	…	…	2.61	…
	Min	1.43	…	…	…	…	…	1.70	…	…	…	…	7.53	…
	Max	3.76	…	…	…	…	…	6.41	…	…	…	…	19.57	…
TTCP %	No. Det	3	10	5	12	1	8	50	8	1	7	5	5	6
	Mean	2.50	13.46	13.10	12.36	39.72	18.33	27.34	31.85	32.85	16.01	19.02	2.75	9.46
	Std. Error	0.21	0.97	1.33	1.50	…	1.72	0.98	1.82	…	2.94	2.84	0.22	2.90
	Min	2.09	8.68	8.40	4.33	…	10.81	8.42	24.67	…	7.12	12.00	1.96	3.97
	Max	2.81	18.74	16.41	20.02	…	25.98	38.67	38.26	…	26.17	24.60	3.22	22.15
CaO %	No. Det	1	10	5	12	1	8	46	8	0	7	4	0	6
	Mean	0.43	1.04	1.04	0.98	0.79	0.67	0.73	0.80	…	0.72	0.66	…	0.91
	Std. Error	…	0.07	0.07	0.05	…	0.06	0.03	0.12	…	0.05	0.13	…	0.09
	Min	…	0.57	0.83	0.72	…	0.41	0.38	0.36	…	0.52	0.31	…	0.56
	Max	…	1.32	1.17	1.26	…	0.97	1.14	1.39	…	0.84	0.90	…	1.08

Table A.12 – XRD analysis results for α-TCP, TTCP and CaO obtained from bone specimens heated to 1400 °C, grouped by species. For elephant and monkey the 'mean' values represent data from one individual from each species and so no standard error of the mean, minimum or maximum values are presented. The phase α-TCP was only detected in chicken, human AUS and rat bone specimens and CaO was not detected in rat or monkey bone specimens

A.5 – KENDALL'S TAU CORRELATION RESULTS (GROUPED BY SPECIES)

		Rat									
		Unheated			600 °C						
		HAP <00ℓ>	HAP a	HAP c	Mass Loss	HAP <00ℓ>	HAP a	HAP c	β-TCP %	β-TCP a	β-TCP c
Unheated	HAP <00ℓ>		------ 0	------ 0	------ 0	------ 0	------ 0	------ 0	------ 0	------ 0	------ 0
	HAP a	-0.400 0		------ 0	------ 0	------ 0	------ 0	------ 0	------ 0	------ 0	------ 0
	HAP c	0.000 0	0.200 0		------ 0	------ 0	------ 0	------ 0	------ 0	------ 0	------ 0
600 °C	Mass Loss	0.400 5	-0.200 5	-0.600 5		0.800 5	-0.400 5	-0.600 5	-0.200 5	-0.400 5	-0.600 5
	HAP <00ℓ>	-0.600 5	0.800 5	0.400 5	-0.400 5		-0.200 5	-0.400 5	-0.400 5	-0.600 5	-0.800 5
	HAP a	-0.200 5	0.800 5	0.400 5	-0.400 5	0.600 5		0.000 5	0.400 5	0.600 5	0.400 5
	HAP c	-0.800 5	0.200 5	-0.200 5	-0.200 5	0.400 5	0.000 5		-0.200 5	0.000 5	0.200 5
	β-TCP %	0.600 5	-0.400 5	0.000 5	0.000 5	-0.600 5	-0.200 5	-0.400 5		0.800 5	0.600 5
	β-TCP a	-0.600 5	0.800 5	0.000 5	0.000 5	0.600 5	0.600 5	0.400 5	-0.600 5		0.800 5
	β-TCP c	-0.800 5	0.600 5	0.200 5	-0.200 5	0.800 5	0.400 5	0.600 5	-0.800 5	0.800 5	
		HAP <00ℓ>	HAP a	HAP c	Mass Loss	HAP <00ℓ>	HAP a	HAP c	β-TCP %	β-TCP a	β-TCP c
		Unheated			600 °C						
		Chicken									

Table A.13 – Chicken and rat: Kendall's Tau correlation results for bone mineral characteristics obtained from XRD analysis of unheated bone and bone heated to 600 °C and mass change results for bone heated to 600 °C, tested against each other. Unheated rat bone was not investigated using XRD analysis. In each test result 'box' the correlation coefficient is presented above the number of individuals used for the test. A grey shaded box indicates $p < 0.05$ and a black box indicates $p < 0.01$

		Chicken									
		1400 °C									
		Mass Loss	HAP %	HAP a	HAP c	β-TCP %	β-TCP a	β-TCP c	α-TCP %	TTCP %	MgO %
Unheated	HAP <00ℓ>	0.400 5	-0.400 5	-0.600 5	0.400 5	0.600 5	-0.600 5	0.800 5	0.333 3	0.333 3	0.800 5
	HAP a	0.200 5	0.200 5	0.800 5	-0.600 5	-0.400 5	0.000 5	-0.600 5	-0.333 3	-1.000 3	-0.600 5
	HAP c	0.200 5	0.200 5	0.400 5	0.200 5	-0.400 5	0.000 5	-0.200 5	-0.333 3	1.000 3	-0.200 5
600 °C	Mass Loss	0.200 5	-0.600 5	-0.400 5	-0.200 5	0.800 5	-0.400 5	0.200 5	0.333 3	-1.000 3	0.200 5
	HAP <00ℓ>	0.000 5	0.400 5	1.000 5	-0.400 5	-0.600 5	0.200 5	-0.800 5	-0.333 3	-0.333 3	-0.800 5
	HAP a	0.400 5	0.000 5	0.600 5	-0.400 5	-0.200 5	-0.200 5	-0.400 5	-0.333 3	-0.333 3	-0.400 5
	HAP c	-0.600 5	0.200 5	0.400 5	-0.600 5	-0.400 5	0.800 5	-0.600 5	-1.000 3	-0.333 3	-0.600 5
	β-TCP %	0.000 5	-0.400 5	-0.600 5	0.400 5	0.200 5	-0.200 5	0.800 5	-0.333 3	0.333 3	0.800 5
	β-TCP a	0.000 5	0.000 5	0.600 5	-0.800 5	-0.200 5	0.200 5	-0.800 5	-0.333 3	-1.000 3	-0.800 5
	β-TCP c	-0.200 5	0.200 5	0.800 5	-0.600 5	-0.400 5	0.400 5	-1.000 5	-0.333 3	-0.333 3	-1.000 5

Table A.14 – Chicken: Kendall's Tau correlation results for bone mineral characteristics obtained from XRD analysis of bone heated to 1400 °C and mass change results for bone heated to 1400 °C, each tested against bone mineral characteristics obtained from XRD analysis of unheated bone and bone heated to 600 °C and mass change results for bone heated to 600 °C. In each test result 'box' the correlation coefficient is presented above the number of individuals used for the test. A grey shaded box indicates $p < 0.05$ and a black box indicates $p < 0.01$

		Rat									
		1400 °C									
		Mass Loss	HAP %	HAP a	HAP c	β-TCP %	β-TCP a	β-TCP c	α-TCP %	TTCP %	MgO %
Unheated	HAP <00ℓ>	------	------	------	------	------	------	------	------	------	------
		0	0	0	0	0	0	0	0	0	0
	HAP a	------	------	------	------	------	------	------	------	------	------
		0	0	0	0	0	0	0	0	0	0
	HAP c	------	------	------	------	------	------	------	------	------	------
		0	0	0	0	0	0	0	0	0	0
600 °C	Mass Loss	-0.200	0.400	-0.200	-0.200	-0.200	0.200	-0.600	0.333	0.600	0.800
		5	5	5	5	5	5	5	4	5	5
	HAP <00ℓ>	-0.400	0.200	0.000	0.000	0.000	0.400	-0.400	0.000	0.800	1.000
		5	5	5	5	5	5	5	4	5	5
	HAP a	-0.400	-0.600	0.000	0.400	0.000	-0.400	0.400	0.000	-0.400	-0.200
		5	5	5	5	5	5	5	4	5	5
	HAP c	-0.200	0.000	0.600	-0.200	0.600	0.200	0.600	-0.667	-0.200	-0.400
		5	5	5	5	5	5	5	4	5	5
	β-TCP %	0.200	-0.400	-0.600	0.600	-0.600	-1.000	0.200	0.667	-0.200	-0.400
		5	5	5	5	5	5	5	4	5	5
	β-TCP a	0.000	-0.600	-0.400	0.400	-0.400	-0.800	0.400	0.333	-0.400	-0.600
		5	5	5	5	5	5	5	4	5	5
	β-TCP c	0.200	-0.400	-0.200	0.200	-0.200	-0.600	0.600	0.000	-0.600	-0.800
		5	5	5	5	5	5	5	4	5	5

Table A.15 – Rat: Kendall's Tau correlation results for bone mineral characteristics obtained from XRD analysis of bone heated to 1400 °C and mass change results for bone heated to 1400 °C, each tested against bone mineral characteristics obtained from XRD analysis of bone heated to 600 °C and mass change results for bone heated to 600 °C. Unheated rat bone was not investigated using XRD analysis. In each test result 'box' the correlation coefficient is presented above the number of individuals used for the test. A grey shaded box indicates $p < 0.05$ and a black box indicates $p < 0.01$

		Rabbit						
		Unheated			600 °C			
		5	5	5	5	5	5	5
		HAP <00ℓ>	HAP a	HAP c	Mass Loss	HAP <00ℓ>	HAP a	HAP c
Unheated	HAP <00ℓ>		-0.200	0.000	0.000	0.400	-0.400	0.400
	HAP a	0.800		0.400	0.400	0.000	0.000	0.400
	HAP c	-0.600	-0.400		-0.200	-0.200	0.200	0.600
600 °C	Mass Loss	0.600	0.400	-0.600		0.600	0.200	-0.200
	HAP <00ℓ>	0.400	0.200	-0.400	0.800		0.200	0.200
	HAP a	0.000	0.200	-0.400	0.000	0.200		-0.200
	HAP c	-0.400	-0.200	0.800	-0.400	-0.200	-0.200	
		HAP <00ℓ>	HAP a	HAP c	Mass Loss	HAP <00ℓ>	HAP a	HAP c
		5	5	5	5	5	5	5
		Unheated			600 °C			
		Deer						

Table A.16 – Deer and rabbit: Kendall's Tau correlation results for bone mineral characteristics obtained from XRD analysis of unheated bone and bone heated to 600 °C and mass change results for bone heated to 600 °C, tested against each other. In each test result 'box' the correlation coefficient is presented above the number of individuals used for the test. In each test result 'box' the correlation coefficient is presented above the number of individuals used for the test. A grey shaded box indicates p < 0.05 and a black box indicates p < 0.01

		Deer									
		1400 °C									
		5	5	5	5	5	5	5	5	5	5
		Mass Loss	HAP %	HAP a	HAP c	β-TCP %	β-TCP a	β-TCP c	TTCP %	CaO %	MgO %
Unheated	HAP <00ℓ>	0.200	0.600	0.200	0.200	0.200	0.000	0.200	-0.200	0.600	0.000
	HAP a	0.000	0.400	0.400	0.400	0.000	0.200	0.000	0.000	0.400	0.200
	HAP c	-0.200	-0.200	-0.600	0.200	-0.600	-0.400	-0.600	0.600	-0.200	0.000
600 °C	Mass Loss	0.600	0.200	0.200	0.200	0.200	0.000	0.200	-0.200	0.600	0.000
	HAP <00ℓ>	0.800	0.000	0.000	0.400	0.000	-0.200	0.000	0.000	0.400	0.200
	HAP a	0.000	-0.400	0.400	0.000	0.400	0.600	0.000	0.000	-0.400	0.600
	HAP c	-0.400	0.000	-0.400	0.400	-0.800	-0.200	-0.800	0.800	0.000	0.200

Table A.17 – Deer: Kendall's Tau correlation results for bone mineral characteristics obtained from XRD analysis of bone heated to 1400 °C and mass change results for bone heated to 1400 °C, each tested against bone mineral characteristics obtained from XRD analysis of unheated bone and bone heated to 600 °C and mass change results for bone heated to 600 °C. In each test result 'box' the correlation coefficient is presented above the number of individuals used for the test. A grey shaded box indicates $p < 0.05$ and a black box indicates $p < 0.01$

		Rabbit									
		1400 °C									
		5	5	5	5	5	5	5	5	4	5
		Mass Loss	HAP %	HAP a	HAP c	β-TCP %	β-TCP a	β-TCP c	TTCP %	CaO %	MgO %
Unheated	HAP <00*l*>	0.000	-0.800	-0.600	0.600	-0.200	-0.200	1.000	0.800	-0.333	-0.600
	HAP a	0.400	0.000	0.200	0.200	0.200	1.000	-0.200	0.000	-0.667	0.200
	HAP c	-0.200	0.200	0.000	0.400	-0.400	0.400	0.000	0.200	0.000	0.400
600 °C	Mass Loss	1.000	-0.200	0.400	-0.400	0.800	0.400	0.000	-0.200	-0.667	0.000
	HAP <00*l*>	0.600	-0.200	0.000	0.000	0.400	0.000	0.400	0.200	-0.667	0.000
	HAP a	0.200	0.600	0.400	-0.400	0.400	0.000	-0.400	-0.200	0.000	0.800
	HAP c	-0.200	-0.200	-0.400	0.800	-0.400	0.400	0.400	0.600	-0.333	0.000

Table A.18 – Rabbit: Kendall's Tau correlation results for bone mineral characteristics obtained from XRD analysis of bone heated to 1400 °C and mass change results for bone heated to 1400 °C, each tested against bone mineral characteristics obtained from XRD analysis of unheated bone and bone heated to 600 °C and mass change results for bone heated to 600 °C. In each test result 'box' the correlation coefficient is presented above the number of individuals used for the test. A grey shaded box indicates $p < 0.05$ and a black box indicates $p < 0.01$

		Sheep						
		Unheated			600 °C			
		6	6	6	6	6	6	6
		HAP <00ℓ>	HAP a	HAP c	Mass Loss	HAP <00ℓ>	HAP a	HAP c
Unheated	HAP <00ℓ>		-0.467	-0.333	-0.333	0.200	-0.276	0.200
	HAP a	0.286		0.600	0.333	-0.200	0.276	-0.200
	HAP c	0.000	0.000		-0.067	-0.067	-0.138	0.200
600 °C	Mass Loss	0.143	-0.143	0.429		0.467	0.966	-0.867
	HAP <00ℓ>	0.429	-0.143	-0.143	0.286		0.414	-0.333
	HAP a	0.000	0.286	0.000	0.000	-0.429		-0.966
	HAP c	0.357	-0.071	-0.071	-0.071	0.071	0.071	
		HAP <00ℓ>	HAP a	HAP c	Mass Loss	HAP <00ℓ>	HAP a	HAP c
		8	8	8	8	8	8	8
		Unheated			600 °C			
		Goat						

Table A.19 – Goat and Sheep: Kendall's Tau correlation results for bone mineral characteristics obtained from XRD analysis of unheated bone and bone heated to 600 °C and mass change results for bone heated to 600 °C, tested against each other. In each test result 'box' the correlation coefficient is presented above the number of individuals used for the test. In each test result 'box' the correlation coefficient is presented above the number of individuals used for the test. A grey shaded box indicates p < 0.05 and a black box indicates p < 0.01

		Goat									
		1400 °C									
		8	8	8	8	8	8	8	8	8	8
		Mass Loss	HAP %	HAP a	HAP c	β-TCP %	β-TCP a	β-TCP c	TTCP %	CaO %	MgO %
Unheated	HAP <00*l*>	0.286	-0.143	0.071	-0.286	-0.571	-0.429	0.143	0.286	0.286	0.214
	HAP a	-0.286	0.143	-0.357	0.143	0.000	0.143	0.143	-0.286	-0.143	0.643
	HAP c	0.143	0.000	-0.071	-0.143	0.000	0.143	-0.286	0.000	0.286	0.071
600 °C	Mass Loss	0.429	-0.143	0.214	-0.571	-0.143	-0.286	-0.286	0.143	0.714	0.071
	HAP <00*l*>	0.429	-0.571	0.071	-0.286	-0.286	-0.714	-0.143	0.714	0.286	-0.214
	HAP a	0.000	0.714	0.214	-0.143	-0.286	0.143	0.000	-0.714	0.143	0.643
	HAP c	0.357	0.071	0.429	-0.071	-0.500	0.214	0.500	0.071	0.071	0.000

Table A.20 – Goat: Kendall's Tau correlation results for bone mineral characteristics obtained from XRD analysis of bone heated to 1400 °C and mass change results for bone heated to 1400 °C, each tested against bone mineral characteristics obtained from XRD analysis of unheated bone and bone heated to 600 °C and mass change results for bone heated to 600 °C. In each test result 'box' the correlation coefficient is presented above the number of individuals used for the test. A grey shaded box indicates $p < 0.05$ and a black box indicates $p < 0.01$

		Sheep									
		1400 °C									
		6	6	6	6	6	6	6	6	6	6
		Mass Loss	HAP %	HAP a	HAP c	β-TCP %	β-TCP a	β-TCP c	TTCP %	CaO %	MgO %
Unheated	HAP <00ℓ>	0.067	0.200	0.200	-0.200	0.067	-0.200	0.067	-0.200	0.467	0.067
	HAP a	-0.067	-0.200	-0.200	0.733	-0.067	0.467	-0.333	0.200	-0.733	-0.067
	HAP c	-0.200	-0.333	-0.600	0.333	0.067	0.333	-0.200	0.333	-0.600	-0.467
600 °C	Mass Loss	0.600	0.467	0.467	0.067	0.067	-0.200	0.067	-0.467	-0.067	0.600
	HAP <00ℓ>	0.600	0.733	0.467	-0.200	-0.200	-0.200	-0.200	-0.733	0.200	0.333
	HAP a	0.690	0.414	0.552	0.138	0.138	-0.138	0.138	-0.552	0.000	0.690
	HAP c	-0.733	-0.333	-0.600	-0.200	-0.200	0.067	-0.200	0.600	-0.067	-0.733

Table A.21 – Sheep: Kendall's Tau correlation results for bone mineral characteristics obtained from XRD analysis of bone heated to 1400 °C and mass change results for bone heated to 1400 °C, each tested against bone mineral characteristics obtained from XRD analysis of unheated bone and bone heated to 600 °C and mass change results for bone heated to 600 °C. In each test result 'box' the correlation coefficient is presented above the number of individuals used for the test. A grey shaded box indicates p < 0.05 and a black box indicates p < 0.01

		Pig						
		Unheated			600 °C			
		7	7	7	7	7	7	7
		HAP <00ℓ>	HAP a	HAP c	Mass Loss	HAP <00ℓ>	HAP a	HAP c
Unheated	HAP <00ℓ>		0.683	-0.195	0.195	0.098	-0.195	0.098
	HAP a	-0.061		-0.048	0.333	0.143	-0.143	-0.238
	HAP c	-0.121	0.212		-0.143	-0.143	0.143	-0.143
600 °C	Mass Loss	-0.091	0.545	0.121		0.810	0.333	-0.524
	HAP <00ℓ>	-0.182	0.212	0.394	0.061		0.524	-0.524
	HAP a	0.030	0.242	0.061	0.576	-0.061		-0.619
	HAP c	0.121	-0.333	0.091	-0.606	0.212	-0.485	
		HAP <00ℓ>	HAP a	HAP c	Mass Loss	HAP <00ℓ>	HAP a	HAP c
		12	12	12	12	12	12	12
		Unheated			600 °C			
		Dog						

Table A.22 – Dog and pig: Kendall's Tau correlation results for bone mineral characteristics obtained from XRD analysis of unheated bone and bone heated to 600 °C and mass change results for bone heated to 600 °C, tested against each other. In each test result 'box' the correlation coefficient is presented above the number of individuals used for the test. In each test result 'box' the correlation coefficient is presented above the number of individuals used for the test. A grey shaded box indicates $p < 0.05$ and a black box indicates $p < 0.01$

		Dog											
		1400 °C											
		12	12	12	12	12	12	12	12	12	12	12	12
		Mass Loss	HAP %	HAP a	HAP c	β-TCP %	β-TCP a	β-TCP c	TTCP %	CaO %	MgO %	Sex	Age
Unheated	HAP <00ℓ>	-0.091	-0.212	-0.091	-0.030	0.061	-0.364	-0.182	0.121	-0.121	0.121	-0.055	0.018
	HAP a	0.667	-0.242	0.061	-0.424	0.394	-0.333	0.273	-0.394	0.030	0.091	-0.550	-0.312
	HAP c	0.242	0.000	0.121	0.000	0.030	-0.212	-0.030	0.152	-0.030	-0.576	-0.275	0.092
600 °C	Mass Loss	0.697	-0.212	0.030	-0.636	0.667	-0.303	0.364	-0.485	-0.242	0.182	-0.330	-0.569
	HAP <00ℓ>	0.121	-0.121	-0.182	0.121	-0.091	-0.212	-0.091	0.152	0.030	-0.273	-0.385	0.239
	HAP a	0.394	-0.394	-0.152	-0.697	0.788	-0.485	0.364	-0.364	-0.303	0.182	0.165	-0.752
	HAP c	-0.606	0.061	-0.242	0.485	-0.455	0.091	-0.273	0.455	0.030	-0.212	0.165	0.532

Table A.23 – Dog: Kendall's Tau correlation results for bone mineral characteristics obtained from XRD analysis of bone heated to 1400 °C and mass change results for bone heated to 1400 °C, each tested against bone mineral characteristics obtained from XRD analysis of unheated bone and bone heated to 600 °C and mass change results for bone heated to 600 °C. In each test result 'box' the correlation coefficient is presented above the number of individuals used for the test. A grey shaded box indicates $p < 0.05$ and a black box indicates $p < 0.01$

		Pig									
		1400 °C									
		7	7	7	7	7	7	7	7	7	7
		Mass Loss	HAP %	HAP a	HAP c	β-TCP %	β-TCP a	β-TCP c	TTCP %	CaO %	MgO %
Unheated	HAP <00*l*>	0.390	0.390	0.350	-0.488	-0.390	-0.293	-0.488	-0.293	-0.098	0.098
	HAP a	0.429	0.048	0.195	-0.143	-0.238	-0.143	-0.333	0.048	-0.238	-0.048
	HAP c	-0.238	0.143	0.098	-0.048	0.048	-0.048	0.143	-0.048	0.238	0.048
600 °C	Mass Loss	0.524	0.143	-0.488	-0.238	-0.143	-0.429	-0.238	-0.238	-0.333	-0.333
	HAP <00*l*>	0.524	0.333	-0.293	-0.238	-0.333	-0.429	-0.429	-0.429	-0.143	-0.143
	HAP a	0.048	0.238	-0.390	-0.333	-0.238	-0.524	-0.143	-0.333	0.333	0.143
	HAP c	-0.048	-0.238	0.195	0.143	0.238	0.333	0.143	0.333	-0.143	-0.143

Table A.24 – Pig: Kendall's Tau correlation results for bone mineral characteristics obtained from XRD analysis of bone heated to 1400 °C and mass change results for bone heated to 1400 °C, each tested against bone mineral characteristics obtained from XRD analysis of unheated bone and bone heated to 600 °C and mass change results for bone heated to 600 °C. In each test result 'box' the correlation coefficient is presented above the number of individuals used for the test. A grey shaded box indicates $p < 0.05$ and a black box indicates $p < 0.01$

		Human UK						
		Unheated			600 °C			
		8	8	8	8	8	8	8
		HAP <00ℓ>	HAP a	HAP c	Mass Loss	HAP <00ℓ>	HAP a	HAP c
Unheated	HAP <00ℓ>		0.143	0.429	0.429	-0.214	-0.071	0.071
	HAP a	-0.091 47		-0.286	0.143	-0.071	0.214	0.071
	HAP c	0.057 47	0.230 47		0.286	-0.071	-0.071	0.214
600 °C	Mass Loss	-0.082 47	0.123 47	-0.140 47		0.357	0.214	-0.500
	HAP <00ℓ>	0.145 47	-0.093 47	0.199 47	-0.066 50		0.571	-0.857
	HAP a	-0.178 47	0.297 47	-0.358 47	0.123 50	-0.388 50		-0.429
	HAP c	0.072 47	-0.086 47	0.221 47	-0.212 50	0.229 50	-0.108 50	
		HAP <00ℓ>	HAP a	HAP c	Mass Loss	HAP <00ℓ>	HAP a	HAP c
		Unheated			600 °C			
		Human AUS						

Table A.25 – Human UK and human AUS: Kendall's Tau correlation results for bone mineral characteristics obtained from XRD analysis of unheated bone and bone heated to 600 °C and mass change results for bone heated to 600 °C, tested against each other. In each test result 'box' the correlation coefficient is presented above the number of individuals used for the test. In each test result 'box' the correlation coefficient is presented above the number of individuals used for the test. A grey shaded box indicates p < 0.05 and a black box indicates p < 0.01

		Human AUS											
		1400 °C											
		Mass Loss	HAP %	HAP a	HAP c	β-TCP %	β-TCP a	β-TCP c	TTCP %	CaO %	MgO %	Sex	Age
Unheated	HAP <00ℓ>	-0.033 47	0.009 47	-0.051 47	0.119 47	-0.107 47	0.112 47	0.025 47	0.096 47	-0.098 43	-0.232 47	0.047 47	0.148 47
	HAP a	0.110 47	-0.064 47	0.396 47	-0.251 47	0.251 47	0.154 47	0.205 47	-0.241 47	0.132 43	0.195 47	-0.185 47	-0.303 47
	HAP c	-0.086 47	0.003 47	-0.128 47	0.212 47	-0.278 47	-0.006 47	-0.209 47	0.354 47	-0.074 43	-0.275 47	-0.120 47	0.390 47
600 °C	Mass Loss	0.579 50	0.301 50	0.125 50	-0.167 50	0.056 50	-0.019 50	0.157 50	-0.376 50	0.239 46	0.239 50	-0.088 50	-0.226 50
	HAP <00ℓ>	-0.158 50	0.264 50	-0.280 50	0.314 50	-0.448 50	-0.128 50	-0.351 50	0.220 50	0.016 46	-0.037 50	-0.228 50	0.374 50
	HAP a	0.094 50	-0.177 50	0.435 50	-0.296 50	0.538 50	0.324 50	0.482 50	-0.388 50	0.127 46	0.345 50	-0.006 50	-0.597 50
	HAP c	-0.189 50	-0.088 50	-0.167 50	0.449 50	-0.289 50	0.260 50	-0.092 50	0.385 50	-0.159 46	-0.078 50	-0.058 50	0.372 50

Table A.26 – Human AUS: Kendall's Tau correlation results for bone mineral characteristics obtained from XRD analysis of bone heated to 1400 °C, mass change results for bone heated to 1400 °C, sex and age data, each tested against bone mineral characteristics obtained from XRD analysis of unheated bone and bone heated to 600 °C and mass change results for bone heated to 600 °C. In each test result 'box' the correlation coefficient is presented above the number of individuals used for the test. A grey shaded box indicates $p < 0.05$ and a black box indicates $p < 0.01$

		Human UK											
		1400 °C											
		8	8	8	8	8	8	8	8	8	8	8	8
		Mass Loss	HAP %	HAP a	HAP c	β-TCP %	β-TCP a	β-TCP c	TTCP %	CaO %	MgO %	Sex	Age
Unheated	HAP <00ℓ>	0.714	0.286	0.214	0.143	-0.214	0.214	0.429	-0.286	0.071	0.500	-0.049	-0.071
	HAP a	0.286	0.000	0.357	-0.286	0.071	0.357	0.143	-0.429	0.071	0.214	-0.244	-0.357
	HAP c	0.286	0.429	0.214	0.286	-0.357	0.357	0.143	0.000	0.214	0.071	0.342	0.071
600 °C	Mass Loss	0.429	-0.143	0.214	-0.429	0.357	0.357	0.429	-0.286	0.071	0.357	0.244	-0.500
	HAP <00ℓ>	-0.214	-0.357	0.143	-0.500	0.571	0.000	0.071	-0.071	0.286	-0.143	0.342	-0.429
	HAP a	-0.214	-0.357	0.429	-0.357	0.429	0.143	0.214	-0.071	0.286	-0.286	0.244	-0.714
	HAP c	0.071	0.500	0.000	0.643	-0.714	0.143	-0.214	0.071	-0.143	0.000	-0.342	0.429

Table A.27 – Human UK: Kendall's Tau correlation results for bone mineral characteristics obtained from XRD analysis of bone heated to 1400 °C, mass change results for bone heated to 1400 °C, sex and age data, each tested against bone mineral characteristics obtained from XRD analysis of unheated bone and bone heated to 600 °C and mass change results for bone heated to 600 °C. In each test result 'box' the correlation coefficient is presented above the number of individuals used for the test. A grey shaded box indicates $p < 0.05$ and a black box indicates $p < 0.01$

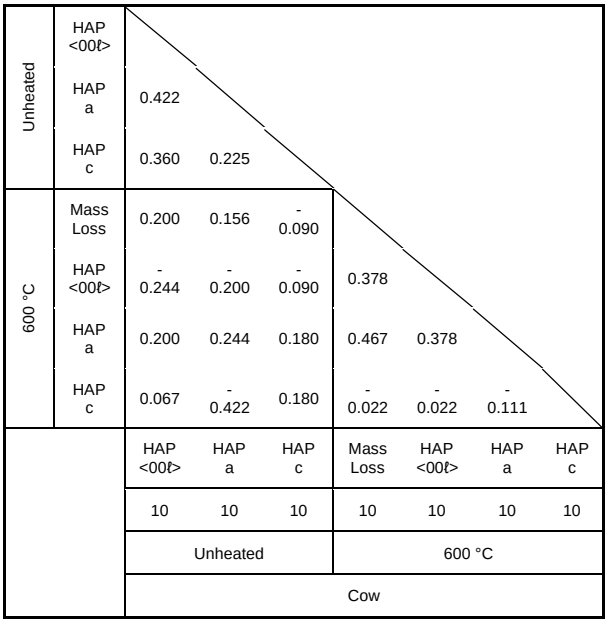

Table A.28 – Cow: Kendall's Tau correlation results for bone mineral characteristics obtained from XRD analysis of unheated bone and bone heated to 600 °C and mass change results for bone heated to 600 °C, tested against each other. In each test result 'box' the correlation coefficient is presented above the number of individuals used for the test. In each test result 'box' the correlation coefficient is presented above the number of individuals used for the test. A grey shaded box indicates p < 0.05 and a black box indicates p < 0.01

		Cow											
		1400 °C											
		10	10	10	10	10	10	10	10	10	10	10	10
		Mass Loss	HAP %	HAP a	HAP c	β-TCP %	β-TCP a	β-TCP c	TTCP %	CaO %	MgO %	Sex	Age
Unheated	HAP <00ℓ>	0.467	0.067	0.067	0.022	0.022	0.333	0.156	-0.067	-0.333	0.511	0.316	-0.316
	HAP a	0.422	0.111	-0.244	-0.200	-0.022	-0.156	-0.067	-0.289	-0.022	0.111	-0.316	-0.527
	HAP c	0.180	0.315	-0.225	0.135	-0.225	0.045	0.000	0.135	-0.090	-0.045	0.333	0.000
600 °C	Mass Loss	0.556	0.244	0.156	-0.333	-0.156	-0.200	-0.111	-0.422	0.200	0.244	0.316	-0.316
	HAP <00ℓ>	0.022	-0.022	0.067	-0.333	0.200	-0.289	0.067	-0.156	0.556	-0.022	0.632	0.527
	HAP a	0.467	0.067	0.244	-0.600	0.200	0.067	0.422	-0.422	0.289	0.333	-0.316	-0.738
	HAP c	-0.378	-0.067	-0.067	0.333	0.067	0.200	0.200	0.333	-0.289	0.200	0.632	0.527

Table A.29 – Cow: Kendall's Tau correlation results for bone mineral characteristics obtained from XRD analysis of bone heated to 1400 °C, mass change results for bone heated to 1400 °C, sex and age data, each tested against bone mineral characteristics obtained from XRD analysis of unheated bone and bone heated to 600 °C and mass change results for bone heated to 600 °C. In each test result 'box' the correlation coefficient is presented above the number of individuals used for the test. A grey shaded box indicates $p < 0.05$ and a black box indicates $p < 0.01$

		Human AUS												
		600 °C												
		3	3	3	3	3	3	3	3	3	3	3	3	3
		Ca %	P %	Atomic Ca/P	Total N %	Total C %	Total H %	Fe ppm	K ppm	Mg ppm	Na ppm	Sr ppm	F ppm	Cl ppm
Unheated	HAP <00ℓ>	1.000	1.000	-1.000	-0.333	-0.333	0.333	-0.333	-0.333	0.333	1.000	0.333	0.333	1.000
	HAP a	-0.333	-0.333	0.333	-0.333	1.000	0.333	-0.333	-0.333	-1.000	-0.333	-1.000	0.333	-0.333
	HAP c	-0.333	-0.333	0.333	-0.333	1.000	0.333	-0.333	-0.333	-1.000	-0.333	-1.000	0.333	-0.333
600 °C	Mass Loss	-0.333	-0.333	0.333	-0.333	1.000	0.333	-0.333	-0.333	-1.000	-0.333	-1.000	0.333	-0.333
	HAP <00ℓ>	-0.333	-0.333	0.333	-0.333	1.000	0.333	-0.333	-0.333	-1.000	-0.333	-1.000	0.333	-0.333
	HAP a	0.333	0.333	-0.333	0.333	-1.000	-0.333	0.333	0.333	1.000	0.333	1.000	-0.333	0.333
	HAP c	0.333	0.333	-0.333	-1.000	0.333	1.000	-1.000	-1.000	-0.333	0.333	-0.333	1.000	0.333
1400 °C	Mass Loss	0.333	0.333	-0.333	0.333	-1.000	-0.333	0.333	0.333	1.000	0.333	1.000	-0.333	0.333
	HAP %	1.000	1.000	-1.000	-0.333	-0.333	0.333	-0.333	-0.333	0.333	1.000	0.333	0.333	1.000
	HAP a	-0.333	-0.333	0.333	-0.333	1.000	0.333	-0.333	-0.333	-1.000	-0.333	-1.000	0.333	-0.333
	HAP c	1.000	1.000	-1.000	-0.333	-0.333	0.333	-0.333	-0.333	0.333	1.000	0.333	0.333	1.000
	β-TCP %	-1.000	-1.000	1.000	0.333	0.333	-0.333	0.333	0.333	-0.333	-1.000	-0.333	-0.333	-1.000
	β-TCP a	0.333	0.333	-0.333	-1.000	0.333	1.000	-1.000	-1.000	-0.333	0.333	-0.333	1.000	0.333
	β-TCP c	0.333	0.333	-0.333	-1.000	0.333	1.000	-1.000	-1.000	-0.333	0.333	-0.333	1.000	0.333
	TTCP %	-0.333	-0.333	0.333	1.000	-0.333	-1.000	1.000	1.000	0.333	-0.333	0.333	-1.000	-0.333
	CaO %	-0.333	-0.333	0.333	-0.333	1.000	0.333	-0.333	-0.333	-1.000	-0.333	-1.000	0.333	-0.333
	MgO %	-1.000	-1.000	1.000	0.333	0.333	-0.333	0.333	0.333	-0.333	-1.000	-0.333	-0.333	-1.000
	Age	1.000	1.000	-1.000	-0.333	-0.333	0.333	-0.333	-0.333	0.333	1.000	0.333	0.333	1.000

Table A.30 – Human AUS: Kendall's Tau correlation results for bone mineral characteristics obtained from ICP-AES, P-IC and C-GC of bone specimens heated to 600 °C tested against characteristics obtained from XRD analysis of unheated bone specimens, bone specimens heated to 600 °C and to 1400 °C and for mass change results for 600 °C and 1400 °C. In each test result 'box' the correlation coefficient is presented above the number of individuals used for the test

		Cow														
		600 °C														
		6	6	6	6	6	6	6	6	6	6	6	6	6	6	6
		Ca %	P %	Atomic Ca/P	Total N %	Total C %	Total H %	Fe ppm	K ppm	Mg ppm	Na ppm	Sr ppm	F ppm	Cl ppm	CO_3 %	SF
Unheated	HAP <00ℓ>	-0.333	-0.276	-0.072	-0.467	-0.467	0.000	-0.200	0.333	-0.067	-0.600	0.200	-0.467	0.733	0.200	-0.333
	HAP a	0.467	0.276	-0.072	0.600	0.067	0.000	-0.467	-0.200	0.467	0.200	-0.333	0.067	-0.067	-0.067	0.200
	HAP c	-0.138	0.500	-0.741	0.276	-0.276	-0.143	-0.828	0.552	0.000	-0.276	0.276	0.000	0.000	0.276	0.552
600 °C	Mass Loss	-0.200	-0.414	0.072	-0.067	-0.333	0.138	-0.333	0.200	0.067	-0.200	0.067	-0.067	0.600	-0.200	0.067
	HAP <00ℓ>	-0.733	0.138	-0.501	-0.333	-0.333	-0.414	-0.333	0.733	-0.467	-0.200	0.867	0.200	0.067	0.067	0.333
	HAP a	-0.200	0.138	-0.358	-0.067	-0.600	-0.414	-0.333	0.200	0.333	-0.467	0.067	-0.600	0.333	-0.467	0.600
	HAP c	-0.467	-0.138	-0.215	-0.333	0.200	0.276	-0.067	0.467	-0.733	-0.467	0.333	-0.067	0.333	0.333	0.067
1400 °C	Mass Loss	-0.200	-0.138	-0.215	-0.067	-0.600	-0.138	-0.333	0.200	0.333	-0.200	0.067	-0.333	0.600	0.067	-0.200
	HAP %	-0.067	0.000	-0.215	0.067	-0.467	0.000	-0.467	0.067	0.467	-0.067	-0.067	-0.200	0.467	-0.200	0.067
	HAP a	-0.200	-0.552	0.501	-0.600	-0.333	-0.138	0.467	-0.333	0.067	-0.200	0.067	-0.600	0.600	-0.600	-0.333
	HAP c	-0.333	0.000	-0.215	0.067	0.333	0.138	-0.200	0.333	-0.600	0.200	0.467	0.600	-0.333	0.467	-0.333
	β-TCP %	-0.067	0.414	-0.215	-0.200	0.333	-0.138	0.333	0.333	-0.333	-0.333	0.200	-0.200	-0.067	0.200	0.200
	β-TCP a	-0.333	-0.414	0.358	-0.733	-0.467	-0.276	0.333	-0.200	-0.067	-0.333	0.200	-0.733	0.467	-0.467	-0.467
	β-TCP c	-0.067	0.138	-0.215	-0.467	-0.200	-0.414	0.333	0.067	-0.067	-0.333	-0.067	-0.733	0.200	-0.333	0.200
	TTCP %	-0.200	-0.138	0.072	-0.067	0.467	0.276	0.200	0.200	-0.733	0.067	0.333	0.467	-0.200	0.600	-0.200
	CaO %	0.067	0.276	-0.215	-0.067	-0.600	-0.690	-0.333	-0.067	0.333	0.067	0.067	-0.333	-0.200	-0.467	0.333
	MgO %	-0.467	-0.690	0.358	-0.600	-0.333	0.138	0.200	-0.067	-0.200	-0.200	0.333	-0.333	0.867	-0.467	-0.200
	Age	-0.527	0.000	-0.222	-0.105	0.527	0.222	0.105	0.527	-0.949	0.105	0.738	0.738	-0.105	0.527	-0.105

Table A.31 – Cow: Kendall's Tau correlation results for bone mineral characteristics obtained from ICP-AES, P-IC, C-GC and IR spectroscopy of bone specimens heated to 600 °C tested against characteristics obtained from XRD analysis of unheated bone specimens, bone specimens heated to 600 °C and to 1400 °C and for mass change results for 600 °C and 1400 °C. In each test result 'box' the correlation coefficient is presented above the number of individuals used for the test